1 2 9 0

UNIVERSIDADE Ð COIMBRA

Rim Erragued

SEPARATION OF HIGH ADDED VALUE PHENOLIC
COMPOUNDS FROM OLIVE LEAF EXTRACT USING
MEMBRANE TECHNOLOGY

December 2023

Co-supervision PhD thesis, submitted to the Department of Chemistry, Faculty of Sciences of Sfax, University of Sfax and the Department of Chemical Engineering, Faculty of Sciences and Technology, University of Coimbra

Institutions:

CIEPQPF – Chemical Process Engineering and Forest Products Research Centre Department of Chemical Engineering, University of Coimbra

Laboratory of Electrochemistry and Environment, National School of Engineers of Sfax, University of Sfax

Supervisors:

Professor Licínio Manuel Gando de Azevedo Ferreira

Professor Mohamed Bouaziz

Acknowledgements

I am filled with a sense of accomplishment and gratitude as I approach the final stages of my doctoral program. Throughout this journey, I have received invaluable support and guidance that has been instrumental. I am deeply grateful to the individuals and institutions who have believed in my abilities and have contributed to the completion of this thesis. It is with great pleasure that I acknowledge their invaluable support.

I would like to extend my heartfelt thanks to my supervisor at the University of Sfax, **Professor Doctor Mohamed Bouaziz**, for being an excellent mentor who provided valuable guidance and feedback. I am grateful for his scientific insights and engaging discussions over the years since I began my PhD journey. I am also extremely grateful for his prompt availability and timely responses to my doubts.

I also want to extend my sincere appreciation to my supervisor at the University of Coimbra, **Professor Doctor Licínio Ferreira**, for his guidance in the development of this thesis and for being a constant source of support. I would like to express my deepest gratitude to him for his innovative ideas that provided me with the foundation I needed to begin my work. I am grateful for his expertise and for his willingness to share his knowledge and insights with me. I am also thankful to all of my co-authors for their contributions, which were invaluable in the development of this thesis.

My over-whelming thanks go to the entire committee for giving me the opportunity to go for doctoral research. I express my deepest respect to **Prof. Raja Ben Amar** (University of Sfax) who gave me honor of accepting the jury presidency. I also express my gratitude to **Prof**. **Hermínio José Cipriano de Sousa** (University of Coimbra) and **Prof. André Deratani** (University of Montpellier) for accepting to devote their precious time to the thesis revision. For the same occasion, i would like to thank **Prof. Ali Bougatef** (University of Sfax) for agreeing to examine and judge this thesis.

I am grateful to the CIEPQPF research centre at the Department of Chemical Engineering, for providing the necessary resources for my research. I would also like to thank electrochemistry and environment laboratory (LEE) at the national engineering school of Sfax for its necessary

support. I am also thankful to Nicolaus Copernicus University in Toruń for the opportunity to collaborate on my PhD.

Professor Maria Graça Carvalho and Professor Thabet Yangui deserves special mention for their constant support throughout my PhD journey. They were always available to help me, whether it was for personal or professional issues. I am also grateful to my colleagues and friends at the University of Sfax and University of Coimbra, particularly Manorma, Andreia, Patricia, Raffaela, Solange, Ons, Ines, and Jonathan for creating a warm and supportive environment.

I want to express my heartfelt gratitude to my friends, especially Afef, Lotfi and Amina, who were always there for me when I needed them. I would like to express my appreciation for their friendship and for being such an integral part of my life. Thank you for being there for me, no matter how far apart we may be. Your support means the world to me.

I would like to express my sincere gratitude to my parents Amor Erragued and Omzine Hasni, my siblings Mouna, Abdrazak, Chaima, Asma and Ahlem and my nieces Assil, Yassmine, Youssef and Yazid for their love, emotional support and encouragement, even though they live miles away from me. Despite the distance, they have always been there for me, offering a listening ear and a comforting presence whenever I needed it. Even though they are not directly involved in my research, their belief in me and their encouragement has been an invaluable source of strength and inspiration.

I would like to express my special thanks to my great father, **Amor Erragued**, who passed away during my Ph.D. Unfortunately, God chose not to have him with me in these final moments. I want you to know that your belief in my abilities and your efforts in my education allowed me to wholeheartedly focus on my research and coursework. It enabled me to pursue my passion and work towards achieving my goals. I will never forget your favor, and I promise that I will make you proud of me.

Finally, I want to thank everyone who has been part of my journey for their support. Their love and encouragement have been integral to my journey.

Resumo

As folhas de oliveira (OL) são consideradas um subproduto da oliveira, gerado a partir do cultivo e processo de produção de azeite de oliva. A grande quantidade de compostos fenólicos presentes nas folhas de oliveira tem atraído o interesse dos pesquisadores, e muitos estudos têm relatado que as folhas de oliveira oferecem efeitos benéficos, como capacidade antioxidante, efeito anti-hipertensivo, redução do colesterol, cardioproteção, anti-inflamatório e comocoadjuvante no tratamento da obesidade.

Nos últimos anos, diferentes estudos foram realizados para a separação e recuperação desses compostos fenólicos do extrato de folhas de oliveira (OLE). No âmbito desta tese, foi dada ênfase à preparação e aplicação de membranas de matriz mista (MMMs) para a recuperação de compostos fenólicos.

O trabalho começou com a caracterização de diferentes amostras de folhas de oliveiraobtidas de várias variedades, regiões de coleta e períodos de amostragem para analisar a variabilidade em sua concentração total de compostos fenólicos. Verificou-se que os compostos fenólicos nas folhas de oliveira mudavam com base na variedade de oliveira, região de coleta e período de amostragem. Posteriormente, a variedade de oliveira, região de coleta e período de amostragem foram fixados para minimizar o efeito da variação na concentração total de compostos fenólicos no desempenho das membranas utilizadas durante a filtração do extrato de folhas de oliveira (OLE).

Neste estudo, os compostos fenólicos foram separados com eficácia do extrato de folhas de oliveira usando uma membrana comercial de nanofiltração (NF) de poliétersulfona (PES) em folha plana. Além disso, membranas de matriz mista (MMMs) foram meticulosamente preparadas para aprimorar o processo de separação. Antes de efetuar os testes de NF, o OLE foi submetido a um processo preliminar de ultrafiltração (UF) para remover sólidos suspensos e compostos macromoleculares, permitindo assim reduzir os fenómenos de colmatação no processosubsequente de NF.

A primeira abordagem integra a técnica de extração com solvente e separação por membrana usando uma membrana comercial de nanofiltração (NF) de poliétersulfona (PES) em folha plana.

Por meio da otimização cuidadosa usando um desenho de experiências do tipo "CompostoCentral" (CCD), o estudo determinou as seguintes condições ótimas: uma temperatura de extração de 50°C por 90 minutos e 0,03 g/mL, com etanol:água, 75%/25% (v/v). A nanofiltração subsequente a 30 bar de pressão demonstrou um desempenho excepcional, coeficiente de rejeição para compostos fenólicos e flavonoides. O concentrado resultante, rico em oleuropeína, mostrou uma capacidade antioxidante significativa, tornando-o inestimável para aplicações nas indústrias de alimentos, cosméticos e farmacêutica.

Quanto à abordagem para a separação de polifenóis do extrato de OLE usando MMMs, foram preparadas membranas de NF usando óxido de zinco revestido por nanopartículas de polianilina (ZnO-PANI), bem como membranas de NF com nanopartículas à base de carbono (carvão ativado - CA), utilizando uma variedade de concentrações de nanopartículas através do método de inversão de fase.

No caso da membrana preenchida com ZnO-PANI, as nanopartículas foram auto- sintetizadas, caracterizadas e incorporadas na matriz de PES em diferentes cargas (0 a 0,6% em peso). ZnO-PANI foi usado para adsorver compostos fenólicos totais (TPC) do OLE em diferentes concentrações iniciais do adsorbato e diferentes níveis de pH. O modelo de Langmuir descreveu melhor a adsorção de TPC do que o modelo de Freundlich. A incorporação de ZnO- PANI melhorou significativamente as propriedades da membrana, incluindo porosidade, tamanhodo poro e hidrofilicidade, até 0,2% em peso, resultando em uma permeabilidade aprimorada. O desempenho de nanofiltração (NF) das membranas foi avaliado para rejeição de TPC em várias pressões (10-30 bar), rejeição de oleuropeína (OLP) a 30 bar e resistência ao fouling. As MMMs exibiram permeabilidade aprimorada em comparação com as membranas de PES nãopreenchidas. A membrana preenchida com 0,2% em peso de ZnO-PANI apresentou o equilíbrio ideal entre fluxo de permeado e rejeição de oleuropeína. Esses resultados sugeriram que as MMMs à base de ZnO-PANI preparadas podem separar efetivamente o TPC do OLE, alcançando100% de rejeição de OLP.

No caso da membrana preenchida com CA, as nanopartículas foram incorporadas na matriz de Psf com cargas de 0 a 0,9% em peso. Essas membranas foram caracterizadas por meio de experiências de filtração de água e OLE e outras propriedades físicas, como morfologia de superfície e porosidade por técnicas de microscopia (MEV e AFM), rugosidade de superfície e

hidrofilicidade. A eficiência das membranas preparadas na separação de TPC do OLE foi avaliada sob várias pressões. A membrana com o melhor desempenho geral, principalmente em termos de filtração de OLE, foi selecionada para investigações adicionais para otimizar variáveis operacionais (pH, temperatura e pressão) para melhorar a rejeição de TPC. As condições operacionais ideais para NF usando membranas à base de 0,3% de CA foram em torno de pH 2,7,25°C e 30 bar para a melhor rejeição de TPC. Além disso, sob condições otimizadas, essas membranas alcançaram 100% de rejeição de oleuropeína. Esses resultados sugeriram que as MMMs preparadas podem separar TPC do OLE com elevada eficiência e menor grau de colmatação.

Palavras-chave: compostos fenólicos; oleuropeína; folhas de oliveira; membranas; nanopartículas.

Abstract

Olive leaves (OL), is considered a by-product of olive tree, which is generated from the cultivation and olive oil production process. The large amount of phenolic compounds present in olive leaves has attracted the interest of researchers and many studies have reported that olive leaves provide beneficial effects such as antioxidant capacity, antihypertensive, cholesterol lowering, cardioprotective, anti-inflammatory and as a coadjuvant in the treatment of obesity.

In recent years, different studies were performed for the separation and recovery of these phenolic compounds from olive leaves extract (OLE).Within the framework of this thesis, the major emphasis was given to preparation and application of mixed matrix membranes (MMMs) for phenolic compounds recovery.

The work started with the characterization of different olive leaves samples obtained from various cultivars, collection regions, and sampling periods to analyze the variability in their total phenolic compound concentration. It was found that phenolic compounds in olive leaves changed based on the olive cultivar, collection region, and sampling period. Subsequently, the olive tree cultivar, collection region, and sampling period were fixed to minimize the effect of total phenolic compound concentration variation on the performance of the membranes used during the filtration of olive leaf extract (OLE).

In this study, phenolic compounds were effectively separated from olive leaf extract using a commercial polyethersulfone (PES) flat sheet nanofiltration (NF) membrane. Additionally, MMMs were meticulously prepared to enhance the separation process. Before all NF experiments, OLE was subjected to a preliminary ultrafiltration (UF) process to remove suspended solids and macromolecular compounds, thus allowing to reduce the fouling phenomena in the subsequent NF process.

The first approach integrates solvent extraction and membrane separation technique using a commercial polyethersulfone (PES) flat sheet nanofiltration (NF) membrane. Through careful optimization employing a Central Composite Design (CCD), the study determined the optimal parameters: an extraction temperature of 50°C for 90 min and 0.03 g/mL, with ethanol: water, 75%/25 % (v/v). Subsequent nanofiltration at 30 bar demonstrated exceptional performance,

indicating a high rejection coefficient for phenolic compounds and flavonoids. The resulting concentrate, rich in oleuropein, showed significant antioxidant capacity, making it invaluable for applications in the food, cosmetic, and pharmaceutical industries.

Regarding the approach for separating of polyphenols from OLE extract using MMMs, NF membranes using zinc oxide coated by polyaniline (ZnO-PANI) nanoparticles (NPs) , as well as NF membranes with carbon-based NPs (activated carbon - AC) ,were prepared using a range of NPs concentrations through the phase inversion method.

In the case of membrane filled with ZnO-PANI, NPs were self-synthesized, characterized, and incorporated into the PES matrix at varying loadings (0 to 0.6 wt%). ZnO-PANI was used for adsorbing TPC from OLE at different initial adsorbate concentration and different pH levels. Langmuir model described the adsorption of TPC better than Freundlich model. The incorporation of ZnO-PANI significantly enhanced membrane properties, including porosity, pore size, and hydrophilicity, up to 0.2 wt%, resulting in improved permeability. The nanofiltration (NF) performance of the membranes was evaluated for TPC rejection at various pressures (10-30 bar), oleuropein (OLP) rejection at 30 bar, and fouling resistance. MMMs exhibited enhanced permeability compared to unfilled PES membranes. The membrane filled with 0.2 wt% ZnO-PANI displayed the optimal balance between permeate flux and oleuropein rejection. These findings suggested that the prepared ZnO-PANI-based MMMs can effectively separate TPC from OLE, achieving 100% rejection of OLP.

In the case of membrane filled with AC, NPs were incorporated in Psf matrix with loadings from 0 to 0.9 wt %. These membranes were characterized by water and OLE filtration experiments and other physiological properties, such as surface and pore morphology by microscopy techniques (SEM and AFM), surface roughness and hydrophilicity. The efficiency of prepared membranes in separating of TPC from OLE was evaluated under various pressures. The membrane with the best overall performance mainly in terms of OLE filtration was selected for additional investigations into optimizing operational variables (pH, temperature, and pressure) to improve the rejection of TPC. The optimal operating conditions for NF using 0.3% AC-based membranes were around pH 2.7, 25°C and 30 bar for the best TPC rejection. Moreover, under optimized conditions, these membranes achieved 100% oleuropein rejection. These findings

suggested that the prepared MMMs can effectively separate TPC from OLE with minimalfouling.

Overall, this work demonstrates the potential for the separation and purification of bioactive compounds from OLE using commercial membranes and mixed matrix membranes. The recovery and valorization of high added value phenolic compounds can contribute to health, pharmaceuticals, cosmetics, environmental sustainability, economic growth, research, food preservation, and waste reduction.

Keywords: phenolic compounds; oleuropein; olive leaves; membranes; nanoparticles.

Table of contents

List of Tables

List of Figures

CHAPTER 1 :Introduction

1.1 Background

The olive tree (*Olea europaea L.*) is one of the oldest known cultivated plants. It is usually native to Mediterranean countries and its cultivation has spread globally during the past two decades due to the healthiness attributed to the consumption of olive oil. More than 8 million ha of olive trees are cultivated worldwide; almost 98% of them are in the Mediterranean basin (Peralbo-Molina and Luque de Castro, 2013).The estimated total world production of olive oil in 2020/2021 accounts for 3,034,000 tons, 93.4% of which is produced by European International Olive Council (IOC) member countries and its main destination is human consumption (IOC, 2022). In addition to olive oil, olive trees are also cultivated for table olive production. Table olives and olive oil are two of the most representative foods of the traditional Mediterranean diet (Obied et al., 2012).

By-products derived from olive trees and olive oil extractions are generally known as "olive by-products" (Molina-Alcaide and Yáñez-Ruiz, 2008). A high number of by-products and residues derived from both olive tree cultivation and the olive processing industry are obtained yearly; most of them have no practical applications. Olive leaves, one of these by-products, canbe found in large amounts in olive oil industries. Leaves represent 10% of the weight of olives collected for oil extraction (Herrero et al., 2011). Furthermore, they also accumulate in large volumes on farms during the pruning of the trees (Govaris et al., 2010). It has been estimated thatpruning produces 25 kg of by-products (twigs and leaves) per tree annually.

A typical olive tree pruning lot includes leaves (approximately 25% by weight), thin branches (approximately 50% by weight), and thick branches or wood (approximately 25% by weight), although the proportions may vary depending on culture conditions, tree age, productionand/or local pruning practice. In the Mediterranean region, residual biomass from olive tree pruning yield ranges from 1 to 5 and from 4 to 11 t/ha, for Spanish and Italian orchards, respectively (Spinelli and Picchi, 2010), making of residues a huge, cheap, and unexploited source of energy or chemicals. Olive leaves are usually burned or ground together with the remainder of the olive tree pruning by-products, i.e., branches (Romero-García et al., 2014) and are then directly thrown away as by-products, potentially causing environmental damage and wasting a resource (Xie et al., 2015).

Thus, this residue is a very abundant vegetable material with increasing cost for producers due to their removal, storage and elimination. Nevertheless, olive leaves are a potential source of various chemicals that can be transformed into products with significant added value (Quirantes-Piné et al., 2012; Rahmanian et al., 2015).

The interest of olive leaves, as a matrix rich in antioxidants, have increase with the aim to be further use in food and food supplements. In food industry, there is an increasing interest in producing functional foods for their health beneficial. The incorporation of such extracts in food industry may contribute to the health benefit of the consumers significantly and also to prolong the shelf life of food products (Bouaziz, Fki, Jemai, Ayadi, & Sayadi, 2008). Enrichment of oils with olive leaves, olive leaf extract as well as with the main secoiridoid compound (oleuropein) has been reported in literature (Erbay and Icier, 2010). Moreover, the enrichment of refined olive and refined olive-pomace oils with oleuropein, oleuropein aglycone and hydroxytyrosol rich extracts has proven to inhibit the deterioration of oil rancidity by improving stability (Bouaziz et al., 2008).

Olive leaf extracts have been recently marketed as dietary product (Briante et al., 2002). Commercial products in the form of herbal teas or food supplements are available all over the world, as complete dried leaves, powder, extracts or tablets (Tsimidou and Papoti, 2010). It has been shown that encapsulation of olive leaf extracts with the aid of β-cyclodextrin increases the aqueous solubility of the polyphenolic residue from olive leaf (Mourtzinos et al., 2007).

Therefore, research has been directed toward exploring the potential of agro-industrial residues as valuable resources for biorefineries (see **Fig.1.1**), given their significance in both environmental impact and economic value, highlighting the need for valorization of wasted by- products that can yield similar or even higher contents of bioactive compounds than the final product (Ayala-Zavala et al., 2011). As a result, these bioactive compounds can be used as an important source to produce nutraceuticals or to be included in functional food thanks to their potential health benefits.
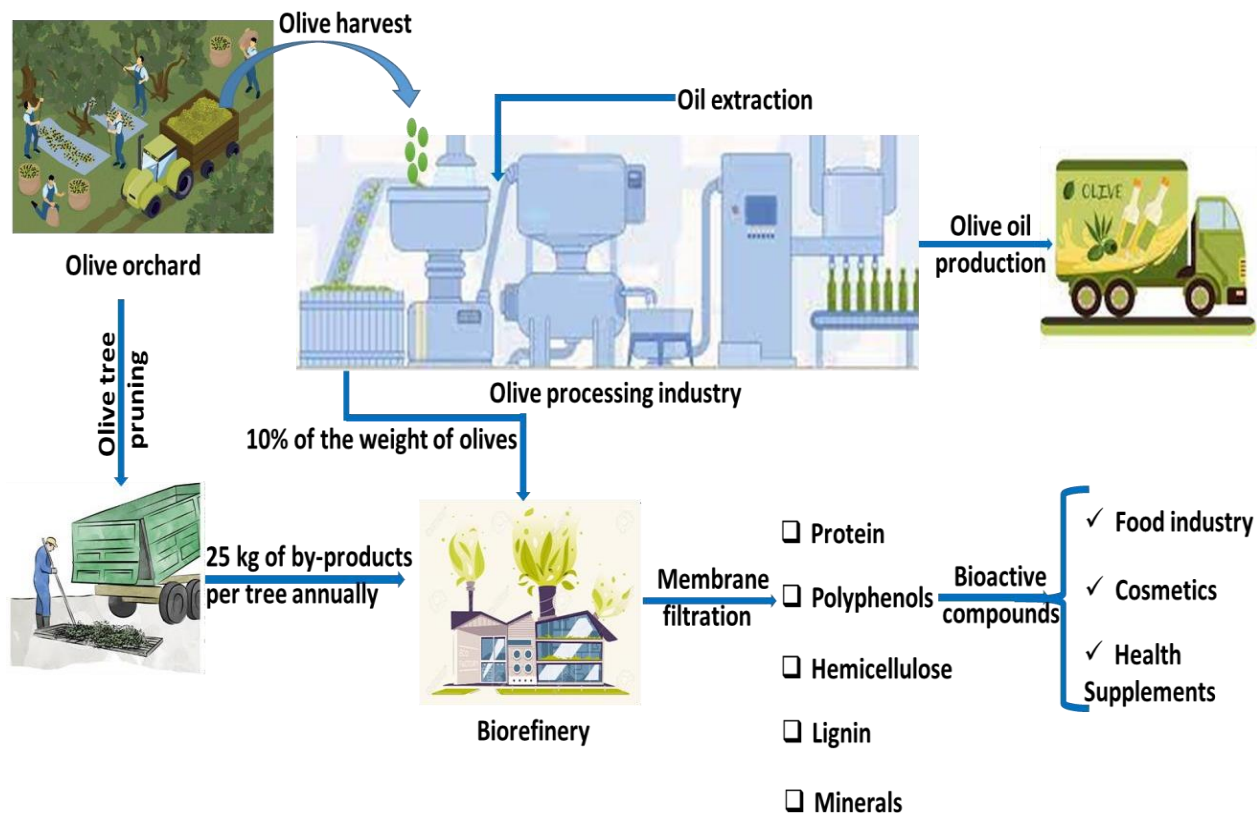
Figure 1.1: Valorization of olive leaf by-product.

1.2 Motivation

The motivation behind this work can be attributed to several factors:

1. Waste Utilization: Olive leaf waste generated from olive oil production can be a significant environmental concern. By utilizing membrane filtration, it is possible to extract useful compounds from these leaves, reducing waste and making the olive oil production process more sustainable.

2. Phytochemical Extraction: Olive leaves contain various phytochemicals, including polyphenols, flavonoids, and triterpenoids, which have antioxidant, anti-inflammatory, and antimicrobial properties. Membrane filtration helps extract and concentrate these valuable compounds for medicinal or nutritional applications.

3. Health Benefits: Compounds extracted from olive leaves have been associated withseveral health benefits, such as reducing blood pressure, improving cardiovascular health, and

enhancing the immune system. Membrane filtration allows for the concentration of these compounds, making it easier to incorporate them into dietary supplements or functional foods.

4. Cosmetic and Pharmaceutical Applications: Extracts from olive leaves are used in cosmetic and pharmaceutical products due to their skin-nourishing and antimicrobial properties. Membrane filtration enables the production of high-quality extracts for these applications.

5. Research and Development: Scientists and researchers often use membrane filtration techniques to isolate specific compounds from olive leaves for research purposes. Understanding the chemical composition of olive leaves can lead to the development of new drugs, supplements, or technologies.

In summary, the motivation behind membrane filtration of olive leaves extract stems from the desire to harness the beneficial compounds present in the leaves for various applications, ranging from health and wellness products to environmental sustainability initiatives and scientific research.

1.3 Research gap

To enhance the functional and nutritional properties of natural extracts rich in polyphenols, concentration methods must be applied, thus boosting the added value of the final product. Many conventional methods were used for extract concentration, including adsorption, chromatography, electrophoresis, vacuum distillation and freeze–drying. However, these methods impose some constraints including high operational and energy costs or the use of high temperatures that can degrade thermosensitive compounds such as phenolic species (Mello et al., 2010). Membrane filtration is considered as a simple and effective separation tool. This process offers several advantages, namely the isolation of polyphenols from natural extracts without significant variations in pH and temperature, and low chemical and energy consumption (Humpert et al., 2016; Kevlich et al., 2017).

Despite the various studies on the application of membranes (both polymeric and ceramic) in the recovery of polyphenols from natural extract, some constraints such as considerable reduction in permeate flux, molecular weight cut-off (MWCO) and separation efficiency are crucial for their commercial use. In this context, the use of morphologically and physiochemically modified

membranes (MMMs) for the separation of phenolic compounds from olive leaf extract can be an interesting subject of investigation.

However, to best of our knowledge, no work has been done on the use of MMMs for filtration of olive leaf extract, which justifies the need of this work for bioactive compounds recovery from olive leaves. Moreover, the study of the operating conditions during the filtration process can be considered another interesting aspect, as these have a determining effect on the separation performance (Arkell et al., 2014; Wallberg and Jönsson, 2006). Therefore, in this workthese aspects are focused in order to develop an efficient and economical separation process for the recovery of the high added value compounds from olive leaf extract.

1.4 Objectives

The main objective of the thesis is to separate high added value phenolic compounds from olive leaf extract using a system of ultrafiltration (UF) and nanofiltration (NF) commercial and modified membranes using suitable nanoparticles (see **Fig. 1.2**). The modification of membranes was intended to improve their performance in terms of permeate flux, membrane resistance to fouling and separation of phenolic compounds, in particular oleuropein. In order to achieve this general objective of the thesis, specific objectives are required, which are also shown in **Fig. 1.2**.

- Sampling and physicochemical characterization of olive leaf extract ;
- Preliminary selection of extraction solvents ;
- Optimization of phenolic compounds extraction from olive leaves ;
- Assessment of the application of a commercial membrane for the separation of phenolic compounds from olive leaf extract;
- Preparation and characterization of different MMMs;
- Assessment of the prepared MMMs application for the separation of phenolic compounds from olive leaf extract;
- Optimization of the NF system to improve filtration and separation efficiency.

1.5 Thesis outline

This thesis is divided into eight chapters to allow a better understanding of work presented and to improve the readability of the document. The first chapter provides a detailed introduction

of the work, the motivation behind this study and the main objectives achieved throughout the development of this research. Then, the 2nd chapter is devoted to a brief literature review of topics required for understanding of the work. It includes review of literature regarding olive leaves biomass and its composition, phenolic compounds, oleuropein and its benefits, membrane technology, preparation of mixed matrix membranes using nanoparticles (NPs) and their applications.

Further, chapters from 3 to 7 covers the experimental work, key observation of the work performed as part of this thesis and include various research articles published in peer-reviewed journals. In this regards, Chapter 3 deals with the methods used for sampling and characterization of olive leaves extract to analyze its physiochemical composition. The study was performed to avoid any interference, which can be caused by difference in composition, during filtration of this olive leaves extract.

Followed by Chapter 4, which briefly describes the selection of the best solvent for the extraction of phenolic compounds from olive leaves. The optimization of extraction conditions were also performed to improve polyphenols yield. Further, filtration of olive leaf extract using commercial PES membrane is discussed. Following chapter 5 deals with the preparation of ZnO-PANI nanoparticles and their characterization. Further, the adsorption tests towards phenolic compounds using these nanoparticles is discussed. In addition, this chapter addresses the preparation of NF mixed matrix membranes with different ZnO-PANI nanoparticles content. Further, characterization of different prepared membranes is discussed.

Next chapter address the application of NF ZnO-PANI membranes (prepared in previous chapter) for olive leaves extract filtration in dead-end mode and the analysis of their performance for oleuropein rejection is discussed.

Chapter 7 deals with the preparation of NF mixed matrix membranes with different carbon-based nanoparticles and their application. In this chapter the methods for fabrication and characterization of prepared NF membranes were included. Followed by the assessment of applicability of the prepared NF membranes for filtration of olive leaves extract (obtained from UF process). Further, chapter 7 addresses the study of optimization of operating variables during the NF process to improve the filtration and separation performance.

Lastly, chapter 8 is dedicated to the main conclusions obtained from the work performed in this thesis, along with possibilities for future work.
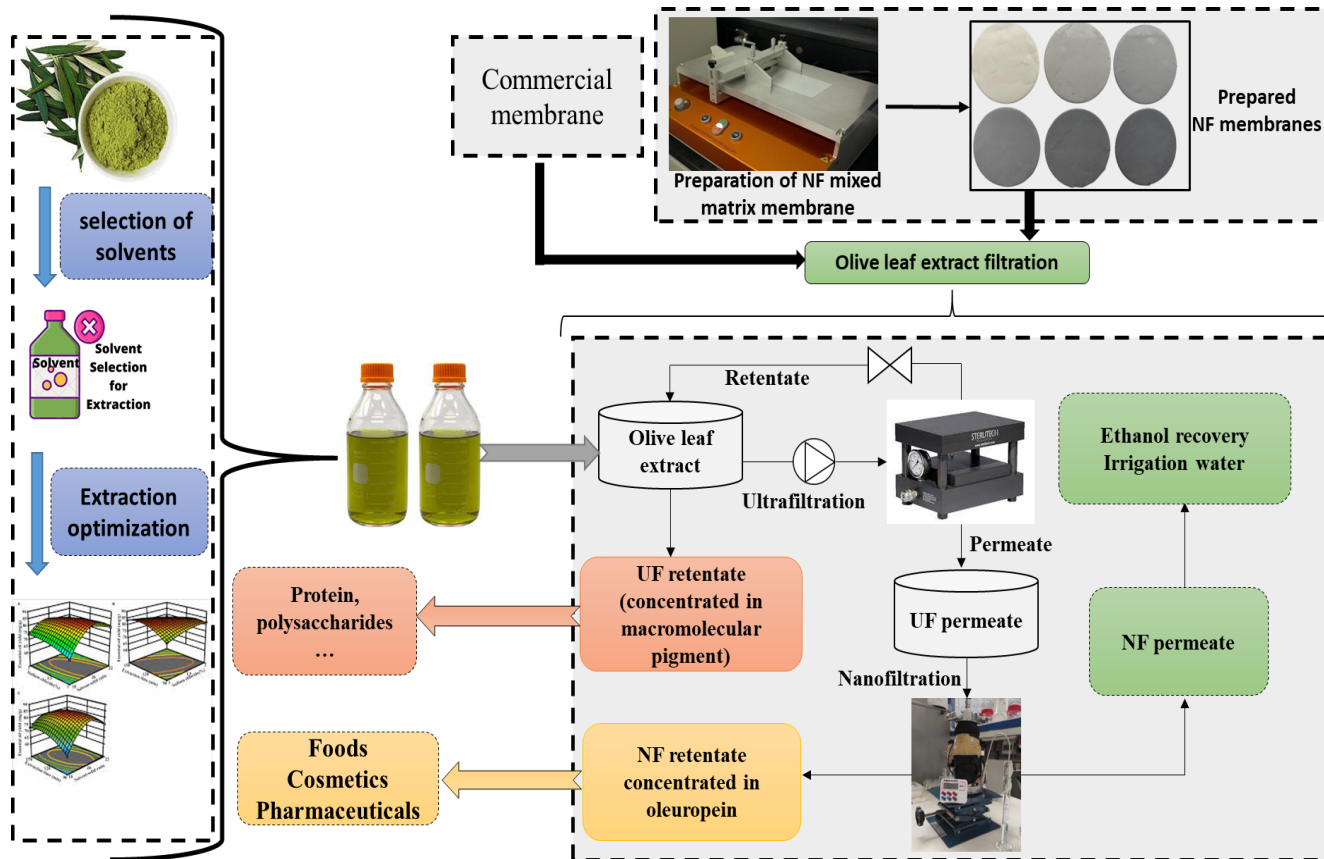
Figure 1.2: Overview of the work performed in the framework of this thesis.

CHAPTER 2: State of the art

2.1 Olive tree

Olive tree (*Olea europaea L.*), a member of the Oleaceae (Gilani et al., 2010), is a drought-tolerant plant essentially native to the Mediterranean climate (Mannina et al., 2010). It is universally planted in tropical and subtropical regions (Ray et al., 2015), predominantly in Greece, Italy, Spain, Australia, Portugal, France, Cyprus, Israel, Jordan, USA, Morocco, Turkey, and Tunisia (Caballero et al., 2003). The Mediterranean region, representing above 90% of the cultivated area, is estimated to be above 11 million hectares in 2017 (Zipori et al., 2020).

2.2 Olive leaves

2.2.1 Huge biomass

The leaves of the olive tree are within easy reach either from the olive orchard or from the residues remained after agricultural (Rahmanian et al., 2015) and industrial by-products (Contreras et al., 2020). The olive mill leaves constitute a relatively sizable portion, in the range of 4–7% (Contreras et al., 2020), up to 10% of overall weight of processing olives (Abaza et al., 2015) and account for almost 5% of overall yield from olive oil by-products (Lama-Muñoz et al., 2020) (**Fig.2.1 a**). During the horticultural system, a significant proportion of leaf residue is also generated. In the course of pruning (**Fig.2.1 b and c**), depending on variations in geography, horticultural routine, and tree lifetime, the amount of leaf by-products roughly accounts for 25% of total weight of pruned residue (Romero-García et al., 2014). In addition, during the harvest, leaves can be picked with the olives (**Fig. 2.1 d**).

The increment of these residues represents a major problem through its adverse effect on environmental sustainability, as a large proportion of leftovers is underexploited and/or inadequately disposed of, e.g., through incineration (Talhaoui et al., 2015a). There is an increased awareness that this underutilised biomass could be regarded as a valuable/health-promoting resource, if properly exploited, with great market potential in the food and dietary system.

Figure 2.1: Olive leaves, a byproduct of the olive oil industry, generated in large quantities during the harvest (a and b), in oil mills (c), and after pruning olive trees (d).

2.2.2. Composition of olive leaves

The fresh leaves of the olive tree are characterized by a dry matter content of around 50%. **Table 2.1** shows the overall chemical composition of olive leaves according to various authors. Several factors (e.g., sampling period, cultivar, age of olive tree, and climatic changes) affect olive leaf composition (Souilem et al., 2017).The leaves are particularly rich in carbohydrates. The organic matter consists of proteins, lipids, phenolic monomers and polymers (such as tannins), and mainly polysaccharides (such as cellulose, hemicelluloses).

Table 2.1: Overall chemical composition of olive leaves (expressed in g per 100 g) according to several authors.

Composition (in %)	Souilem et al., 2017	Boudhrioua et al., 2009	Erbay and Icier, 2009	Martin-Garcia et al., 2006	Garcia-Gomez et al., 2003
Water	49.8 a	46,2-49,7 a	49,8 a	41,4 a	nd
Proteins	7.6 a	5,0-7,6 a	5,4 a	7,0 b	nd
Lipids	1.1 a	1,0-1,3 a	6,5 a	3,2 b	6,2 b
Minerals	4.5 a	2,8-4,4 a	3,6 a	16,2 b	26,6 b
Carbohydrates	37.1 a	37,1-42,5 a	27,5 a	nd	nd
Raw fibers	nd	nd	7,0 a	nd	nd
Cellulose	nd	nd	nd	nd	19,3 b
Hemicellulose	nd	nd	nd	nd	25,4 b
Lignin	nd	nd	nd	nd	30,4 b
Total polyphenols	nd	1,3-2,3 b	nd	2,5 b	nd
Soluble tannins	nd	nd	nd	nd	nd
Condensed tannins	nd	nd	nd	0,8 b	nd

[a] Results reported in fresh olive leaves.

[b] Results reported in dry olive leaves.
nd : not determined

The protein content is low in olive leaves. **Table 2.2** presents the composition of olive leaves in amino acids, which is particularly diverse.

Table 2.2: Amino acid composition of fresh olive leaves (expressed in mg/100 g dry matter) (according to Altop et al., 2018).

Amino acid	Concentration
Aspartic acid	511.04
Glutamic acid	769.72
Serine	182.67
Glycine	328.90
Histidine	32.73
Arginine	116.68
Threorine	197.45
Alanine	405.45
Proline	441.35
Tyrosine	269.25
Valine	433.96
Methionine	69.69
Isoleucine	409.68
Leucine	622.43
Phenylalanine	380.11
Lysine	206.42
Tryptophan	158.38
Essential amino acids	2510.85
Non-essential amino acids	3025.06
Total amino acids (without cysteine)	5535.91

The mineral composition of olive leaves is presented in **Table 2.3**. The most abundant mineral in the leaves is iron, with a concentration between 68.24 - 88.95 g/kg of dry matter.

Table 2.3: Mineral composition of olive leaves (expressed in grams per kilogram of dry matter) (according to Pasković et al., 2020).

Minerals	Concentration
Calcium (Ca)	11.45 - 25.07
Phosphorus (P)	1.36 - 1.67
Manganese (Mg)	8.00 - 10.14
Potassium (K)	5.28 - 7.85
Iron (Fe)	68.24 - 88.95
Copper (Cu)	11.09 - 16.19
Zinc (Zn)	22.17 - 25.85
Magnesium (Mn)	46.74 - 67.68

2.2.3. Phenolic compounds in olive leaves

2.2.3.1 Generalities on phenolic compounds

a. Definition and localization of phenolic compounds

Phenolic compound are a large class of secondary natural metabolites. They constitute the most important group of phytochemical organic compounds in the plant kingdom with around 8000 phenolic structures (Alara et al., 2021). Their structure comprises an aromatic ring, containing one or more hydroxyl substituents (**Fig.2.2**). They can range from simple phenolic molecules to highly polymerized compounds. The most phenolic compounds occur naturally as conjugates with mono- and polysaccharides, associated with one or more phenolic groups. In addition, they also can be linked to esters and methyl esters (Vuolo et al., 2019).
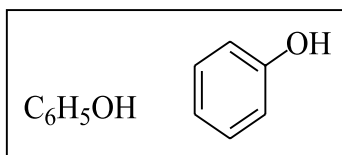
Figure 2.2: Structure and chemical formula of simple phenol.

Phenolic compounds are primarily located in soluble form within the vacuoles. They can also accumulate in plant cell walls, such as lignin (a heteropolymer of coniferyl, p-coumaryl, and sinapyl alcohols) or certain flavonoids (Robards et al., 1999; Macheix et al., 2003).

b. Classification of phenolic compounds

The term phenolics covers a very large and diverse group of chemical compounds. These compounds can be classified in a number of ways.

Harborne and Simmonds (1964) classified phenolic compounds into groups based on the number of carbons in the molecule (see **Table 2.4**).

Table 2.4: Classification of phenolic compounds (according to Harborne and Simmonds, 1964).

Structure	Class
C6	Simple phenolics
C6-C1	Phenolic acids and related compounds
C6-C2	Acetophenones and phenylacetic acids
C6-C3	Cinnamic acids, cinnamyl aldehydes, cinnamyl alcohols, coumarins, isocoumarins and chromones
C15	Chalcones, aurones, dihydrochalcones, flavans, flavones, flavanones, flavanonols, anthocyanidins, anthocyanins
C30	Biflavonyls
C6-C1-C6, C6-C2-C6	Benzophenones, xanthones, stilbenes
C6, C10, C14	Quinones
C18	Betacyanins
Lignans, neolignans	Dimers or oligomers
Lignin	Polymers
Tannins	Oligomers or polymers
Phlobaphenes	Polymers

c. Biological activities of phenolic compounds

Natural plants represent an important source of phenolic compounds that are useful in a wide range of applications, especially those with biological activities (Zhang et el., 2022). The biological activities relating to polyphenols are relatively diverse. It appears that each chemical class of polyphenols is used for its distinct benefits (Martin and Andriantsitohaina, 2002). It is worth knowing that phenolic compounds play an essential role in natural antioxidant, antimicrobial, and anti-inflammatory effects, as well as in the treatment of diseases such as obesity, cancer, and diabetes (Zhang et el., 2022).

Phenolic compounds are scavengers of free radicals, which are harmful products of aerobic metabolism leading to oxidative stress in the organism. Multiple in-vitro, in-vivo, and epidemiological studies have shown that polyphenols are of great interest in the prophylaxis and treatment of cardiovascular and neurological diseases, cancer, and aging-related disorders, mainly due to their remarkable antioxidant activity (Yahfouf et el., 2018, Zhang et al., 2015). Theclaimed anti-inflammatory activity also appears to be related to antioxidant power.

Complementarily, the metal chelation ability is another protective effect of polyphenols which is especially noticeable against the toxicity caused by heavy metals. Compounds such as proanthocyanins, curcumin, resveratrol, caffeic acid, or oleuropein, have been extensively investigated, and their structures have been the basis to design new drugs with enhanced activity for the treatment of cancers and microbial infections (Vidal-Casanella et al., 2021). Recently, dozens of studies have been published regarding the possible use of polyphenols to treat SARS-CoV-2 based on previous evidence on the phenolic activity against different viruses(Montenegro-Landívar et al., 2021). The use of phenolic compounds for pharmaceutical applications is not new. Oriental traditional medicine is a good example, with herbs, plants and spices rich in polyphenols acting as active principles. The food industry has also incorporated polyphenols as natural additives in food products, cosmetics, and packaging (Chemat et al., 2019,Santhosh et al., 2021).In addition phenolic compounds posses others   biological activities (see **Fig 2.3**).
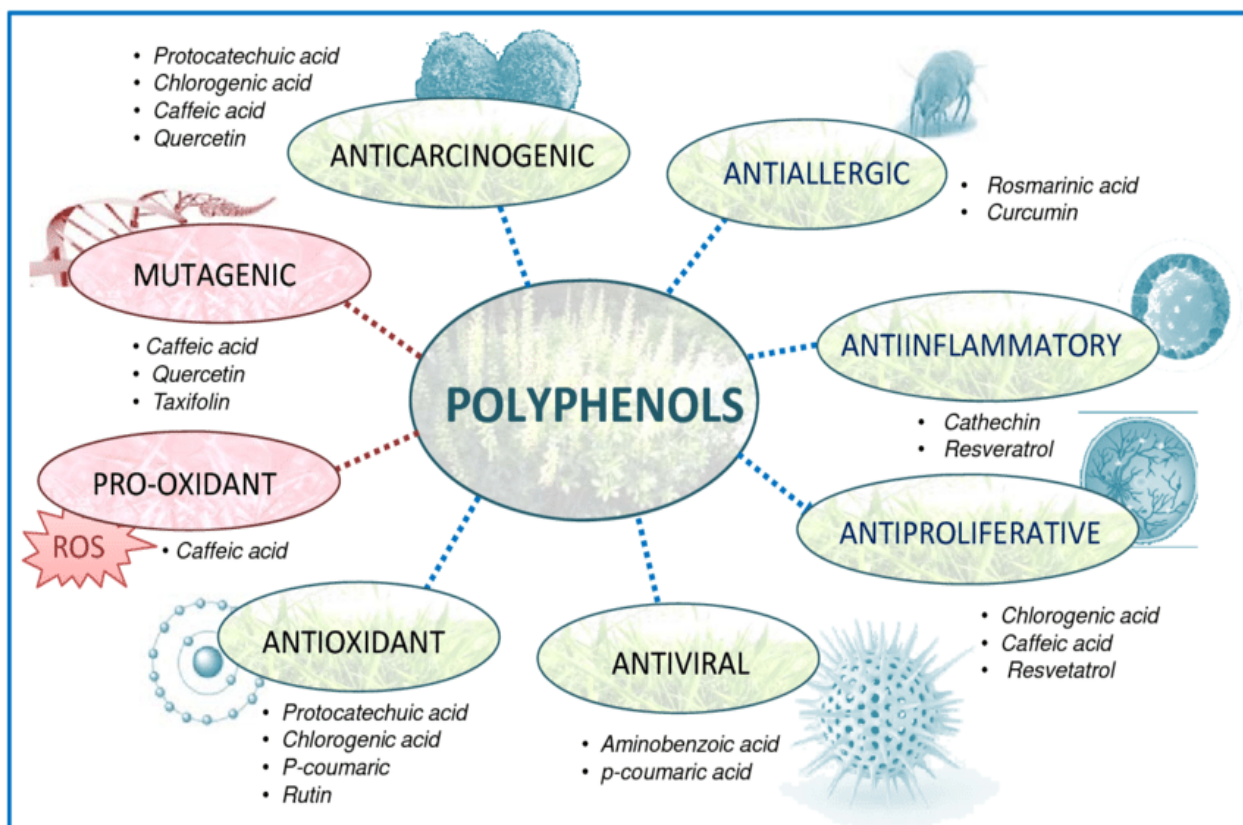
Figure 2.3: Biological effects of polyphenols.

2.2.3.2. Determination of phenolic compounds in olive leaves

a. Extraction of phenolic compounds from olive leaves

Extraction is one of the most important steps in sample pre-treatment for polyphenolsanalysis. Generally, it is a separation process where the distribution of the analyte (in this case, a phenolic compound) between two immiscible phases is made in order to arrive at the appropriate distribution coefficient (Talhaoui et al., 2015a). A great number of extractions procedures have been developed to determine phenolic compounds fraction in olive leaves.

The most commonly extraction system used has been the solid–liquid extraction (SLE) by maceration of the olive leaves in a solvent. Common extraction solvents used for olive leaves are methanol, ethanol, acetone, ethyl acetate, and diethyl ether, as well as aqueous alcohol mixtures as the usual solvents for extraction of polyphenols (Altıok et al., 2008; Le Floch et al., 1998; Talhaoui et al., 2014).

Nowadays, the application of SLE is slowly starting to decline because of the big necessity to low the costs by reducing solvent consumption, and to accelerate the extraction process. Thus, other modern extraction and isolation techniques have been used as alternative. These modern techniques include: microwave-assisted extraction (MAE), pressurized liquid extraction (PLE), supercritical fluid extraction (SFE), and ultrasound-assisted extraction (UAE) (**Table 2.5**).

The MAE has gained much attention in plants and particularly in olive leaves analytical chemistry for its major advantages including short extraction time, low-energy requirement, high extraction efficiency, and minimum degradation of target components (Capote et al., 2008; Taamalli et al., 2012b).

The PLE, is a technique which uses conventional solvents and performs a fully automated extraction under constant pressure and various controllable parameters like temperature, static extraction time, extraction cycles etc. (Xynos et al., 2014). The use of organic solvents at high pressures and temperatures above their normal boiling point enables to achieve fast and efficient extraction of the analytes from solid matrices. The PLE technique limits the use of organic solvents, hereby making possible the use of solvent allowed for food uses such as water and

ethanol, while obtaining higher extraction yields and faster extraction processes (Quirantes-Piné et al., 2012).

The SFE is more environmentally friendly, avoiding the use of large amounts of toxic solvents, as well as being rapid, automatable. The intrinsic low viscosity and high diffusivity of supercritical CO_2 has permitted faster and more efficient separation, and relatively clean extracts. In addition, the absence of light and air during extraction reduces the degradation of analytes that occur in traditional extraction techniques (Lamuela-Raventós et al., 2014).

The UAE has been proved to be drastically faster and more efficient than conventional extraction in olive leaves (Japón-Luján et al., 2006a). This is because this method is a powerful aid in accelerating various steps of the analytical process. In fact, it facilitates and speeds up operations such as the extraction, the homogenization, and various others (Garcia-Salas et al., 2010) (**Table 2.5**).

The comparison between those sophisticated techniques applied on olive leaves, showed that MAE is the auxiliary energy that requires shorter extraction time, meanwhile UAE needs less solvent than the others. SPE shows intermediate values in extraction time as well as in the percentage of ethanol in the solvent mixture (Japón-Luján and Luque de Castro, 2006). On the other hand, Taamalli et al. (2012a) reported that each technique was more adequate than others for the extraction of each particular class of compounds. In fact, MAE and conventional extraction showed to be more efficient for extracting more polar compounds such as oleuropein derivatives, apigenin rutinoside and luteolin glucoside. However, SFE was the best extraction procedure for apigenin and diosmetin.

The analysis of phenolic compounds in olive leaves was first elaborated by spectrophotometric techniques; the most used method was Folin-Ciocalteu for the determination of total phenolic compounds. However, the identification of single phenolic compounds presentin olive leaves is only possible performing a previous separation of the compounds present in the samples (Gómez-Caravaca et al., 2014). The use of gas chromatography (GC) and nuclearmagnetic resonance (NMR) have been reported as possible techniques for phenolics characterization in olive leaves (Briante et al., 2002). NMR spectroscopy has found interesting application in the analysis of complex mixtures without previous separation of the individual components in the mixture, but it has been increasingly recognized for its non- invasiveness,

rapidity and sensitivity to a wide range of compounds in one single measurement (Christophoridou and Dais, 2009). GC although needs reagents derivatizing as samples pre- treatments, it has the advantages of lower detection limits and better separations (Saitta et al., 2010).

Nevertheless, high/ultra performance liquid chromatography (HPLC/UPLC) coupled to diode-array detection (DAD) and/or coupled to mass spectrometry (MS) is the most used to quantify and characterize phenolic compounds olive leaves (**Table 2.5**). This powerful analytical technique provides shorter times of analysis, acquires a high degree of versatility not found in other chromatographic systems and it has the ability to easily separate a wide variety of chemical mixtures.

Table 2.5: Main extraction systems and analytical methods used to determine phenolic compounds in olive leaf.

Extraction system	Analytical technique	Olive leaf cultivar	Phenolic compounds described	References
Solid–liquid extraction with different combinations of solvents (acetone, methanol, ethanol, dichloromethane, ethyl acetate, petroleum ether, dichloromethane) and/or water	HPLC-DAD	5 Spanish cultivars.	oleuropein, hydroxytyrosol, luteolin-7-glucoside,apigenin-7-glucoside, verbascoside, tyrosol, vanillic acid, diosmetin-7-glucoside, caffeic acid, luteolin, rutin, diosmetin, vanillin, catechin	(Benavente-garcía et al., 2000)
	HPLC-DAD	14 French cultivars	rutin, verbascoside, luteolin 7-glucoside, apigenin 7-glucoside, oleuropein, oleuroside, coumarin	(Savournin et al., 2001)
	Gas Chromatography detector and Flame Ionization Detector (GC-FIL)	'Moraiolo	tyrosol, hydroxytyrosol, syringic acid, gallic acid, ferulic acid, oleuropein, oleuropein aglycon	(Briante et al., 2002b)
	HPLC-DAD-MS	10 Greek cultivars	oleuropein, tyrosol, hydroxytyrosol, elenolic acid	(Agalias et al., 2005)
	HPLC-DAD	23 Portuguese cultivars	luteolin 7,4′-O-diglucoside; luteolin 7-O-glucoside; rutin; apigenin 7-O-rutinoside, apigenin 7-O-glucoside; luteolin 4´-O-glucoside; luteolin; apigenin; diosmetin	(Meirinhos et al., 2005)
	HPLC-DAD-MS	'Arbequina'	oleuroepin, luteolin-7-O-glucoside, verbascoside,luteolin-4-O-glucoside, hesperidin	(Malik and Bradford, 2006)
	HPLC- APCI-MS	11 Italian cultivars	hydroxytyrosol, rutin, verbascoside, luteolin-7-glucoside, luteolin-4′-o-glucoside, oleuropein, oleuropein aglycon, ligstroside aglycon	(Silva et al., 2006)
	NMR and HPLC-DAD	'Manaki'	secologanoside, oleuropein, oleoside dimethyl-ester, 6′-e-p-coumaroyl-secologanoside, 6′-O-[(2e)-2,6-dimethyl-8-hydroxy- 2-octenoyloxy] secologanoside	(Karioti et al., 2006)
	HPLC-DAD	'Koroneiki'	luteolin diglucoside, rutin, luteolin glucoside, luteolin rutinoside, apigenin rutinoside, luteolin glucoside, oleuropein	(Mylonaki et al., 2008)

Table 2.5: Main extraction systems and analytical methods used to determine phenolic compounds in olive leaf. (Continuation)

HPLC-DAD	Not cited	oleuropein, verbascoside, luteolin-7-O-glucoside, luteolin-4-o-glucoside	(Malik and Bradford, 2008)
HPLC-DAD-MS	11 Greek cultivars and 'Picual' 'Frantoio	oleuropein, luteolin 7-O-glucoside, luteolin, 4´-O-glucoside, luteolin, luteolin glucosides, verbascoside.	(Papoti & Tsimidou, 2009)
HPLC-DAD	'Picual'	oleuropein, tyrosol, hydroxytyrosol	(Ortega-García, Blanco, Peinado, & Peragón, 2009)
HPLC –DAD	Not cited	caffeic acid, vanillin, rutin, oleuropein, catechin	(Lee et al., 2009)
HPLC-MS-ESI	'Picholine'	oleuropein, oleuroside, ligstroside, verbascoside and isomers, luteolin-7-o-glucoside, luteolin-glucoside and isomers, oleuropein, oleuroside, ligstroside, quercetin, diosmetin aglycon and isomers	(Laguerre et al., 2009)
HPLC -DAD	'Picual','Verdial', 'Arbequina', 'Frantoio	hydroxytyrosol, tyrosol, oleuropein	(Ortega-García & Peragón, 2010)
HPLC-MS	'Koroneiki', 'Megaritiki' 'Kalamon'	secologanoside, dimethyloleuropein, oleuropein diglucoside, luteolin-7-o-glucoside, rutin, oleuropein, oleuroside, quercetin, ligstroside, verbascoside	(Kiritsakis et al., 2010)
HPLC-DAD-MS	11 Greek cultivars and 'Picual', 'Frantoio'	hydroxytyrosol glucoside, hydroxytyrosol, verbascoside, luteolin 7-O-glucoside, luteolin 4-O-glucoside, oleuropein, oleuropein derivative, luteolin	(Goulas et al., 2010)
HPLC-DAD	Not cited	hydroxytyrosol, tyrosol, luteolin-7-O-glucoside, verbascoside, apigenin-7-O-glucoside, oleuropein	(Hayes at al., 2011)
HPLC and Mid-Infrared Spectroscopy.	Six Tunisian cultivars	oleuropein	(Aouidi et al., 2012)
HPLC-DAD	Six Italien cultivars	Catechin, rutin, verbascoside, luteolin-7-glucoside, luteolin-7-rutinoside, luteolin-3-O-glucoside, luteolin-4-o-glucoside, luteolin, diosmetin-7-glucoside, diosmetin, apigenin-7-rutinoside, apigenin-7-glucoside, oleuropein.	(Scognamiglio et al., 2012)
HPLC-DAD-	'Kalamon'	oleuropeosides (oleuropein and verbascoside), flavones (luteolin, apigenin-7-	(Botsoglou at

Table 2.5: Main extraction systems and analytical methods used to determine phenolic compounds in olive leaf. (Continuation)

	ESI-TOF- MS		o-glucoside, luteolin-7-O-glucoside and luteolin-4-O-glucoside) and flavonols (rutin)	al., 2013)
	HPLC-DAD-ESI-TOF- MS	'Sikitita', 'Arbequina', 'Picual'	oleoside,hydroxytyrosol-hexose and isomers, secologanoside and isomers,tyrosol glucoside, elenolic acid glucoside and isomers, oleuropein aglycon, luteolin diglucoside, luteolin glucoside, demethyloleuropein, rutin, luteolin rutinoside, luteolin glucoside and isomers, verbascoside, apigenin rutinoside, oleuropein diglucoside and isomers, chrysoeriol-7-O-glucoside, methoxyoleuropein and isomers, oleuropein and isomers, oleuroside, ligstroside, luteolin	(Talhaoui et al., 2014)
	HPLC-DAD-ESI-TOF- MS	'Arbosana', 'Arbequina', 'Picual' 'Sikitita', 'Changlot Real', 'Koroneiki	oleoside,hydroxytyrosol-hexose and isomers, secologanoside and isomers,tyrosol glucoside, elenolic acid glucoside and isomers, oleuropein aglycon, luteolin diglucoside, luteolin glucoside, demethyloleuropein, rutin, luteolin rutinoside, luteolin glucoside and isomers, apigenin rutinoside, oleuropein diglucoside and isomers, chrysoeriol-7-O-glucoside, methoxyoleuropein and isomers, oleuropein and isomers, oleuroside, ligstroside, luteolin.	(Talhaoui et al., 2015b)
	HPLC-DAD-MS	'Chetoui', 'Chemchali'	six hydroxybenzoic acids (gallic, protocatechuic, 4-hydroxybenzoic, 3-hydroxybenzoic, vanillic, cinnamic acids), eight hydroxycinnamic acids (chlorogenic, caffeic, ferulic, p-, m- and o-coumaric, cinnamic and rosmarinic acids), phenolic alcohol (hydroxy- tyrosol), three flavonoids (catechin, luteolin and apigenin), phenolic acids (hydroxyphenylacetic and phenylacetic acids), one secoiridoid (oleuropein	(Brahmi et al., 2014)
Microwave-assisted extraction (MAE)	HPLC- Triple quadrupole mass detector (QQQ)-MS	'Picual'	hydroxytyrosol, verbascoside, luteolin-7-glucoside, apigenin-7-glucoside, oleuropein, luteolin, apigenin, diosmetin	(Capote et al., 2008)
	HPLC-DAD-MS	'Picual', 'Arbequina', 'Lechín'	verbascoside, luteolin-7-glucoside,apigenin-7-glucoside, oleuropein	(Japón-Luján and Luque de Castro, 2008)
	HPLC ESI-TOF-MS and ESI-IT-MS2	'El Hor'	quinic acid, secologanoside, vanillin, hydroxytyrosol, elenolic acid glucoside and isomers, oleuropein aglycon derivative, luteolin diglucoside, luteolin diglucoside and isomers, 2-(2-ethyl-3-hydroxy-6-propionylcyclohexyl) ac glucoside, rutin, luteolin rutinoside and isomers, 10-hydroxy-oleuropein, luteolin glucoside and isomers, oleuropein glucoside, apigenin rutinoside,	(Taamalli et al., 2012b)

Table 2.5: Main extraction systems and analytical methods used to determine phenolic compounds in olive leaf. (Continuation)

			syringaresinol, diosmin and isomer, taxifolin, apigenin-7-glucoside, chryseriol-7-O-glucoside, 2″- methoxyoleuropein and isomers, oleuropein and isomers, luteolin, quercetin, pinoresinol, acetoxypinoresinol, apigenin.	
Pressurized liquid extraction (PLE)	HPLC–DAD	Not cited	verbacoside, apigenin-7-glucoside, luteolin-7-glucoside, oleuropein	(Japón-Luján and Luque de Castro, 2006)
	HPLC-ESI-QTOF-MS	'Hojiblanca'	quinic acid, oleoside/secologanoside, hydroxytyrosol, p-hydroxybenzoic acid, elenolic acid diglucoside, p-coumaric acid, vanillin, oleoside methyl ester 7-epiloganin, 7-epiloganin, elenolic acid glucoside, luteolin-7,4-O-diglucoside, hydroxyoleuropein, luteolin-7-O-rutinoside, rutin, verbascoside, hydroxytyrosol acetate, luteolin-7-O-glucoside, oleuropein diglucoside and isomers, apigenin-7-o-rutinoside, luteolin-4-O-glucoside, luteolin-3-O-glucoside,oleuropein and isomers, oleuroside, lucidumoside and isomers, 6′-O-[2,6- -dimethyl-8-hydroxy-2-octenoyloxy] secologanoside, ligstroside, luteolin	(Quirantes-Piné et al., 2012)
Supercritical Fluid Extraction (SFE)	Mass Spectrometric Screening	Not cited	tyrosol, hydroxybenzoic acid, cinnamic acid, hydroxytyrosol, protocatechuic acid, caffeic acid, homovanillic acid, syringic acid, elenolic acid 4-methoxytectochysin, caftaric acid, cirsimaritin, fertaric acid, chlorogenic acid, ligstroside, oleuropein	(Le Floch et al., 1998)
Supercritical Fluid, Pressurized liquid, microwave-assisted extractions	HPLC-ESI-TOF-MS/IT-MS2	Six Tunisian cultivars	quinic acid, secologanoside, vanillin, hydroxytyrosol, elenolic acid glucoside and isomers, oleuropein aglycon derivative, luteolin diglucoside, luteolin diglucoside and isomers, 2-(2-ethyl-3-hydroxy-6-propionylcyclohexyl) ac glucoside, rutin, luteolin rutinoside and isomers, 10-hydroxy-oleuropein, luteolin glucoside and isomers, oleuropein glucoside, apigenin rutinoside, syringaresinol, diosmin and isomer, taxifolin, apigenin-7-glucoside, chryseriol-7-O-glucoside, 2″- methoxyoleuropein and isomers, oleuropein and isomers, luteolin, quercetin, pinoresinol, acetoxypinoresinol, apigenin	(Taamalli et al., 2012a)
Ultrasound Assisted Extraction (USAE) + Solid–liquid extraction	HPLC-DAD and GC-MS	Not cited	verbacoside, luteolin-7-glucoside, 3, apigenin-7-glucoside, 4, oleuropein.	(Japón-Luján et al., 2006 a)
	HPLC-DAD-MS2	'Serrana'	caffeoyl,oleuropein, verbascoside, luteolin-7-o-glucoside and isomer, apigenin-6,8-diglucoside, luteolin-7-O-rutinoside, oleuropein glucoside, apigenin rutinoside, apigenin-7-O-glucoside, luteolin	(Ahmad-Qasem et al., 2013)

b. Composition of olive leaves in phenolic compounds

The content of phenolic compounds in olive leaves varies between 2.8 mg/g of dry matter (Altiok et al., 2008) and 44.3 mg/g of dry matter (Boudhrioua et al., 2009). It can even exceed 250 mg/g of dry matter (Mylonaki et al., 2008).

The chemical composition of olive leaves varies according to many factors such as olive variety, climatic conditions, tree age, wood proportion, agricultural practices, genetics, temperature, and extraction procedures (Rahmanian et al., 2015). Recently, many studies have examined olive leaves from various cultivars using different separation techniques, e.g. reverse-phase HPLC with diode-array detection with or without coupling to mass spectrometry (MS) (Bilgin & Sahin, 2013; Silva et al., 2006; Taamalli et al., 2010).

Olive leaves contain a large variety of phenolic derivatives, and consist of simple phenols (the most common and important low-molecular weight phenolic compounds), flavonoids (flavones, flavanones, flavonols, 3-flavanols), and secoiridoids (**Fig. 2.4**). Hydroxytyrosol has been widely described as one of the main components of simple phenols in olive leaves (Altıok et al., 2008; Benavente-García et al., 2000; Bouallagui et al.,2011; Fu et al., 2010; Goulas et al., 2009; Taamalli et al., 2012b). Flavonoids are one of the most common and widely distributed group of olive leaves polyphenols (Abaza et al., 2011; Heimler et al., 1992) and consist of two aromatic rings linked through three carbons that usually form an oxygenated heterocycle (Škerget et al., 2005). They can be present in the aglycone form (quercetin, apigenin, luteolin, diosmetin) or in the glycosylated form (quercetin-7-O-rutinoside, luteolin- 7-O-rutinoside, luteolin-7-O-glucoside, luteolin-5-O-glucoside) (Briante et al., 2002a; Laguerre et al., 2009).

However, secoiridoids, which are a subclass of iridoids (monoterpene derivatives with an iridane ring) derived from the cleavage of the cyclopentane ring at the 7, 8 bond containing phenol moieties, are restricted to the Oleaceae family and are the main family ofcompounds contained in olive leaves (Pérez-Trujillo et al., 2010; Quirantes-Piné et al., 2012; Ranalli et al., 2006; Ye et al., 2014). Among them, oleuropein is the main phenolic compound in olive leaves (Benavente-García et al., 2000; Fu et al., 2010; Kiritsakis et al., 2010). In addition to their diversity, phenolic compounds are found in olive leaves at

different concentration levels. The quantitative determination has widely been reported in scientific researches. The ranges of individual phenolic compounds contents in the literature are reviewed in **Table 2.6**.

Therefore, due to the increasing demand for the replacement of chemical additives by natural ones, olive leaves extracts could be considered as an important, easily available and inexpensive raw material to be considered as natural compounds. Romero-García et al. (2014) reviewed different applications of olive leaves, within the context of a biorefinery based on olive biomass. These authors reported health and medical food applications but also in supplemented foods or even nutraceuticals (Kashaninejad et al., 2020).

Secoiridoids

Oleuropein (R₁=OH, R₂=Glc)
Ligstroside aglycone)R₁=H, R₂=OH)
Oleuropein aglycone (R₁=OH, R₂=OH)

Flavonoids

Flavonols

Quercetin (R₁=OH, R2=OH)
Isorhamnetin (R₁=OH, R2=OCH3)
Rutin (R₁=Rut, R2=OH)

Flavanols

Catechin (R₁=OH, R₂=H)
Gallocatechin (R₁, R₂=OH)

Flavones

Apigenin (R₁=H, R₂=OH)
Luteolin (R₁,R₂=OH)

Simple phenols

Phenylethanoids

Tyrosol (R₁=H, R₂=OH)
Hydroxytyrosol (R₁,R₂=OH)

Hydroxybenzoic acids

p-hydroxybenzoic acid (R₁,R₃=H,R₂=OH)
Gallic acid (R₁,R₂,R₃=OH)

Hydroxycinnamic acids

p-coumaric acid (R=H)
Caffeic acid (R=OH)
Ferulic acid (R=OCH3)

Figure 2.4: Examples of phenolic compounds from olive leaves. Glc (Glucose); Rut (Rutinose).

Table 2.6: Concentration levels of main phenolic compounds in olive leaves.

Class	Phenolic compounds	Range (mg/kg dry extract)	References	Range (mg/kg dry leaf)	References	Range (mg/kg fresh leaf)	Reference
Secoiridoids	oleuropein aglycone	14.8×10^3	(Quirantes-Piné et al., 2013)	170–280	(Talhaoui et al., 2014)		
	oleuropein glucoside	6600	(Quirantes-Piné et al., 2013)	430–16.4×10^3	(Ahmad-Qasem et al., 2013, Ahmad-Qasem et al., 2014; Talhaoui et al., 2014)		
	demethyloleuropein	2300	(Quirantes-Piné et al., 2013)	1340–6380			
	oleuropein	6.97×10^3 - 441×10^3	(Quirantes-Piné et al., 2013)	24.7–143.2×10^3	(Afaneh et al., 2015; Ahmad-Qasem et al., 2013, Ahmad-Qasem et al., 2014; Brahmi et al., 2013; Japón-Luján et al., 2006b ; Lee et al., 2009; Malik and Bradford, 2008; Ortega-García & Peragón, 2010; Savournin et al., 2001; Talhaoui et al., 2014; Tayoub et al., 2012)	236.14–8610	(Agalias et al., 2005; Mert et al., 2013; Ranalli et al., 2006)
	ligstroside	12,400	(Quirantes-Piné et al., 2013)	600–3840	(Ahmad-Qasem et al., 2014; Talhaoui et al., 2014)		
	oleuroside			2010–7000	(Savournin et al., 2001; Talhaoui et al., 2014)		
	methoxyoleuropein			870–2190	(Talhaoui et al., 2014)		
	oleoside	10,800	(Quirantes-Piné et al., 2013)	390	(Talhaoui et al., 2014)		
	secologanoside	7300	(Quirantes-Piné et al., 2013)	1820–3680	(Talhaoui et al., 2014)		
Flavonoids	*flavones*						
	luteolin			10.1–5600	(Ahmad-Qasem et al., 2014; Brahmi et al., 2013; Liakopoulos & Karabourniotis, 2005; Meirinhos et al., 2005; Savournin et al., 2001; Talhaoui et al., 2014)		

Table 2.6: Concentration levels of main phenolic compounds in olive leaves. (continuation)

luteolin glucoside	507–10,500	(Herrero et al., 2011; Quirantes-Piné et al., 2013)	85.2–11.1x10^3	(Ahmad-Qasem et al., 2013; Brahmi et al., 2013; Japón-Luján et al., 2006b ; Liakopoulos & Karabourniotis, 2005; Malik and Bradford, 2008; Meirinhos et al., 2005; Savournin et al., 2001; Talhaoui et al., 2014)
luteolin diglucoside			0.0–121.4	(Meirinhos et al., 2005)
luteolin rutinoside			67–2700	(Ahmad-Qasem et al., 2013; Ahmad-Qasem et al., 2014; Liakopoulos & Karabourniotis, 2005; Talhaoui et al., 2014)
apigenin	1–480	(Herrero et al., 2011; Quirantes-Piné et al., 2013	4.6–339.5	(Brahmi et al., 2013; Meirinhos et al., 2005)
apigenin glucoside	12–680	(Herrero et al., 2011; Quirantes-Piné et al., 2013)	122.7–1261.3	(Ahmad-Qasem et al., 2014; Japón-Luján et al., 2006b ; Liakopoulos & Karabourniotis, 2005; Meirinhos et al., 2005; Savournin et al., 2001)
apigenin diglucoside			90–480	(Ahmad-Qasem et al., 2013)
apigenin rutinoside			7.3–1130	(Ahmad-Qasem et al., 2013; Brahmi et al., 2013; Japón-Luján et al., 2006b ; Liakopoulos & Karabourniotis, 2005; Malik and Bradford, 2008; Meirinhos et al., 2005; Savournin et al., 2001; Talhaoui et al., 2014)
diosmetin	1–37	(Herrero et al., 2011)	traces −350.8	(Meirinhos et al., 2005)
chrysoeriol-7-O-glucoside			580–840	(Talhaoui et al., 2014)

flavonols

Table 2.6: Concentration levels of main phenolic compounds in olive leaves. (Continuation)

Category	Compound						
	rutin			13.8–3500	(Lee et al., 2009; Meirinhos et al., 2005; Savournin et al., 2001; Talhaoui et al., 2014)		
	quercetin rutinoside			654–1210	(Liakopoulos & Karabourniotis, 2005)		
	quercetin	1–129	(Herrero et al., 2011)				
	flavan3-ols catechin			0.8–64.2	(Brahmi et al., 2013)		
Simple phenols	*simple phenols*						
	tyrosol			90–660	(Ortega-García & Peragón, 2010)	8.2–410.74	(Agalias et al., 2005; Ranalli et al., 2006)
	tyrosol glucoside			860–1280	(Talhaoui et al., 2014)		
	hydroxytyrosol	30.8–11,400	(Herrero et al., 2011; Lalas et al., 2011; Quirantes-Piné et al., 2013)	2.1–1120	(Brahmi et al., 2013; Ortega-García & Peragón, 2010)	11.94–479.28	(Agalias et al., 2005; Ranalli et al., 2006)
	hydroxytyrosol glucoside			340–790	(Talhaoui et al., 2014)		
	phenolic aldehyde vanillin			1.3–8.2	(Lee et al., 2009)		
	phenolic acids vanillic acid			12.8–110.1	(Brahmi et al., 2013)		
	caffeic acid	1–60	(Herrero et al., 2011)	1.4–4.5	(Lee et al., 2009)	1350–22.190x10^3	(Mert et al., 2013)
	gallic acid			7.4–55.8	(Brahmi et al., 2013)		
	cinnamic acid			5.4–44.5	(Brahmi et al., 2013)		
	hydroxycinnamic acid					5040–32.69x10^3	Mert et al., 2013)

Table 2.6: Concentration levels of main phenolic compounds in olive leaves. (Continuation)

syringic acid	174–447	(Briante et al., 2002b)	5.2–13.7	(Brahmi et al., 2014)		
ferulic acid			7–91.4	(Brahmi et al., 2013; Liakopoulos & Karabourniotis, 2005)		
verbascoside	29x10^3	(Quirantes-Piné et al., 2013)	300–18.6x10^3	(Ahmad-Qasem et al., 2013, Ahmad-Qasem et al., 2014; Japón-Luján at al., 2006b ; Savournin et al., 2001; Talhaoui et al., 2014)		
isoverbascoside	17,200	(Quirantes-Piné et al., 2013)				
p-hydroxybenzoic acid			0.6–23.8	(Brahmi et al., 2013)		
cholorogenic acid			3.4–3.8	(Brahmi et al., 2013)	6140–70.71x10^3	(Mert et al., 2013)
protocatechuic acid			2.3–61.0	(Brahmi et al., 2013)		
Hydroxyphenylacetic acid			14.7–45.7	(Brahmi et al., 2013)		
Other compounds						
elenolic acid					99.6–662.92	(Agalias et al., 2005; Ranalli et al., 2006)
elenolic acid glucoside	5600	(Quirantes-Piné et al., 2013)				
elenolic acid diglucoside			270–1370	(Talhaoui et al., 2014)		

2.2.3.3 Oleuropein: benefits, content and method of quantification in olive leaves

All parts of the olive tree and its oil contain oleuropein, but the leaves of olive tree are the richest source of this compound (Rahmanian et al., 2015).Oleuropein is classified   as the ester formed by 3,4-dihy-droxyphenyl ethanol (hydroxytyrosol)   and   the glucoside of elenolic acid (**Fig.2.5**) (Coppa et al., 2020). The compound was firstly detected in olives in 1908 and described by Bourquelot and Vintilesco as a green thin solid with a melting point of 89°C (De Leonardis et al., 2008). Oleuropein is almost absent in olive oil due to its high solubility in water and enzymatic degradation during oil extraction (Paiva-Martins and Pinto, 2008). Olive leaves may contain 60–

90 mg/g of oleuropein in dry mass (Ansari et al., 2011). However, the oleuropein content depends on several factors, including olive variety, plant region, sea-son, olive maturation during harvesting, and the type of olive processing (Al-Rimawi et al., 2014; Hassen et al., 2015).
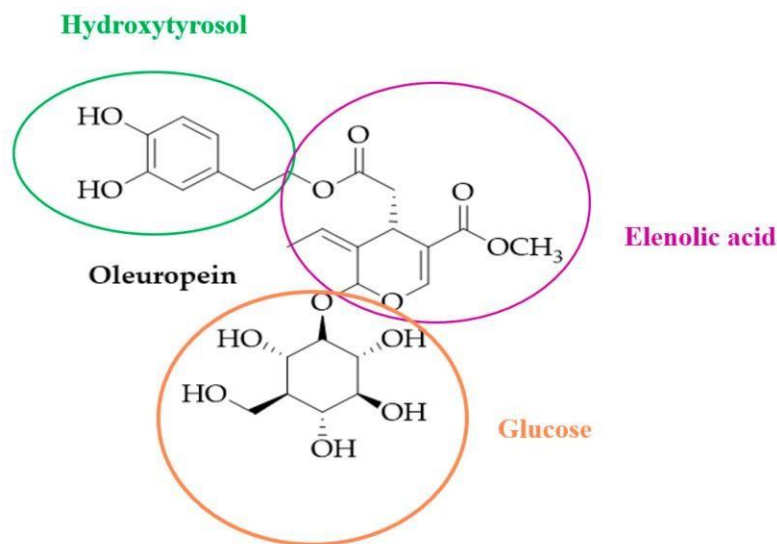
Figure 2.5: Chemical structure of oleuropein.

It has been reported that oleuropein possesses many beneficial effects on human health, such as antioxidative (Benavente-Garcia et al., 2000), antimicrobial (Pereira et al., 2007), antiviral (Micol et al., 2005), anti-ischemic (Andreadou et al., 2006), anti-inflammatory (Visioli et al., 1998) and hypolipidemic (Jemai et al., 2008) properties. In addition, oleuropein has shown cardioprotective (Andreadou et al., 2006) and neuroprotective

(Omar, 2010) effects. In vitro studies have demonstrated that oleuropein acts as an antitumor compound (Hamdi and Castellon, 2005), inhibits platelet-activating factor activity (Andrikopoulos et al., 2002) and might be a modulator of metabolism. It improves lipid metabolism to protect against obesity problems (Polzonetti et al., 2004). Furthermore, oleuropein intervenes in the developmental processes of olive fruits and tree. It also defends olive tree against the attack of pathogens and insects (Malik and Bradford, 2006).

According to the bibliographic review (**Table 2.7**), the quantification of oleuropein in olive leaves is most frequently carried out using high performance liquid chromatography (HPLC). The mobile phases used in this technique can be normal phase or reverse phase. Solvents can be eluted in isocratic or gradient mode. Oleuropein is detected at a wavelength of 280 nm. In addition to this technique, Ranalli et al., (2006) also used gas chromatography (HRGC) for the quantification of oleuropein in olive leaves and showing no difference between the results obtained by this technique and those obtained by HPLC.

Table 2.7: Literature review on techniques and conditions for measuring oleuropein in olive leaves.

						Analytical conditions					
Analytical technique	Detector	λ (nm)	column	Flow rate (mL/min)	T (°C)	Mobile phases	Elution system	t (min)	t_r (min)	Content of OLP	References
HPLC	Diode array detector.	280	C18 LiChrospher 100 analytical column (5µm, 250mm×4mm)	1	30	-(A) acetic acid/water (2,5: 97,5) - (B) acetonitrile	Gradient	60	22.2	13,4% (134,4 mg OLP per g of olive leaf extract)	Altiok et al., 2008
HPLC	UV detector (SPD-10Avp)	280	C-18 Shim-pack VP–ODS (4,6 - 250 mm)	0.6	40	-(A) 0,1% phosphoric acid in water -(B)70% acetonitrile in water	Gradient	50	37.5	14% (data are reported on a dry mass basis)	Bouaziz et al., 2008
HPLC	UV detector (SPD-10Avp)	280	C-18 Shim-pack VP–ODS (4,6 - 250 mm)	0.6	40	-(A) 0,1% phosphoric acid in water -(B) 70% acetonitrile in water	Gradient	50	39	15, 13 g of extract containing 6, 8 g of OLP per 100g of fresh olive leaves.	Bouaziz et Sayadi, 2005
HPLC	UV detector (SPD-10Avp)	280	Shim-pack, VP-ODS (4,6mm×250mm)	0.5	40	-(A) 0,1% phosphoric acid in water -(B)70acetonitrile in water	Gradient	40	37.5	4,32 g/100 g dry weight	Jemai et al., 2008
RP-HPLC	Diode array detector	280	a reversed-phase Spherisorb ODS2 (250 x 4,6 mm, 5 µm particle size) column	0. 9	40	-(A)water/formic acid (19:1) -(B) methanol	Gradient	40	28	26,47 mg/g in olive leaf lyophilized extract	Pereira et al., 2007
RP-HPLC	UV-visible detector.	280	Waters Spherisorb ODS2 (250 x 4,6 mm, 5 µm particle size) column	1	RT	-(A) mixture of 2% acetic acid in water (pH 3,1) -(B) methanol	Gradient	70	37	11,43 -14,25 (% w/w) of Leaf Extracts	Paiva-martins et al., 2007

Table 2.7: Literature review on techniques and conditions for measuring oleuropein in olive leaves. (Continuation)

HPLC	Diode array detector.	280	C18 LiChrospher 100 analytical column (250 x 4,6 mm, 5 µm particle size)	1	30	-(A) acetic acid/water (2,5: 97,5) -(B)acetonitrile	Gradient	60	22.7	abundance of OLP in olive leaf extract (absolute content dry basis) :24%	Benavente - Garcia et al., 2000
RP-HPLC	Mass spectrometer	280	- XTerraR RP18; 3,5 µm, 4,6 x 10mm x 150mm column	1	Not cited	-(A) water/ acetic acid (99,9: 0,1) -(B)acetonitrile/ acetic acid (99,9: 0,1)	Gradient	80	31.9	3,26 à 8,48 mg/ 100g leaves	Kiritsakis et al., 2010
HPLC	Photodiode array detector	280	Waters Symmetry C18 (5 µm 0 (3,9 mm x150 mm) column	1	35	-(A)100% acetonitrile -(B)0,02% trifluoroacetic acid in water	Gradient	65	Not Cited	in frozen leaves: 36,4±1,06 mg/g fresh wt	Malik et Bradford, 2008
RP-HPLC	Spectrophotometer	280	Reversed silica phase adsorboshere XL C18 90 A column (250 mmx4,6 mm, 5 µm)	1	RT	acetonitrile/water (21: 79) mixture acidified with o-phosphoric acid (up to pH3)	Isocratic	35	25	0,9 à 8,55 g/kg fresh weight	Ranalli et al., 2006
HPLC	Diode array detector	280	-Lichrospher 100 RP-18 (250mm×4 mm, 5µm). -Kromasil 5 C-18 column (15mm×4,6 mm, 5µm) protected with a steel holder	Different debit	RT	- (A) 6% acetic acid, 2 mM sodium acetate, in water). - (B) Acetonitrile.	Gradient	45	18	22,61 mg/g dry leaves	Japon-Lujian et al., 2006a
RP-HPLC	UV detector	240	a reverse phase column (Erbasil 100-S-C18, 230mm × 8mm × 4 mm)	1	Not cited	-(A)H_2O/AcOH (99:1). -(B) Methanol.	Gradient	60	Not cited	37,7 mg/ 100g extract	Briante et al., 2004
HRGC	Not cited	Not cited	30 m x 0,32 mm id, 0,1 µm HP-1 capillary column coated with dimethylpolysiloxane	Column Pressure: 40 kPa	320	hydrogen	Isocratic	Not cited	Not cited	0,8 à 8,61 g/kg fresh weight	Ranalli et al., 2006

2.3 Membrane technology

Membranes are thin, porous physical barriers used to separate different components from a mixture or solution. They are semi-permeable, which means that they allow some substances to pass through while blocking others. The ability of a membrane to allow certain substances to pass through is known as its "selective permeability." This property is determined by factors such as the size, shape, charge, and solubility of the molecules being separated (Baker et al., 2004).

In a separation process using a membrane, the mixture or solution being treated is known as the "feed" (F). The species that are rejected (retained) by the membrane and remain in the feed solution are known as the "retentate" (R). While the components thatpass through the pores and are collected on the other side are known as the "permeate" (P). The size of the pores primarily determines which species are rejected and which will pass through the membranes (see the **Fig. 2.6**).

Membranes are widely used in a variety of industries, including food processing, pharmaceuticals, biorefineries, and biotechnology. They offer numerous advantages over other separation techniques, such as low chemical and energy requirements, and can be easily adapted to different processes. Overall, the use of membranes in various industries is increasing due to their versatility and efficiency in separating different species (Kolah et al., 2013).
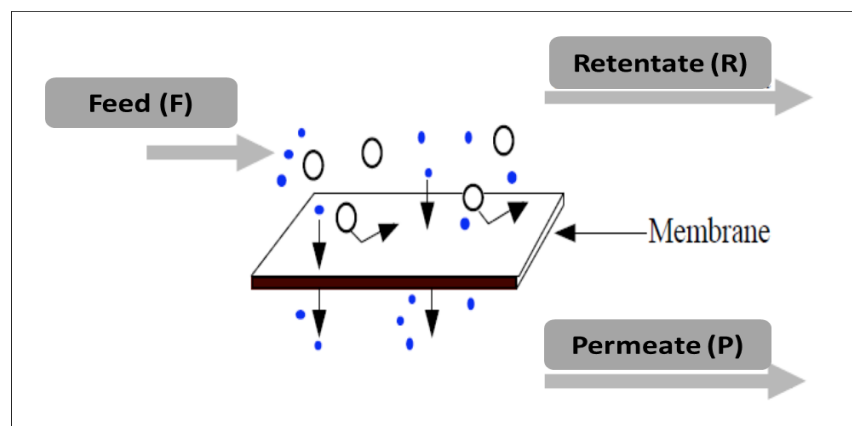
Figure 2.6: Schematic representation of membrane module showing components of filtration process.

2.3.1 Types of membrane

Membranes can be classified based on various aspects such as manufacturing material (e.g. polymeric and ceramic), fabrication methods (e.g. phase inversion, stretching, and electrospinning, etc.), application module configuration (e.g. flat sheet, spiral bound and hollow fiber, etc.) and pore size (e.g. microfiltration (MF), ultrafiltration (UF) and nanofiltration (NF), etc.) (El-Ghaffar and Tieama, 2017; Lalia et al., 2013; Othman et al., 2021). The type of membranes is selected depending on the specific requirements of their intended application. For example, some applications require high temperature and pressure resistance, chemical stability in extreme pH conditions, the desired flow rate, or specific separation characteristics (Pendergast and Hoek, 2011; Warsinger et al., 2018).

Ceramic membranes, which are typically made from materials such as alpha-aluminum oxide (Al_2O_3) and titanium dioxide (TiO_2), are known for their thermal, mechanical and chemical stability but have limitation associated with their high cost. Polymeric membranes, on the other hand, have low cost and are made from polymers such as polyvinylidene fluoride, polyether sulfone, and cellulose acetate. These membranes are generally more sensitive to high pressure and thermal conditions and have higher separation efficiency compared to ceramic membranes.

In recent years, MMMs have grown increasingly popular in addition to ceramic and polymeric membranes. These membranes are fabricated from polymeric materials by adding inorganic or organic nanoparticles into their structure in order to enhance their separation efficiency, flux, hydrophilicity or hydrophobicity, and fouling resistance (Jhaveri and Murthy, 2016). These membranes combine the advantageous characteristics of polymeric membranes (e.g., low cost and fabrication simplicity) with those of ceramic membranes (e.g., thermal and mechanical strength) ((Pendergast and Hoek, 2011)). Further details of MMMs development and applications are discussed in following subsection.

2.3.2 Characteristics of membrane filtration processes

a. Pore size

One of the key characteristics of a membrane filtration process is the size of the pores. Membrane processes are often classified based on the pores size, which can range from less than 1 nanometer (nm) (virtually non-porous) to 10 micrometers (μm) (microfiltration (MF)) (see **Fig. 2.7**).
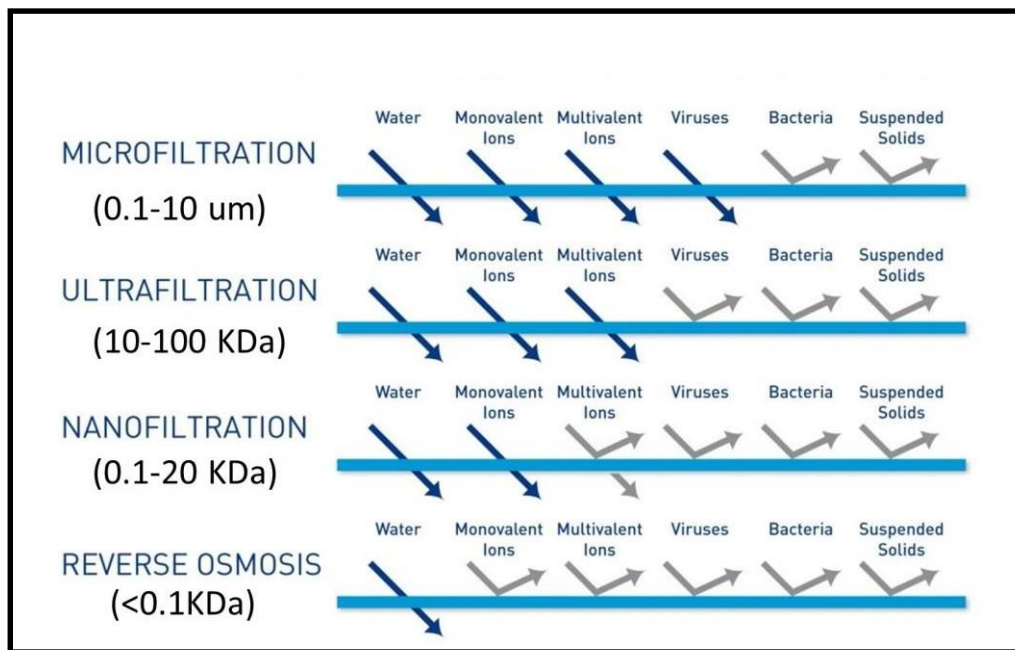
Figure 2.7: Filtration spectrum of different types of membranes.

b. transmembrane pressure (TMP)

For a pressure driven membrane, the transmembrane pressure (TMP) serves as the driving force to push the feed solution through the membrane. The required TMP typically increases as the pore size decreases, moving from microfiltration to reverse osmosis. TMP shows great influence on the filtration performance of membranes in terms of flux, rejection and membranes fouling.

c. Mode of operation

The mode of operation i.e., cross flow and dead-end filtration, can affect the performance of the membrane by influencing the formation and thickness of a "filter cake"

on the surface of the membrane. A filter cake is a layer of accumulated contaminants that can build up on the membrane surface over time, increasing the resistance to flow and reducing the efficiency of the separation. The formation of a filter cake is more common in microfiltration and ultrafiltration processes, as the feed streams for these processes often contain substances with high molecular weights (MWs) that tend to accumulate more easily on the membrane surface.

In cross flow filtration, the feed solution flows is tangentially to the membrane surface, which can reduce the deposition of the filter cake and allow the process to operate in an almost continuous mode. In contrast, in dead-end filtration, the feed solution flows perpendicular to the membrane surface, which can lead to the rapid formation of a filter cake. This makes dead-end filtration a batch process, as the filter cake must be removed or allowed to accumulate before the process can continue. In dead-end filtration, the resistanceof the filter cake can exceed the membrane resistance, becoming the dominant factor in the performance of the membrane (Krawczyk, 2013). The schematic representation of cross flow and dead-end filtration operations is shown in **Fig. 2.8.**
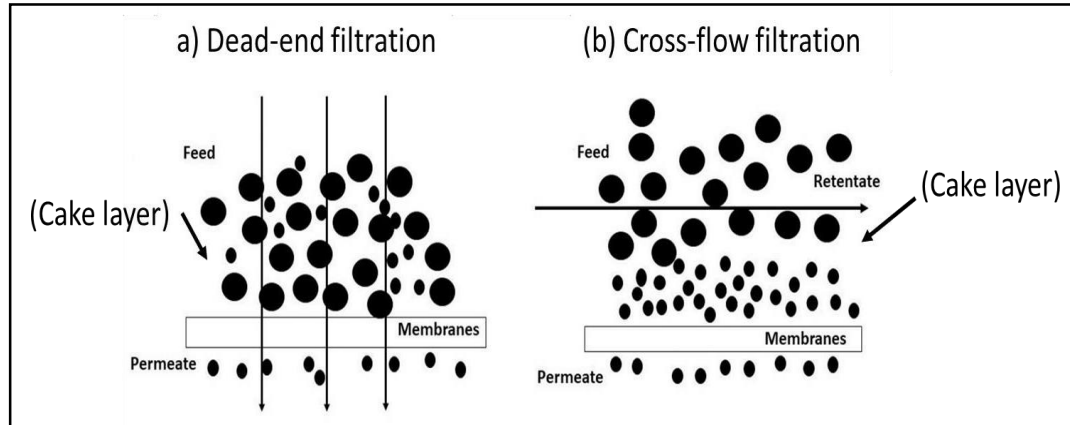
Figure 2.8: Separation scheme of membrane filtration (a) Cross flow (b) Dead- end filtration.

Overall, the efficiency of a membrane filtration process depends on a combination of factors, including the pore size, TMP, feed characteristics, membrane type, and mode of operation. Some of the key characteristics of different pressure-driven membrane are

summarized in **Table 2.8** (Van der Bruggen et al., 2003; Pendergast and Hoek, 2011; Jhaveri and Murthy, 2016; Kevlich et al., 2017; Lalia et al., 2013; Warsinger et al., 2018).

Table 2.8: Characteristics of MF, UF, NF and RO membranes.

Characteristics	MF	UF	NF	RO
Pore size (nm)	100-10,000	1-100	0.5-2	<0.5
TMP (bar)	0.5-3	1-10	5-30	20-150
Permeability (l/h.m^2.bar)	>1000	10-1000	1.5-30	0.05-1.5
MWCO (kDa)	100-5000	10-100	0.1-20	<0.1

2.3.3 Fouling of membrane

Despite the numerous advantages of membranes in separation processes, including efficiency, environmental friendliness, and cost-effectiveness, one of the major challenges in their use is membrane fouling. Fouling occurs when contaminants accumulate on the surface of the membrane or to its pores, reducing its performance in terms of flux and separation efficiency (Jhaveri and Murthy, 2016; Warsinger et al., 2018).

Membrane fouling can be reversible and irreversible that requires frequent cleaning to restore the original flux or membrane replacement, which increases the operational cost of filtration process. The irreversible fouling of membranes can be explained by different mechanisms e.g. irreversible cake layer formation, intermediate or complete pore blockage, and the adsorption of small molecules in pore walls. Cake formation and pore blockage can be caused by large molecules in the feed, while small molecules can enter the pores and reduce their effective size, leading to an increase in membrane resistance and a reduction in flux (Baker et al., 2004; Bet-Moushoul et al., 2016). While the reversible fouling is mainly due to formation of concentration polarization (CP) across membrane surface (see **Fig.2.9**). Its effect can be reversed by changing process conditions such as cross flow velocity or turbulence.
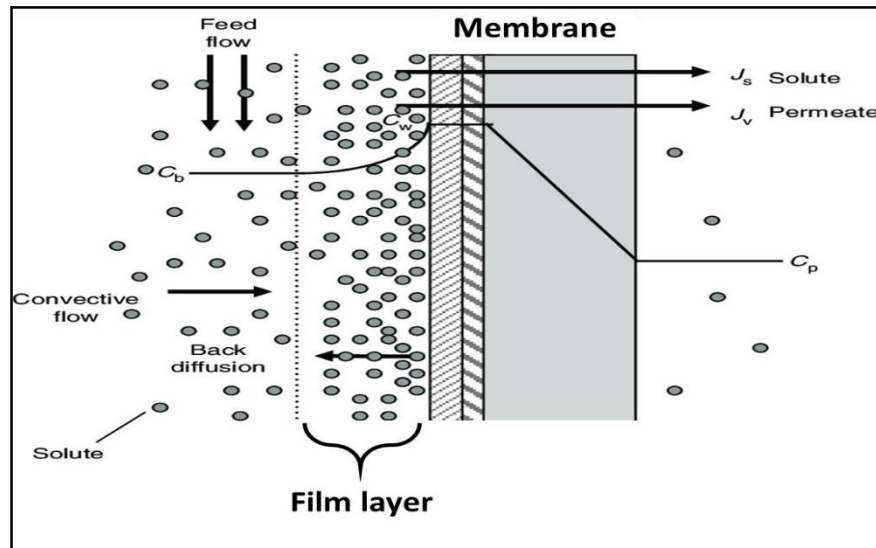
Figure 2.9: Schematic representation of concentration polarization.

The fouling of membranes is a complex process, and much research has focused on understanding its mechanisms and developing new fouling-resistant membranes. The nature of the membrane material and the feed can influence fouling, with hydrophobic membranes tending to foul more easily than hydrophilic membranes, and hydrophobic solutes more likely to be adsorbed by membranes (Rezakazemi et al., 2018). Development of MMMs with more hydrophilic surface can improve the fouling resistance of membranes and increase their operational lifetime. In this thesis, the possibilities of using MMMs for the separation of TPC and purification of oleuropein from olive leaves streams are explored. Consequently, the focus of the further state-of-the-art analysis is on MMMs and membranes applicable in the recovery of polyphenols, including additional details on membrane fouling.

2.4 Mixed matrix membranes (MMMs) and their applications

MMMs, also known as hybrid or nanocomposite membranes (NCM), are the result of new developments in the field of membrane technology to exploit the advantageous features of both polymeric and ceramic membranes (see **Table 2.9**). They are made by incorporating inorganic and organic nanomaterials, such as ceramic particles, metal-organicframeworks (MOFs), carbon nanotubes (CNT), into a polymer matrix (Esfahani et al., 2019).

Different nanomaterials are used for the preparation of MMMs by adding them to the polymeric membrane structure by dispersing over surface or embedding into matrix (see **Fig**. **2.10**). They can also enhance the various characteristics of membranes such as stability, flux, and selectivity allowing it to more effectively separate specific molecules or ions.

These membranes have high permeability and fouling resistance and sometime specific features like photocatalytic (Leong et al., 2014) and antibacterial effect (Chen et al., 2013; Yu et al., 2013) can be imparted to these membranes depending on the application. They were originally developed for gas separation, but have been used in a variety of applications including water treatment, toxin extraction from human plasma, pervaporation, blood purification, lithium cell batteries, sensors, and more (Pendergast and Hoek, 2011; Garcia-Ivars et al., 2014; Golemme and Santaniello, 2019; Guo and Kim, 2017; Lalia et al., 2013; Li et al., 2016a; Rahimpour et al., 2008; Warsinger et al., 2018; Zhao et al., 2011; Zinadini et al., 2014).

Table 2.9: Comparative study of characteristics of polymeric, ceramic, and MM membranes.

Features	Polymeric membrane	Ceramic membrane	MMMs
Casting method	Phase inversion Stretching Track Etching Electrospinning	Sol-gel process Hydrothermal synthesis	Phase inversion Stretching Track Etching Electrospinning
Fabrication ease	Yes	Yes	Yes
Thermal stability	Low-moderate	High	Moderate-high
Flux	Low- high	High	High
Tunable selectivity	No	Yes	Yes
Operating cost	Moderate- high	Low-moderate	-
Constraints	Fouling Low membrane life Low chemical resistance Low temp. resistance	Scale-up Costly materials Low selectivity Fouling	Compatibility of nanoparticles Notfully developed technology
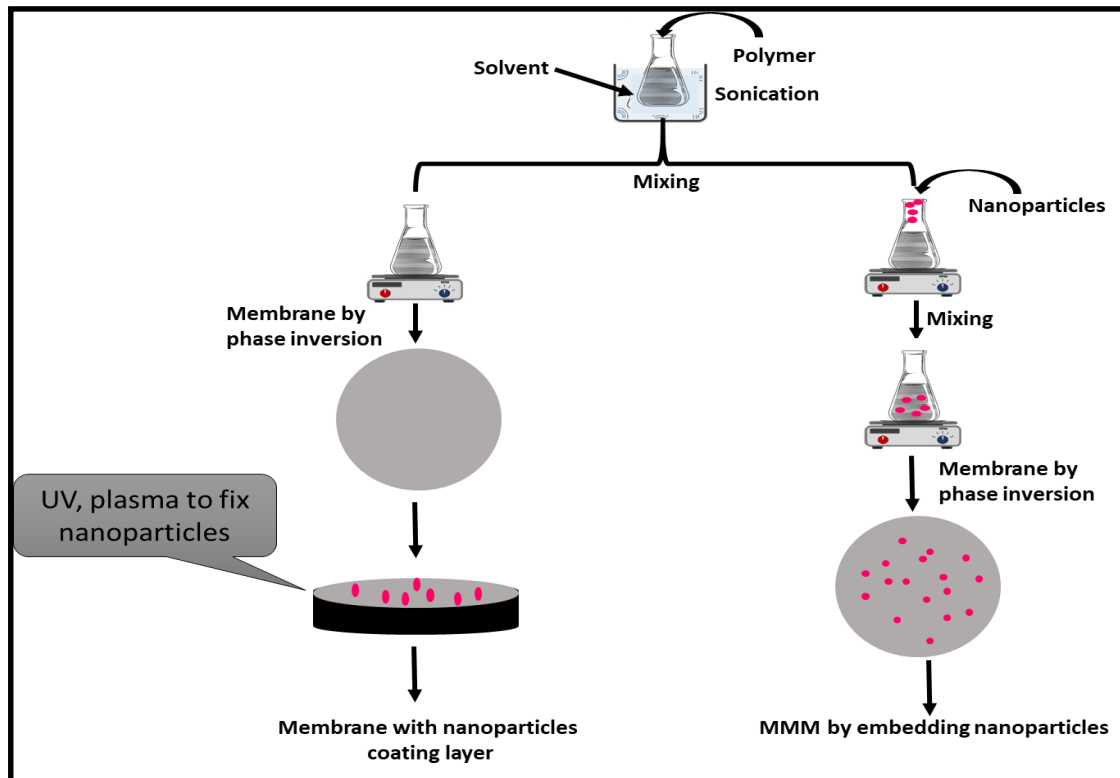
Figure 2.10: Schematic representation of preparation process for mixed matrix membranes bysurface coating and by embedding nanoparticle to polymeric membranes matrix.

For the preparation of MMMs, different type of nanoparticles (NPs), such as porous, nonporous, organic and inorganic materials (e.g., CNT, activated carbon, zeolites, PEG, SiO_2, Al_2O_3, TiO_2, ZnO) are used depending on their application (Bet-Moushoul et al., 2016; Garcia-Ivars et al., 2014; Jhaveri and Murthy, 2016; Lewis et al., 2021). For instance,as the hydrophobic membranes are more prone to fouling, while hydrophilic membranescan get swollen and lose their mechanical strength and rejection efficiency when exposed toaqueous feed solutions. One way to address these issues is to use hydrophilic NPs to modify hydrophobic polymeric membranes (Garcia-Ivars et al., 2014).

There are two main methods for incorporating NPs into polymeric membranes: coating the pre-prepared membranes with NPs, or mixing NPs into the dope solution and casting the membrane (see **Fig. 2.10**) (Diagne et al., 2012; Esfahani et al., 2019; Gohari and Abu-Zahra, 2018; Jamshidi Gohari et al., 2014; Li et al., 2014b; Moghimifar et al., 2014). The coating method is easier and more scalable, but the NPs can be washed away from the

membrane surface over time. The most commonly used method for fabricating polymeric membranes with NPs is the phase inversion process, which can produce hollow fiber or flat sheet membranes. Phase inversion is a broad category that includes evaporation induced phase inversion, thermally induced phase inversion, vapor induced phase inversion, and immersion precipitation (Van der Bruggen et al., 2003; Leong et al., 2014; Li et al., 2014b; Mohammad et al., 2015; Qadir et al., 2017; Tijink et al., 2014; Yang et al., 2009; Zhu et al., 2019). The most frequently used technique for fabricating modified polymeric membranes is non-solvent induced phase inversion and is the focus of further state-of-the-art included in **Table 2.10**.

Table 2.10: State of art for MMMs characteristics and their applications.

Application	Polymer	Filler	Membrane synthesis method & operation	Performance		Modification* and Primary goal achieved	Ref.
				PWF (L/m^{2}h)	Rejection (%)		
Cu (II) Removal from Water	PES	APTES modified γ- Al$_2$O$_3$	PIIP method; DEF system	54.3 at 4 wt% filler	87% at 4 w% filler	E; increased the thermal stability, HP, total porosity, BET surface area, and glass transition temperature.	(Gohari and Abu-Zahra, 2018)
Concentration of Kraft Black	PES support	GO	Vacuum filtration on PES supports; DEF system	-	98% for lignin	C; (up to 98%) lignin rejection under realistic process conditions.	(Rashidi and Yusup, 2017)
Tested for Humic Acid (HA) performance	PS-UF	GO	PIIP method; DEF system	108.403-133.61	95.58- 99.41	E; improved water permeability, HA rejection and anti-fouling, HP properties	(Akhair et al., 2017)
Tested by filtering BSA solution and 3 different Mw organic dyes	PES	(rGO)/ TiO$_2$	NSIPI method; DEF system	23.1 - 45	RG19 – 99.4; DY12- 95.4; RB21- 81.4;	E; improved water permeability and fouling resistance, dye removal better at 0.1 wt. % filler.	(Safarpour et al., 2016)
Tested for separation of dyes at different operating temp.	CA -UF	TiSiO$_4$	PIIP method (for 12 h at 25°C); CFF system	72.1 ± 2.0 to 134.4 ± 1.6	68	E; Improved HP, fouling properties, permeability, and thermal stability	(Dasgupta et al., 2014)
Tested by inhibition zone and filtration of bacterial suspension	CA -UF	n-Ag	PIIP method; DEF system	-	-	E; High flux, higher BSA rejection for 30 nm n-Ag; Better antibacterial performance	(Mollahosseini et al., 2012)
Tested for HA filtration and 6 different organic dyes with different Mw	PES	ZnO	PIIP method; DEF system	-	-	E; better dye rejection, HP, permeability, lower flux decline	(Balta et al., 2012)

*C: coated, E: embedded; HP: hydrophilicity; CAP: corona air plasma, Pm: membrane permeability and R$_m$: membrane resistance

CHAPTER 3: Characterization of olive leaf extract

3.1 Introduction

Phenolic profile of olive leaves is known to be affected by several agronomical and technological factors such as leaf age, degree of ripeness, geographical origin, cultivar, phonological stage during sampling, proportion of brunches on the tree, moisture content, degree of contamination with soil and industrial processes employed for extraction (El et al., 2009, Papoti et al., 2009). Several studies have been carried out to investigate some of the effects mentioned above (Vinha et al., 2005; Japón-Luján et al., 2006; Veličković et al., 2008). In this research, our attention have been directed towards investigating the effect of cultivar, geographical origin, and sampling time.

The polyphenol profile of olive leaves can vary significantly based on the cultivar, which refers to different varieties of the olive tree (Olea europaea).Different olive cultivars have distinct genetic traits, and these traits can influence the types and amounts of polyphenols present in their leaves. Therefore, the choice of olive cultivar can have a significant impact on the polyphenol profile of olive leaves, which in turn can influence the potential health benefits associated with consuming products derived from these leaves. Many studies have been carried out to investigate the effect of cultivar of the profile of polyphenols (Di Donna et al., 2010; Mohamed et al., 2018).

The phenolic compounds content in olive leaves can be influenced by the geographical origin of the olive tree. Therefore, the specific polyphenol composition and concentration in olive leaves can vary based on environmental factors such as climate, soil type, altitude, and sunlight exposure. Different regions have varying climates, including temperature, humidity, and precipitation patterns, which can influence the production and accumulation of polyphenols in olive leaves. For example, olive trees grown in regions with moderate temperatures and sun exposure might produce more polyphenols as a defense mechanism against environmental stressors. Additionally, the composition of the soil, including its nutrient content and pH levels, can affect the availability of minerals and nutrients to the olive tree, thereby influencing the production of polyphenols. These geographical factors play a crucial role in shaping the polyphenol profile of olive leaves. Numerous research studies have been conducted to explore the influence of geographical origin on the polyphenol profile (Zakraoui et al., 2023; Bilgin and Şahin, 2013).

Moreover, the polyphenol content in olive leaves can vary throughout the year due to seasonal changes. For example, in some regions, the polyphenol content might be higher in spring when the plant is actively growing and producing new leaves. Therefore, the time of the year when leaves are harvested can significantly impact the polyphenol levels. Numerous research endeavors have been undertaken to explore the impact of the sampling duration on the polyphenol profile (Wang et al., 2019; Lorini et al., 2021).

3.2 Materials and Methods

3.2.1 Materials

3.2.1.1 Plant materials

Samples of olive leaves, utilized in this study, were collected from five different cultivars (Chemlali, Chetoui, Chemchali, Oueslati and Jarboui), in the same experimental field of the Chaal (Sfax, Tunisia) in winter 2019. In order to observe the effect of the harvest period, four samples of Chemlali leaves were also collected in spring, summer, autumn and winter 2020. Finally, five samples of Chemlali were picked from the following different sites in Tunisia: Gafsa, Sfax, Monastir, Sousse, and Mednin. These origins are located in various parts of Tunisia and exhibit different climate properties, ranging from humid to windy air, and varying altitudes. After collecting, the leaves were washed, dried, milled and stored at ambient temperature in the dark.

3.2.1.2 Chemicals

Ethanol was provided from Merck and were of >99.8% mass fraction purity. Folin- Ciocalteu reagent, sodium carbonate and gallic acid were purchased from Sigma–Aldrich. Distilled water from a Millipore Milli-Q water purification system was used to prepareolive leaves extract.

3.2.2 Methods

3.2.2.1 Extraction of total phenolic compounds from olive leaves

The extraction of olive leaves was carried out as described below. Briefly, 1.2 g of olive leaves powder was immersed into 40 mL of ethanol/water, 75/25% (v/v), followed by

a 90 min mixing in a shaking bath at 120 rpm and 50°C. After extraction, the mixture was subjected to vacuum pump using sintered glass at 0.45 μm, then centrifuged (Sorvall ST 16 R, Thermo Scientific, Leicestershire, UK) at 4000 rpm for 15 min. The extract obtained was stored in a refrigerator until analysis.

3.2.2.2 Total phenols determination

Total phenolic compounds (TPC) was determined using the Folin-Ciocaltaeu method described by Szyd1owska-Czerniak et al., (2012). In this method, 100 μL of the extract was mixed with 100 μL of Folin-Ciocalteu solution, and then incubated at 25°C for 5 min. Afterwards, 300 μL of saturated Na_2CO_3 (0.333 g/mL) was added to each sample for another 30 min of incubation at 40°C. The absorbance was recorded at $\lambda = 765$ nm. A calibration curve was drawn with gallic acid at different concentrations (2–20 mg/mL, $R^2 = 0.988$). The results were expressed as milligram gallic acid equivalents (GAE) per gram of olive leaf powder (mg GAE/g OLP).

3.3 Results and Discussion

3.3.1 Effect of cultivar

Many factors are able to affect the actual phenolic content of olive leaves, either qualitatively or quantitatively (Di Donna et al., 2010; Markakis et al., 2010; Bilgin and Şahin, 2013). Genotype is among the most important factors, contributing to most of the differences in phenolic profile (Fabbri et al., 2008; Ben Salah Abdelmelek and Abderraba, 2012; Petridis et al., 2012).The phenolic extracts of Chemlali, Chetoui, Chemchali, Oueslatiand Jarboui cultivars were screened for the range of phenolic compounds. All extracts were found to contain high and varying amounts of phenolic compounds as shown in **Table 3.1.** These findings are in agreement with those described in previous researches, which reported that olive leaves can represent a good source of phenolic compounds (Quirantes- Pinéeet al., 2012; Talhaoui et al., 2015). In our study, significant differences were observed for total phenolic contents in extracts. As shown in **Table 3.1**, the highest amount was found in Chemlali (50.5 mgGAE/OLP), while the lowest was registered in Jarboui extract (28.36 mgGAE/OLP). It can be hypothesized that the significant differences observed for total phenols may be related to genetics (Kallithraka et al., 2004; Felhi et al., 2016).

Table 3.1: Total phenolic compounds in the leaves of different cultivars.

Varieties		Chemlali	Chetoui	Chemchali	Oueslati	Jarboui
TPC	Our study	50.5 ± 0.45	49.52 ± 0.22	44.21 ± 0.56	33.35± 0.81	28.36 ± 0.39
(mgGAE/OLP)	Previous studies	48.23 ± 0.26	47.47 ± 0.45	34.55 ± 0.6	28.97 ± 0.9	18.96 ± 0.85

3.3.2 Effect of geographical origin

Figure 3.1 represents the variation in the total phenolic content of olive tree leaves grown in five different geographical locations. There were clear differences in the total phenolic content among leaves from different geographical locations. Our results support previous reports indicating possible differences in total phenolic content among samples from different origins. For instance, among the various sample locations, the region of Sfax exhibited the highest total phenolic values. This can be explained by the variations in weather, climate, and soil composition in these locations.
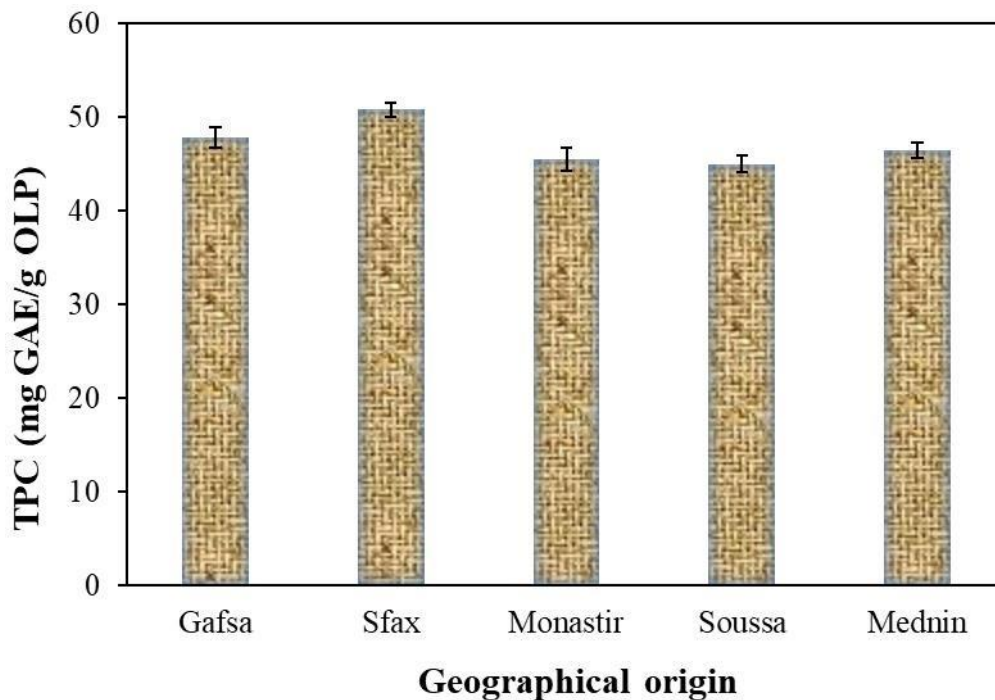
Figure 3.1: Total phenolic content in the chemlali olive leaves from different geographical origins.

3.3.3 Effect of sampling time

As shown in **Fig.3.2**, the level of phenolics in Chemlali olive leaves varied extensively with the harvesting season. TPC exhibited fluctuations from 54.51 to 45.11 mgGAE/gOLP. The maximum level of TPC (about 54.51 mgGAE/gOLP) was detected in winter (November), whereas minimal level was found in summer (April) (45.11 mgGAE/gOLP). This result was contrary to the study of Papoti et al., (2009) who observed an increase in TPC in "Picual" olive leaves from August to November. The changes in TPC may be correlated with the augmentation of the polyphenol protein oxidase content and activity in olive leaves, which is consistent with the finding described by Wang et al., (2019). This suggests that winter may be the best period to obtain phenolic compounds from Chemlali olive leaves.
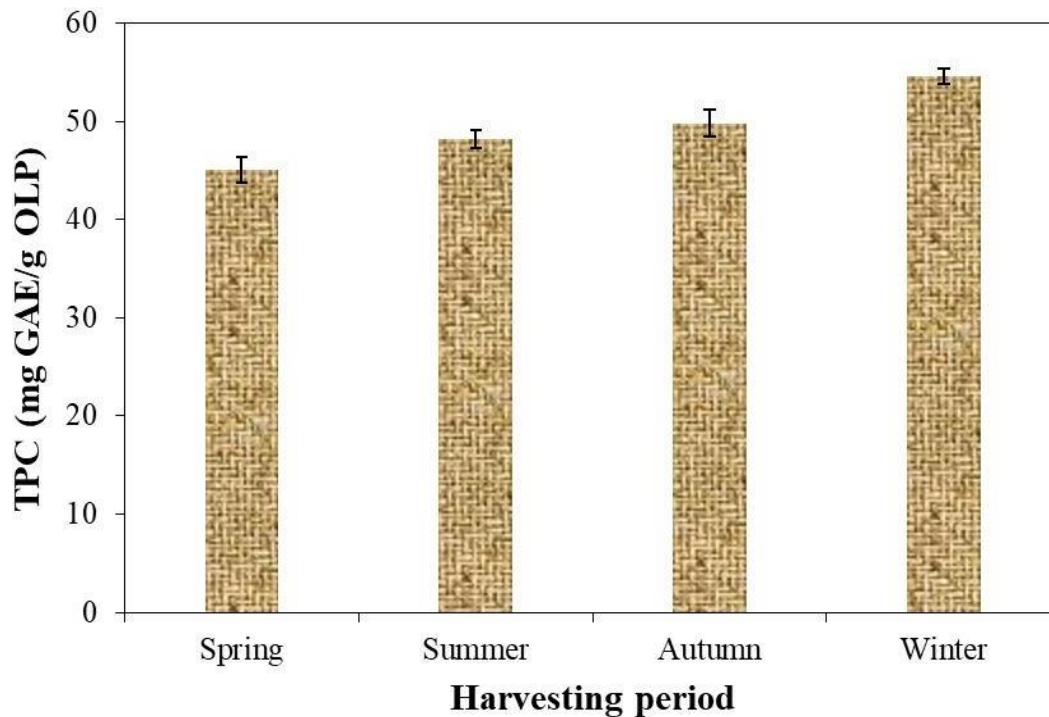
Figure 3.2: The seasonal variation of total phenolic content in Chemlali olive leaves during the year 2020.

3.4 Conclusions

The total phenolic content of olive leaf samples collected from Tunisia is influenced by the cultivar, geographical region, and harvesting time. The highest TPC was observed in samples from the chemlali cultivar, particularly in the region of Sfax. Additionally, TPC was found to be highest in samples collected during winter (November) compared to other seasons. Based on these findings, it is concluded that chemlali olive leaves from the Sfax region, harvested in November, will be used for subsequent experiments in this thesis.

CHAPTER 4: Integration of solvent extraction and membrane processes to produce an oleuropein extract from olive leaves

This Chapter is based on the publication:

4.1 Abstract

The integration of solvent extraction and membrane separation technology was used to recover and concentrate oleuropein from olive leaves. In this study, the effect of extraction solvent (type, composition) on the content of total phenolic compounds (TPC) extracted from olive leaves was investigated. Experimental results showed that ethanol: water, 75/25% (v/v), gives the highest TPC. Thus, to establish the parameters to obtain hydroethanolic olive leaves extract with the highest content of total phenolic compounds, a Central Composite Design was performed. The extract obtained at 50°C for 90 min, within

0.03 g/mL, was subjected to crossflow ultrafiltration (UF) to remove suspended solids in the feed and to reduce fouling phenomena, followed by a stirred dead-end nanofiltration (NF) using a commercial flat sheet membrane at different pressure (10, 20 and 30 bar). The nanofiltration (at 30 bar) showed a high rejection coefficient towards phenolic compounds and flavonoids contents. Fractions coming from UF and NF (at 30 bar) revealed that the highest content of oleuropein was 119.01 mg/g corresponding to NF retentate, high antioxidant capacity (DPPH method). It can be concluded that the integration of solvent extraction and membrane separation technology is efficient for the recovery and concentration of oleuropein and phenolic compounds from olive leaves. The obtained concentrate is of interest for preparing formulations to be used in the food, cosmetic and pharmaceutical industries.

Keywords: Olive leaves; Central composite design; Phenolic compounds; Crossflow; Dead-end; Oleuropein.

4.2 Graphical abstract
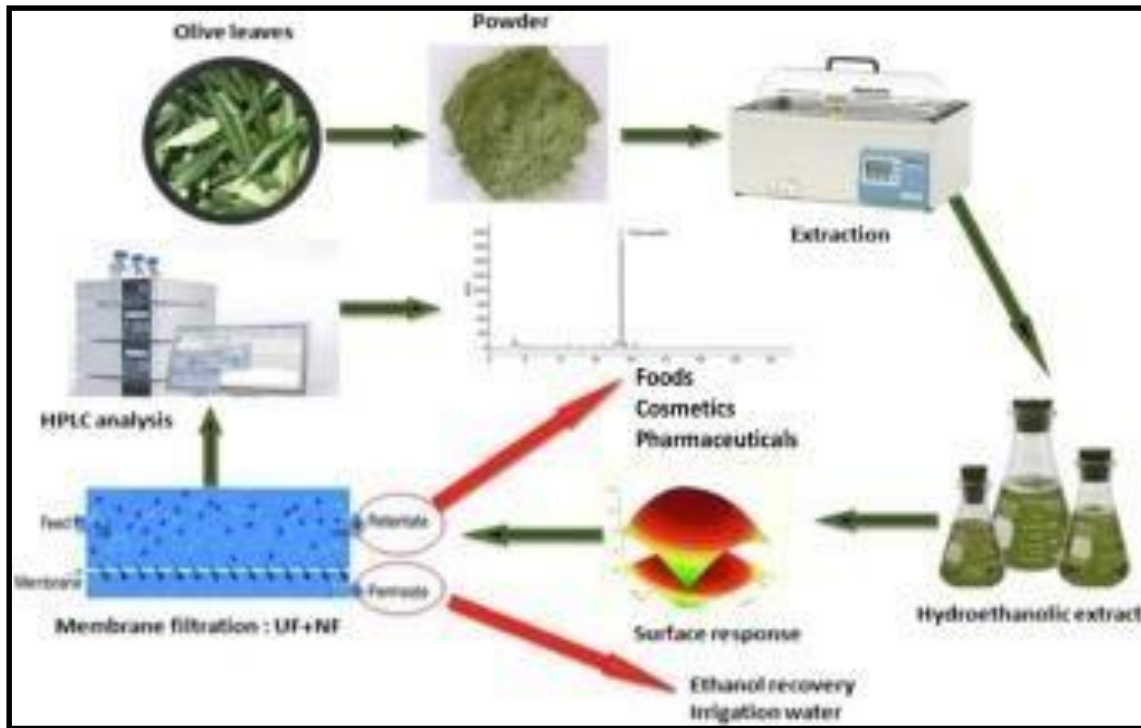
Figure 4.1: Graphical abstract.

4.3 Introduction

In recent years, the agronomic, cosmetic, and pharmaceutical industries have increased their interest in natural extracts from plants and by-products (Cifá et al., 2018). They have gained considerable attention for their high potential as a source of low-cost phytochemicals (Da Rosa et al., 2019). Olive tree is one of the most important sources rich in natural antioxidant products because of its phenolic contents in fruits (Ben Othman et al.,2008), oil (Arslan et al., 2012) and leaves (Bouaziz et al., 2005; Ahmad-Qasem et al.,2013).

Annually, many by-products and residues are obtained from both olive harvesting and oil extraction where most of them have no practical applications (Martín-García et al., 2020). Olive leaves, one of these by-products are regarded as a cheap, renewable and

abundant raw material (Khemakhem et al., 2017) and containing the highest content in bioactive compounds (Da Rosa et al., 2021).

Olive leaves have been used in traditional medicine as a cardioprotective, antidiabetic, and anticholesterolemic agent (Del Contreras et al., 2020). Recently, several scientific reports have demonstrated the antihypertensive (Susalit et al., 2011), anticarcinogenic (Bouallagui et al., 2011), anti-inflammatory, hypoglycemic, antimicrobial, and hypocholesterolemic effects of olive leaves (Lee et al., 2010). All these positive effects seem to be at least partially related to antioxidant action (Dekanski et al., 2011), mainly related to low molecular weight polyphenols such as oleuropein. Accordingly, bioactive compounds found in olive leaves could be used not only in medical treatments, cosmetics, and pharmaceutical industry, but they can also be applied in the food industry as food supplements to improve stability and nutritional characteristics (Talhaoui et al., 2014).

Most of the studies have reported oleuropein as the most prominent phenolic compound present in the leaves and varies from 1% to 14% depending upon the harvesting time of the leaves compared to olive oil and olive mill wastewater which contain only (0.005–0.12%) and (0.87%), respectively (Stamatopoulos et al., 2012) . Numerous investigations in vitro and in vivo have been shown oleuropein many health benefits, such as antioxidant (Jemai et al., 2009), antibiotic (Naleini et al., 2015), anti-inflammatory (Park et al., 2017), antibacterial (Yuan et al., 2018), antiviral (Ma et al., 2001), anti-cancer (Sherifet al., 2018) and anti-diabetic (Al-Azzawie et al., 2006). Currently, bioactive components, such as oleuropein, have also been applied for the preparation of dietary supplements, nutraceuticals, functional food ingredients or cosmeceuticals (Vural et al., 2021).Consequently, the separation and recovery of oleuropein from olive leaves quite necessary and has attracted the attention of many researchers, because natural active compounds are safer for human health than synthetic chemicals (Khemakhem et al., 2017).

The profile of phenolic compounds in any plant leaf is usually carried out after extracting them using a suitable solvent. The extract quality and extraction efficiency are normally affected by several factors such as the extraction technique, type of solvent used and its concentration, the liquid–solid ratio, time and temperature of extraction etc. (Dahmoune et al., 2015). Regarding extraction method, soxhlet and simple maceration

extraction (Yateem et al., 2014), moderate electric extraction (Cokgezme et al., 2022), dynamic ultrasound-assisted extraction (Vural et al., 2021), pressurized liquid extraction (Jaski et al., 2019) and superheated liquid extraction (Japon-Luján et al., 2006) can be used.

To enhance the functional and nutritional properties of extracts, concentration methods must be applied, thus boosting the added value of the final product. Conventional methods used for extract concentration include adsorption, chromatography, electrophoresis, vacuum distillation and freeze–drying. These methods may involve high operational and energy costs or the use of high temperatures that can degrade thermosensitive compounds such as phenolic species (Mello et al., 2010).

Membrane technology could be a promising technology for the concentration of these sensitive biologically active compounds (Avram et al., 2017). The main advantages offered by this process are energy savings, low costs, no additives, selectivity and easy scaling up (Arend et al., 2017). This technique is based on the principle of selective permeation of the solute molecules through either polymeric or inorganic semi-permeable membranes (Murakami et al., 2011; Kiai et al., 2014; Cassano et al., 2013). Concentration by nanofiltration of bioactive compounds from a large variety of products has been found to be extremely efficient (Bras et al., 2015). In fact, Khemakhem et al., (2017) used a sequence of different membrane operations (micro-, ultra, and nano-filtrations) in order to concentrate oleuropein from aqueous extract of olive leaves. Likewise, Dammak et al., (2015) applied nanofiltration to concentrate aqueous oleuropein feed. However, there areno reports in the literature dealing with the integration of the solvent extraction, cross-flow UF and dead-end NF to obtain extracts concentrated in bioactive compounds from hydroethanolic olive leaves. Therefore, the integration of solvent extraction, which is an efficient technique to recover compounds, with membrane filtration, which has the abilityto concentrate sensible bioactive compounds, such as flavonoids and secoiridoids, without damaging them, can contribute to defeat the difficulties in obtaining a concentrated product.To the best of our knowledge, this is an innovative approach in the concentration and purification of phenolic compounds, mainly oleuropein.

The main goal of this work was to produce a stream rich in oleuropein from extract of olive leaves. Initially, the effect of extraction solvent on the recovery of total phenolic content has been investigated. Afterwards, an experimental central composite design (CCD)coupled with response-surface methodology was adopted to optimize the extraction conditions (solvent type, temperature, solid-to-liquid ratio and extraction time) in order to maximize the recovery of phenolic compounds from olive leaves. After that, the extract was processed by crossflow ultrafiltration (UF) followed by dead-end nanofiltration (NF) using different pressure drops. Different fractions were characterized in terms of total phenolics content, flavonoids content, antioxidant capacity and composition profile byHPLC-DAD.

4.4 Materials and Methods

4.4.1. Materials

Olea.europaea (variety Chemlali) leaves were collected from Sfax (Tunisia) in the middle of November 2020. Before the extraction processes, the leaves were washed and dried in the oven for 20 min, then milled and stored in darkness at 25°C. The same raw material lot was used in the whole optimization study.

4.4.2. Chemicals

For extraction experiments, ethanol was purchased from Fisher Chemical, and water was distilled using a Milli-Q system (Millipore, Bedford, MA, USA). For HPLC-DAD analysis, acetronitrile $\geq$ 99.9% and phosphoric acid (85%) was purchased from Carlo Erba and Sigma-Aldrich, respectively, and ultrapure water was obtained by the aforementioned Milli-Q system. Standard compounds used for the quantification were: Oleuropein (OLP) $\geq$ 98% is from Sigma-Aldrich. Tyrosol $\geq$ 99% and Hydroxytyrosol $\geq$ 98% are from Extrasybthese; Vanilic Acid $\geq$ 98.5% is from Acros Organics.

4.4.3. Methods

4.4.3.1. Extraction of phenolic compounds from olive leaves

a. Preliminary selection of solvents

Phenolic compounds were extracted from leaves of Olea.europaea according to the methods described by Szydłowska-Czerniak et al., (2012) with slight modifications. Briefly, 4 g of olive leaf powder was placed in a test flask and extracted with 40 mL of different solvents. The solvents used for the extraction were: (100% of water, 100% of ethanol, water (25%)/ethanol (75%), water (50%)/ethanol (50%), water (75%)/ethanol (25%). The flasks were sealed and continuously stirred in a shaking bath at 30°C during180 min. Then, the five extracts were centrifuged at 4000 rpm for 15 min in a centrifuge (NAHITA bleu, Modibas + centrifuge, mod.2741) and the supernatants were collected and stored at 4°C until further use. The extractions were repeated in triplicate for each studied solvent, and extracts were characterized in terms of phenolic contents (TPC).

b. Design of Experiments

In this study, a three-variable-three-level central composite design (CCD) was applied to determine the optimum conditions of the extraction of phenolic compounds from olive leaves. The independent variables were temperature (X_1), solid-to-solvent ratio (X_2) and extraction time (X_3), known to affect extraction yield and phenolic compounds contents (Carbone et al., 2020). The selection of the best combination of these variables was based on the highest value of total phenolic compounds (TPC) of the obtained extract. The total phenolic compounds (Y) was defined as the response variable for the experimental design.

The experimental design included 15 runs where each run was replicated twice. Each variable was coded at three levels, − 1, 0, +1, whereas temperature between 30 and 50°C; solid-to-solvent ratio between 0.03 and 0.15 g/mL and extraction time between 30 and 90 min (**Table 4.1**). In this context, the range of values of each variable was selected based on both the literature data and preliminary experiments.

Table 4.1: Independent variables and coded levels for Central Composite Design (CCD).

Independent variables	Coded variables	Levels		
		-1	0	1
Temperature (°C)	X_1	30	40	50
Solid-to-solvent ratio (g/mL)	X_2	0.03	0.09	0.15
Extraction time (min)	X_3	30	60	90

The predicted response for TPC (Y) was based on the following second-order polynomial equation shown below (Eq.4.1):

$$Y = \beta_0 + \beta_1 X_1 + \beta_2 X_2 + \beta_3 X_3 + \beta_{12} X_1 X_2 + \beta_{13} X_1 X_3 + \beta_{23} X_2 X_3 + \beta_{11} X_1^2 + \beta_{22} X_2^2 + \beta_{33} X_3^2 \qquad (4.1)$$

where Y is the response variable (TPC); X_1, X_2 and X_3 represent the independent variables selected; βi and βij are the regression coefficients of the model.

4.4.3.2. Membrane filtration experiments

The filtration process of olive leaf extract, performed through the combination of two membrane operations, is presented in **Fig. 4.2**. First, the feed stream was pre-treated in a cross-flow ultrafiltration system. Then, the ultrafiltration permeate was treated by a dead-end nanofiltration system.
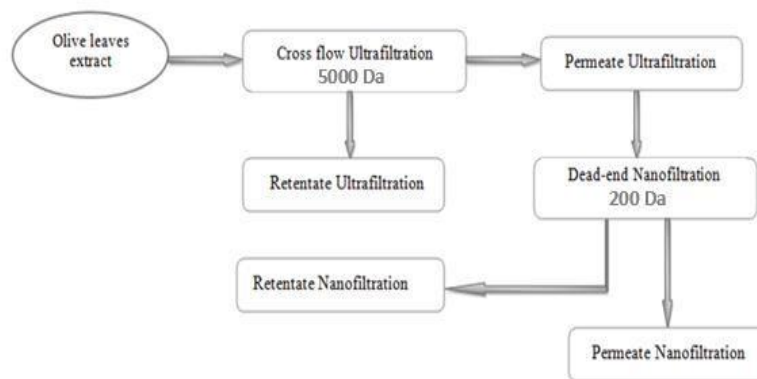
Figure 4.2: Schematic diagram of the membrane filtration process.

a. Crossflow ultrafiltration

Olive leaf extract was subjected to a preliminary UF process to remove suspended solids and macromolecular compounds, thus allowing to reduce the fouling phenomena in the subsequent NF process. The filtration experiments were carried out in a cross-flow membrane filtration unit (Sepa CF II Membrane Cell system, Sterlitech Corporation), with an effective membrane area of 140 cm^2, as shown in **Fig. 4.3**.
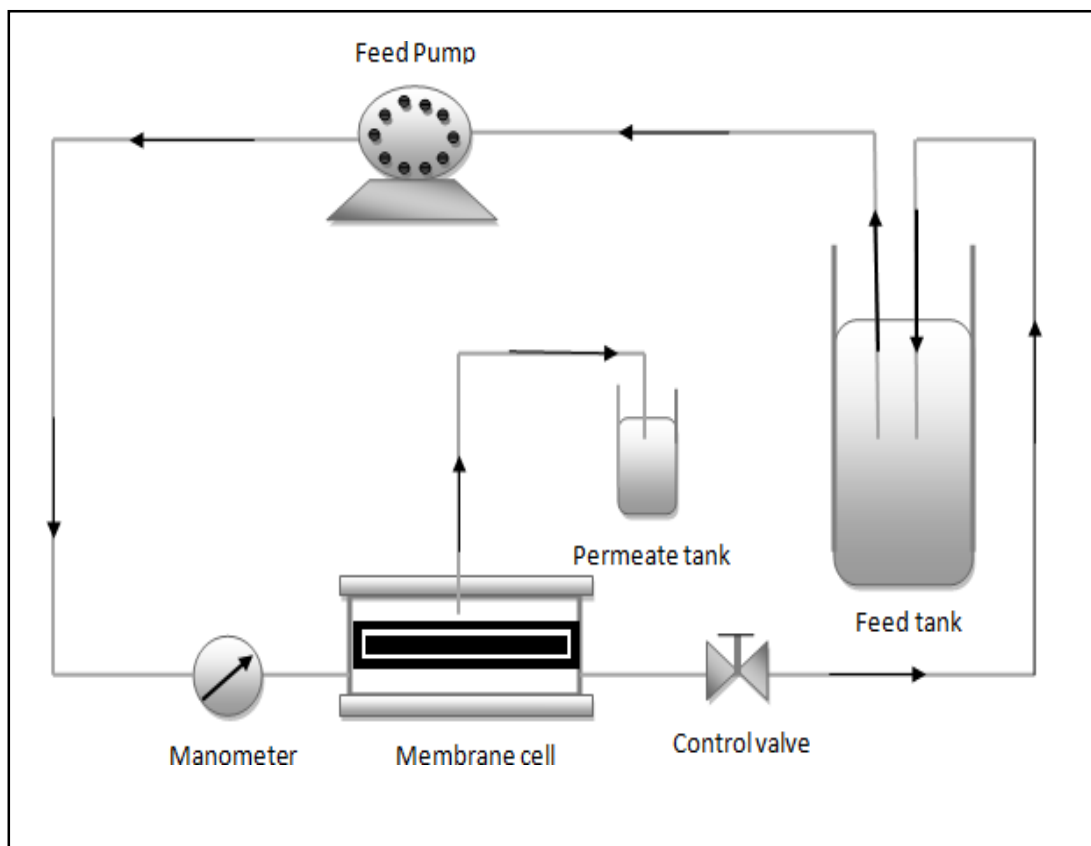
Figure 4.3: Schematic representation of crossflow ultrafiltration set-up.

This apparatus consists on a membrane module, a diaphragm pump (Hydra-Cell, Wanner Engineering, Inc.), a feed tank, a rotameter and valves to regulate pressure. The membrane used UP005 P was supplied by Germany advanced separation technologies (MICRODYN NADIR). Characteristics of the membrane module are reported in **Table 4.2**.

Table 4.2: Characteristics of the UF and NF membrane modules.

Characteristics	UF membrane	NF membrane
Manufacturer	Microdyn Nadir	Microdyn Nadir
Membrane Material	Polyethersulfone	Polyethersulfone
NMWCO (Da)	5.000	200
Configuration	Flat sheet	Flat sheet
Membrane surface area (m^2)	0.014	-
Typical operating pressure (bar)	5	40
Operating temperature (°C)	Maximum 50	5-95
Operating pH range	0.0-14.0	0.0-14.0
Thickness (μm)	210-250	210-250

UF experiments were performed by using an extract volume of 5 L according to a batch concentration configuration, where the permeate was collected and continuouslymeasured over time into a clean tank with the concentrate being recirculated back into the feed tank. The UF system was performed at a feed flow rate of 50 mL/min and at a constant transmembrane pressure (TMP) of 4 bar until reaching a volume reduction factor (VRF) of 2.3, corresponding to a phenolic compounds recovery factor of 33.01%. The feed reservoir temperature was maintained approximately at 25°C. The limit pressure of 4 bar was considered taking into account the membrane supplier's recommendation.

The permeate flux (J) through the ultrafiltration membrane, at a given pressure, was defined as the volume permeated per unit area and per unit time, according to Eq. (4.2):

$$J = \frac{V_p}{A_m t}$$

(4.2)

where Vp (L) is the volume of permeate, Am (m^2) is the membrane area, and t (h) is the operation time.

A cleaning-in-place procedure was used to recover the original water permeability after each experiment. The unit was rinsed with tap water, then a 1% NaOH solution was recirculated through the membrane module at a (TMP) of 2 bar, and an average temperature of 25°C for 60 min. Finally, the circuit was rinsed with distilled water until pH 7.

b. Dead-end nanofiltration

The clarified olive leaves extract was used as feed solution of the NF process. NF experimental runs were performed in dead-end filtration mode, at room temperature (RT) and stirring speed of 750 rpm/min, using bench scale filtration equipment (Sterlitech HP4750 Stirred Cell).

The stirred cell equipment has a volume capacity of 300 mL and is suitable for effective membrane area of 14.6 cm^2 .The filtration equipment was connected to a nitrogen gas cylinder to obtain the operational transmembrane pressure (TMP) for the filtration experiment. Characteristics of the membrane module are shown in **Table 4.2**. The experimental setup can be seen in **Fig. 4.4**.
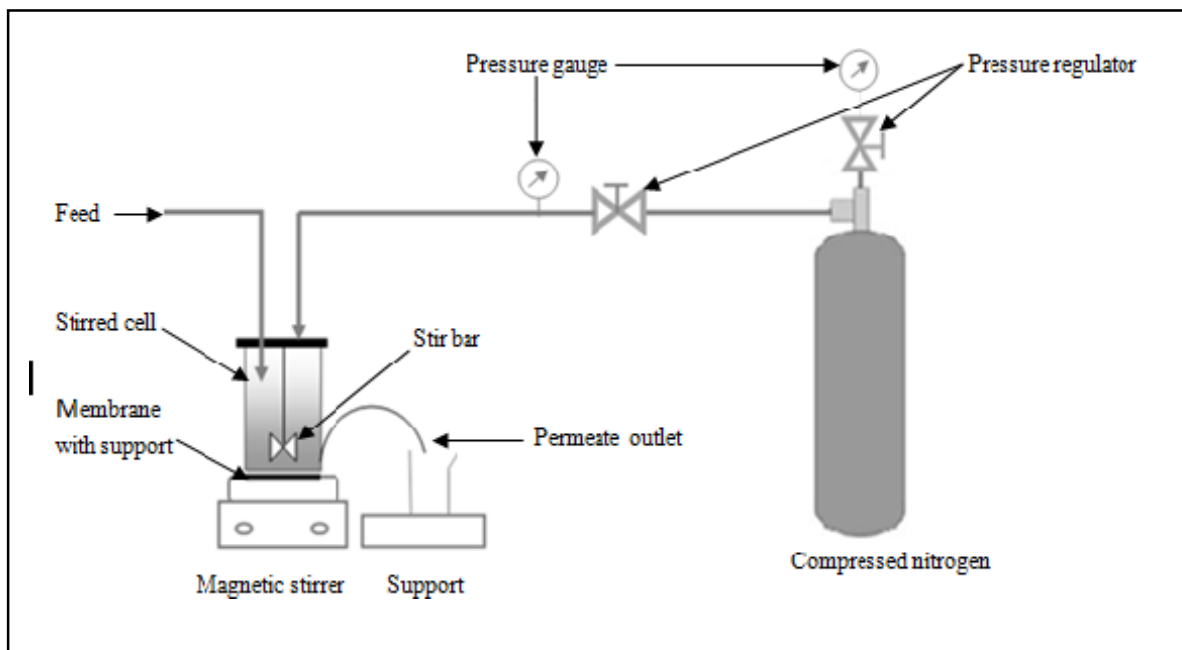
Figure 4.4: Shematic representation of dead-end set-up.

After each experiment of olive leaves extract filtration, the membrane was cleaned with 0.2 M NaOH solution to remove foulants from the membrane surface and pores. Subsequently, pure water flux (PWF) and hydraulic permeability (Lp) were tested to see if

there was any kind of change from initial values. The TMP used for NF experiments were 10, 20 and 30 bar and permeate samples were collected during 6 h.

c. Determination of pure water flux (PWF)

To evaluate the hydraulic permeability of membrane (Lp), water filtration was carried out at different pressure values (1, 2, 3 and 4 bar) for the ultrafiltration process and (5, 10, 20 and 30 bar) for the nanofiltration process. Lp values expressed in (L/m^2 h bar) were calculated according to Eq. (4.3).

$$L_p = \frac{V_w}{tA_m\Delta P} = \frac{J_w}{\Delta P} \tag{4.3}$$

where Vw (L), t (h), and Jw (L/m^2 h) represent the volume of permeate passing through the membrane, time for permeate collection, and PWF, respectively.

The PWF presents a linear relationship, for the filtration of distilled water, when plotted as a function of operational TMP. The slop of this straight line gives the average hydraulic permeability of the membrane in the pressure range used during the filtration experiment.

d. Determination of rejection coefficient (R) and volume reduction (VRF)

To evaluate the performance of UF and NF membranes towards specific compounds, the rejection coefficient (R) of each membrane was determined by the following equation:

$$R = (1 - \frac{Cp}{Cf}) \times 100 \tag{4.4}$$

where Cp and Cf are the concentration of a specific compound in the permeate and feed solution, respectively.

The volume reduction factor (VRF) is defined as the ratio between the initial feed volume and the volume of the resulting retentate. Thus, this factor is calculated as follows:

$$VRF = \frac{V_o}{V_f} \tag{4.5}$$

where V_o and V_f are the initial and final volumes for each process.

4.4.3.3. Analytical methods

a. Determination of total phenolic content (TPC)

Total phenolic compounds (TPC) was determined using the Folin-Ciocaltaeu method described by Szyd1owska-Czerniak et al. (2015). In this method, 100 µL of the extract was mixed with 100 µL of Folin-Ciocalteu solution, and then incubated at 25°C for 5 min. Afterwards, 300 µL of saturated Na_2CO_3 (0.333 g/mL) was added to each sample for another 30 min of incubation at 40°C. The absorbance was recorded at λ = 765 nm. A calibration curve was drawn with gallic acid at different concentrations (2–20 mg/mL, R^2 = 0.988). The results were expressed as milligram gallic acid equivalents (GAE) per gram of olive leaf powder (mg GAE/g OLP).

b. Determination of total flavonoids content (TFC)

Total flavonoids were determined in triplicate according to Costa et al., (2014). Inbrief, 1 mL of extract was mixed with 4 mL of distilled water and 300 µL of sodium nitrite $NaNO_2$ (25%). After 5 min of incubation at RT, 300 µL of 10% $AlCl_3$ were added to the mixture. After waiting 1 min, 2 mL of sodium hydroxide (1 M) and 2.4 mL of ultrapure water were also added. Absorbance measurements were performed at 510 nm. A calibrationcurve was prepared with catechin (50–450 mg/L; r = 0.998), and results were expressed as mg of catechin equivalents CAE per gram of olive leaves powder (mg CAE/g OLP).

c. Determination of the antioxidant activity by the DPPH method

DPPH free-radical scavenging activities of different olive leaves extract were determined as described by Szyd1owska-Czerniak et al., (2019). In this procedure, 0.5 mL of each olive leaf extract (or Trolox standard solutions in the concentration range 0.02–0.10 µmol/mL) was added to 1.5 mL of methanol and 0.5 mL of DPPH methanolic solution (304.0 mmol/mL) used as the source of free radicals. The mixtures were shaken vigorously and then left in the dark for 15 min. After this time, the absorbance was measured at 517nm against a reagent blank (2 mL of methanol + 0.5 mL of DPPH methanolic solution)

using a T60 UV–vis spectrophotometer in a 1 cm -disposable plastic cell. The scavenging of DPPH (x) was calculated as follows:

$$\%x = \frac{A_{control} - A_{sample}}{A_{control}} \times 100 \qquad (4.6)$$

where $A_{control}$ = absorbance of DPPH radical + methanol; A_{sample} = absorbance of DPPH radical + olive leaf extracts (or standard solutions).

However, the results of DPPH measurements for olive leaves extracts samples were obtained from the following linear relationship: f (concentration of Trolox) = DPPH scavenging (in %) for five Trolox standard solutions. Therefore, the DPPH values were expressed as micromoles of Trolox equivalents per gram of olive leaves (µmol Trolox/g OLP).

d. High-performance liquid chromatography (HPLC) analysis

HPLC quantification analyses of polyphenols present in different was performed on a Shimadzu Prominence UFLC chromatograph system. Phenolic compounds were separated on a Eurospher 100-5C18 RP column (250 × 4 mm id, 5 mm, Germany) and then analyzed using a DAD (SPDM20A) detector. The method applied was based on the one proposed by Mulinacci et al., (2001). The mobile phase was a mixture of A and B solutions: (A) is water adjusted to pH 3.20 with phosphoric acid and (B) acetonitrile. The elution gradient applied for a duration of 80 min as follow: 100–89% A (0–3 min), 89–87% A (3–41 min), 87–80% A (41–55 min), 80–75% A (55–70 min), 75–100% A (70–71 min), and finishing with an isocratic elution (100% A) during 9 min. The column temperature was maintained at 30°C and the mobile flow rate was fixed at 1 mL/min. Samples are filtered by 0.1 µm microfilter and the injection volume was 10 µL. The chromatographic profiles were measured at 215 and 280 nm. The tests were performed in duplicate.

The phenolic compounds were identified by comparing the retention times with those from standard solutions prepared with the pure substances in acetonitrile. Calibration curves were used to quantify the main compounds.

4.4.3.4. Statistical analysis

The results obtained are expressed as an average ± standard deviation (SD) of three measurements for all analytical determinations carried out in this study. Statistical analysis was done with JMP software (Version Pro 7.0, SAS) to find the desirability function and response surfaces of the response model. The statistical significance of the main effects, the interactions and the quadratic terms, regression coefficients and model fitting were evaluated by analysis of variance (ANOVA). The adequacy of the model was checked by the coefficient of determination R^2 and adjusted coefficient of determination R^2_{adj}. While the effect of type solvent on the TPC in the first stage and the correlation between the determined antioxidant activity applying DPPH test, oleuropein content and TPC were statistically assessed by ANOVA, using STATISTICA 5.5, to find significant differences among the different results. The statistical significance of each result was determined at 5% probability level ($p < 0.05$).

4.5. Results and discussion

4.5.1. Solvent screening

The effect of extraction solvent on TPC content was investigated by extracting the phenolic compounds from a fixed quantity of olive leaves and varying the composition of water–ethanol mixtures. Five different solvents mixtures of ethanol and water were employed as solvent: 100%, 75%, 50%, 25% and 0% (v/v). The results presented in **Fig. 4.5** showed that the highest extraction yield was obtained when the olive leaves are extracted with 75% ethanol aqueous mixture (v/v) with a value of 51.22 ± 1.07 mg GAE/g OLP followed by 50% ethanol (43.71 ± 0.16 mg GAE/g OLP), and 25% (33.88 ± 0.77 mg GAE/gOLP).

Regarding the pure water or pure ethanol, the amount of TPC extracted using these solvents is low; 24 ± 0.89 and 6.64 ± 0.31 mg GAE/g OLP for ethanol and water, respectively. Statistically, there is a significant difference in the TPC content with a change of solvent (type and composition) which is indicated by different small letters (a, b, c, d and

e). The result achieved was also found for other plant matrixes that reported that ethanol alone was less effective than hydroalcoholic mixtures, showing that the use of water as a co-solvent with organic solvents increases the amount of TPC extracted from olives leaves (Alonso-Riano et al., 2020 ; Kashaninejad et al., 2020).
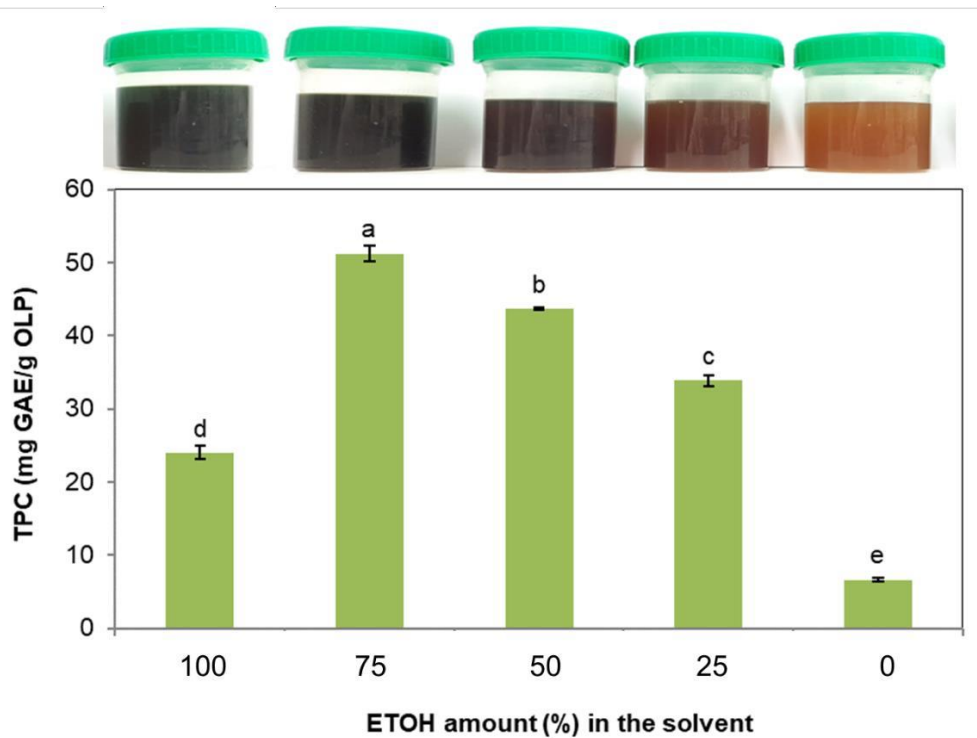
Figure 4.5: Olive leave extracts were obtained by using different solvents mixtures and their TPC contents.

The better efficiency of ethanol–water mixtures to improve TPC extraction compared to pure ethanol and water solvents has been explained considering the double effect of water and ethanol mixtures, since water swells the plant matrix, while ethanol could disrupt the bonding between the solute and the plant matrices (Kashaninejad et al., 2020). The addition of water to organic solvents, such as ethanol, helps to create a more polar medium that facilitates the extraction of compounds that are soluble in organic solvents and/or water (Socaci et al., 2018). Therefore, the mixture of water and EtOH as solvent agent exhibited the best performance to extract polyphenols of all the extractants used. Another explanation

might be the high dielectric constant of water, which leads to an increase in the polarity indices of EtOH with its water solution (Şahin et al., 2013).

Other values of TPC extraction yields found in the literature by using ethanol aqueous mixtures as solvent can be found in **Table 4.2**. In general, solvent mixtures with ethanol content higher than 50% (v/v) yielded good results for the different olive cultivars in terms of TPC and the most abundant phenolic compound in olive leaves, oleuropein. Regarding the different extraction methods, in general, the conventional extraction resulted in good extraction yields compared to other methods more energetically costly, such as Ultrasound-Assisted Extraction. Different TPC values were determined for the different olive cultivars, but in most cases, the values ranged from 10 to 100 mg GAE/g OLP for extraction times varying between 10 and 180 min, similar to the values obtained in this work.

The extracted color by using different ethanol aqueous mixtures can be appreciated in **Fig. 4.5**. The extraction of different pigments can be observed in the variation of the color of the liquid extract from light orange, by using water as solvent, to a more greenish color by using pure ethanol as solvent. The increase in the green color by increasing the amount of ethanol in the extraction solvent indicates the presence of chlorophylls in these extracts (Kashaninejad et al., 2020).

Table 4.3: Comparison of TPC and oleuropein content of olive leaves extracts from different olive leaves cultivars by using different extraction solvents (type/composition) and techniques.

Solvent	Extraction technique	Variety	S/L Ratio (g/mL)	TPC (mg GAE/gOLP)	T (°C)	t (min)	Oleuropein (mg/gOLP)	Reference
80 % EtOH	UAE	var. Serrana	0.03	66 ± 8	-	15	65 ± 2	(Ahmad-Qasem et al.,2013)
80 % EtOH	CE	Serrana de Espadán	0.05	37.6 ± 0.8	50	60	31 ± 2	(Kashaninejad et al., 2020)
75 % EtOH	CE	Chemlali	0.1	51.22 ± 1.07	50	180	Unknown	This work
70 % EtOH	CE	Istrska belica	0.2	32.7	25	120	27.3 ± 1.1	(Cifá et al., 2018)
70 % EtOH	UAE	Coratina	0.05	139 ± 2	35 ± 5	30	Unknown	(Difonzo et al., 2017)
70 % EtOH	UAE	Istrska belica	0.2	138.4	25	120	38.1 ± 1.8	(Cifá et al., 2018)
70 % EtOH	MAE	Arbequina	0.02	129.99	44	10	Unknown	(Da Rosa et al., 2019)
60 % EtOH	Soxhlet	Picual	0.06	42.9 ± 0.4	-	240	65.77	(Lama-Munoz et al., 2020)
60 % EtOH	DM	Picual	0.08	41.1	55	-	31.8	(Lama-Munoz et al., 2019a)
60 % EtOH	UAE	Picual	0.07	35.8 ± 0.6	-	17.9	69.91	(Lama-Munoz et al., 2019b)

Continuation

50 % EtOH	PLE	cv. Oblica	0.5	62.99 ± 0.43	80	10	Unknown	(Putnik et al., 2017)
50 % EtOH	UAE	Tavşan yüreği	0.05	20.37 ± 0.63	25	40	Unknown	(Şahin et al., 2013)
50 % EtOH	CE (pH =2)	Agrielia	0.2	≈30	25	180	Unknown	(Lafka et al., 2013)
47% EtOH	UAE	Picual	0.05	22.3 ± 0.8	RT	50	4.2 ± 0.2	(Del Contreras et al., 2020)
EtOH	UAE	Tavşan yüreği	0.05	10.15 ± 0.10	25	60	Unknown	(Şahin et al., 2013)
EtOH	UAE	Picual	0.05	14.1 ± 0.9	RT	30	14 ± 6	(Del Contreras et al., 2020)
EtOH	CE (pH =2)	Agrielia	0.2	≈36	25	180	Unknown	(Lafka et al., 2013)
Water	MAE	Hojiblanca	0.1	21.84 ± 0.37	50	22.5	Unknown	(Martín-García et al., 2020)
Water	CE	Chemlali	0.02	2.89	30	60	2.65	(Khemakhem et al., 2017)
Water	UAE	Tavşan yüreği	0.02	6.58 ± 0.22	25	20	Unknown	(Şahin et al., 2013)

CE : Conventional Extraction. DM : Dynamic Maceration. UAE: Ultrasound-Assisted Extraction. PLE: Pressurized Liquid Extraction.MAE: Microwave-assited extraction.

4.5.2. Extraction optimization

4.5.2.1. Fitting the model

To define the mathematical modeling of the experiments shown in **Table 4.4**, a second order polynomial equation Eq. (4.7) was generated to describe the relationship between the TPC of olive leaves and operational conditions (temperature, solid/liquid ratio and extraction time).

$$TPC = 25.43 + 12.56\,X_1 - 0.29\,X_2 + 0.09\,X_3 - 15.28\,X_1X_2 - 0.01\,X_1X_3 - 0.14\,X_2X_3 + 8.17X_1^2 - 0.83X_2^2 + 1.51X_3^2 \tag{4.7}$$

Table 4.4: The matrix of a central composite design for three factors with the total phenolic content (experimental and predicted) in the olive leaf extracts.

| Run | Coded Factors | | | Uncoded Factors | | | TPC (mg GAE/g OLP) | |
	X_1	X_2	X_3	Temperature, ^oC (X_1)	Solid-to-Solvent) Ratio, (g/mL) (X_2)	Extraction Time, min (X_3)	Experimental	Predicted
1	-1	-1	-1	30	0.03	30	6.39±0.22	6.47
2	-1	+1	-1	30	0.15	30	39.05±0.08	36.75
3	-1	0	0	30	0.09	60	17.23±0.00	21.04
4	-1	-1	+1	30	0.03	90	6.52±0.48	6.96
5	-1	+1	+1	30	0.15	90	38.72±0.36	36.67
6	0	0	-1	40	0.09	30	25.72±0.72	26.84
7	0	-1	0	40	0.03	60	29.23±0.00	24.88
8	0	0	0	40	0.09	60	26.45±0.40	25.43
9	0	0	0	40	0.09	60	26.49±0.68	25.43
10	0	+1	0	40	0.15	60	18.92±0.09	24.30
11	0	0	+1	40	0.09	90	27.12±0.14	27.03
12	+1	-1	-1	50	0.03	30	60 .42±0.55	62.20
13	+1	+1	-1	50	0.15	30	32.04±0.26	31.33
14	+1	0	0	50	0.09	60	48.95±0.01	46.17
15	+1	-1	+1	50	0.03	90	60.63±0.21	62.66
16	+1	+1	+1	50	0.15	90	31.56±0.46	31.21

An analysis of variance ANOVA is an important statistical tool widely used to further verify the accuracy of models; it was performed to determine if the quadratic model is significant. ANOVA results for the model shown in **Table 4.5** indicated that the model was highly significant ($p < 0.01$), as clear from the high value of the F-test and low p-value.

The linear regression coefficient of experimental value vs predicted ($R^2 = 0.9800$) indicates that only 2.04% of the total variations are not explained by the model. For a good statistical model, the adjusted determination coefficient (R^2_{adj}) should be close to R^2. As shown in **Table 4.5**, both the regression coefficients were close to 1 ($R^2 = 0.9800$ and $R^2_{adj} = 0.9759$), this indicates a high degree of correlation between the experimental and the predicted values **Fig. 4.6**.

The coefficient of variation (CV = 4.75%) and root mean square error (RMSE = 2.8968) were very low, which highlights that the experimental and predicted values are very close.

Accordingly, a high degree of precision and a good precision of the experimental values (Fratoddi et al., 2018; Dairi et al., 2021). Therefore, the proposed model is adequate and could work well for the prediction of phenolic compounds extraction from olive leaves in the range of experimental variables. The significance of each coefficient measured using p- and F-values listed in **Table 4.5**. A smaller p-value and greater F-value mean that the studied variables are significant in the considered response (Dahmoune et al., 2014). The proposed model has a p-value < 0.001, which means that it is significant and can be used to optimize the different extraction variables. The independent variable (X_1) and the quadratic terms (X_1^2) significantly affect the extraction of TPC within a 95 % confidence interval. In addition, the interaction between the temperature (X_1) and the solid-to-solvent ratio (X_2) is significant (p < 0.01). Meanwhile, temperature (X_1) has the dominant effect on the extraction of TPC from olive leaves.

Table 4.5: Estimated regression coefficients for the quadratic polynomial model and the analysis of variance (ANOVA) for the experimental results for phenolic compounds extraction.

Parameter	Estimated coefficient	Standard deviation	Sum of Square	Degree of Freedom	F-value	P > F	Significance
Model	-	-	7455.05	9	98.71	<0.001	**
Intercept							
Q_0	25.43	0.9697	-	-	-	-	
Linear							
X_1	12.56	0.6477	3159.09	1	376.46	<0.0001	**
X_2	-0.29	0.6477	1.68	1	0.20	0.6582	ns
X_3	0.09	0.6477	0.17	1	0.02	0.8853	ns
Interaction							
X_1X_2	-15.28	0.7241	3739.93	1	445.68	<0.0001	**
X_1X_3	-0.01	0.7241	0.0016	1	0.00	0.9891	ns
X_2X_3	-0.14	0.7241	0.33	1	0.03	0.8445	ns
Quadratic							
X_1^2	8.17	1.2615	352.64	1	42.02	<0.0001	**
X_2^2	-0.83	1.2615	3.67	1	0.43	0.5152	ns
X_3^2	1.51	1.2615	12.03	1	1.43	0.2439	ns
Statistics							
R^2	0.9800	-	-	-	-	-	
R_{adj}^2	0.9759	-	-	-	-	-	
RMSE	2.8968	-	-	-	-	-	
CV %	4.75	-	-	-	-	-	

X_1: Temperature (°C); X_2: solid-to-solvent ratio (mg/L); X_3: extraction time (min). ** indicate significance at $p < 0.001$ and ns indicates not significant.
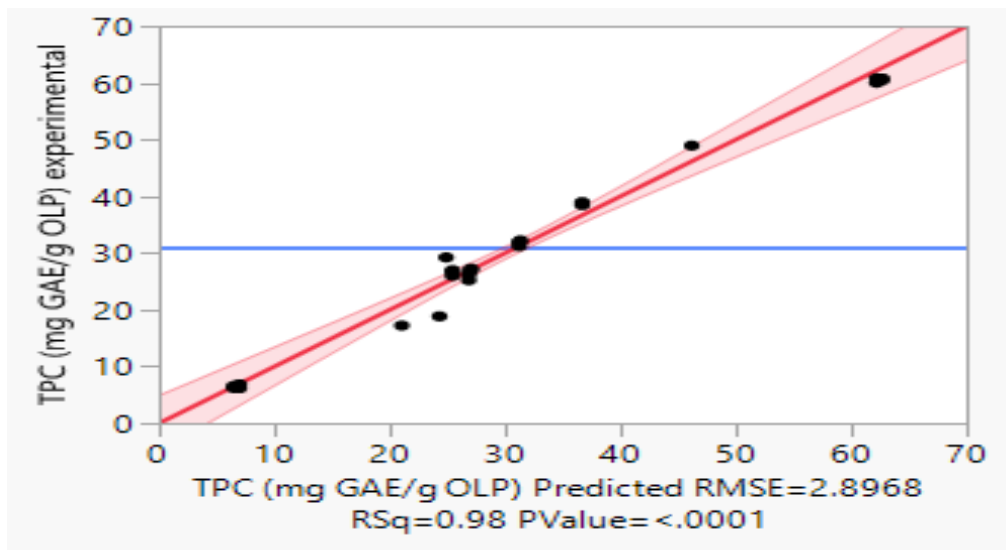
Figure 4.6: Experimental vs predicted value for phenolic compounds extraction.

4.5.2.2. Analysis of desirability function and response surface

To achieve the optimum extraction conditions and to visualize the effects of the independent variables on the TPC extraction from olive leaf extract, the desirability function and response surfaces were generated.

The desirable function (DF) was used to find the optimal value for all the investigated variables. Profiling the desirability of responses involves specifying the DF for each dependent variable by assigning predicted values over a scale in the range of 0.0 (undesirable) to 1 (very desirable) (Khodadoust et al., 2018). **Fig. 4.7** presents the desirability function graphs for each parameter. Hence, the predicted optimal values for the independent variables were as follows: T = 50°C; solid-to-solvent ratio = 0.03 g/mL;extraction time = 90 min.
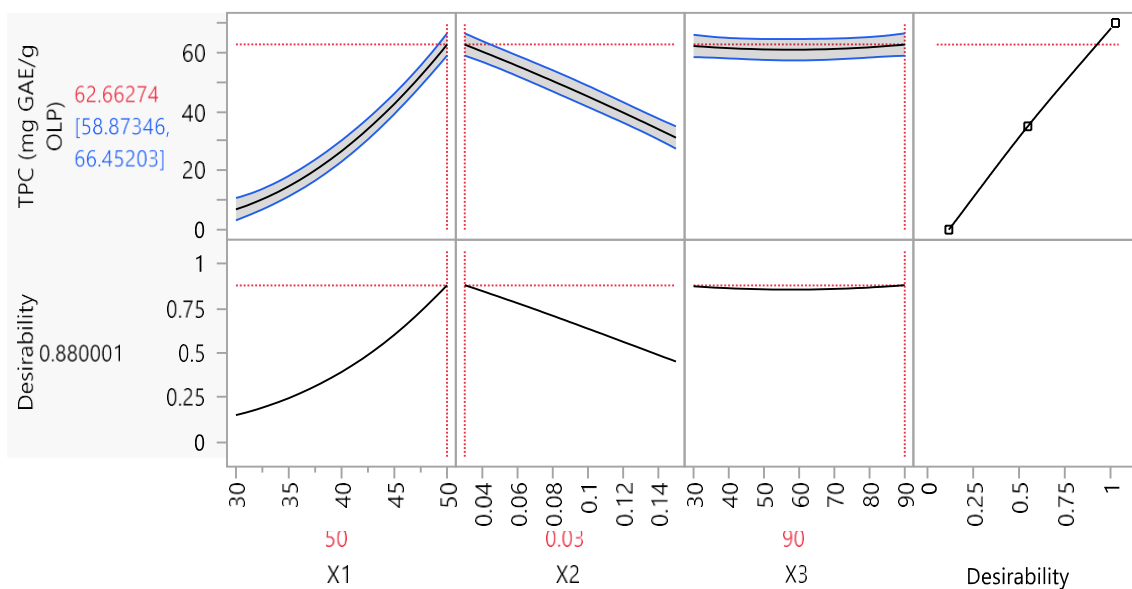
Figure 4.7: Profiles for predicted values and desirability function for the extraction of total phenolic compounds from olive leaf extract. Red lines indicate optimized values for each process parameter (X_1 = Temperature, X_2 = solid-to-solvent ratio, X_3 = extraction time).

The effects of independent variables on TPC are shown in 3D response surfaces (**Fig. 4.8A–C**). The response 3D surface is the graphical representation of the regression equation

and is very helpful to judge the effect of each pair of independent variables at different combination levels on the extraction of phenolic compounds, with the remaining independent variables fixed at zero level (Liu et al., 2013). The plots allow not to obtain only the values that lead to the optimal conditions, but also the mutual interactions between variables on TPC.

In the present study, a strong interaction between the extraction temperature and solid-to-solvent ratio was found (**Fig. 4.8A**). By increasing the temperature up to 50°C and decreasing the solid-to solvent ratio to 0.03 g/mL, the maximum content of phenolic compounds was obtained. On the other hand, decreasing temperatures to 30°C and increasing the solid-to-solvent ratio to 0.15 g/mL resulted in a minimal TPC yield. These results are justified by the fact that the driving force during mass transfer is the concentration gradient between the solid and the bulk of the liquid, which is higher when a lower solid-to solvent ratio (S/L) is used. Lower S/L values promote an increase in the surface contact of the plant matrix with the solvent, with a consequent increase in extraction yields, which will be positively influenced by the increase in the temperature of the extraction medium due to the greater diffusivity of the solvent within the solid matrix.

Considering the combined effect of the temperature and extraction time on total phenolic compounds, the response surface plot suggests that the highest TPC value can be obtained when the two factors increased (**Fig. 4.8B**). Similar results were also observed by Yingngam et al., (2014) for phenolic compounds extraction from Cratoxylum formosum ssp. formosum leaves using Central composite design and Bashi at al. (2012) for phenolic compounds extraction from Yarrow (Achillea beibrestinii) using Box-Behnken design.

Finally, as shown in **Fig. 4.8C,** the effect of the ratio S/L and time on TPC was not obvious. For an X_2 in the range of (0.06–0.1 g/mL) and different values of X_3, the highest TPC value was obtained.
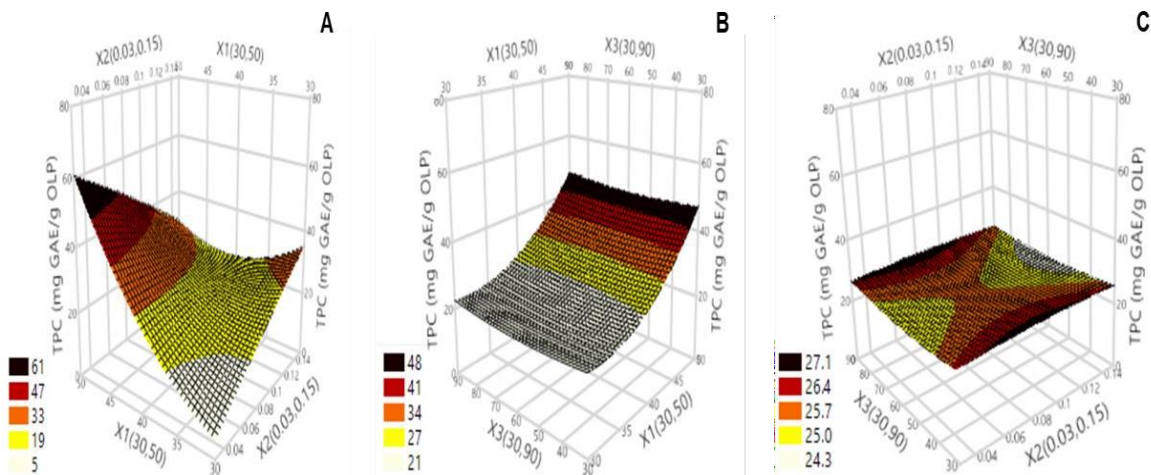
Figure 4.8: Response surface of olive leaf extract as a function of (a) X_1 = Temperature and X_2 = Solid-to-solvent ratio; (b) X_1 = Temperature and X_3 = time; (c) X_2 = Solid-to-solvent ratio and X_3 = time.

4.5.3. Membrane filtration process

4.5.3.1. Determination of pure water flux (PWF)

The water permeability of the membrane was found to be 6.012 and 0.68 (L/ h m^2 bar) for UF and NF membranes, respectively. These values were determined from the slope resulting from the linear fit when the permeate flux was expressed as a function of TMP.

4.5.3.2. Permeate flux of UF and NF processes

Permeate flux of crossflow UF system at 4 bar and dead-end NF system at 10, 20 and 30 bar were measured with time. **Fig. 4.9** shows permeate flux (J) decline in terms of liters of permeate produced per unit time and area (L/h m^2) in ultrafiltration (a) and nanofiltration (b) processes up to VRF of 2.3 and 3.5 respectively.

As shown in **Fig. 4.9A**, the initial permeate flux of the UF membrane of about 34.42 L/h m^2 declined gradually over time and finally reached a reduction of 55.12%. A similar trend was observed for the NF system. These results are similar to that observed byCassano et al., (2013) during the fractionation of olive mill wastewaters by membrane

separation, Khemakhem et al., (2017) during the fractionation of aqueous olive extract by membrane separation and Benedetti et al. (2015) in the treatment of tofu whey by nanofiltration processes. This behavior can be explained by the increase of the thickness of the gel layer over the membrane surface. This increases the resistance against the solvent flow, and the permeate flux decreases (Conidi et al., 2019).

The permeate flux of the NF system declined very rapidly during the initial filtration step and after a certain period, it reached an almost stationary value, as shown in **Fig. 4.9B**. The reduction in permeate flux in the NF process was about 50%, 50.7% and 50.9% at 10, 20 and 30 bar, respectively. Arend et al., (2017) and De Santana Magalhães et al. (2019) observed the same profile for the permeate flux in the separation of phenolic compounds from strawberry juice by NF and pequi fruit extract by direct NF, respectively. According to these authors, this decrease can be justified by the concentration polarization, deposition of solute molecules on the membrane surface and filling of the pores.

Besides that, as can be seen in **Fig. 4.9B**, initial and steady-state permeate flux measured for the NF membrane during the filtration of the olive leaves extract increased byincreasing the applied pressure, as expected.
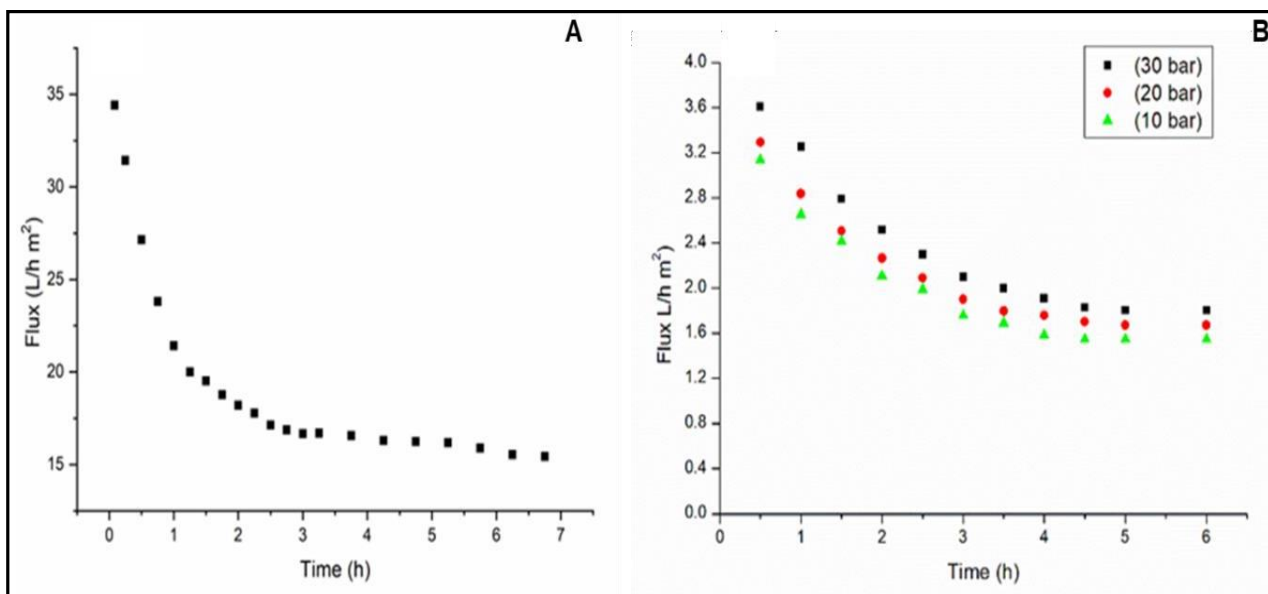
Figure 4.9: Permeate flux behavior of olive leaves extract during UF (a) and NF (b) processes.

4.5.3.3. Performance of UF and NF membranes in the extract filtration process

a. Total phenolic and flavonoid contents

Analyses of total phenolic compounds in different samples coming from the UF andNF treatment are reported in **Fig. 4.10A**. Results showed a low rejection coefficient of crossflow UF membrane towards phenolic compounds of about 33.01%. On the contrary, the rejection factor of those compounds by the dead-end NF membrane was 95.2% at 30 bar. This result can be explained by the low MWCO of this membrane, which was 200 Da and the molecular weight of the analyzed compounds which are in the range of 140 and 610g/mol (Conidi et al., 2017). Vitor Pereira at al., (2020) also found a low rejection coefficient of 42% for UF membrane compared to 69% obtained for NF membrane during the concentration of phenolic compounds from grape marc. The most important mechanismof rejection is the physical sieving, which hinders the permeation of solutes larger than the membrane MWCO (Bellona et al., 2004). UF membrane clarified the feed solution and allows most phenolic compounds to permeate through the membrane. A concentration of phenolic compounds of 39.01 mg GAE/g OLP was found in the UF permeate. An analogous result was obtained by Cassano et al., (2013). A high rejection value wasobtained by dead-end NF membrane thus fulfilling our main objective, which is to concentrate phenolic compounds from the hydroethanolic extract of leave olives. Therejection coefficient can be affected by the membrane's material and surface charge, andthe possibility of complexation of compounds with other molecules (Pereira et al., 2020). Physical sieving of molecules larger than the MWCO of the membrane is the majormechanism of solute rejection by NF. Every phenolic compound with MWCO more than 200 Da will be strongly retained (95%) by the membrane used (Khemakhem et al., 2017). Consequently, the rejection of NF membranes towards phenolic compounds decreased by increasing the MWCO of the membrane (Conidi et al., 2012). These results are very similarto those reported by M. Avram et al., (2017), who were able to obtain 100% retention to concentrate polyphenols from blueberry pomace extract using NF250. In addition, Bras et al., (2015) achieved a rejection near 100% for phenolic compounds from Cynara cardunculus var. altilis.

According to the experimental result presented in **Fig. 4.10A**, phenolic compounds were 3 times more concentrated using the dead-end NF membrane to reach 120.43 mg GAE/gOLP, as is clear from the color of the NF retentate shown in **Fig. 4.11**. However, the NF permeate was a clear solution (see **Fig. 4.11**). This result is confirmed by De Santana Magalhães et al., (2019) who have used direct and sequential membrane filtrations toconcentrate phenolic compounds from pequi (Caryocar brasiliense Camb.) fruit extract and Cassano et al., (2013) who have used the UF and NF techniques to fractionate olive mill wastewaters.

Fig. 4.10B displays rejection coefficient values towards flavonoids of 29.05 and 95.27% for UF and NF at 30 bar, respectively. The high rejection exhibited by the NF membrane for flavonoids is explained by that the majority of them had a higher molecular weight than MWCO of the NF membrane (Khemakhem et al., 2017). The process of nanofiltration started with 22.20 mg CAE/g OLP for the feed and finished with 75.92 mg CAE/gOLP for the extract in the retentate. Concentration values of feed and NF retentate indicate that flavonoids were concentrated approximately 4 times.
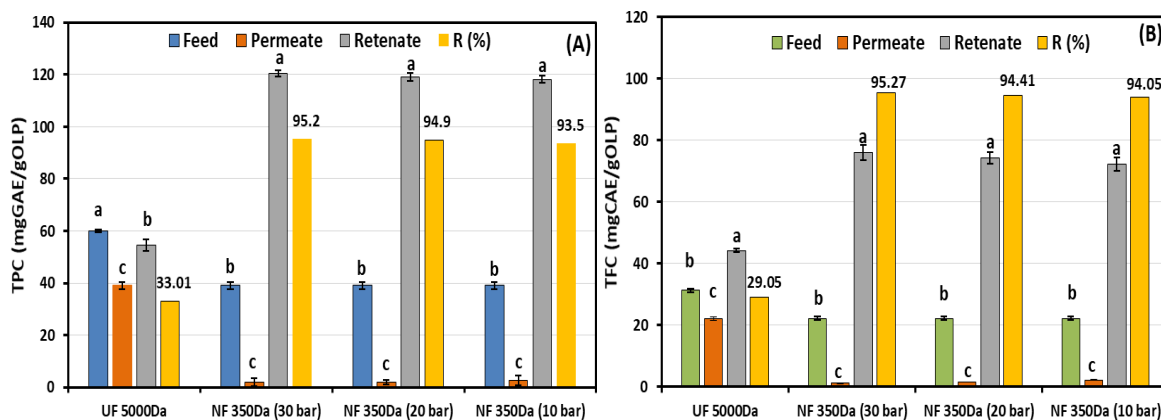
Figure 4.10: Total phenolics (A) and flavonoids (B) contents in feed stream, retentate and permeate of cross-flow ultrafiltration system and dead-end nanofiltration system processes. a–c Different letters in the same line indicate significant differences (p < 0.05) between fractions of the same membrane.

From **Fig. 4.10A-B** can also be observed that the highest rejection coefficient of TPC
and TFC achieved were approximate 95.2 and 95.27%, respectively, at 30 bar followed by
20 bar. Thus, the rejection of TPC and TFC are slightly enhanced by increasing theoperating
pressure in the range of 10–30 bar. The transport of permeate from pressure- driven
membrane can be a result of convection (due to pressure gradient) or diffusion (due to
concentration gradient). At high pressure the diffusion transport does not have much
relevance, mainly being convection, and consequently the pressure gradient, directly
proportional to the permeate flow. Conversely, under low pressure, the diffusion transport
mainly contributes to the permeate flow, which tends to minimize the concentration gradient,
hence the concentration in permeate increases and the rejection decreases (Manorma et al.,
2021).

Based on the results cited above, dead-end NF proved to be a good alternative for the
concentration of phenolic compounds and flavonoids in the hydroethanolic extract of olive
leaves. Furthermore, these data were obtained by clean technology without causing
nutritional degradation.
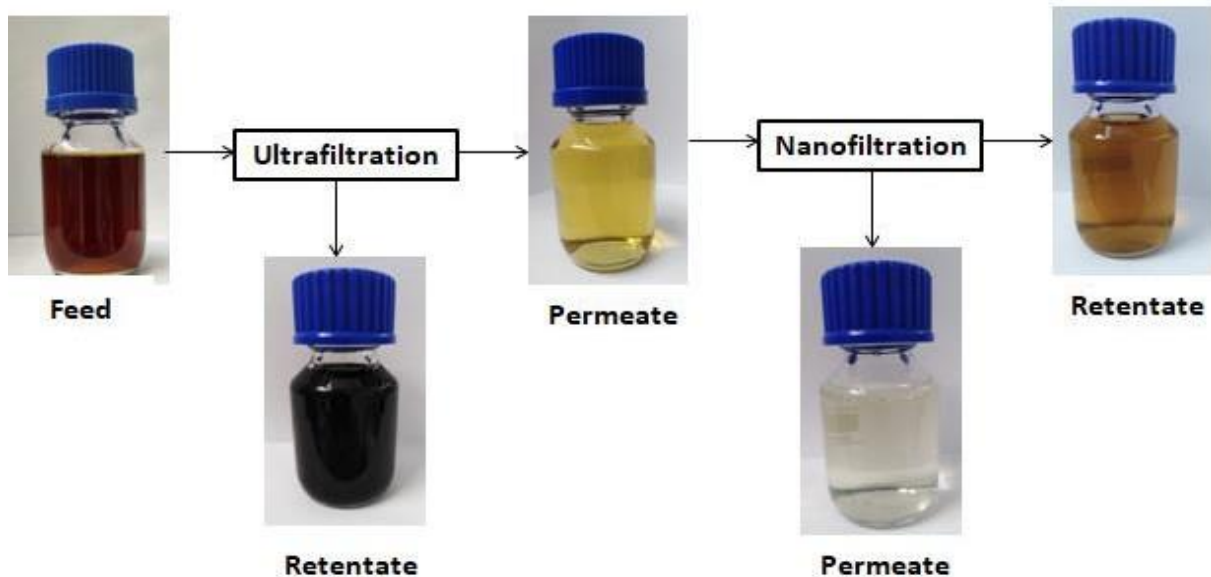
**Figure 4.11: Permeate and retentate samples obtained by clarification and
concentration of olive leaves by cross flow UF and dead-end NF.**

b. Quantification of polyphenols by HPLC-DAD analysis

The concentrations of main polyphenols in permeate and retentate produced by UF and NF at (30 bar), determined by HPLC analysis, are reported in **Table 4.6**. Feed, permeate and retentate chromatographic profiles are shown in **Fig. 4.12(a)–8(e).** Results presented in **Table 4.6** and **Fig. 4.12** highlight that the highest presence of polyphenols detected in the original olive leaf extracts corresponds to oleuropein with a concentration of 77.83 mg/gOLP. Different rejection values by UF membrane of about 43, 28.2, 23.2 and 37.7% were found for oleuropein (Mw = 540 g/mol), vanillic acid (Mw = 168.14 g/mol), tyrosol (Mw = 138.164 g/mol) and hydroxytyrosol (Mw = 154.16 g/mol), respectively, due to differences in their low molecular weights. These results confirm previous studies concerning the lower rejections of UF membranes obtained towards low molecular weight polyphenols (Khemakhem et al., 2017; Dekanski et al., 2011). The amount of oleuropein found in the retentate fraction of the UF experiment was 17.38 mg/g OLP. This behavior could be attributed to higher adsorption of phenolic compounds for PES membranes due to polar interactions (mainly van der Waals interactions and hydrogen bonds) between membrane components and polyphenols (Cassano et al., 2016). On the contrary, 100% rejection of oleuropein was achieved with NF membrane (200 Da), avoiding completely theloss of these compounds into the permeate. Similar results have been reported by Cassano et al., (2013), in the fractionation of olive mill wastewaters using NF 90 and Avram et al., (2017), in the concentration of phenolic compounds from blueberry pomace extract using NF270 and NF245 exhibiting 100% rejection towards low molecular weight polyphenols. In our work, the main goal is to produce a fraction of hydroethanolic extract rich in oleuropein from olive leaves. According to the nanofiltration results, NF PES 200 membrane showed a good performance in terms of concentration of oleuropein considering that the retentate fraction enriched in oleuropein contained 119.01 mg/gOLP.

Table 4.6: Analysis of identified polyphenols in feed stream, retentate and permeates of cross-flow ultrafiltration system and dead-end nanofiltration system processes and the antioxidant capacity (DPPH) of fractions.

Membrane type	Sample	Oleuropein (mg/gOLP)	R_O (%)	Vanilic acid (mg/gOLP)	R_V (%)	Tyrosol mg/gOLP)	R_T (%)	Hydroxytyrosol (mg/gOLP)	R_H (%)	DPPH (µmol of Trolox/gOLP)	R_{DPPH} (%)
UF 5000 Da	Feed	77.83±00[a]	43	6.93±00[a]	28.2	0.99±00[a]	23.2	4.86±00[a]	37.77	627.89 ±0.01[b]	22.88
	Retentate	17.38±00[b]	-	1.76±00[b]	-	0.22±00[b]	-	3.03±00[b]	-	445.21±12[a]	-
	Permeate	43.66±00[c]	-	4.97±00[c]	-	0.76±00[c]	-	2.8±00[c]	-	851.85±0.08[c]	-
NF 200 Da 30 bar)	Feed	43.66±00[b]	100	4.97±00[b]	100	0.76±00[b]	100	2.8±00[b]	100	445.21±0.05[b]	94.7
	Retentate	119.01±00[a]	-	12.57±00[a]	-	1.97±00[a]	-	7.13±00[a]	-	23.2±0.12[a]	-
	Permeate	0±00[c]	-	0±00[c]	-	0±00[c]	-	0±00[c]	-	1423.4±0.09[c]	-

[a–c]Different letters in the same column indicate significant differences ($p < 0.05$) between fractions of the same membrane.
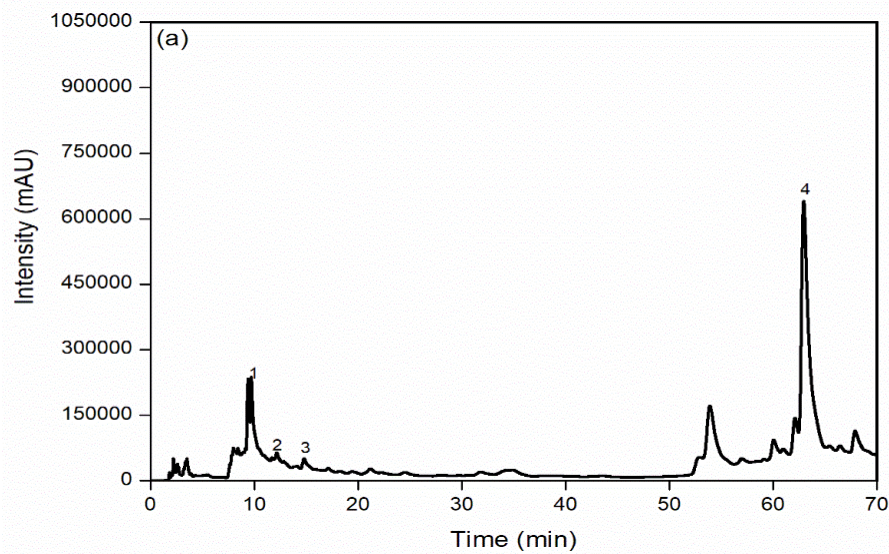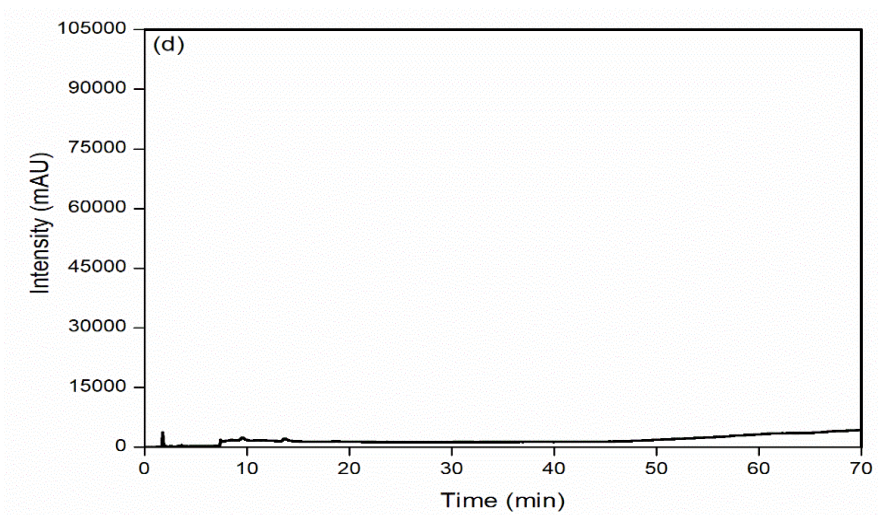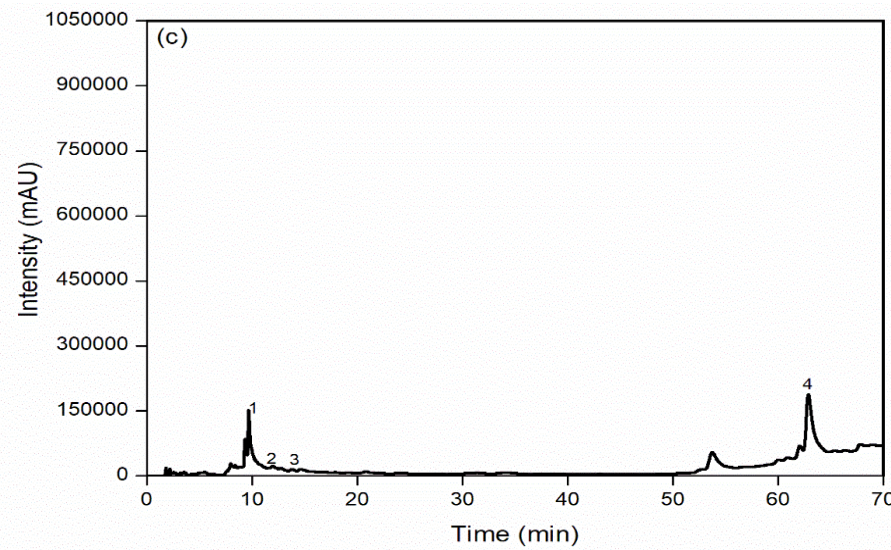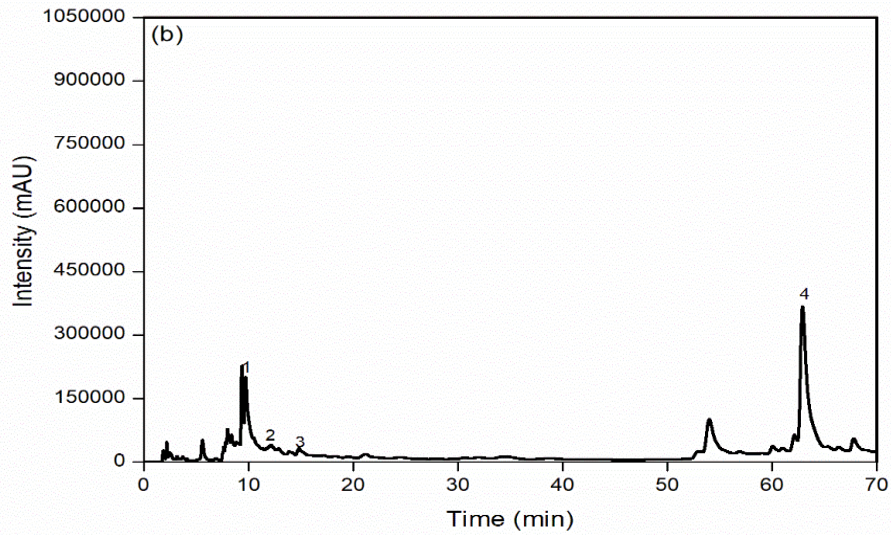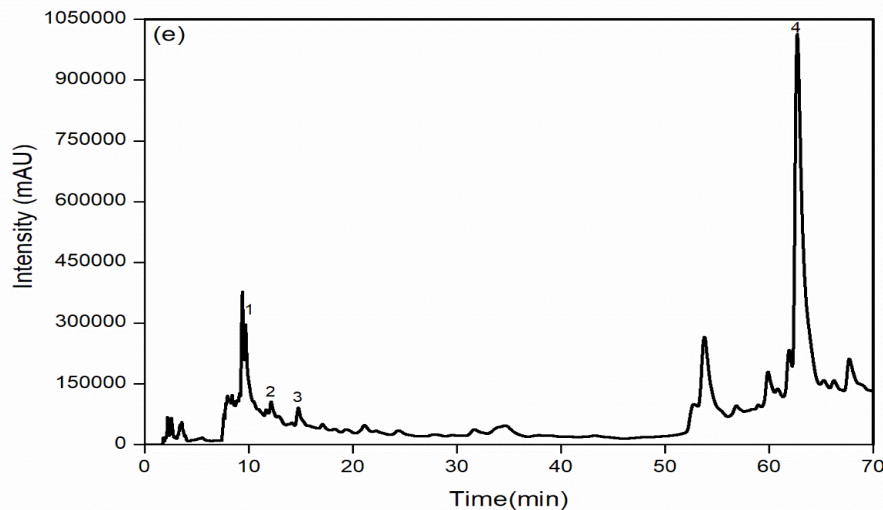
Figure 4.12: HPLC chromatograms of polyphenols in feed (a); permeate UF (b); retentate UF (c) permeate NF (d) and retentate NF (e). (1) Hydroxytyrosol; (2) Tyrosol; (3) Vanilic acid; (4) oleuropein.

c. Antioxidant capacity

The antioxidant capacity determined by the DPPH method of each sample coming from crossflow UF and dead-end NF processes are presented in **Table 4.6**. According to the obtained results, the DPPH assay indicated that the retentate from the dead-end NF can be considered the richest fraction in antioxidants, containing 1423.4±0.09 µmol of Trolox/gOLP. These results are consistent with those reported by Arend et al., 2017 and Conidi et al., (2015) who found that the NF process improved the antioxidant activity of strawberry and bergamot juice, respectively. This result may be can be explained by the high presence of phenolic compounds, mostly oleuropein in olive leaves hydroethanolic extract. Therefore, the DPPH values of all fractions were correlated with polyphenols and oleuropein contents. A high correlation (p < 0.01) was obtained between total phenolic contents and antioxidant activity ($R^2 = 0.975$). In addition, a significant correlation (p < 0.01) was obtained between oleuropein contents and DPPH values ($R^2 = 0.978$). The strong correlation coefficients between DPPH values and oleuropein content can be explained by the fact that in olive leaf extract the antioxidant activity is attributed mainly to the oleuropein content, which, according to Yateem, H et al., (2014) is one of the major phenolic compounds in olive leaves. Furthermore, Goulas et al., (2010) established that

secoiridoids (primarily oleuropein) are responsible for 15–51% of the DPPH• scavenging activity of olive leaf extracts. In fact, different reports are found in the literature, whereby some authors suggested no relationship between total phenol compounds and antioxidative activity (Yu et al., 2002; Babbar et al., 2011). Nevertheless, other studies have found a linear correlation between phenolic content and antioxidant activities in fruits, vegetables, grain and olive oils (Alu'datt et al., 2011). In addition, Orak et al., (2019), Altiok et al., (2008) and Kiritsakis et al., (2010) showed a high correlation between the total phenol content and antioxidant capacities of various cultivars of olive leaves extracts. Thus, it can be concluded that the antioxidant activity of olive leaf extract is directly affected by the levels of total phenols and oleuropein (Khemakhem et al., 2017).

4.6. Conclusions

Extract rich in total phenolics, oleuropein, and higher antioxidant capacity was obtained from olive leaves by solvent extraction and concentrated by membrane filtration. In this study, the optimum operating condition that maximizes the extraction of phenolic compounds was found using the mixture ethanol: water, 75/25% (v/v). A fractional factorial design and desirability profile were used for the optimization of the process variables (temperature, solid-to-solvent ratio and extraction time) and to investigate their interactions. The optimum conditions for the highest recovery of phenolic compounds from olive leaves were 50°C, 30 mg/L and 90 min. In addition, the results obtained from the crossflow UF showed that the process was efficient in clarifying the olive leaf extract and the use of its permeate for the NF process in dead-end mode, due to the lower rejection coefficient towards phenolic compounds, flavonoids and oleuropein. The NF process presented a high rejection coefficient for the studied compounds. Eventually, a purified fraction (NF retentate) enriched in polyphenols, mainly oleuropein, was obtained. Accordingly, the produced retentate fraction exhibited the highest antioxidant activity and can be considered of interest for nutraceutical applications. The extraction and concentration of bioactive compounds from olive leaves using the integration of solvent extraction and UF and NF processes is promising and should be investigated on a pilotscale for possible industrial applications.

CHAPTER 5 :Novel polyethersulfone mixed matrix adsorptive nanofiltration membrane fabricated from embedding zinc oxide coated by polyaniline

This Chapter is based on the publication:

5.1 Abstract

Novel mixed matrix polymeric membranes were prepared by incorporating self-produced zinc oxide coated by polyaniline (ZnO-PANI) nanoparticles into polyethersulfone (PES) matrix using phase inversion method. Nanoparticles were synthesized, characterized and incorporated in PES matrix with loadings from 0.05 to 0.6 wt% ZnO-PANI demonstrated effectiveness as a low-cost adsorbent, especially at a loading of 0.2 wt% ZnO-PANI was used for adsorbing total phenolic compounds (TPC) from olive leaf extract (OLE) at different initial adsorbate concentration (49.92–466.59 mg/L) and pH (2–6). ZnO-PANI proved to be an effective and low-cost adsorbent to remove TPC from OLE. Langmuir model described the adsorption of TPC better than Freundlich model. Effect of incorporated nanoparticles on membranes morphology and hydrophilic properties studied using contact angle measurement, water content, membrane pore size and porosity, SEM, FTIR and pure water flux. Prepared membranes showed a significant increment in porosity, pore size and hydrophilicity by addition of ZnO-PANI in the casting solution up to 0.2wt%. This led to a considerable improvement in permeability, which decreased with higher additive concentration. During OLE filtration tests (10-30 bar) using bare PES and 0.2 wt% ZnO-PANI/PES membranes, 0.2 wt% ZnO-PANI/PES showed the highest permeate flux and good TPC rejection (83-87%). Bare PES exhibited impressive TPC value rejections (85-92%) and better fouling resistance. Using 0.2 wt% ZnO-PANI achieved a balanced permeate flux and TPC rejection. The research emphasizes the practical applicability of these membranes in various industries due to their enhanced efficacy in removing phenolic compounds from natural extracts, offering a balanced approach between permeate flux and TPC rejection.

Keywords: Olive leaves; Phenolic compounds; ZnO-PANI nanoparticles; Adsorptive removal; PES/ZnO-PANI membranes.

5.2 Graphical abstract
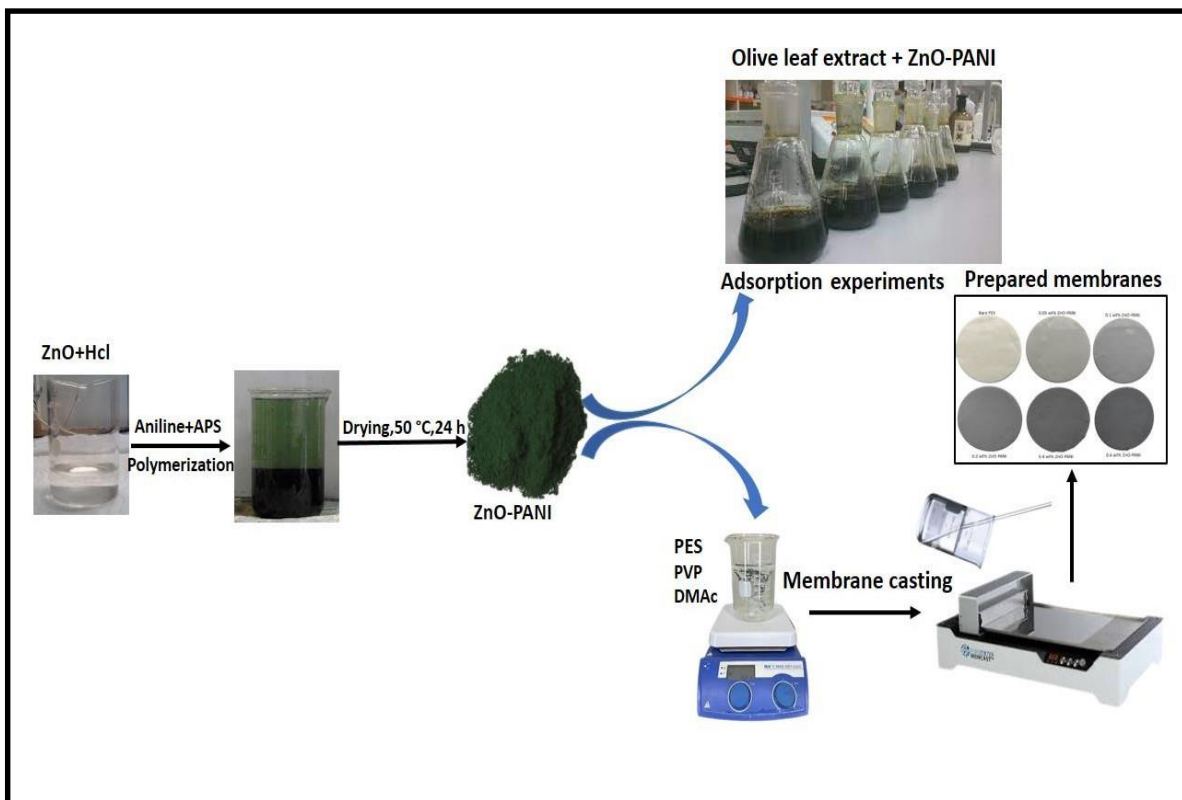
Figure 5.1: Graphical abstract.

5.3 Introduction

In the last several years, nanofiltration (NF) has become progressively an efficient practical application in wide fields, such as water and wastewater treatment, desalination, food processing, concentration and purification, removal of dyes, pharmaceutical and chemical industries (Zinadini et al., 2017; Vatanpour et al., 2012; Bagheripour et al., 2016). This is owing to advantages from this technology to name a few such as high separation efficiency, simplicity of operation, low cost, lower energy and chemical consumption and environment friendly (Zinadini et al., 2017). Therefore, preparing NF membranes with special adapted characteristics such as high water permeability, high rejection and good antifouling performances is a necessary step in solutions treatment, purification and concentration (Hosseini et al., 2019). The surface characteristics of NF membranes and

their microscopic morphology are practically crucial due to their effect on the process effectiveness (separation performance and antifouling behaviour) (Zangeneh et al., 2019). Fouling phenomenon is a blind spot of pressure-driven NF membrane which diminishes the permeate flux, membrane lifetime and separation efficiency (Guo et al., 2017; Nasrollahi et al., 2018). It is believed that the improving surface hydrophilicity is effective for enhancing the fouling resistance of NF membranes (Wang et al., 2018; Wang et al., 2019; Vatanpour et al., 2011). There have been some extensive efforts in enhancing the hydrophilicity and antifouling ability of NF membranes through various methods such as surface grafting, coating, polymers blending, embedding with nanoparticles and functionalization of polymer (Rahimi et al., 2015; Rahimpour et al., 2012; Hosseini et al., 2016).

Recently, the incorporation of hydrophilic nanoparticles into the polymer matrix is well known as an excellent method which attracts more attention, often referred as mixed matrix membranes (MMMs) (Hosseini et al., 2019; Wang et al., 2018).These are polymeric membranes containing some organic, inorganic or hybrid nanoparticles. The incorporation of nanoparticles into a polymer matrix for membrane preparation offers several benefits, which can enhance the performance and functionality of the resulting membranes. Nanoparticles increase the porosity of the membrane, enhancing water permeability. This is crucial in applications like water filtration and wastewater treatment where high flux rates are desired. In addition, incorporating nanoparticles into polymer matrix can modify the selectivity of the membrane, making it more effective at separating specific molecules or ions from a mixture. This is vital in processes like nanofiltration and reverse osmosis, where specific molecule sizes need to be filtered out. Furthermore, nanoparticles can create a repulsive force against foulants, reducing membrane fouling. This is significant for long-term applications as fouling can severely impact membrane performance. Moreover, the use of these nanoparticles as additives can improve the thermal, mechanical, and chemical stability of polymeric membranes (Zangeneh et al., 2019).

When porous microfiltration (MF) and ultrafiltration (UF) membranes are considered for separation processes, the type of polymer used does not seem important. On the contrary, when dense membranes are considered, the selection of polymer becomes crucial for extended life and membrane performance (Mukherjee et al., 2016).Various polymers,

such as polysulfone (Psf), polyethersulfone (PES), cellulose acetate (CA), polyvinylidene fluoride (PVDF) and polyetherimide (PEI) are used for the preparation NF and UF membranes by phase inversion method (Bagheripour et al., 2016). Among the different polymers, polyethersulfone (PES) is considered a superior candidate for the preparation of membranes. It offers various advantages, namely suitable chemical properties, excellent thermal stability, environmentally friendly, high pH resistance, as well as wide pore size range and good mechanical properties (Rahimi et al., 2015).

In the last years, many kinds of fillers have been utilized to prepare MMMs, including TiO_2 (Vatanpour et al., 2012), SiO_2 (Shen et al., 2011), ZnO (Sharma et al., 2022), Fe_3O_4 (Bubela et al., 2023), carbon nanotubes (CNTs) (Manorma et al., 2021), graphene oxide (GO) (Xia et al., 2015), activated carbon (Aghili et al., 2017), zeolite (Sohail et al., 2023) and polyaniline (Daraei et al., 2012). These nanofillers, when used as additives in the polymeric matrix, resulted in enhanced membrane characteristics (morphology, porosity, hydrophilicity), improved antibiofouling properties, as well as the thermal, mechanical, and chemical stability of the membranes (Zinadini et al., 2017 ; Vatanpour et al., 2012 ; Rahimpour et al., 2012; Manorma et al., 2021 ; Zangeneh et al., 2019; Hosseini et al., 2016).

ZnO is considered an excellent nanofiller due to their various advantageous features, like low cost, nontoxicity, high hydrophilicity, as well as good chemical and physical stability (Zinadini et al., 2017; Sharma et al., 2022). Latest research by Sharma et al., (2022) revealed that blending ZnO nanoparticles with polyethersulfone (PES) ultrafiltrationmembrane led to a lower contact angle and higher hydrophilicity, which was effective to reach greater water flux.

In addition to metal oxides, some polymeric materials such as polyaniline (PANI) can be a great suggestion for MMMs preparation. PANI is one of the most promising conducting polymers due to its facile synthesis, high environmental and thermal stability, relatively low cost (Baruah et al., 2016). This makes it usable in many fields such as separation processes for water and wastewater treatment applications (Bagheripour et al., 2016). Thus, PANI is considered as an effective adsorbent, which has good adsorption performance for heavy metal ions and organic pollutants (Zhou et al., 2017).

Coating Zinc oxide by Polyaniline and its incorporating into PES matrix membrane results in a novel membrane type that combine the distinctive properties of both ZnO and PANI.This innovative approach transforms ZnO-PANI nanoparticles into a double-edged sword, enhancing the water flux and surface hydrophilicity through the presence of ZnO in the matrix, while achieving a high rejection of polyphenols due to polyaniline. Moreover, by integrating adsorption and membrane filtration, polyphenols recovery efficiency is maximized, offering a sustainable approach for various applications.

The novelty of this study stems from several key aspects. Firstly, it requires the synthesis and successful incorporation of ZnO-PANI nanoparticles into the PES matrix, representing an innovative application of these nanoparticles to improve polymeric membranes. Secondly, the study delves into the application of ZnO-PANI as an adsorbentto remove total phenolic compounds (TPC) from olive leaf extract (OLE), a unique application in the field of adsorption, considering the significance of phenolic compounds across various industries. The research also scrutinizes the effect of these incorporated nanoparticles on membrane morphology and hydrophilic properties through an array of analyses, including contact angle measurements, water content, pore size, porosity, SEM, FTIR, and pure water flux. These investigations shed light on how ZnO-PANI incorporation into PES matrix influences membrane structure and properties, a crucial aspect in membrane technology. Lastly, the study evaluates the performance of the prepared membranes in terms of permeate flux, TPC rejection, and fouling resistance during OLE filtration tests. OLE was pretreated by a commercial UF membrane to improve the efficiency of the NF process and remove high molecular weight compounds. In summary, the novelty of this work lies in the synthesis and incorporation of ZnO-PANI nanoparticles into a PES membrane matrix, their application in TPC recovery from OLE, and the comprehensive evaluation of membrane properties and performance, highlighting their practical significance in real-world applications.

5.4 Materials and Methods

5.4.1. Materials

Olea.europaea (variety Chemlali) leaves were collected from Sfax region (Tunisia) in mid-November 2021, immediately transferred to the laboratory, and dried in the oven at 40°C for 30 min. After that, samples were milled and kept in darkness at room temperature (RT) until used for the extraction process.

5.4.2. Chemicals

For the extraction process, ethanol was purchased from Fisher Chemical, and water was distilled using a Milli-Q system (Millipore, Bedford, MA, USA). Aniline ($C_6H_5NH_2$) monomer. Ammonium persulfate (APS) $((NH_4)_2S_2O_8)$, zinc oxide (ZnO) and hydrochloric acid (HCl) were supplied by Merck for synthesis of nanocomposites. For the preparation of membranes, polyethersulfone (PES, Mw = 60,000 g/mol), polyvinylpyrrolidone (PVP, Mw = 29,000 g/mol) and N, N-Dimethylacetamide (DMAc) were purchased from Sigma Aldrich. The selection of PVP with a MW of 29000 g/mol was based on extensive preliminary experiments and literature reviews. The compounds utilized as standard references for quantification were: Oleuropein (OLP) ≥ 98% is from Sigma-Aldrich, Tyrosol ≥99% and Hydroxytyrosol ≥ 98% are from Extrasybthese.

5.4.3. Extract Preparation

5.4.3.1. Extraction of total phenolic compounds (TPC) from olive leaves

Olive leaf extract was prepared according to the method proposed by Aleksandra Szydłowska-Czerniak et al., (2012), with minor modifications. Shortly, 1.2 g portion of ground olive leaves was added to 40 mL of ethanol/water, 75/25% (v/v) in an erlenmeyer flask. After that, the erlenmeyer was capped and continuously stirred in a shaking bath at 50°C. After 90 min of extraction, the sample was filtered with a sintered glass at 0.45 μm using a vacuum pump, then centrifuged (NAHITA bleu, Modibas+ centrifuge, mod.2741)

at 4000 rpm for 15 min and the supernatant was collected and kept in a refrigerator until further use.

5.4.3.2. Determination of total phenolic compounds (TPC)

Total phenolic compounds (expressed as mg gallic acid equivalents (GAE)/g of leaf powder) was determined by the Folin-Ciocalteu method as previously described by Erragued et al., (2022). A calibration curve (2–20 mg/mL; $R^2 = 0.9996$) was prepared and absorbance measured at 765 nm using a PG Instruments T6 UV/Vis spectrophotometer (England).

5.4.3.3. High-performance liquid chromatography (HPLC) analysis

The quantitative analyses of polyphenols found in the feed, permeate, and retentate produced from a 0.2 wt% ZnO-PANI/PES membrane was performed using an HPLC system (Waters separation model 2695). Polyphenols were subjected to separation using a Brisa LC2 C18 column (250 × 4.6 mm id, 5 μm, Spain). Following the separation process, the analysis of the polyphenols was carried out using a Waters 2487 dual-absorbance detector. The used mobile phase consisted of a combination of two solutions: Solution A, which was water adjusted to pH 3.20 using phosphoric acid, and Solution B, which was acetonitrile. The mobile phase flowed at a rate of 1 mL/min. The elution gradient used lasted for 80 min and was carried out as follows: starting with 100–89% A (0–3 min), then 89–87% A (3–41 min), followed by 87–80% A (41–55 min), 80–75% A (55–70 min), 75–
100% A (70–71 min), and finally concluding with an isocratic elution at 100% A for 9 min. The temperature of the column and the sampler were adjusted to 30°C and 25°C, respectively. Prior to injection, the samples were filtered using a 0.1 μm microfilter, and theinjection volume for each sample was set to 10 μL. Chromatographic profiles were measured at wavelengths of 215 nm and 280 nm. To identify polyphenolic compounds,their retention times were compared with those obtained from a standard solution. The standard solution consisted of pure standards dissolved in acetonitrile.

5.4.4. Synthesis of ZnO-PANI nanoparticles

PANI coated ZnO nanocomposites (ZnO-PANI) were synthesized in-situ by chemical oxidation polymerization as shown in **Fig. 5.2**. The methodology described by Goswami et al., (2019) was followed with slight modification. PANI coating was developed on ZnO nanoparticles in 1 M HCl medium where the nanoparticles were pre-dispersed. Initially, 2g of ZnO powder was dispersed into 500 mL HCl (1 M) using ultrasonic bath for 45 min to activate the ZnO surface. Then, 490 μL of aniline was mixed with the ZnO nanoparticles dispersed in HCl solution under magnetic stirring for 30 min in an ice bath (0–5°C). After that, 1.225 g of APS oxidant dissolved in 250 mL of 1 M HCl was added drop by drop to the above solution by keeping the reaction temperature in the range of 0–5°C. The mixture vessel was further stirred continuously overnight at 25°C. Finally, the resulting dark green solution was filtered using glass Buchner funnel G_4 (5-15μm) and the precipitate was washed repeatedly with distilled water. The obtained product was dried in an oven at 50°C for 24 hours and stored in a desiccator.
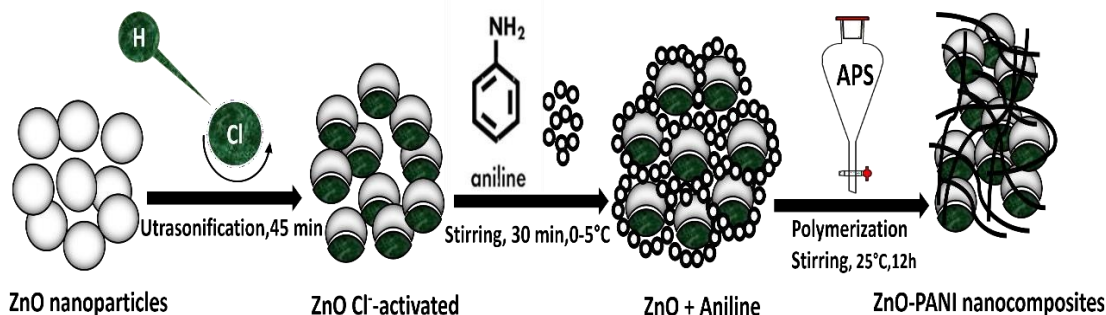
Figure 5.2: Scheme of preparation of ZnO-PANI nanocomposites.

5.4.5. Characterization of ZnO-PANI nanoparticles

UV–Vis adsorption spectra were recorded using a Lambda 650 UV–Vis spectrophotometer (PerkinElmer, US) in the wavelength range from 200 to 800 nm. SEM-EDX technique (model ZEISS, Merlin) was utilized to study the morphological features and to confirm the formation of ZnO-PANI nanocomposite. The size distribution of ZnO- PANI was measured using dynamic light scattering (DLS) using the ZetaSizer Nano ZS.

5.4.6. Adsorption experiments

Different batch adsorption experiments were carried out to study the effects of solution pH and initial concentration of the adsorbate on the adsorption capacity of the ZnO-PANI nanocomposite. The adsorption experiments were done in 50 mL conical flasks. 20 mL of the adsorbate was taken in conical flask with 100 mg of the adsorbent (this particular weight ratio was chosen to maintain consistency with previous studies and to facilitate comparisons with the existing literature). The solutions were then agitated constantly using a shaking bath at 150 rpm and at a fixed temperature during 7 h. Samples were taken out from flasks and the solutions were separated from the adsorbent by vacuum filtration and centrifuged for 15 min at 4000 rpm. The concentration of residual phenolic compounds in the supernatant solutions was determined using UV–Vis spectrophotometry (**section 5.4.3.2**). Experiments were performed three times under identical conditions and data were presented as averages with standard deviations.

The adsorption capacity was calculated using Eq. (5.1)

$$q_e = \frac{(C_0 - C_e)V}{m} \tag{5.1}$$

where, q_e is the equilibrium uptake (mg/g), C_0 and C_e are the initial and equilibrium concentration (mg/L) of the adsorbate respectively, V is the volume of the solution (L) and m is the adsorbent dosage (g).

5.4.6.1. Effect of pH on adsorption capacity

The effect of solution pH on adsorption was studied by varying the pH of the adsorbate solution from 2.4 to 6.3. The experiment was conducted using naturel olive leaf extract with a known concentration of total phenols (460 mg/L) at 30°C. The initial pH of the extracts was adjusted using 0.1 M NaOH and 0.1 M HCl solutions. pH of the solutions were measured by a pH meter (pH c1020 from Consort). The olive leaf extract used in this study have a pH of 4.7 before adsorbent addition and pH adjustment.

5.4.6.2. Effect of initial adsorbate concentration on adsorption capacity

To study the effect of initial adsorbate concentration on phenolic compounds adsorption, experiments were carried out for five different initial concentrations at 30°C.

The initial concentration of olive leaf extract (466.59 mg/L) and concentrations of 226.6 mg/L, 113.5 mg/L, 66.36 mg/L and 49.92 mg/L, which were obtained through dilution of the initial extract by factors of 25, 50, 100, and 250, respectively were used in this study. 20mL of the adsorbate solution was placed in contact with 100 mg of adsorbent under stirring for 7 h.

5.4.6.3. Isotherm models

Two isotherm models were applied to analyze the data in this work, namely, Freundlich and Langmuir isotherm equations.

The Freundlich isotherm equation is expressed by Eq. (5.2):

$$q_e = C_e^{1/n} \tag{5.2}$$

where K_F and $1/n$ represent the Freundlich adsorption constant and adsorption intensity of the adsorbent respectively (Majumdar et al., 2018).

The Langmuir isotherm equation is given by Eq. (5.3) (Salem et al., 2016):

$$q_e = \frac{b\, q_{max}\, C_e}{1 + C_e} \tag{5.3}$$

where q_{max} (mg/g) is the maximum adsorption capacity of the adsorbent and b (L/mg) is the Langmuir adsorption constant.

One of the essential characters of the Langmuir isotherm is the separation factor R_L which is dimensionless and can be expressed by Eq. (5.4):

$$R_L = \frac{1}{1 + bC_0} \tag{5.4}$$

where C_0 (mg/L) is the initial adsorbate concentration. The value of R_L should lie between 0 and 1 for favorable adsorption.

5.4.7. Preparation of PES/ZnO-PANI nanofiltration membranes

NIPS method (non-solvent induced phase separation) was used to prepare mixed matrix PES NF membranes. Five MMMs and one bare PES membrane (used as reference) were prepared. The compositions of casting solutions consisting of DMAc as a solvent, PES, PVP and desired concentration of ZnO-PANI is presented in **Table 5.1**. Firstly, precise amount of ZnO-PANI were dispersed in DMAc using an ultrasonic bath. Then, PES (20

wt%) and PVP (1 wt%) were added in the above mixer and the solutions were agitated overnight at RT for their complete dissolution.

In order to better dispersing of the nanocomposites in the PES matrix and avoid the formation of ZnO-PANI aggregates, the sonication was again used for 30 min. The solutions were put in a vacuum oven at 50°C to ensure air bubbles removal.

After that, homogenous casting solution is formed and a membrane of 250 μm was casted on a smooth glass plate using an automatic film applicator (Elcometer 4340). The glass plate was immediately submerged into nonsolvent bath (distilled water) until the membrane film was detached from the glass plate. The formed film was again immersed in fresh distilled water container for 24 h to guarantee the complete extraction of DMAc. Finally, the membranes were naturally dried by hiding them between two filter papers for 24 h at RT.

Table 5.1: Composition of the membrane casting solution.

Membrane type	PES (wt %)	PVP (wt %)	ZnO-PANI (wt %)	DMAc (wt %)
Bare PES	20	1	0	79.0
0.05 wt%	20	1	0.05	78.95
0.1 wt%	20	1	0.1	78.9
0.2 wt%	20	1	0.2	78.8
0.4 wt%	20	1	0.4	78.6
0.6 wt%	20	1	0.6	78.4

5.4.8. Characterization of NF membranes

5.4.8.1. Membrane water content

Equilibrium water content (EWC) was determined by gravimetric weight analysis using Eq. (5.5). The procedure consisted of immersing a certain weight of dry membrane in water for 24 h and then drying its surface with filter paper and immediately weighing it. After that, the membranes were dried in an oven at 40°C for 24 h and weighed again. The difference between dry and wet weight indicated the water content (weight rise percent) of each membrane. In order to reduce the errors, all experiment were performed in triplicates.

$$E(\%) = \frac{m_1 - m_2}{m_1} \times 100 \tag{5.5}$$

where m_1 and m_2 are wet and dry membrane weights (g), respectively.

5.4.8.2. Membrane Porosity and mean pore size

The obtained values from the determination of water content were used for determining the average porosity of the prepared membranes by the following equation (5.6):

$$(\%) = \frac{\dfrac{m_1 - m_2}{\rho_w}}{V_m} \times 100 \tag{5.6}$$

where ρ_w and V_m are water density (g cm^{-3}) and membrane pieces volume (cm^3), respectively.

The mean pore radius size (r_m) of the prepared membranes was evaluated by theGuerout–Elford–Ferry equation (Eq. (5.7)) based on pure water flux and porosity results.

$$r_m = \sqrt{\frac{(2.9 - 1.75\varepsilon)8\mu_w l Q_w}{\varepsilon A_m \Delta P}} \tag{5.7}$$

where ε is the membrane porosity, μ_w (Pa.s) is the water viscosity (8.9×10^{-4}), l (m) is membrane thickness, Q_w (m^3 s^{-1}) is the volume of water passing through the membrane per unit time, A_m (m^2) is membrane active area and ΔP (Pa) is the operating pressure.

5.4.8.3. Water contact angle

Surface hydrophilicity for all prepared membranes was evaluated by contact angle goniometry. Water contact angles (WCA) were measured using the sessile drop method with an OCA 20 goniometer (Dataphysics, Germany). To determine the contact angles in the static mode, a droplet of deionized water (10 µl) was dropped on the membrane surface.Afterwards, the formed angle was measured by fitting the Young-Laplace equation to the drop profile. In order to diminish the experimental error, the contact angle was measured at six random locations on each membrane and the average value was calculated.

5.4.8.4. Scanning electron microscopy (SEM)

The surface and cross section morphology of membranes was observed by field emission scanning electron microscopy (FE-SEM) technique using the TESCAN MAIA3 electron microscope in the secondary electrons mode. Prior to performing SEM analysis, the dry membranes samples were transversely cut and glued to carbon tape on a support

and lately sputtered with 6 nm Iridium using the sputter Quorum Q150T ES.SEM observations were obtained at 3 kV, under vacuum conditions.

5.4.8.5. Fourier transform infrared spectroscopy (FTIR)

ATR-FTIR was performed by Jasco FT/IR-4200 equipment to analyze the structure and surface chemistry to confirm the existence of ZnO-PANI nanoparticles on the structure and surface of the membranes. The analysis was performed with the resolution of 4 cm^{-1} and total 64 scans were taken from 600 cm^{-1} to 4000 cm^{-1}.

5.4.8.6. Nanofiltration tests

First, the comparative filtration performance of the prepared membranes was analyzed by water filtration tests. Thereafter, based on the comprehensive characterization studies conducted on different prepared membranes, a specific type was carefully chosen to evaluate its performance towards TPC rejection. The clarified olive leaf extract was used as feed solution of the NF process.

The experiments were carried out in a dead-end cell filtration mode, at constant temperature and stirring rate, using a bench scale filtration equipment (Sterlich HP 4750 stirred cell). The system contains of a stainless steel filtration cell with an effective membrane surface area of 14.6 cm^2 and a volume capacity of 300 mL. The filtration cell was connected to a nitrogen gas cylinder with the pressure control valve and gauge.

The water filtration test was performed to evaluate the hydraulic permeability (L_p) and resistance (R_m) which were considered as primary properties to select the optimal membrane. To evaluate the hydraulic permeability of membrane, pure water filtration was carried out at different pressure values (5, 10, 15, 20, 25 and 30 bar) and the permeate was collected at intervals of 5 min. L_p (L/ (m^2 h bar)) values were calculated according to Eq. (5.8).

$$L_p = \frac{V_m}{tA_m\Delta P} = \frac{J_w}{\Delta P} \tag{5.8}$$

where V_w (L), t (h), and J_w (L/(m^2 h)) represent the volume of permeate passing through the membrane, time for permeate collection, and the PWF, respectively. The PWF shows a linear straight-line relation, for the filtration of distilled water, when plotted as a function of

operating TMP. The slope of this straight line gives the average hydraulic permeability of the membrane over the pressure range used during the filtration.

The R_m (1/m) is the overall resistance imposed by membrane during the filtration process and was calculated using Eq. (5.9).

$$R_m (m^{-1}) = \frac{1}{L_p \mu_w}$$
(5.9)

where μ_w (Pa s) is the dynamic viscosity of water, at the same temperature used during the filtration test.

To evaluate the performance of the selected membrane in concentrating TPC from OLE, filtration tests were conducted at feed temperature of 25 °C using variable TMP.

It is important to remind that the feed (OLE) was the permeate coming from the UF process, without any other modification. The collected permeate samples were analyzed to determine TPC and OLP concentrations. The TPC concentration was determined using UV–Vis spectrophotometry (detailed in **section 5.4.3.2**), while the OLP concentration was determined using HPLC (detailed in **Section 5.4.3.3**), thus allowing to calculate rejection values for TPC and OLP, as given by Eq. (5.10).

$$Rejection\ (\%) = (1 - \frac{C_p}{C_f}) \times 100$$
(5.10)

where C_p and C_f are the concentrations of TPC or OLP in the permeate and feed solution, respectively.

The fouling study was carried out for bare PES and 0.2% ZnO-PANI/PES membranes that were being evaluated for filtering OLE. Following the OLE filtration process, the membranes were subjected to a cleaning procedure. Initially, it was washed with distilled water, and subsequently, a chemical cleaning was carried out using 0.2 M NaOH at a temperature of 25°C under 20 bar. Once the cleaning process was completed, the PWF and the hydraulic permeability were tested at 20 bar pressure conditions. The flux recovery (FR) was assessed to evaluate the antifouling ability of bare PES and 0.2% ZnO-PANI/PES membranes. This was done by utilizing the permeability data of the new membrane ($L_{p,i}$) and the used membrane after cleaning ($L_{p,f}$). Equation (5.11) was employed to calculate the flux recovery (FR) based on these permeability values.

$$(\%) = \frac{L_{p,f}}{L_{p,i}} \times 100 \tag{5.11}$$

where $L_{p,i}$ and $L_{p,f}$ represent the initial hydraulic permeability and the hydraulic permeability regained after filtration of OLE, followed by cleaning with a 0.2 M NaOH solution, respectively.

5.5. Results and discussion

5.5.1. Characterization of nanoparticles

Optical absorption spectra of the ZnO nanoparticles and ZnO-PANI nanocomposite determined by UV-vis spectrophotometry are shown in **Fig. 5.3**.

The ZnO-PANI nanocomposite absorption spectra reveals the existence of two characteristic absorption peaks, the first one is fixed at around 335 nm and attributed to $\pi - \pi^*$ transition of the benzenoid ring (Alves et al., 2012; Dhole et al., 2018; Mostafaei et al., 2012), whereas the second one is a strong wide absorption peak at around 650 nm, which is due to electrons being excited to the highest occupied molecular orbital of benzene ring (Gu et al., 2022). These two peaks confirm the formation of polyaniline (Mostafaei et al., 2012).
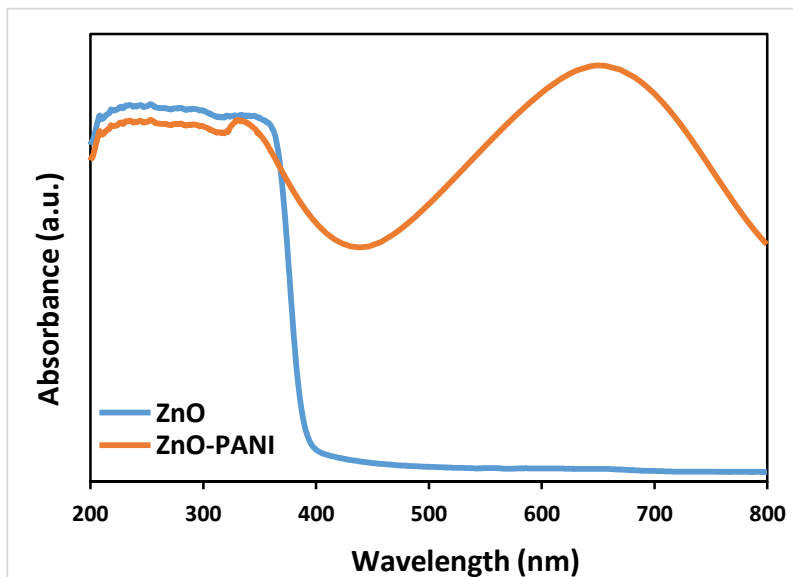
Figure 5.3: UV-visible absorption spectra of ZnO and ZnO-PANI.

Figure 5.4 shows the field-emission scanning electron microscopy micrographs of ZnO nanoparticles **(Fig. 5.4a1)**, PANI **(Fig. 5.4b1)** and ZnO-PANI nanocomposite **(Fig. 5.4c1).** It can be seen that the morphological aspect of ZnO **(Fig. 5.4a1)** has cumulatedgrain structure with non-regular sizes (Maruthi et al., 2021; Thomas et al., 2017), whereas (**Fig. 5.4b1**) PANI as a typical agglomerated structure (Belabed et al., 2021). For the ZnO- PANI nanocomposite **(Fig. 5.4c1)**, the same agglomerated aspect is predominant in the images with a random appearance of few fragments of ZnO nanoparticles, recognized by itsshape of smooth and non-granular plate. This shows clearly that the majority of ZnO nanoparticles is coated by the PANI during the polymerization (Belabed et al., 2021).

The quantitative analysis by EDX is very important and this reflects the purity and chemical composition of the samples. In the present study, the EDX technique was applied to confirm the formation of ZnO-PANI nanocomposite before membrane preparation. On EDX analysis (**Fig. 5.4c2**), these filler nanoparticles confirmed by the presence of Zn peak (**Fig. 5.4a2**) and majority of peaks present in PANI (**Fig. 5.4b2).**
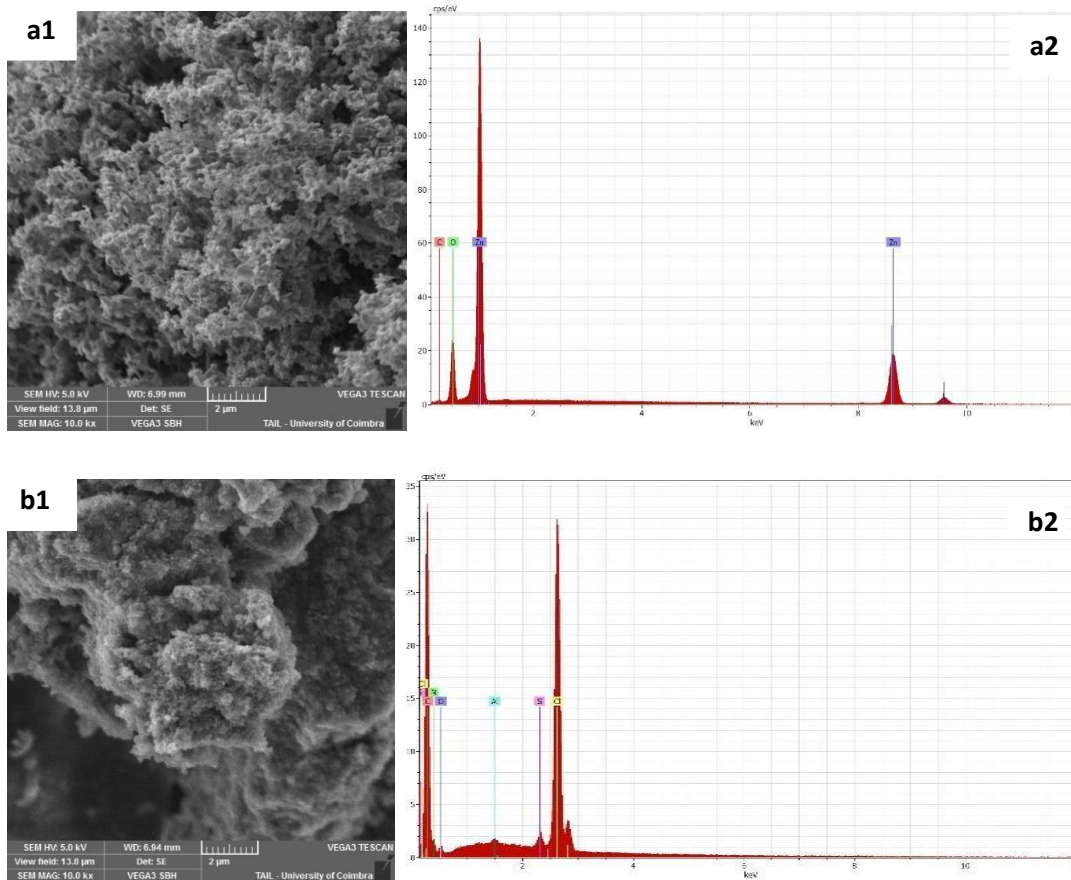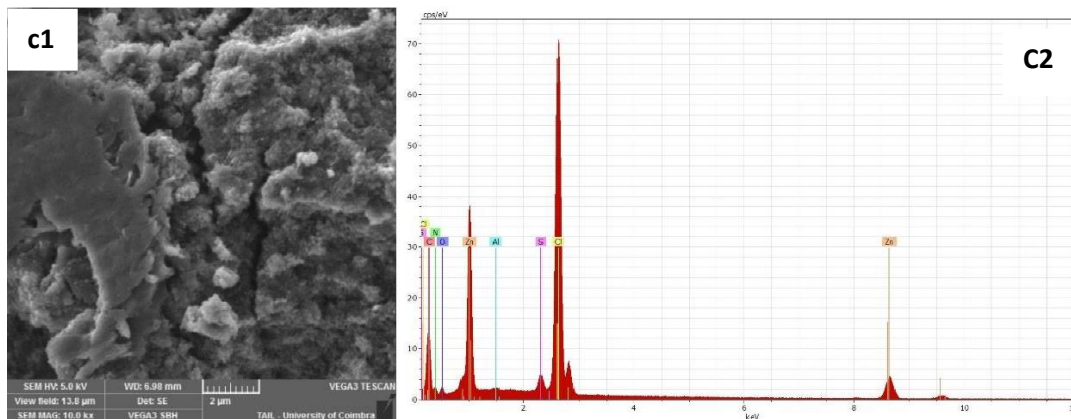
Figure 5.4: SEM and EDX images for (a1, a2) ZnO, (b1, b2) PANI and (c1, c2) ZnO-PANI.

DLS measurements indicate that the particle size distribution of ZnO-PANI particles varies from 255 to 458 nm (**Fig. 5.5**).
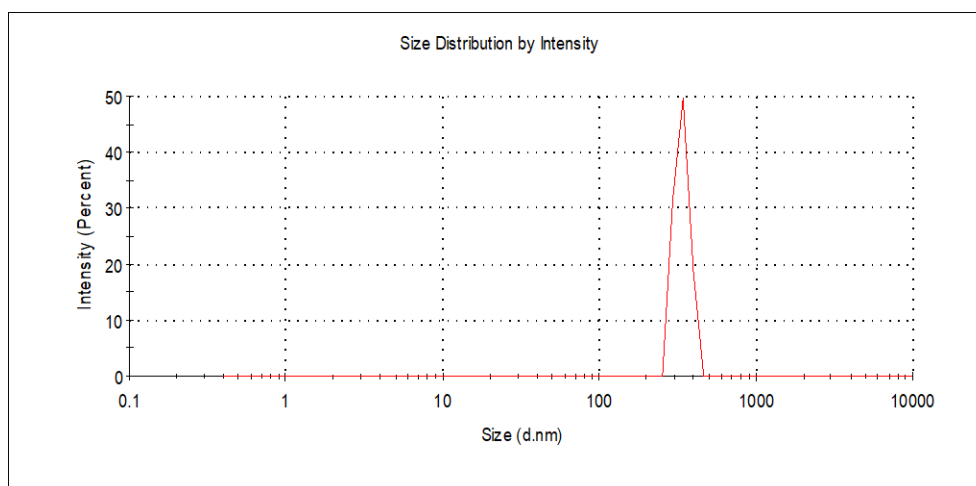
Figure 5.5: Size distribution of ZnO-PANI.

5.5.2. Adsorption of phenolic compounds onto ZnO-PANI

5.5.2.1. Effect of pH on ZnO-PANI adsorption capacity

The solution pH is one of the most critical parameters affecting the adsorption process, essentially on the adsorption capacity (Achak et al., 2014). This is mainly due to fact that pH affects the dissociation of the adsorbate and the surface charge of the adsorbent (Goswami et al., 2019).

Figure 5.6 shows the effect of pH on the adsorption of phenolic compounds onto ZnO-PANI on 20 mL olive leaf extract. Agitation was maintained for 7 h (150 rpm) at $30 \pm 2°C$ and with an adsorbent dosage of 100 mg. It was found that the adsorption of phenolic compounds increased from 13.52 mg/g to 35.36 mg/g for an increase in pH from 2.4 to 6.3. The adsorption capacity of phenolic compounds on ZnO-PANI and similar adsorbent materials depends on several factors, such as the nature of the adsorbate, the physical nature of the adsorbent, and the solution conditions, especially the pH medium (Ahmadiaras et al., 2023).

The significant increase in adsorption capacity from 13.52 mg/g at pH 2.4 to 35.36 mg/g at pH 6.3 can be explained by the electrostatic interactions between the adsorbent and the phenolic compounds molecules. At lower pH (2.4), the adsorbent surface is likely positively charged. Moreover, it is widely known that phenolic molecules remain undissociated when the pH medium is lower than pKa. Therefore, the weak electrostatic interactions between similarly charged particles result in lower adsorption capacity. As the pH increases to around 5 (while the membrane most likely still possessed a positivecharge), there is an increase in TPC adsorption. This phenomenon can be elucidated by the existence of two categories of phenolic compounds present in natural olive leaf extract. These categories include hydroxycinnamic acids, including ferulic acid, p-coumaric acid, chlorogenic acid, and caffeic acid, as well as hydroxybenzoic acids like gallic acid and vanillic acid. These compounds possess primary pKa values due to their carboxylic group, typically around 4.5. Consequently, pH levels above 4.5 facilitate the deprotonation of these phenolic compounds, causing them to carry a negative charge (Hashim et al., 2018). This phenomenon contributes to the higher adsorption capacity observed at higher pH levels. In addition, the increase in adsorption capacity can also be attributed to the formation of hydrogen bonds and π-π interactions between the phenolic compounds and theconjugated structure of polyaniline. These interactions become more prevalent at higher pH values, leading to enhanced adsorption. These results are in agreement with the results found by Stasinakis et al., (2008) and Achak et al., (2014).
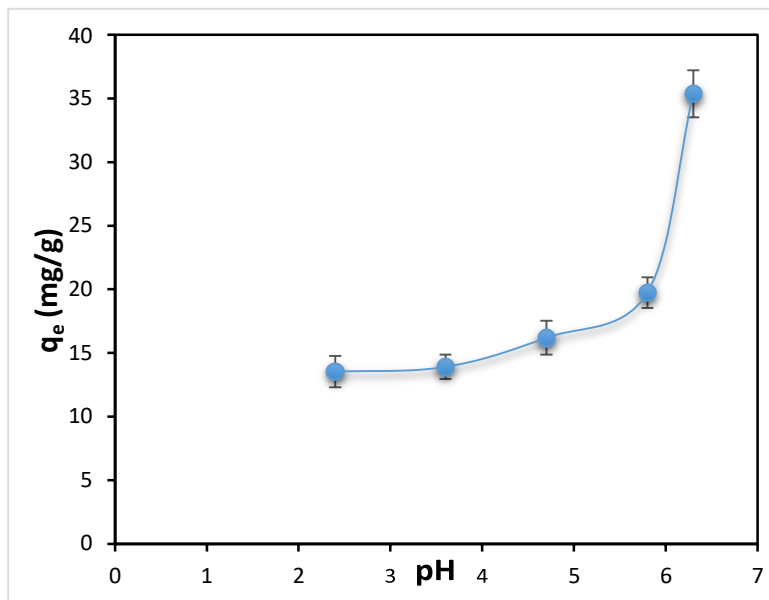
Figure 5.6: Effect of pH on adsorption of phenolic compounds by ZnO-PANI nanocomposite.

5.5.2.2. Effect of initial adsorbate concentration on ZnO-PANI adsorption capacity

The initial concentration of the adsorbate has a significant effect on the phenolic compounds adsorption. In order to identify the effect of adsorbate concentration on phenolic compounds adsorption, a series of experiments were conducted where the initial concentration of olive leaf extract, containing phenolic compounds, was varied from 49.92 to 466.59 mg/L. As clearly seen in **Fig. 5.7**, the adsorption capacity of polyphenols increased with the increase in the initial concentration of the adsorbate. Firstly, the higher initial concentration of the adsorbate provides a larger pool of sorbate molecules in the solution, which leads to a more substantial adsorption onto the solid sorbent. As the adsorbate concentration increases, there is a greater availability of phenolic compounds for interaction with the sorbent's surface. Moreover, the elevated initial concentration of total phenols creates a stronger driving force that helps overcome the mass transfer resistance experienced by phenol molecules between the solid and aqueous phases. This enhanced driving force facilitates the movement of phenolic compounds from the liquid phase onto the solid adsorbent, further promoting the adsorption process. Therefore, increasing the initial adsorbate concentration increases the adsorption capacity of the adsorbate (Goswami et al., 2019; Stasinakis et al., 2008). Another significant consequence of increasing the

initial adsorbate concentration is the increased probability of interactions between polyphenols and the sorbent material. As the concentration of phenolic compounds in the solution rises, more molecules come into contact with the sorbent surface, resulting in an increased chance of successful adsorption onto the sorbent's active sites. It is important to note that these findings are in line with previous studies cited as references (Goswami et al., 2019; Stasinakis et al., 2008).
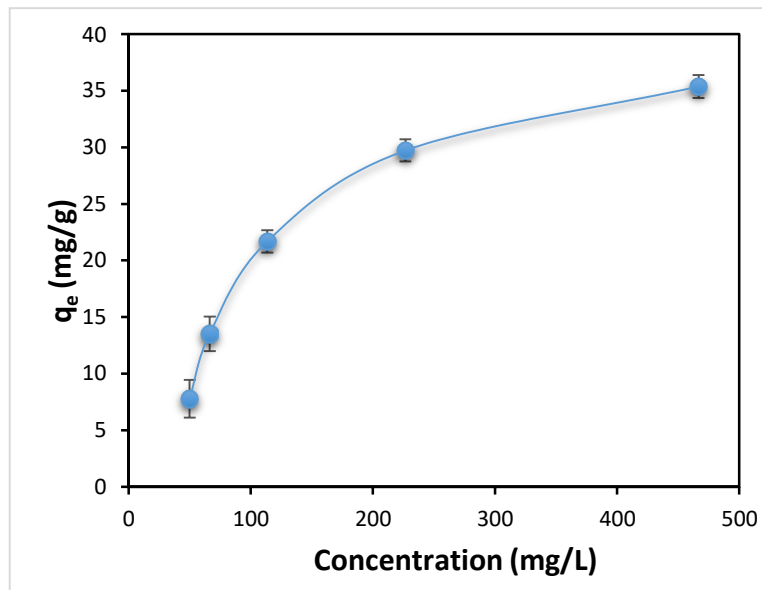
Figure 5.7: Effect of initial concentration of the adsorbate on adsorption capacity.

5.5.2.3. Isotherm studies

Adsorption isotherm is basically important to describe how the adsorbate interacts with the adsorbents and is critical to optimize the use of adsorbents (Zaini et al., 2022). In this study, the experimental data were analyzed by fitting them into Freundlich and Langmuir adsorption isotherm models. Freundlich model suggested that the interactions between adsorbent and adsorbate occur during adsorption (Buthiyappan et al., 2019). The Langmuir isotherm defined that adsorption occurs only on the homogeneous surface through monolayer adsorption. The tested isotherms were evaluated, and the results were presented in **Fig. 5.8**.
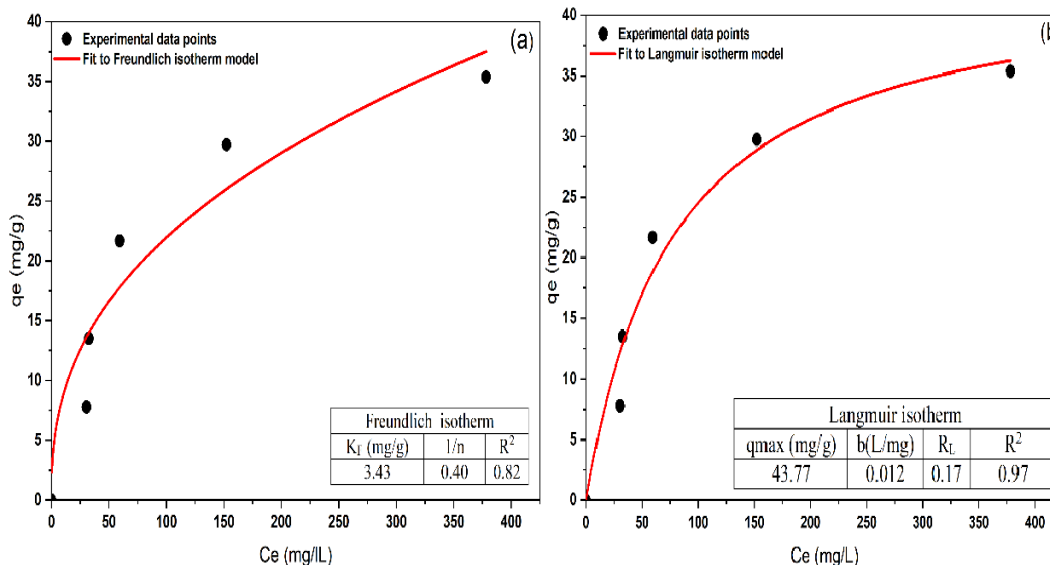
Figure 5.8: (a) Freundlich and (b) Langmuir isotherm plots for phenolic compounds of olive leaf extract.

The table included in **Fig. 5.8** indicated that, the determination coefficient value obtained from Langmuir model ($R^2 = 0.97$) is much higher than that obtained from Freundlich model ($R^2 = 0.82$). Therefore, the adsorption of polyphenols can be better described by the Langmuir model than by the Freundlich model. In addition, the Langmuir isotherm model also showed a high maximum adsorption capacity ($q_{max} = 43.77$ mg/g) and separation factor ($R_L = 0.17$). R_L value indicated the type of Langmuir isotherm to be (irreversible $R_L = 0$, favorable adsorption $0 < R_L < 1$, and linear adsorption $R_L = 1$ or unfavorable adsorption $R_L > 1$). The R_L values between 0 and 1 indicated favorable adsorption (Buthiyappan et al., 2019). The separation factor value in the present work was lesser than one (<1), indicating that the adsorption of the phenolic compounds on ZnO- PANI adsorbent is favorable. Hence, it can be reported that the adsorption of phenolic compounds on the ZnO-PANI surface is a favorable and monolayer adsorption. These results were in close agreement with those previously obtained by Le Minh Tri et al., (2020). They reported that the Langmuir equation is able to describe the mechanism of adsorption of phenolic compounds and confirmed this by adsorbing polyphenols fromeffluents using Fe-nano zeolite.

5.5.3. Characterization of membranes

5.5.3.1. Water content and porosity

Figure 5.9 shows the effect of ZnO-PANI concentration on the water content of prepared membranes. According to the results, the water content of the membrane was initially increased with the addition of a small amount of ZnO-PANI nanoparticles, but thenslightly reduced with a higher concentration of nanoparticles.

The increase of membrane water content may be assigned to hydrophilic characteristic of ZnO-PANI nanoparticles, which enhances the membrane hydrophilicity. During the phase inversion process, hydrophilic ZnO-PANI nanoparticles migrate spontaneously to the membrane/water interface, resulting in a more hydrophile membrane surface. The results obtained from the measurements of the contact angle presented in **Fig.5.11** confirm this explanation. Furthermore, the increase in water content by the increase in ZnO-PANI nanoparticles may be caused by the increase in porosity and pore size (see **Fig. 5.10**). In this situation, there are more available spaces in the membrane structure for water accommodation, leading to an increase in water content. SEM images (**Figs. 5.14c and 5.14d**) also illustrated greater macrovoids in the membrane sub-layer for the modified membranes containing composite nanoparticles (0.1 and 0.2 %wt), compared to bare one that confirms more open structure for water storing.

The reduction of membrane water content at 0.4 wt% of ZnO-PANI loading ratio may be attributed to membrane pore clogging induced by the aggregation of ZnO-PANI, which results to lower porosity and smaller pore size, leading to restriction of the storage of water molecules (Ansari et al., 2015). Indeed, by more adding of nanoparticles content up to 0.4 wt%, it is possible that the pores, cavities and channels in the membrane matrix areencircling and occupied by ZnO-PANI nanoparticles, which lead to water adsorption. The pore filling and clogging phenomenon at high concentration of nanoparticles is demonstrated by SEM analysis. The results of porosity and pore size presented in **Fig. 5.10** reflected the same behaviors that prove this issue. Similar observations were also reported for embedding PANI-co-MWCNT (Bagheripour et al., 2016) and Fe_3O_4-PVP (Hosseini et al., 2019) nanoparticles in PES mix matrix membranes.
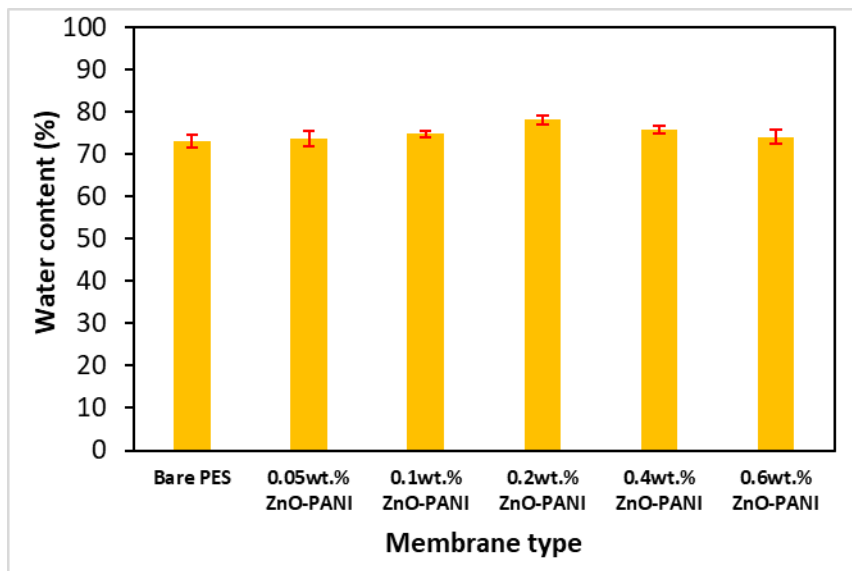
Figure 5.9: The effect of ZnO-PANI nanoparticles concentration on membrane water content.

The results calculated by Eqs. (6) and (7) for porosity and mean pore size, respectively, are presented in **Fig. 5.10**. As seen in this figure, the results of the porosity measurement of all prepared membranes comes within the range of 77–72%. Porosity and mean pore radius are improved with the incorporating of 0.05-0.2%wt of ZnO-PANI nanoparticles in the casting solution compared to the bare PES membrane. Under these conditions, macrovoids within the sub-layer expand, becoming notably larger and more distinct, as illustrated in **Figs 13b**, **c**, and **d**, while nanopores located in the top layer increase in size, clearly depicted in **Fig. 13h**.

This situation can be explained by the influence of the kinetics during the impregnation of the precipitate phase. Mixed hydrophilic ZnO-PANI nanoparticles could accelerate the process of phase inversion, resulting in reduction of skin-layer thickness, and thus the porosity and the mean pore diameter is increased (Wang et al., 2018; Wang et al., 2019). However, porosity and mean pore radius remarkably decreased starting from the use of 0.4 %wt ZnO-PANI nanoparticles. This might be due to increase of the casting solution viscosity at high additive ratio, which reduces the mass exchange rate (Hosseini et al., 2019). Therefore, the formation of membrane with thicker surface, lower porosity and narrower pore size (Xu et el., 2014). Thus, there is an optimum concentration of nanofiller

for obtaining a membrane with thinner skin layer and higher overall porosity (Ghaemi et al., 2015). According to **Fig.5.10**, the optimum amount for ZnO-PANI of prepared membranes is 0.2 wt. %. These results are in line with other similar studies on mixedmatrix membranes (Hosseini et al., 2019; Xu et el., 2014).
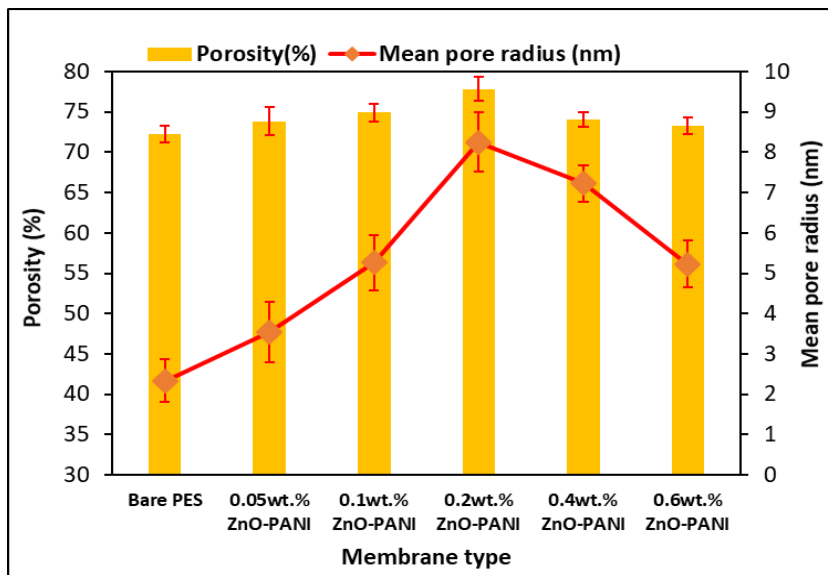
Figure 5.10: The effect of ZnO-PANI nanoparticles concentration on porosity and mean pore size.

5.5.3.2. Membrane surface hydrophilicity

Surface hydrophilicity is one of the main characteristics of the membranes that strongly influences the performance and the antifouling ability. That is usually expressed interms of contact angle for a water drop on the membrane surface to assess the affinity of water for wetting the membrane surface. Generally, a lower contact angle with water signifies a more hydrophilic membrane surface (Zinadini et al., 2017). According to **Fig. 5.11**, it could be comprehended that the angle between the deionized water droplet and membrane surface significantly decreased once the amount of ZnO-PANI nanoparticles increased in the membrane body. This is due to the effect of the high hydrophilic characteristic of these incorporated nanoparticles, which consequently increased the hydrophilicity of the membrane surfaces (Vatanpour et al., 2012). During the preparation of mixed matrix membranes, a significant phenomenon occurs during the phase inversion process in water, whereby the ZnO-PANI nanoparticles within the mixed solution

spontaneously migrate towards the upper layer, eventually reaching the membrane surface. Consequently, the ZnO-PANI nanoparticles adorn the top surface of the prepared membrane, leading to a reduction in interfacial energy and a consequent improvement in membrane hydrophilicity (Wang et al., 2018).

Nevertheless, when embedding 0.4 and 0.6 wt% of ZnO-PANI, an unexpected increase in the contact angle to 61.48°±2.1 and 64.93°±2.2, respectively, was observed. This occurrence could be elucidated by the excessive concentration of ZnO-PANI, resulting in irregular positioning and agglomeration of these nanoparticles on the membrane surface (Rahimi et al., 2015). Consequently, this irregular arrangement diminishes the number of effective functional groups that come into contact with water, leading to the observed increase in contact angle. Similar phenomena were also reported by Wang et al., (2018).
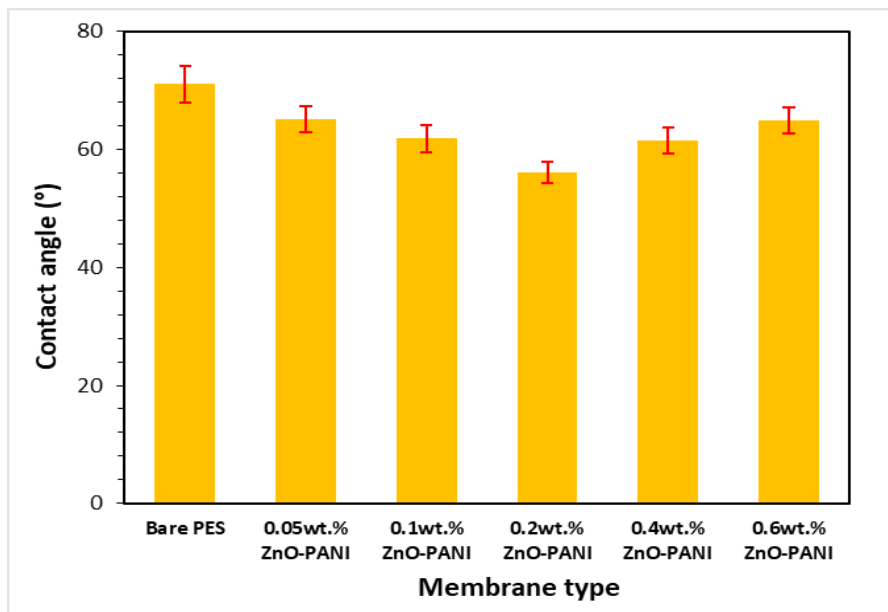
Figure 5.11: Water contact angle of prepared PES membranes.

5.5.3.3. Effect of ZnO-PANI on hydraulic permeability and resistance

The impacts of changes in ZnO-PANI concentration on PWF and subsequently on the permeability and resistance of lab-made membranes are shown in **Fig. 5.12a.** From the results, it is clear that the membranes with higher permeability offered lower resistance against the permeate flow. In addition, it was observed that the PWF and hydraulic permeability of membranes increased with the addition of ZnO-PANI nanoparticles in their

matrix. As seen from **Fig. 5.12b**, the permeability of all the prepared membranes with the ZnO-PANI has improved in comparison to the unfilled PES membrane. The permeability of the prepared mixed matrix membranes had the maximum value when the content of the ZnO-PANI was 0.2 wt% (7.18 L/ (m^2 h bar)) and it declined by 55.3% and 68.3% for 0.4 and 0.6 %wt ZnO-PANI, respectively.

Broadly, two major characteristics which can affect the membrane permeation flux are membrane hydrophilicity and membrane structure (Tseng et al., 2012). Increasing membrane hydrophilicity enhances the water permeability (Almanassra et al., 2023). In addition, higher porosity, larger pore size, thinner skin layer led to higher permeation flux across the membrane. The permeability improvement can be partly explained by the increase of membrane water content/ hydrophilicity, which enhances the permeation flux. Furthermore, it is possible that larger pores and macro-voids in the membrane structure and more porosity made by addition of nanoparticles into the casting solution (0.05, 0.1 and 0.2 wt%) (as observed in **Figs. 5.9 and 5.14**), which facilitates the water transport through the membrane, can be other logical reasons for the improvement in permeability. The addition of 0.4 wt% ZnO-PANI nanoparticles to the PES matrix resulted in a decrease in permeability. This decrease can be attributed to two main factors: a reduction in mean pore size and porosity (Wang et al., 2018) caused by nanoparticle incorporation, and the phenomenon of pore filling/blocking at higher nanoparticle concentrations. These effects limit water traffic through the composite material, as observed in previous studies (Daraei et al., 2012; Mobarakabad et al., 2015).

This observation is in very good agreement with the morphological results, SEM analysis and water content measurements depicted in **Fig. 5.9**. Similar behavior was reported by Zinadini et al., (2014) for GO blended PES membranes.
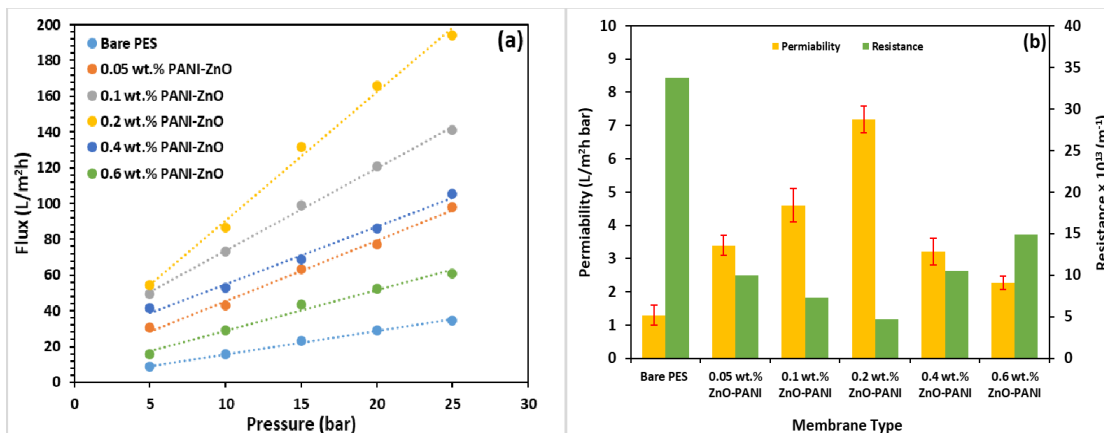
Figure 5.12: (a) Variation of PWF with TMP; (b) Hydraulic permeability and resistance of prepared PES membranes.

5.5.3.4. Surface characterization by FTIR spectroscopy

In order to confirm the embedment of ZnO-PANI in the polymeric matrix, FTIR spectroscopy was carried out on the prepared membranes, and the corresponding spectra are presented in **Fig.5.13**. The FTIR analysis provides valuable insights into the chemical composition and interactions within the materials. In the case of bare PES membrane, two distinctive peaks were observed at 1245 and 1107 cm^{-1}, which can be attributed to the stretching vibrations of S=O asymmetric and S=O symmetric of the PES polymer. These findings correlates well with previously reported studies (Vatanpour et al., 2011; Wang et al., 2015). Upon examining the FTIR spectrum of the PES/ZnO-PANI composite matrix, besides to similar peaks found for bare PES membrane, band at 554 cm^{-1} was found and supposed to be the vibrations of Zn-O (De Peres et al., 2019) . In addition, peaks of C-N and N-B-N were observed at 1149 and 1484 cm^{-1}, confirming that the PANI have been successfully embedded (Bagheripour et al., 2016).

In summary, the FTIR spectra of the prepared membranes, when analyzed and compared, provide strong evidence for the embedment of ZnO-PANI within the polymeric matrix. The presence of Zn-O vibrations and the characteristic C-N and N-B-N peaks serve

as strong confirmation of the successful incorporation of PANI. These findings highlight the immense potential of these composite membranes for diverse practical applications.
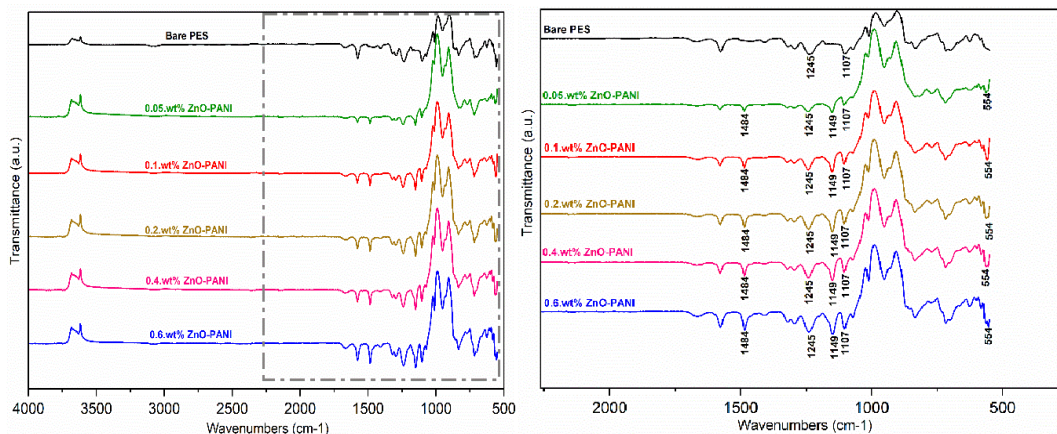
Figure 5.13: FTIR spectra of bare PES membrane and the MMMs with 0.05, 0.1, 0.2, 0.4, and 0.6 wt% of ZnO-PANI nanoparticles incorporated.

5.5.3.5. Morphology characterization by SEM

For the investigation of cross-sectional structure of the composite membranes and the top surface morphology, the SEM analysis has been carried out. All of the prepared PES membranes (bare PES and filled with ZnO-PANI) exhibited a typical asymmetric membrane structure with a porous sub-layer and a dense layer formed at the top-layer, as shown in **Fig.5.14.** .

The cross-sectional SEM image of the unfilled PES membrane (without ZnO-PANI) represents a typical asymmetric structure composed of a thin and dense skin layer and macro-voids in the bottom side (**Fig. 5.14a**). By adding ZnO-PANI to the casting solution, significant changes in the sub-layer and skin layer morphology of the prepared membranes were observed (**Fig. 5.14b–5.14f**). When the content of ZnO-PANI in the casting solution increases up to 0.2 wt%, the quantity of pores and macrovoids volume increase, resulting in membranes with higher porosity in the sub-layer which was proved by porosity measurements (**Fig. 5.10**). This result might be due to thermodynamic instability of casting solution caused by hydrophilic ZnO-PANI nanoparticles. The hydrophilic nature of these nanoparticles is responsible for the fast exchange of solvent and non-solvent during the

phase inversion process, which leads to the formation of larger channels in the sub layer (Rahimpour et al., 2012; Hosseini et al., 2016).
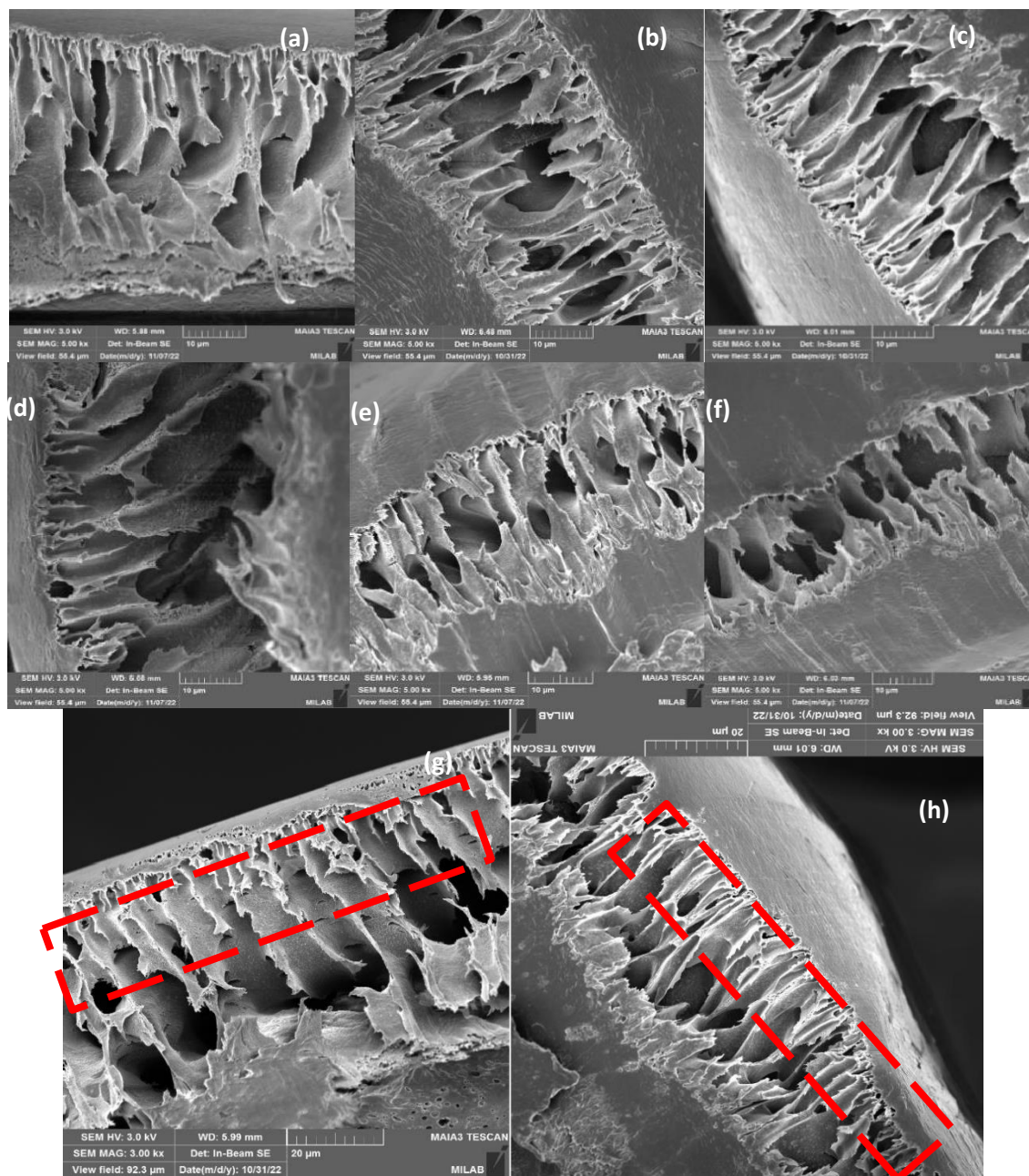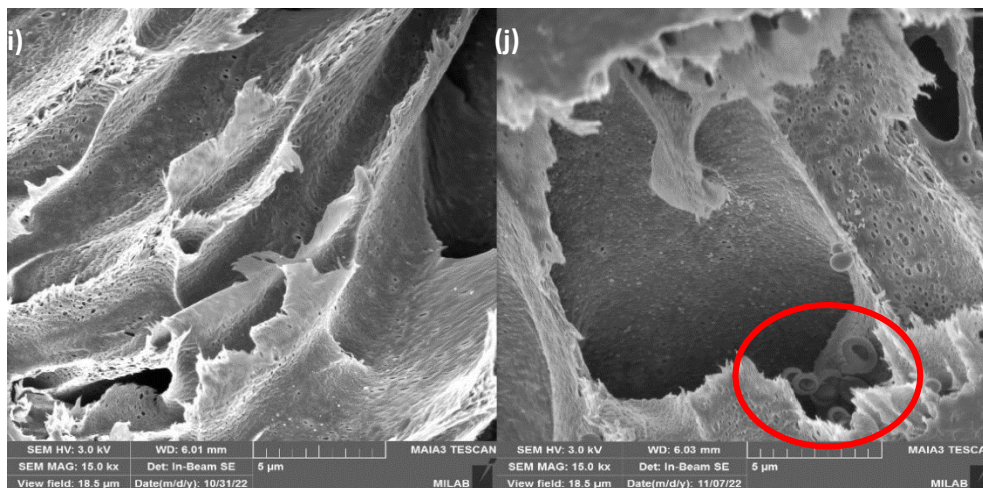
Figure 5.14:Cross-sectional SEM images of PES membranes prepared with: (a) 0 wt.% ZnO-PANI, (b) 0.05 wt.% ZnO-PANI, (c) 0.1 wt.% ZnO-PANI, (d) 0.2 wt.% ZnO-PANI, (e) 0.4 wt.% ZnO-PANI, (f) 0.6 wt.% ZnO-PANI, (g) 0.2 wt.% ZnO-PANI(with clear top layer in red rectangle) ,(h) 0 wt.% ZnO-PANI (with clear top layer in red rectangle),(i) 0.2 wt.% ZnO-PANI (high magnification) and (j) 0.6 wt.% ZnO-PANI (high magnification).

As observed from **Fig. 5.14d**, by adding 0.2 wt% of ZnO-PANI, macrovoids within the sub-layer expanded, becoming notably larger and more distinct, while nanopores located in the top layer increased in size, clearly depicted in **Fig. 5.14h**. This change could facilitate the water transport through the membrane and, consequently, increases the permeability (Nasrollahi et al., 2018). In addition, an obvious change in the sub-layer structure from a finger-like one to a macrovoids one due to the effect of further incorporation of ZnO-PANI into the PES polymeric matrix is observed.

Nevertheless, when the amount of ZnO-PANI in the casting solution is further increased (0.4 and 0.6 wt%), a denser sub-layer structure is formed (**Fig. 5.14e-f**). This is probably due to the strong increase in the viscosity of casting solution with the addition of ZnO-PANI (Rahimpour et al., 2012). These results are in close agreement with those presented in the previous sections in relation to the increase in water content, porosity,mean pore size and hydraulic permeability.

As obvious observed in the high magnification cross section SEM image of 0.2 wt% of PES/ZnO-PANI membrane (**Fig. 5.14i**), no aggregates was detected for ZnO-PANI in the sub-layer structure of the prepared membrane which indicated the homogenous dispersion of ZnO-PANI in the membrane polymer matrix. The aggregates of nanoparticles in sub- layer macrovoids of 0.6 wt. % ZnO-PANI membranes are clearly observed and shown in **Fig. 5.14j**.

In addition, the surface SEM images of 0.2% ZnO-PANI and 0.6% ZnO-PANI membranes are shown in **Fig.5.15**. The SEM images obviously indicate that nanoparticle agglomeration might occur at high concentrations. **Figure 5.15a** shows that when 0.2% ZnO-PANI were added to the membrane casting solution, no nanoparticles were agglomerated in the surface of the membranes, whereas in the surface SEM image (**Fig. 5.14b**) the nanoparticle agglomeration in high concentration of ZnO-PANI was encircledby red lines. This dispersion property is important for the preparation of blend membranes with excellent performance. Furthermore, no crevices were detected on the membrane top surface, signifying that the membranes did not become crisp by the addition of ZnO-PANI and there was no negative impact on the membranes stability.
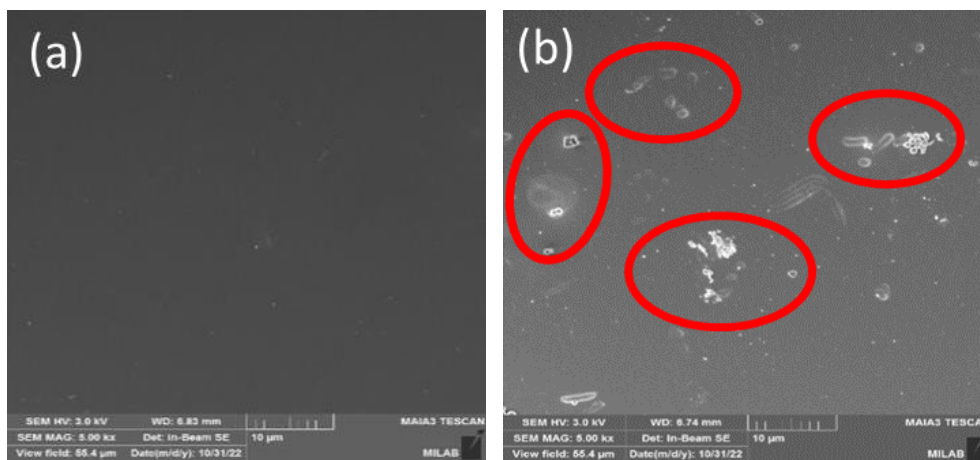
Figure 5.15: FE-SEM images of the top surface of (a) 0.2% ZnO-PANI and (b) 0.6% ZnO-PANI membranes.

5.5.4. Membrane selection

5.5.4.1. Olive leaf extract filtration tests

Figure 5.16a shows the behavior of permeate flux during the filtration of olive leaf extract with time using bare PES and 0.2 wt% ZnO-PANI/PES membrane at different pressures (10, 20 and 30 bar). It is crucial to mention that, a fresh membrane was utilized for each pressure condition. The feed solution is introduced into the filtration system at the beginning of the experiment (batch mode filtration) then, collecting permeate at 75 min intervals for 300 min for each pressure (10, 20, and 30 bar).Afterwards, the membrane was subjected to cleaning using a 0.2 M NaOH solution aiming to restore the original permeate water flux.
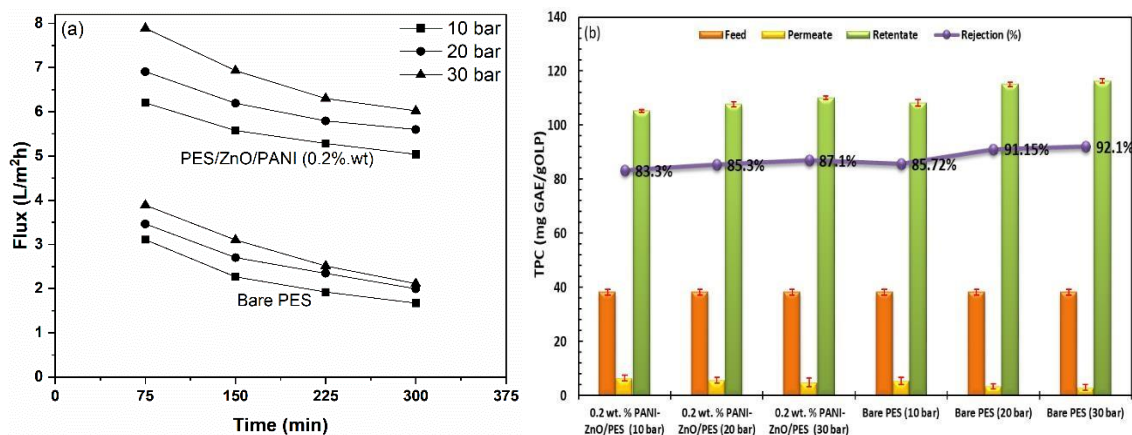
Figure 5.16: Permeate flux behavior of olive leaf extract with time using bare PES and 0.2 wt. % ZnO-PANI/PES at different pressure (a) and total phenolic contents (b) in feed stream, retentate and permeate using 0.2 wt. % ZnO-PANI/PES membrane.

As expected, the increase in applied pressure led to an increase in the permeate flux observed for the olive leaves extract filtration using the 0.2 wt% ZnO-PANI/PES NF membrane and PES bare, as depicted in **Fig. 5.16a**. Moreover, it can be seen a uniform trend between flux variation under different applied pressures for both membranes. In addition, it can be observed that the permeate flux increased with the addition of ZnO- PANI. Remarkably, the 0.2 wt% ZnO-PANI/PES NF membrane exhibits a permeate flux surpassing that of the bare PES membrane under the applied pressures. The observed effect

can be attributed to the enlargement of pore size and enhanced permeability resulting from the addition of ZnO-PANI (Manorma et al., 2021).

For 0.2 wt% ZnO-PANI/PES membrane, the initial decline of the permeate flux was notable during the first 150 min, and it was followed by a gradual decrease, indicating a potential approach a near-stationary state. In case of bare PES, the permeate flux showed a continuous reduction along the filtration time. The permeate samples collected from filtration of olive leaf extract using bare PES and 0.2 wt% ZnO-PANI/PES were analyzed to determine the concentration of TPC and subsequent calculation of rejections were performed. **Figure 5.16b** shows the variation of TPC rejection with the filtration pressure for the both membranes. It can be seen that a rejection of 87% and 92% was obtained from the 0.2 wt% ZnO-PANI/PES and simple PES membranes, respectively, at 30 bar.

It is worth knowing that the rejection from membranes is influenced by several factors, namely membranes pore size, the morphology of these pores and the interaction that occur between the membranes and the solute molecules (Manorma et al., 2021; Hosseini et al., 2018). The reason behind the lowest flux and highest rejection observed in the bare PES membrane can be attributed to its small pore size, as indicated by the mean pore size analysis (**Fig.5.10**) and further supported by the hydraulic permeability analysis.Nevertheless, the rejection of TPC in the 0.2 wt% ZnO-PANI/PES membrane was influenced not only by pore size but also by other factors. Notably, the interaction between the components of the membrane matrix and polyphenols emerged as a significant contributing factor. The high adsorption of TPC onto ZnO -PANI nanoparticles (see **section 5.5.2**) is a clear evidence of these interpretation.

The data presented in **Fig. 5.16b** indicates that the membrane, which was prepared with 0.2% ZnO-PANI/PES and bare PES, showed an increasing trend in TPC rejection as the pressure was increased. This result is consistent with previous findings reported in the literature (Erragued et al., 2022). Permeate transport in pressure-driven membranes can happen through two main mechanisms: convection driven by a pressure gradient, or diffusion driven by a concentration gradient. At lower pressures, the primary means of transport for is diffusion, which leads to an elevation in the concentration of the permeate or a decrease in retention. This happens as diffusion works to minimize the concentration gradient during the permeation process. Conversely, at high pressure, diffusion transport

becomes less significant, with convection playing a dominant role. As a result, the pressure
gradient becomes directly proportional to the permeate flow (Manorma et al., 2021).

The application of MMMs (0.2% ZnO-PANI) exhibited interesting results when it comes
to the recovery of phenolic compounds. Other values of TPC recovery found in the literature
by using other common technologies in various types of matrix can be found in **Table 5.2**.

**Table 5.2: Results from the literature related to the recovery of phenolic compounds
using common technologies.**

Removing methods of TPC	Operating conditions/Notes	Matrix	Results	References
Micellar enhanced ultrafiltration	(anionic surfactant (sodium dodecyl sulfate salt, SDS)/hydrophobic polyvinylidene fluoride membrane)	Olive mill waste water	74% polyphenols was rejected	(El-Abbassi et al., 2011)
Solvent extraction	-Extraction conditions (50°C ,20 min) -solvent (DI water)	Pomegranate's peel	Recovery of 17.78% polyphenols	(Zam et al., 2012)
Adsorption technology	Adsorbent : macroporous adsorbent resins	Blueberries extract	Recovery of 45.6% polyphenols	(Buran et al., 2014)
Coagulation	Electrocoagulation/ aluminium electrodes	Olive mill waste water	Removal of 91% polyphenols	(Adhoum et al., 2004)
Integrated extraction–adsorption process	Adsorbent : macroreticular aliphatic cross-linked polymer resin	Aronia melanocarpa berries extract	Recovery of 82% polyphenols	(Galván D'Alessandro et al., 2013)
Ultrafiltration	100 kDa polysulphone hollow fiber membrane. 35°C / 1.4 bar	Orange press liquor	58.3% total phenolic rejection	(Ruby-Figueroa et al., 2012)
Anaerobic and aerobic (biological technique)	Two-phase anaerobic digester reactors	Olive mill waste water	Phenol removal 70–78%	(Fezzani et al., 2010)

The concentrations of main polyphenols in permeate and retentate produced by 0.2% ZnO-
PANI/PES at 30 bar, as determined by HPLC analysis, and the feed, permeate, and retentate
chromatographic profiles are shown in **Table 5.3** and **Fig. 5.17**, respectively.
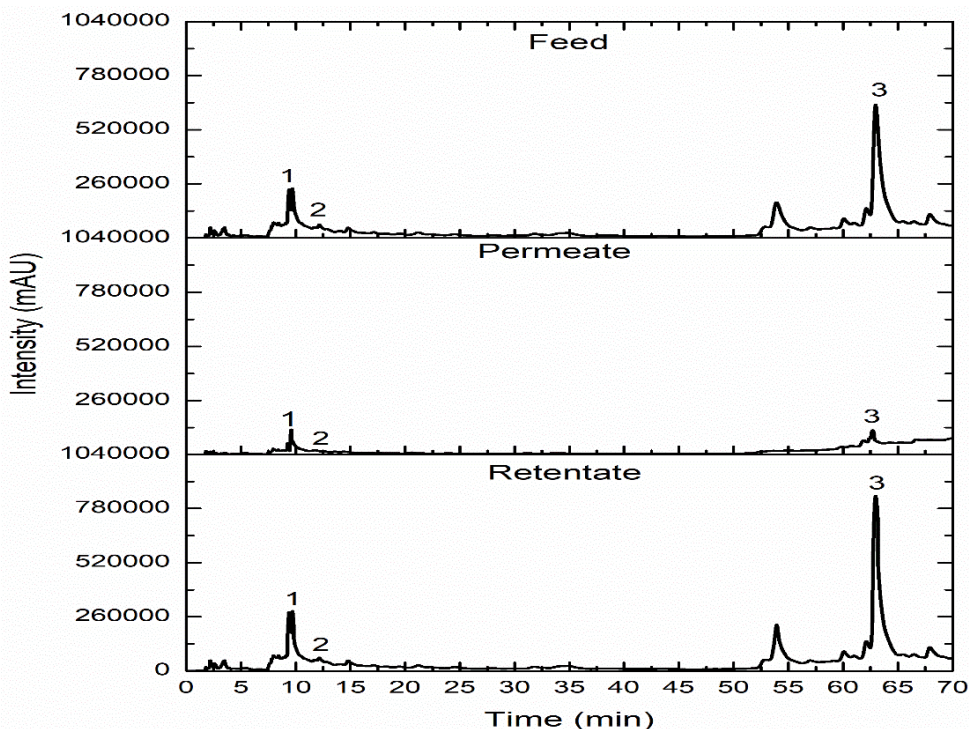
Figure 5.17: HPLC chromatograms of polyphenols in feed, permeate and retentate produced by 0.2% ZnO-PANI (30 bar). (1) Hydroxytyrosol; (2) Tyrosol; (3) oleuropein.

The data displayed in **Fig. 5.17** highlight that the highest presence of polyphenols identified in olive leaf extract is oleuropein, which was measured at a concentration of 41.56 mg/gOLP. The rejection values of oleuropein (Mw = 540 g/mol), tyrosol (Mw = 138.164 g/mol), and hydroxytyrosol (Mw = 154.16 g/mol) using ZnO-PANI/PES membrane were approximately 86%, 100%, and 83%, respectively. The obtained resultscan be explained to higher adsorption of phenolic compounds onto ZnO-PANI nanoparticles surfaces that are incorporated into membrane matrix, as evidenced in **section 5.5.2**. The study conducted by Goswami et al., (2019) demonstrates a successful removal of polyphenols, namely p-nitrophenol and resorcinol, from water using adsorption onto NiO-PANI nanoparticles. Their research findings highlight the potential of these nanoparticles as an efficient method for water treatment, specifically targeting the removal of polyphenolic compounds. In our work, our primary objective is to attain a substantial polyphenol rejection from olive leaf extract while maintaining a high flux rate. Based on the

nanofiltration results, 0.2% ZnO-PANI/PES membrane showed an optimal balance between rejection of TPC due to the strong adsorption affinity of ZnO-PANI nanoparticles, and a significantly high flux, owing to the hydrophilic properties of these nanoparticles.

Table 5.3: Analysis of identified polyphenols in feed stream, retentate and permeates obtained using 0.2% ZnO-PANI/PES membrane at 30 bar.

Membrane	Sample	Oleuropein (mg/g_{OLP})	R_o(%)	Tyrosol (mg/g_{OLP})	R_T(%)	Hydroxytyrosol (mg/g_{OLP})	R_H(%)
0.2% ZnO-PANI/PES	Feed	41.56 ± 00	86	0.74 ± 00	100	3.1 ± 00	83
	Retentate	102.34 ± 00	-	1.99 ± 00	-	5.91 ± 00	-
	Permeate	5.6 ± 00	-	0.00 ± 00	-	0.51 ± 00	-

5.5.4.2. Membrane fouling and cleaning

As previously mentioned, both bare PES and 0.2% ZnO-PANI/PES membranes underwent cleaning using a 0.2 M NaOH solution at 25°C and under a pressure of 20 bar following the filtration of OLE. To assess membrane fouling, the post-cleaning permeate water flux (PWF) was measured under 20 bar. This was done to assess the difference in flux variation compared to the initial flux value. Afterwards, the flux recovery was calculated and presented in **Table 5.4**.The FR of 0.2% ZnO-PANI/PES membrane (45%) was lower than of the unfilled PES membrane (more than 74%). The variation in flux recovery between the two membranes can be attributed to the influence of the utilized nanoparticles. These nanoparticles facilitate the creation of a thin layer cake through the adsorption of phenolic compounds onto the membrane surface. Given that these membranes underwent a single cleaning run, it is evident that flux recovery can be enhanced either through a thorough deep cleaning or by conducting multiple cleaning runs. That's can remove more phenolic compounds stuck in membrane surface and clean membrane pores.

Table 5.4: Comparison between the initial permeability, the permeability after cleaning and flux recovery of bare PES and 0.2% ZnO-PANI/PES membranes.

Membrane type	$L_{p,i}$ (L/(m^2 h bar))	$L_{p,f}$ (L/(m^2 h bar))	FR (%)
Bare PES	1.29	0.96	74.3
0.2% ZnO-PANI/PES	7.18	3.24	45.1

5.6. Conclusions

In the present study, ZnO-PANI nanoparticles was fabricated by simple chemical oxidation polymerization, and the SEM-EDX characterization showed that the ZnO-PANI was successfully prepared. The experimental results showed that adsorption of phenolic compounds is more in high pH medium and with high initial adsorbate concentration. Isotherm studies showed that adsorption of phenolic compounds from OLE was best described by the Langmuir isotherm model. Embedding of various content of synthesized ZnO-PANI nanoparticles into PES mix matrix was done by the non-solvent induced phase inversion method. The FTIR spectrum approved presence of ZnO-PANI in the prepared mixed matrix. This study demonstrated that the morphological and structural properties of the prepared membranes are affected by the presence of ZnO-PANI nanoparticles in the polymeric matrix. Results showed that porosity, pore size, water content and contact angle were improved initially by an increase of ZnO-PANI concentration up to 0.2 wt% in the membrane matrix and then decreased by more additive content. It was found that membrane permeability increased from 1.29 Lm^{-2} h^{-1} bar to 7.18 Lm^{-2} h^{-1} bar comparing bare PES (0% ZnO-PANI) and membrane with 0.2% ZnO-PANI bare PES (0% ZnO- PANI). As a conclusion, membrane embedded with 0.2 wt% ZnO-PANI was selected as the best NF membrane, which provide high flux with good TPC rejection.

CHAPTER 6 :Recovery of oleuropein from olive leaf extract using zinc oxide coated by polyaniline nanoparticle mixed matrix membranes

6.1 Abstract

Zinc oxide coated by polyaniline (ZnO-PANI) nanoparticles were incorporated in polyethersulfone (PES) matrix to evaluate adsorptive removal of oleuropein (OLP) from olive leaf extract (OLE).The effect of nanoparticles on pure water flux (PWF) and permeability was studied. The nanofiltration (NF) performance was investigated by total phenolic compounds (TPC) rejection at various pressures (10-30 bar), OLP rejection at 30 bar and fouling resistance. Results showed improved permeability of ZnO-PANI-prepared membranes compared to unfilled PES membranes. Findings showed that 0.2 wt% of ZnO-PANI had the highest initial permeate flux. In terms of rejection, 0.4 wt% ZnO-PANI offered highest rejection value (90–97%) and 100% for TPC and OLP, respectively. Fouling resistance results showed that bare PES had the best antifouling capacity. By appropriately incorporating ZnO-PANI in the membranes, it became feasible to enhance both flux and rejection efficiency. Out of the various prepared membranes, the 0.2% ZnO- PANI membrane exhibited a favorable equilibrium between permeate flux and oleuropein rejection. It was surprising to discover that utilizing these membranes for OLE filtration, after pre-treatment with ultrafiltration (UF), resulted in a complete 100% rejection of OLP. This indicates a notable and specific separation of OLP from OLE by a ZnO-PANI-based MMM.

Keywords: Olive leaves, Phenolic compounds, Oleuropein, Nanofiltration, Adsorptive removal, PES/ZnO-PANI membranes.

6.2 Graphical abstract
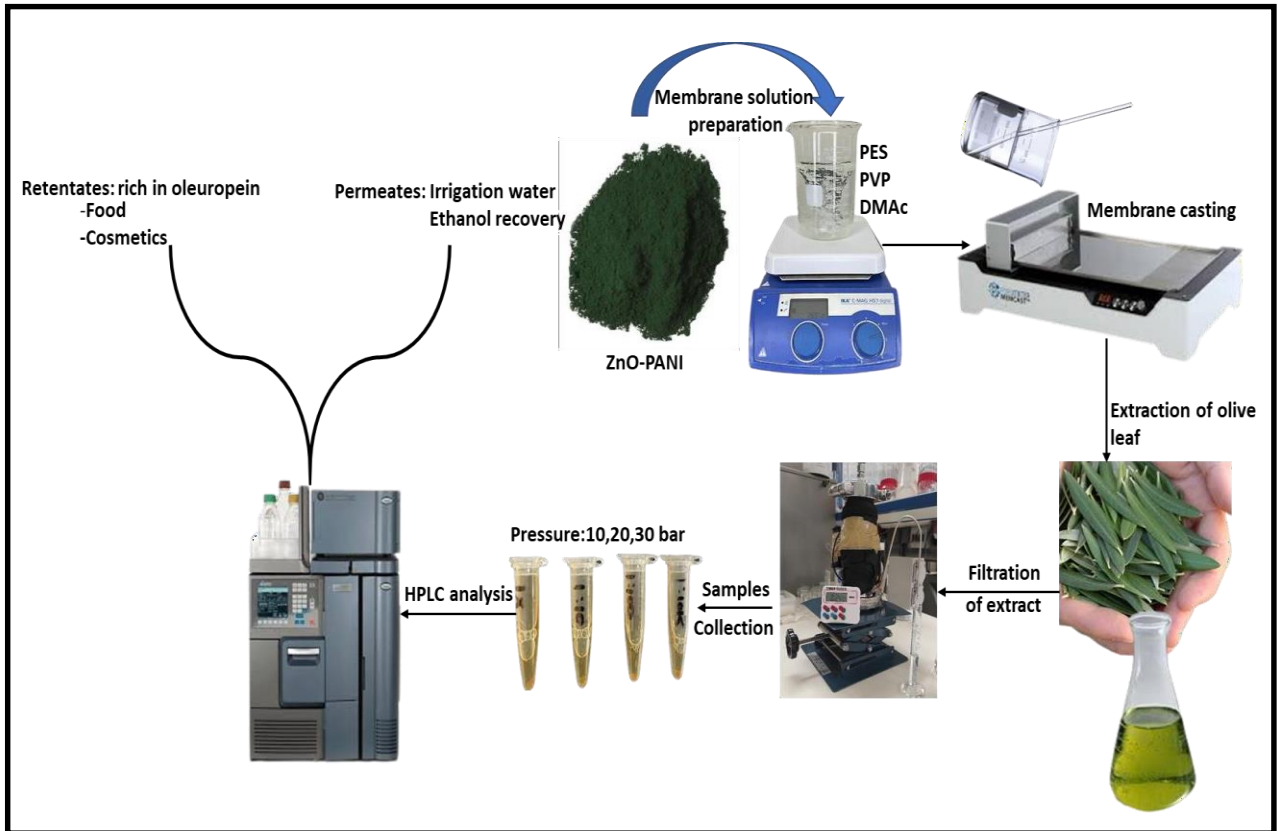
Figure 6.1: Graphical abstract.

6.3 Introduction

Olive tree leaves are easily obtained either from the olive grove or from residues remained after agricultural treatment and industrial waste (Markhali et al., 2020). Olive oil production process generates huge amounts of olive leaves, which is around 10% of the total weight of the olives harvested (Lama-Muñoz et al., 2019). Furthermore, a significant amount of olive leaves, approximately 25 kg per olive tree annually is produced through olive tree pruning (Kashaninejad et al., 2020). Currently, this byproduct is usually disposed of through either incineration or grinding, with the resulting particles spread across agricultural fields in sector (Lama-Muñoz et al., 2019), therefore, its valorization can make the olive sector more profitable and decrease the negative environmental impact of this activity (Contreras et al., 2020).

In this specific context, multiple research endeavors have been conducted with the aim of comprehending the benefits of the abundant bioactive compounds found in these byproducts (Cruz et al., 2017). Olive leaves consist primarily of secoiridoids (oleuropein, ligstroside, dimethyloleuropein) and flavonoids (apigenin, kaempferol, luteolin), alongside various other phenolic compounds (hydroxytyrosol, tyrosol, caffeic acid) (Cifá et al., 2018). These phenolic compounds exhibit a variety of biological characteristics, including antioxidant and anti-inflammatory properties, along with antimicrobial, antiviral, anti-carcinogenic, and advantageous cardiovascular effects (Irakli et al., 2018). As a result, various industries, including the pharmaceutical, cosmetic, and food industries, have been increasingly interested in the possible health advantages of olive leaves.

Literature shows that oleuropein is the dominant phenolic compound present in olive leaves and varies between 17% and 23% depending on the time of harvesting the leaves (Yateem et al., 2014). Diverse studies demonstrate that oleuropein has anti-inflammatory, antioxidant, antimicrobial, anticancer and anti-diabetes properties (Lama-Muñoz et al.,2019; Kashaninejad et al., 2020). Thus, there is an increasing attention in extraction and purification of oleuropein from olive leaves extract because of the growing demand for the substitution of chemical additives by natural ones (Erragued et al., 2022).

In order to promote the functional properties and increase the nutritional benefits of extracts, concentration techniques can be applied to enhance the added value of the final product. In recent years, multiple attempts have been made aiming at the production of phenolic rich concentrated streams include extraction, precipitation, chromatography, electrophoresis, osmotic distillation, freeze concentration (Pereira et al., 2020; Khemakhem et al., 2017). Nevertheless, all of the abovementioned techniques are characterized by some downsides, including the degradation of the thermosensitive compounds due to high temperatures and high consumption of energy, ineffectiveness, and additional chemicals, and therefore, they are cost intensive (Erragued et al., 2020 ; Pereira et al., 2020).

The use of membrane technology is becoming a successful alternative to concentrate these sensitive natural compounds. The membrane technology is advantageous in terms of energy savings, no additives, high removal efficiency, simplicity of operation and clean environmentally benign. This technique is based on the ability to differentiate between

different types of solute molecules, only allowing some molecules to pass through either polymeric or semi-permeable membranes while blocking others under a driving force, which named by selective permeation.

In fact, a variety of polymeric /ceramic membrane techniques specifically microfiltration (MF), UF, and NF are used to recover value-added compounds from a various variety of liquid matrix. In particular, NF membranes are suitable for the retention of phenolic compounds in considerable amounts due to its small pore sizes and in that way produce a stream rich in phenolic compounds, offering special pluses for the fractionation of molecules of similar molecular weight (Tundis et al., 2018 ; Conidi et al., 2012; Mudimu et al., 2012).Unfortunately, this process is still limited due to the inability of polymeric membranes to tolerate high temperature and pH conditions, the relatively poor selectivity of ceramic membranes for TPC separation, and the presence of TPC impurities with comparable molecular masses. Moreover, it diminishes membrane performance by causing a gradual decline in permeate flux under constant pressure, leading to a reductionin membrane lifetime and a rise in transmembrane pressure (TMP) or operational costs.

There have been some excellent advancements have been achieved in this field, particularly with the introduction of mixed matrix membranes (MMMs).These membranes exhibit great promise and are formed by integrating inorganic, organic, or hybrid nanofillers into a continuous polymeric matrix. Moreover, these nanofillers possess the potential to function as a layer coating atop polymeric membranes (Manorma et al., 2021).

Many kinds of fillers used for MMMs preparation; these include: titanium dioxide (TiO_2), aluminum oxide (Al_2O_3), zircona (ZrO_2), silica (SiO_2), graphene oxide (GO), carbon nanotubes (CNTs), graphene, chitosan, Boehmite, zeolites (Zinadini et al., 2017 ; Guo et al., 2017; Rahimi et al., 2015). The use of these nanomaterials as additives leads to the improvement of the surface hydrophilicity, the pore formation and also theenhancement of the antifouling property (Zinadini et al., 2017), as well as provide beneficial effects on the chemical, physical and mechanical properties of simple polymeric membranes. These nanofillers have the potential to bestow distinct characteristics such as antibacterial, antioxidant, and photocatalytic activities, depending on the intendedapplication (Rahimi et al., 2015).

An instance of this is the study conducted by Manorma et al., (2022), wherein they examined the impact of incorporating ZnO nanoparticles into the PSf matrix. The results revealed that adding ZnO up to 0.5% resulted in increased water flux and improved antifouling properties, attributed to the enhanced surface hydrophilicity. Zinadini et al., (2014) prepared the nanocomposite membranes blended with GO nanoparticles in order to investigate their effect on the performance and morphology of PES membrane. The results showed that 0.5 wt% of GO is sufficient to prepare a membrane with mean pore radius, porosity, and water flux higher than bare PES membrane, as well as better water flux, hydrophilicity and antifouling property. Wang et al., (2015), investigated the effect of CNTs nanoparticles mixed in PES membrane on membrane efficiency and revealed that theblended membrane with 0.01 wt% of CNTs presented a better water permeation, surface hydrophilicity and surface roughness compared to unfilled PES membrane.

Among different membrane materials used in separation fields, PES is one of the most promising polymeric materials (Hosseini et al., 2016). It can provide high rigidity, excellent thermal and chemical resistances as well as good mechanical stability (Zinadini et al., 2017; Hosseini et al., 2016; Rahimpour et al., 2012). Furthermore, it is commercially available (Vatanpour et al., 2012), non-harmful/non-toxic and wide pH endurance (Rahimi et al., 2015).In this regard, these properties are adequate factors can distinguish it from others in preparation of NF asymmetric membranes (Nasrollahi et al., 2018).

ZnO is extraordinarily significant nanofiller due to its excellent properties such as commercially abundant, nontoxicity, low cost, high thermal, mechanical, chemical and physical stability, great photocatalytic activity, simple surface functionalization and extremely high surface area (Zinadini et al., 2017; Nasrollahi et al., 2018). These unique features make it a recommended choice for our purpose. In addition to metal oxides, some polymeric materials such as PANI is considered as a promising polymer in different separation processes due to its special features including: easy and inexpensive to produce, environmental and thermal stability, high intrinsic ionic and electronic conductivity as well as relatively low cost (Bagheripour et al., 2016).

Nanostructured ZnO composites have been extensively investigated in many applications such as solar cells, chemical sensors, photocatalysis, optoelectronic, and field

emission (Beek et al., 2004 ; Günes et al., 2007; Yousefi et al.,2010; Huang et al., 2008; Khan et al., 2010; Xu et al., 2009).

So far, to the best of our knowledge, zinc oxide-polyaniline (ZnO-PANI) nanocomposites have not been investigated for phenolic compounds removal. In a previous work, we have employed a simple approach to coat ZnO nanoparticles with PANI, resulting in a composite material that exhibits improved adsorption capability for phenolic compounds. Therefore, the incorporation of zinc oxide coated by polyaniline nanoparticles in MMMs preparation becomes a successful candidate to enhance membrane performance in terms of permeability and high rejection. In addition, in a previous research, a commercial spiral and flat sheet membranes has been investigated in order to recover phenolic compounds, especially oleuropein from olive leaves extract (Erragued et al., 2022 ; Khemakhem et al., 2017). To the best of our knowledge the removal of oleuropein from olive leaf extract using a flat sheet lab-made membrane has not been previously reported. Therefore, in this work an innovative application of lab-made ZnO-PANI-based MMMs to separate OLP from TPC (pre-filtered by UF) was proposed. ZnO-PANI nanoparticles were chosen as the basis for creating MMMs because they possess excellent adsorption affinity for TPC and can be easily synthesized The membranes were created through the non- solvent induced phase inversion technique, and their properties, such as permeability and fouling, were examined by varying the concentrations of ZnO-PANI nanoparticles. The performance of all prepared membranes was tested by TPC rejection at different pressures (10-30 bar) and OLP rejection at 30 bar.

6.4 Materials and Methods

6.4.1. Materials

Olive leaves were obtained from Chemlali cultivar grown in Sfax (Tunisia). Following collection, the raw material was subjected to a 24-hour drying process in a convection oven at 40°C and finely grinded with a blade cutter. Olive leaf powder was kept in the dark environment at room temperature (RT) until the extraction process.

6.4.2. Chemicals

Polyethersulfone (PES, Mw = 60,000 g mol^{-1}), Polyvinylpyrrolidone (PVP, Mw = 29,000 g mol^{-1}) and N, N-Dimethylacetamide (DMAc) were purchased from Sigma Aldrich for preparation of NF membranes. Self-synthesized zinc oxide coated by polyaniline nanoparticles (ZnO-PANI) by chemical oxidation polymerization was used to prepare the membranes as additives. For the extraction of olive leaves, we utilized ethanol procured from Fisher Chemical, along with distilled water obtained via the Milli-Q system from Millipore, Bedford, MA, USA. Acetonitrile (HPLC grade) and phosphoric acid (85%) wereobtained from Carlo Erba and Sigma-Aldrich, respectively, for the purpose of HPLCanalysis. OLP (purity≥ 98% by HPLC), which was used as a standard, was obtained from Sigma-Aldrich.

6.4.3. Preparation of PES/ZnO-PANI nanofiltration membranes

PES/ZnO-PANI nanofiltration membranes were prepared via nonsolvent induced phase inversion process using casting solutions consisting of PES (20 wt%), PVP (1 wt%) and different amounts of ZnO-PANI in DMAc as solvent. First, a desired amount of ZnO- PANI nanoparticles (0.05, 0.1, 0.2, 0.4 and 0.6 wt%) was dispersed in DMAc and kept in ultrasonic cleaner water bath (Ultrasons, J.P. SELECTA) to achieve a suitable dispersion. The membrane identified as 0.05 wt% ZnO-PANI is the result of preparing a casting solution where the ZnO-PANI content, relative to PES + DMAC, was 0.05 wt%, etc. After dispersing ZnO-PANI in a solvent, the mixture was continuously stirred at RT for 24 hours while adding PES and PVP. Afterward, the produced mixtures were ultrasonicated againfor 30 min to avoid the aggregation of ZnO-PANI nanoparticles. Then, the casting solutionswere left in a vacuum oven at 50 °C for 6 h to remove sufficiently the air bubbles. Next, thehomogenous casting solutions were applied onto glass substrates by an automatic film applicator (Elcometer 4340) equipped with a 250 μm thickness casting knife. After casting, the glass substrates were immediately submerged into a non-solvent bath (distilled water), then kept at 25 °C.

After initially phase separation and membrane solidification, the prepared membranes were moved in fresh distilled water containers for 24. Finally, the prepared membranes were kept between filter papers at RT for 1 day for drying. **Fig.6.2** displays the membranes that have been prepared.
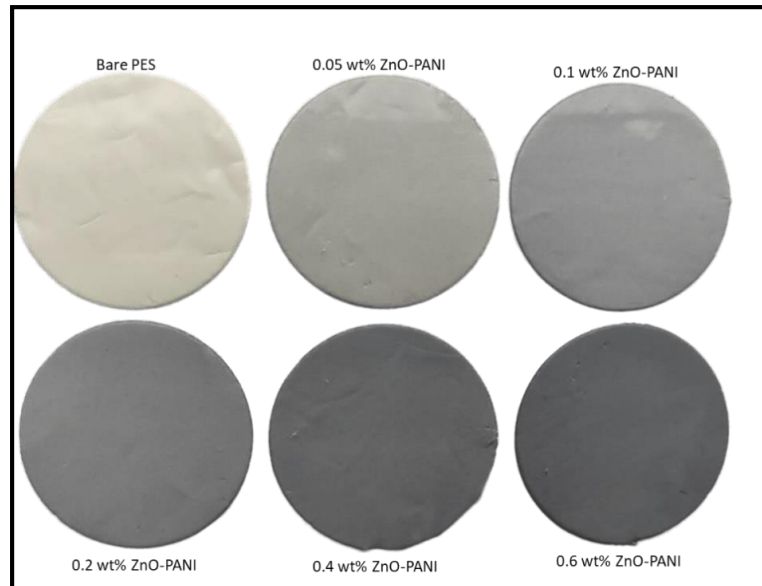
Figure 6.2: Prepared membranes with different concentrations of ZnO-PANI nanoparticles.

6.4.4. Extract preparation

6.4.4.1. Extraction of total phenolic compounds (TPC) from olive leaves

The extraction of olive leaves was carried out as described below. Briefly, 1.2 g of olive leaves powder was immersed into 40 mL of ethanol/water, 75/25% (v/v), followed by a 90 min mixing in a shaking bath at 120 rpm and 50°C. After extraction, the mixture was subjected to vacuum pump using sintered glass at 0.45 μm, then centrifuged (Sorvall ST 16 R, Thermo Scientific, Leicestershire, UK) at 4000 rpm for 15 min. The extract obtained was stored in a refrigerator until analysis.

6.4.4.2. Pretreatment of olive leaves extract

After extraction, OLE underwent an ultrafiltration procedure to eliminate suspended solids and, therefore, reducing the fouling phenomena during NF experiments using the

prepared membranes. The filtration trials were conducted using a crossflow membrane filtration device (Sepa CF II Membrane Cell system, Sterlitech Corporation), which featured a membrane area of 140 cm^2, as illustrated in **Fig. 6.3**.This equipment consists of apermeate and feed tank, a high-pressure diaphragm pump (Hydra-Cell, Wanner Engineering, Inc.), membrane cell system and pressure manometer. The UF unit wasequipped with a UP005 P flat sheet membrane module (hydrophobic polyethersulphone, thickness between 210-250 µm, typical operating pressure 5 bar, maximum operating temperature 50°C, nominal molecular weight cut-off 5000 Da) supplied by Microdyne Nadir (Germany advanced separation technologies). UF experiment was carried out in the batch concentration mode at an operating temperature of 25°C and a transmembrane pressure (TMP) of about 4 bar. Permeate stream was collected and kept in sealed glass bottle in a refrigerator until further use.
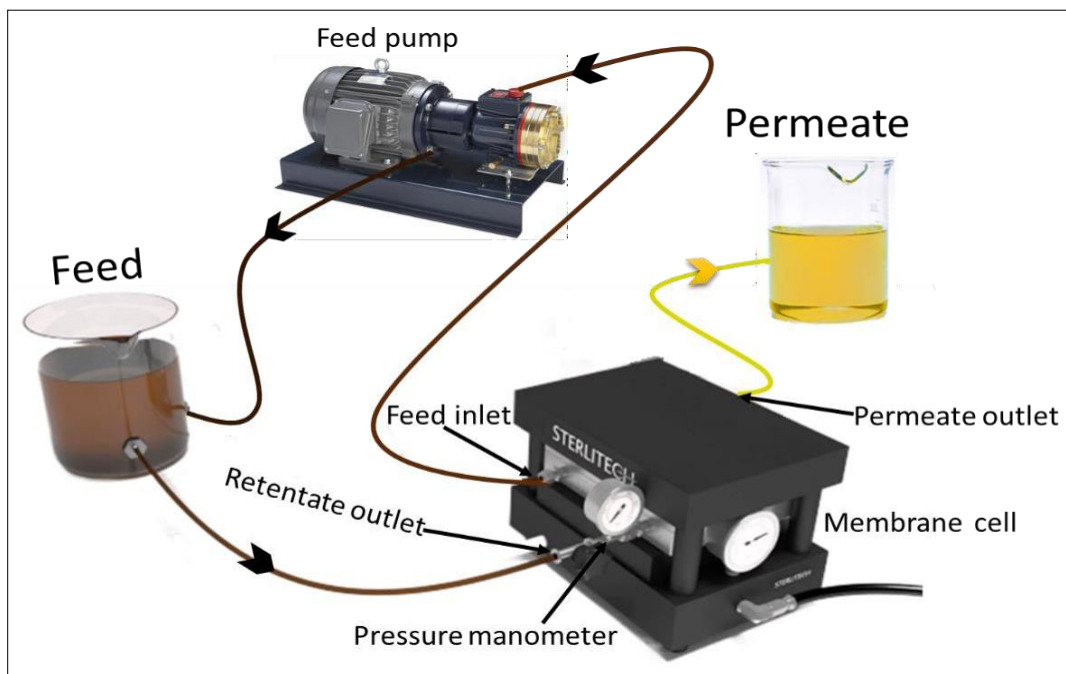
Figure 6.3: Schematic diagram of the ultrafiltration cell in crossflow filtration mode.

6.4.4.3. Determination of total phenolic compounds (TPC)

The analysis of total phenolic compounds (TPC) was performed using the Folin-Ciocaltaeu method. Shortly, 100 µL of extract solution was added to 100 mL of Folin-Ciocalteu reagent. The mixture was then incubated at 25°C for 5 min in the dark. Next,

300 μL of Na_2CO_3 (0.333 g/mL) were added to the mixture. After maintaining the sample at 40 °C in the dark for 30 min, the absorbance at 765 nm was recorded using UV/vis spectrophotometer (PG Instruments T60). A calibration curve was created using gallic acid, and the outcomes were reported as milligrams of gallic acid equivalents (GAE) per gram of olive leaves powder (mg GAE/g_{OLP}).

6.4.4.4. Analysis using high-performance liquid chromatography (HPLC)

The quantification of oleuropein in the different fractions of olive leaf extracts was performed in line with a method previously established by Mulinacci et al., (2001). A HPLC system (Waters 2695 Alliance HPLC) coupled with an UV–VIS multi-wavelength detector was used. The separation was carried out at RT on a Brisa LC2 C18 column (250 ×

4.6 mm id, 5 μm, Spain). The mobile phase consisted of water adjusted to pH 3.20 with phosphoric acid (solvent A) and acetonitrile (solvent B). The conditions of the solvent gradient were the following: 100–89% A (0–3 min), 89-87% A (3–41 min), 87-80% A (41–55 min), 80–75% A (55–70 min), 75–100% A (70–71 min), and finishing with an isocratic elution (100% A) during 9 min. The rate of flow was 1 mL/min. The chromatographic profiles were assessed at 215 and 280 nm after injecting a 10 μL volume. Prior to injection, the samples were filtered using a 0.1 μm microfilter. Peak of oleuropein was identified by congruent retention time compared with standard solution. A calibration curve was prepared at five concentration levels to quantify the amount of oleuropein.

6.4.5. Filtration performance of the prepared NF membranes

A bench scale, stirred dead-end filtration cell system (Sterlitech HP4750 Stirred Cell) was applied to characterize the filtration performance of the prepared membranes. The performance of PES/ZnO-PANI NF membranes was evaluated by measuring pure water flux (PWF), TPC and OLP rejection, and analyzing the occurrence of fouling. The volume capacity and the effective membrane surface area of the module were 300 mL and 14.6 cm^2, respectively. The cell system was pressurized with nitrogen gas to force the liquid through the membrane. Magnetic stirrer was used to reduce concentration polarization of the membranes. The setup of the dead-end filtration system is shown in **Fig. 6.4**.
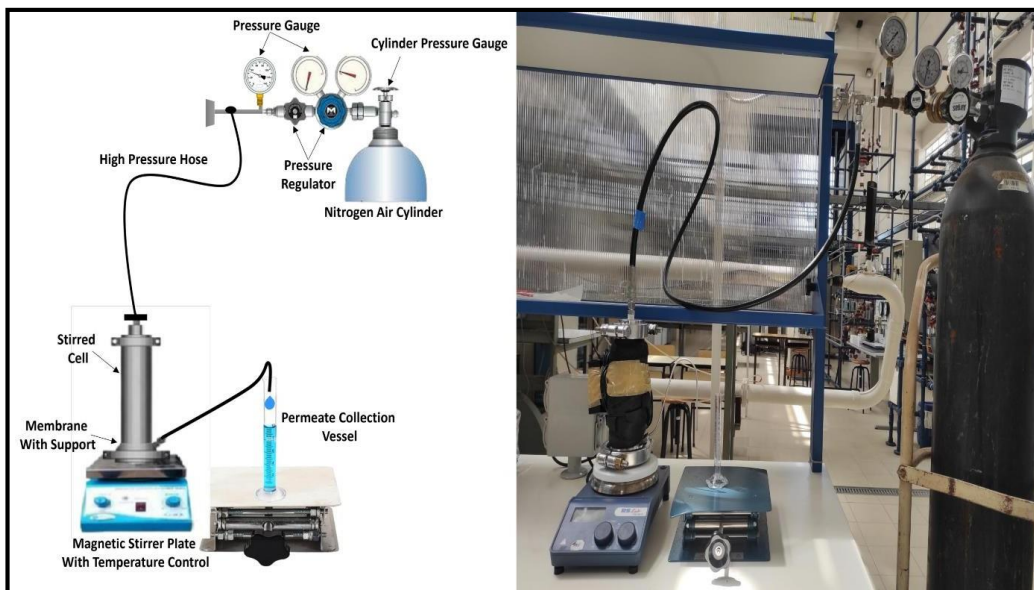
Figure 6.4: Schematic diagram and working lab scale of the dead-end cell.

The primary aim of the water filtration test was to assess the hydraulic permeability (Lp) of the membrane. In order, to determine the hydraulic permeability, pure water filtration was conducted at various pressure levels (5, 10, 15, 20, 25, and 30 bar), and samples of the permeate were collected at 5 min intervals during the process.

First, each membrane was primarily immersed in distilled water for a duration of 30 min. Afterward, the membrane was fixed within the filled cell using more distilled water. Then, the membranes were subjected to compression at 20 bar for 30 min to achieve a stable water flux. Subsequently, the pressure was then adjusted to the designated working pressure. The PWF of all membranes was tested triplicate to obtain an average value. The PWF was calculated by the following Eq. (6.1):

$$J_w = \frac{V_m}{tA_m}$$

(6.1)

J_w $(Lm^{-2}\ h^{-1})$, V_w (L), t (h), and A_m (m^2) stand for the permeate flux, volume of collected permeate, time for permeate collection, and effective membrane area, respectively.

The PWF values obtained were graphed against the operating TMP, yielding a linear curve. The slope of this curve was then utilized to calculate the average hydraulic permeability (as given in Eq. 6.2) within the applied TMP range.

$$L_p = \frac{J_w}{\Delta P} \qquad\qquad (6.2)$$

L_p (L m^{-2} h^{-1} bar^{-1}) represents the hydraulic permeability, while ΔP (Pa) denotes the TMP.

To evaluate the performance of the membranes for concentrating TPC from UF permeate, filtration experiments at feed temperature of 25°C and at variables pressures (10, 20 and 30 bar) were carried out. The feed solution was stirred at the rate of 1000 rpm. Permeate samples were collected at intervals of 75 min then analyzed for determination of total phenolic compounds and oleuropein concentrations by UV–Vis spectrophotometry (**section 6.4.4.3**) and by High-performance liquid chromatography HPLC (**section 6.4.4.4**), respectively, this permits the determination of rejection values for TPC and OLP as provided in Eq.(6.3).

$$Rejection\ (\%) = (1 - \frac{C_p}{C_f}) \times 100 \qquad\qquad (6.3)$$

C_p and C_f represent the concentrations of TPC or OLP in the permeate and feed solutions, respectively.

6.4.6. Fouling analysis

After filtration runs of olive leaf extract, the membranes underwent immediate cleaning using a 0.2 M NaOH solution at 20 bar and RT to reclaim the PWF of the membrane. The Flux Recovery (FR) was then determined using Eq. (6.4), allowing for an assessment of the membrane's resistance to fouling and its reusability properties.

$$(\%) = \frac{L_{p,f}}{L_{p,i}} \times 100 \qquad\qquad (6.4)$$

$L_{p,i}$ and $L_{p,f}$ refer to the initial hydraulic permeability of the membrane and the hydraulic permeability restored after filtering OLE and subsequently cleaning with a 0.2 M NaOH solution, respectively, expressed in units of (Lm^{-2} h^{-1} bar^{-1}).

It is important to know the amount of oleuropein adsorbed on the membrane surface. To calculate the oleuropein adsorbed on the membrane surface, permeate samples coming from the cleaning filtration using NaOH solution were collected for 60 min and then analyzed by HPLC.

6.5. Results and discussion

6.5.1. Hydraulic permeability

The flux/permeability of prepared membranes was analyzed to evaluate the impact of incorporating nanoparticles on filtration efficiency. **Figs 6.5 (a)** and **(b)** illustrate the PWF under various pressures ranging from 5 to 25 bar, along with the average permeability of the membranes.

Fig. 6.5a distinctly illustrates that all MMMs exhibit higher flux in comparison to the basic PES membrane at different operation pressures. Moreover, the PWF of the synthesized membranes increases as the applied pressure increases, which is in agreement with the results reported by other researches (Zinadini et al., 2014). By addition the amount of ZnO-PANI nanoparticles to polymer matrix, the prepared NF membranes showed an increase in permeability compared to bare PES membrane. At first, the permeability increased significantly when ZnO-PANI amount was increased then slightly reduced when the additive is further increased. The findings revealed that the highest permeability rate was observed at 0.2 wt% ZnO-PANI, with 0.1wt% ZnO-PANI following closely in second place. The addition of ZnO-PANI until 0.2% led to an 82% increase in hydraulic permeability in comparison to bare PES membrane.

The improvement in permeability can be related to the increase in surfacehydrophilicity. It was mentioned that a strong correlation exists between water flux and the hydrophilicity of the membrane surface (Zinadini et al., 2017).The hydrophilic characteristic of ZnO-PANI surface increases the hydrophilicity of the membrane surface. This increase leads to an increase in water permeability by enhancing the flow of water molecules within the membrane matrix and facilitating their passage through the membrane(Zinadini et al., 2017; Vatanpour et al., 2012).

In addition, the membrane permeability is closely connected to morphological parameters, including porosity, and mean pore size (Bagheripour et al., 2016). Moreover, by addition of ZnO-PANI nanoparticles into the polymer casting solution, the interaction between polymer-chain and nanoparticles may obstruct the polymer chain, thus enhancing

water permeability due to the formation of additional voids, resulting from the presence of free volumes between the polymer chains and the additive interface. This results in increased porosity, subsequently increased permeability (Rahimi et al., 2015; Vatanpour et al., 2012; Bagheripour et al., 2016). Nevertheless, an inconsiderable decrease appears whenthe amount of ZnO-PANI nanoparticles increased to 0.4 wt%. This effect may be attributed to the combination of low contact angle, porosity and pore size, resulting from the excessive addition of ZnO-PANI nanoparticles. Zinadini et al. (2017) and Bagheripour etal. (2016) both observed comparable phenomena of reduced PWF caused by high nanoparticle concentration, using ZnO/MWCNTs and PANI-co-MWCNT nanoparticles, respectively (Zinadini et al., 2017 ; Bagheripour et al., 2016).
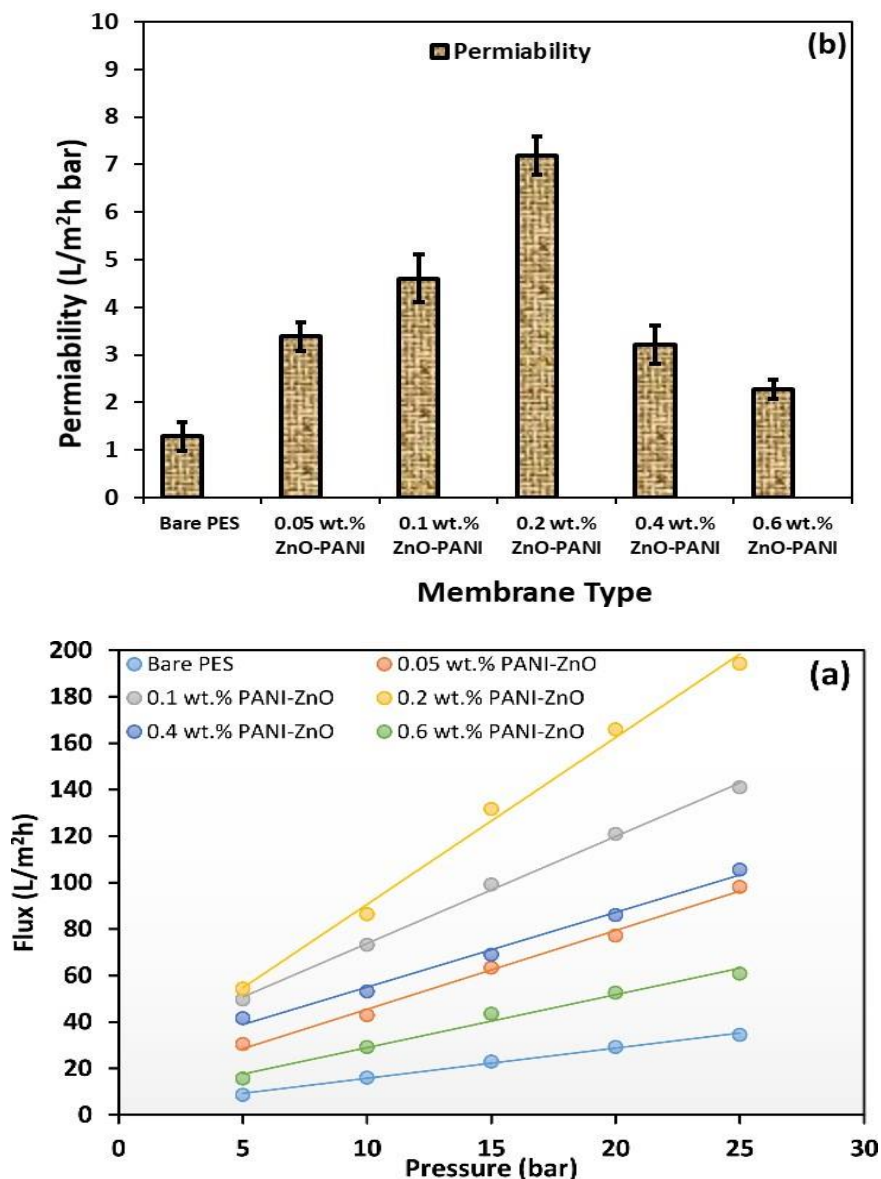
Figure 6.5: (a) Relationship between PWF and TMP; (b) Hydraulic permeability of PES membranes that were fabricated.

6.5.2. Nanofiltration of olive leaves extract

Figure 6.6 illustrates the permeate flux trend over time during the filtration process of olive leaf extract using PES membranes under various pressures (10, 20, and 30 bar).

It is crucial to note that for each pressure level, a fresh membrane was employed, and the filtration process was conducted continuously for a duration of 300 min. Subsequently, the membrane underwent cleaning using a 0.2 M NaOH solution with the objective of restoring the original PWF.

As anticipated, the data presented in **Fig.6.6** demonstrate a consistent trend of increasing flux with higher TMP values for all the membranes tested. Furthermore, an increase in the concentration of ZnO-PANI was found to result in a corresponding increase in the initial flux of permeates from the prepared membranes. For example, at 30 bar, the initial flux of olive leaf extract of the unfilled PES was 3.88 L m^{-2} h^{-1}. But by introducing ZnO-PANI nanoparticles into the casting solution, the initial permeate flux reached 4.50, 7.00 and 7.88 L m^{-2} h^{-1} for 0.05, 0.1 and 0.2 wt% ZnO-PANI/PES membranes, respectively. This can be linked to the rise in pore size and permeability with growing concentration of ZnO-PANI. However, at high concentration of the nanofiller (more than 0.2 wt%), due to phenomenon of agglomeration and plugging of the pore membranes, the initial permeate flux was reduced to 5.58 and 3.95 L m^{-2} h^{-1} for membranes blended by 0.4 and 0.6 wt% Zn0-PANI. Concentration polarization and membrane fouling appeared to be two main factors for the flux mitigation.

It is intriguing to note that the starting flux of 0.2% ZnO-PANI was comparable to that of the 0.1% ZnO-PANI membranes. However, it exhibited a consistent decline throughout the filtration duration. In contrast, permeate flux of 0.1% ZnO-PANI experienced a decline during the initial 75-150 min period, followed by a subsequent stabilization. Furthermore, the permeate flux of 0.6% ZnO-PANI at all pressures are low (3.95 L m^{-2} h^{-1}), then decreased very quick and reaches 1.54 L m^{-2} h^{-1} after 300 min at 30 bar.
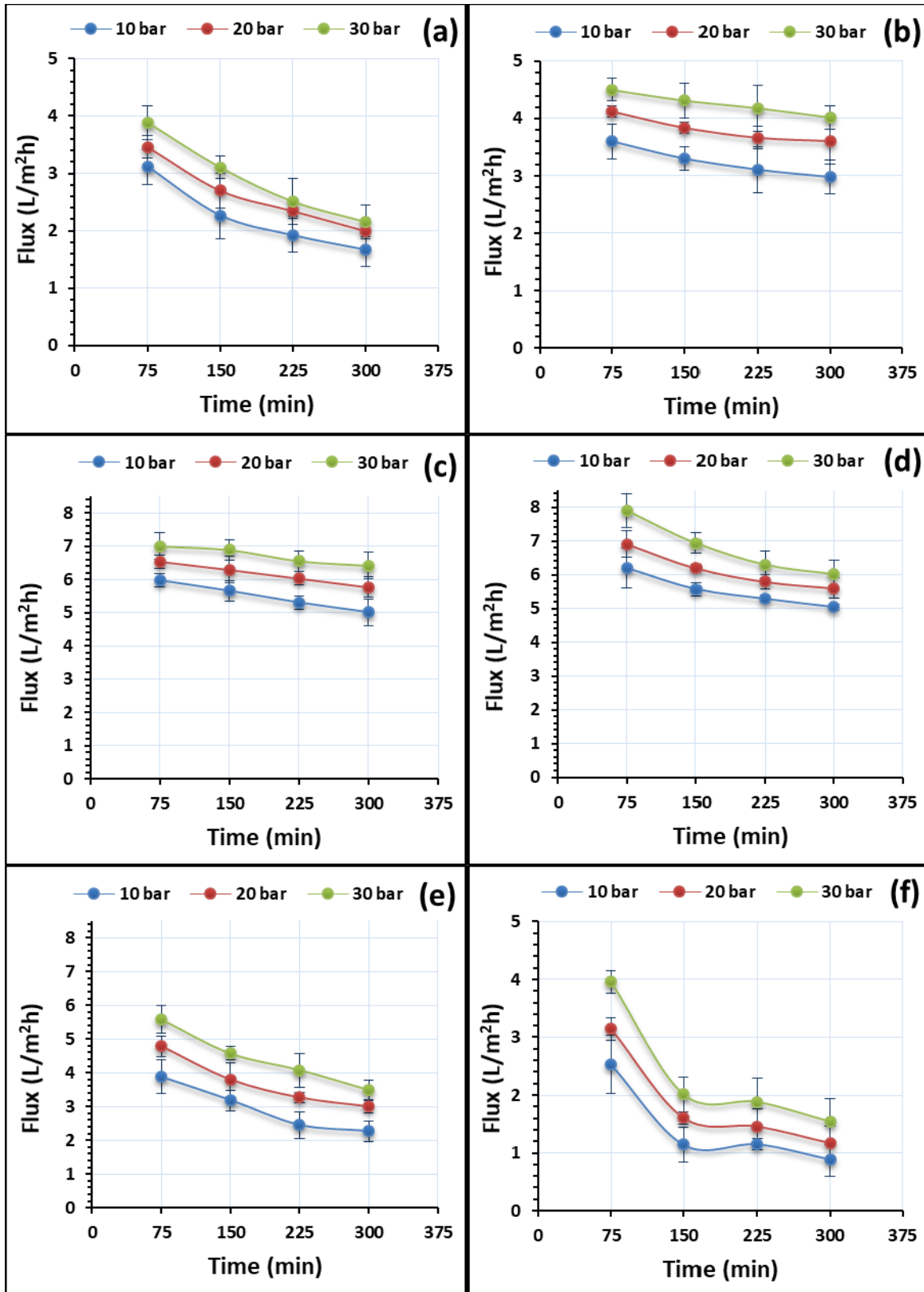
Figure 6.6: Behaviour of permeate flux of olive leaves extracts with time, for each TMP of prepared PES membranes: (a) bare PES; (b) 0.05% ZnO-PANI (c) 0.1% ZnO-PANI, (d) 0.2% ZnO-PANI, (e) 0.4% ZnO-PANI and (f) 0.6% ZnO-PANI.

6.5.3. Total phenolic compounds rejection

This study aimed to examine the nanofiltration performance of the membranes that were prepared, focusing on their ability to remove total phenolic compounds from olive leaf extract. While filtering the extract, we collected permeate samples and analyzed them to determine the concentration of total phenolic c compounds. Subsequently, we carried out calculations to determine the rejections. **Fig. 6.7** illustrates the correlation between the changes in phenolic compound rejection and the duration and pressure of filtration.

As displayed in this figure, the highest rejection for total phenolic compounds was obtained from the 0.4%wt ZnO-PANI (90.5%-97.3%) and simple PES membranes, followed by 0.2%wt, 0.1%wt, and 0.05%wt membranes. A low rejection was obtained by 0.6%wt ZnO-PANI (50.2%-58.2%).

Typically, membrane rejection is influenced by factors such as pore size, pore shape, and the interaction between membrane components and solute molecules (Sharma et al., 2022; Hosseini et al., 2017).Although bare PES showed a relatively low flux (**Fig. 6.7a**), it demonstrated satisfactory rejection capabilities for total phenolic compounds. The reason behind this can be attributed to the presence of a small pore size in this membrane. Nevertheless, concerning the ZnO-PANI-based MMMs, aside from pore size, the predominant factor influencing the removal of phenolic compounds was found to be the interaction between the membrane's constituents and phenolic molecules.

It was expected that the membranes with 0.05 and 0.1 wt% ZnO-PANI would exhibit superior rejections compared to the 0.4 wt% ZnO-PANI membrane because of their reduced pore size. However, these membranes displayed lower values across all pressures.

This can be related to their containing to a low amount of ZnO-PANI nanoparticles, therefore less adsorption capacity.

Figures 6.7(b-e) demonstrate a slight increase in the rejection of phenolic compounds in the prepared NF nanocomposite membranes with the incorporation of ZnO-PANI nanoparticles into the casting solution. As a conclusion, the removal of phenolic compounds is primarily governed by the adsorption mechanism, with the performance of the synthesized membranes being influenced significantly by the concentration and dispersion of ZnO-PANI nanoparticles (Daraei et al., 2012). The declined rejection which appeared using 0.6%wt ZnO-PANI/PES membrane (**Fig. 6.7f**) may be attributed to the critical agglomeration of nanoparticles at high ZnO-PANI density in the casting solution. Therefore, the amount of adsorptive active sites/active surface area decreased, causing a decrease of total phenolic compounds adsorption by nanoparticles, leading to increased transport of phenolic compounds throughout the membrane matrix. Among the prepared membranes, the modified membrane containing 0.4%wt ZnO-PANI composite nanoparticles showed the highest rejection of phenolic compounds (about 97.3%) at 30 bar. In **Fig.6.7** it can also be seen that all membranes indicated a linear trend for membrane rejection towards TPC with pressure and time. This result is in close agreement with the literature (Diawara et al., 2011; Todisco et al., 2002; Cassano et al., 2016 ; Bunani et al., 2013).
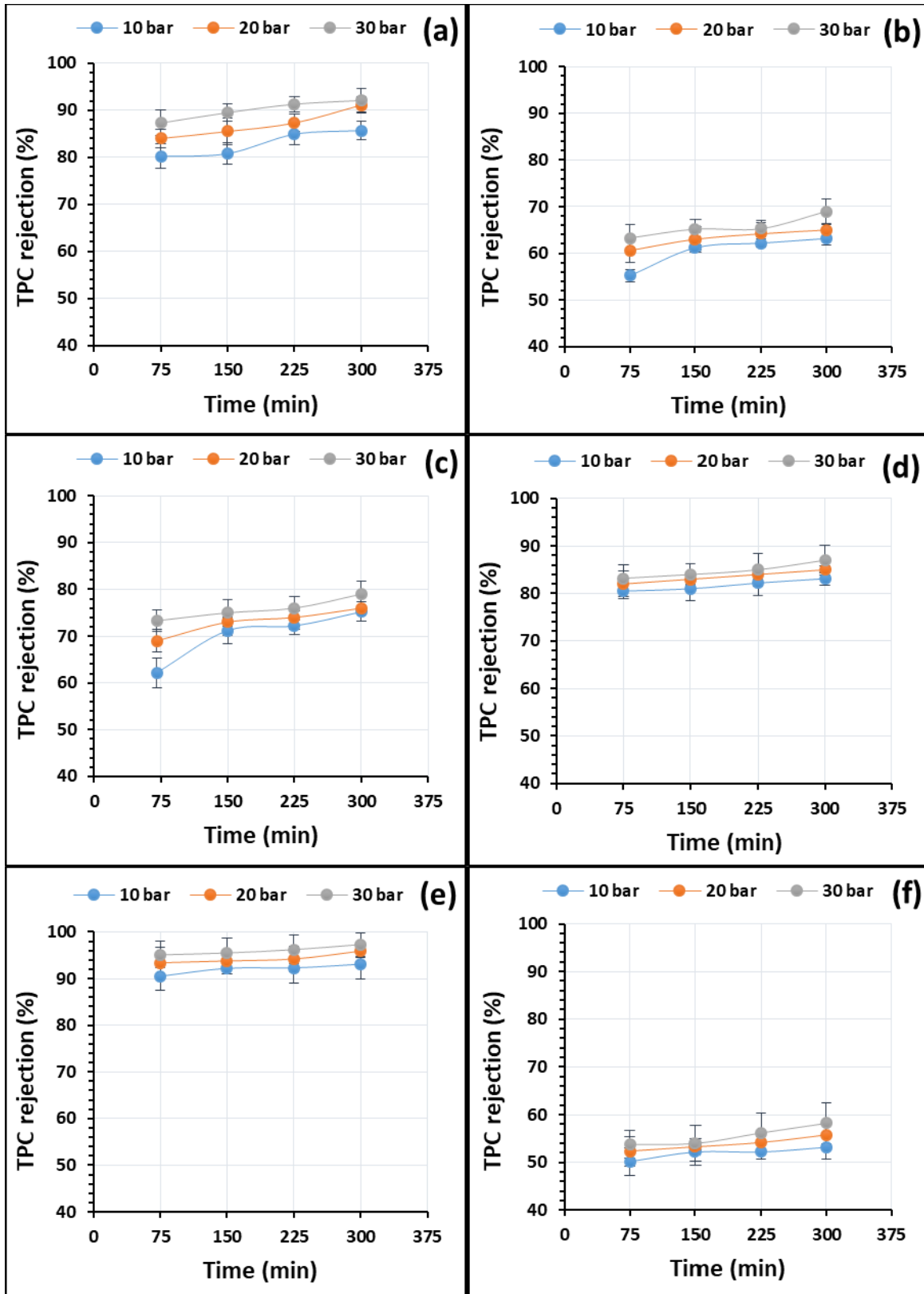
Figure 6.7: Time-dependent rejection of total phenolic compounds for different TMPs of prepared PES membranes: (a) bare PES, (b) 0.05% ZnO-PANI (c) 0.1% ZnO-PANI, (d) 0.2% ZnO-PANI, (e) 0.4% ZnO-PANI and (f) 0.6% ZnO-PANI.

Solute transfer across the membrane is essentially described as being the result of diffusion or convection which are due respectively to a concentration and a pressuregradient across the membrane. At a low pressure, the contribution of the diffusive transport is dominant, so that the concentration in the permeate fraction increases, consequently the retention coefficient decreases. Contrariwise, with increasing pressure, the transport became convective, resulting in a lower concentration of permeate and hence the retention coefficient is higher. In addition, the increase in the rejection coefficient with the extract filtration time extends can be explained by the solute's adsorption onto the membrane pore walls and its deposition on the membrane surface, resulting in narrower pores on the membrane surface with time (Manorma et al., 2021; Van et al., 2002 ; Schaep et al., 1999).This phenomenon can be described as follows: as the filtration process continues, the feed becomes enriched with larger solute molecules that cannot readily traverse through thepores of the membrane. Consequently, these molecules begin to build up on the membrane's surface, resulting in decreased flux and an intensified rejection phenomenon. Nevertheless, these cannot be considered universal laws as various other factors may come into play, such as the intrinsic features of each membrane and the type and composition of the feed being filtered, which also play a significant role (Diawara et al., 2011).

6.5.4. Oleuropein rejection

In order to more deeply study the performance of the prepared membranes, the retentates and permeates fractions obtained after 300 min at 30 bar were analysed by HPLCto determine oleuropein concentration. **Fig. 8.** illustrates the concentrations of oleuropein inthe feed, retentate, and permeate streams corresponding to the various prepared membranes. Chromatographic profiles of feed, retentates and permeates are displayed in **Fig. 6.9**.Results in **Fig. 6.9** shows the dominant polyphenol in the original olive leaf extract to be oleuropein, with a concentration of 44.61 mg/gOLP.

NF prepared membranes exhibited varying rejection values for oleuropein (Molecular weight = 540 g mol^{-1}), ranging from 67% to 100%. From **Figs 6.8** and **6.9,** it is clearly observed that the rejection of oleuropein increases with addition of adsorptive ZnO-PANI nanoparticles and the highest rejection was obtained with 0.4% ZnO-PANI membrane (100%). The reason behind this behavior may be attributed to the greater adsorption capacity of phenolic compounds exhibited by ZnO-PANI nanoparticles. Consequently, as the amount of ZnO-PANI in the membrane rises, more active sites become accessible for the adsorption of oleuropein.

	Bare PES	0.05wt% ZnO-PANI	0.1wt% ZnO-PANI	0.2wt% ZnO-PANI	0.4wt% ZnO-PANI	0.6wt% ZnO-PANI
■ Feed	44.61	44.61	44.61	44.61	44.61	44.61
■ Permeate	0	8.5	6.5	3.2	0	14.5
■ Retentate	118.87	96.28	101.03	110.54	118.22	79.64
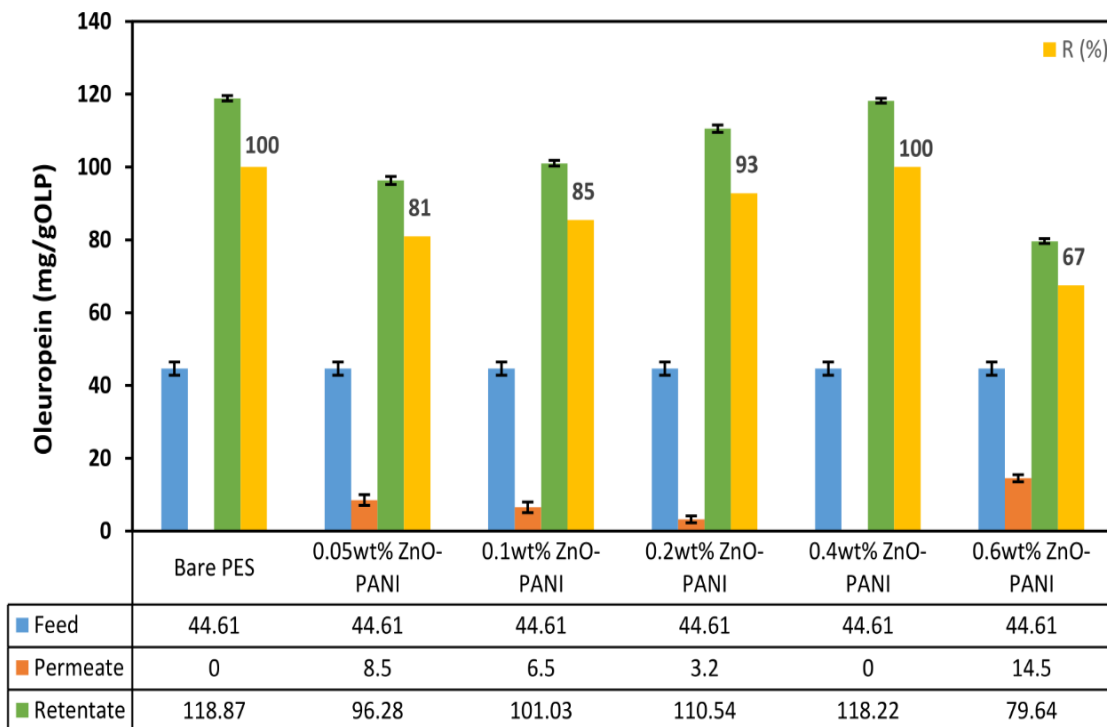
Figure 6.8: Analysis of oleuropein in feed stream, retentates and permeates obtained after 300 min at 30 bar using different prepared membranes.

However, only 67% rejection of oleuropein was achieved with 0.6wt% ZnO-PANI membrane. This reduction may be attributed to the critical agglomeration of nanoparticles at high ZnO-PANI concentration in the casting solution. In addition, the 100% rejection of oleuropein was attained by bare PES as a result of its small pore size and the polar interactions (van der Waals interactions and hydrogen bonds) that occur between membrane components and polyphenols such as oleuropein (Erragued et al.,

2022).However, as mentioned earlier, this membrane exhibits a very low permeate flux.Our main goal in this work was: firstly, to prepare mixed matrix membranes of polyaniline-coated zinc oxide nanoparticles, and secondly, to obtain a hydroethanolic extract enriched with oleuropein from olive leaves. Based on the results obtained, the membrane with 0.4wt% ZnO-PANI demonstrated excellent performance regarding the concentration of oleuropein. It successfully produced a retentate fraction that was enriched in oleuropein, reaching a content of 118.87 mg/gOLP.
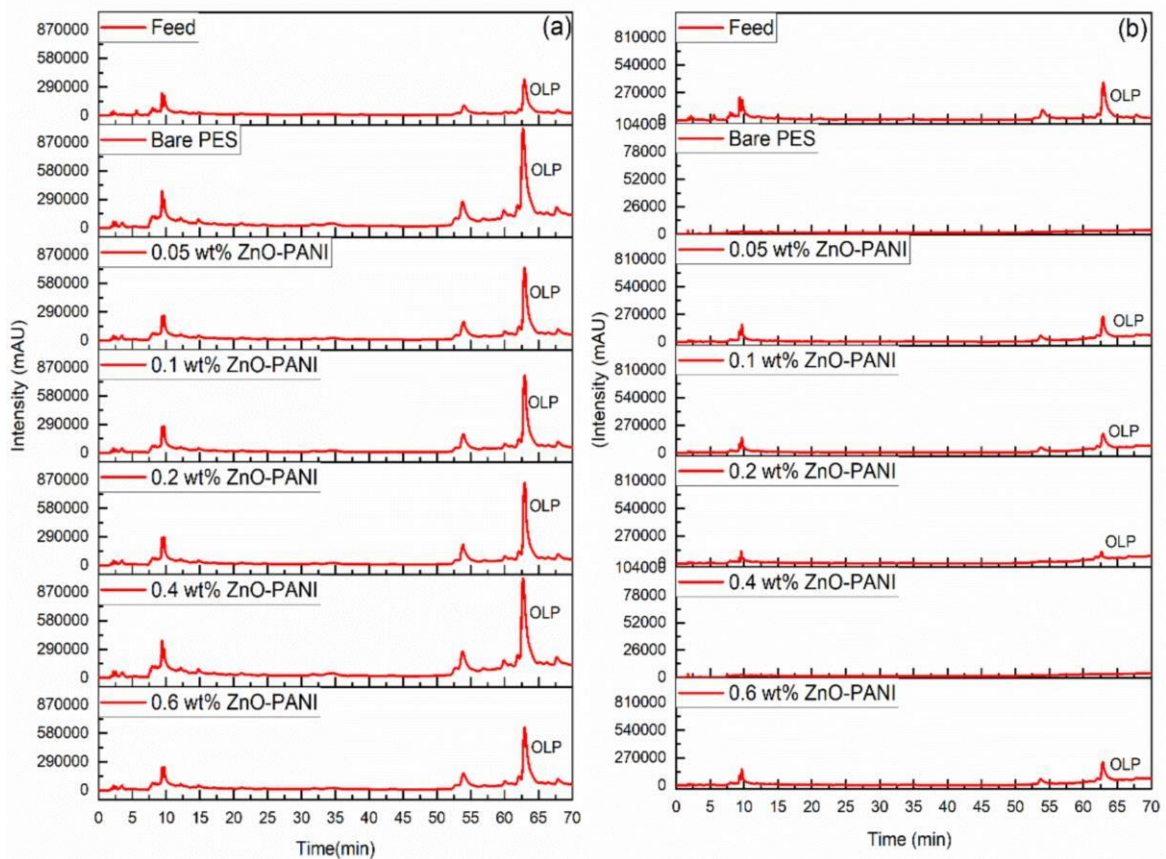
Figure 6.9: HPLC chromatograms of polyphenols (oleuropein) in feed; retentates (a) and permeates (b) obtained after 300 min at 30 bar using different prepared membranes.

6.5.5. Membrane cleaning and fouling analysis

Membrane fouling is considered as unavoidable phenomenon during membrane filtration due to the fouling formation on the membrane surface and/or within the

membrane pores. Fouling phenomena predominantly resulted from the adsorption and deposition of phenolic compounds onto the membrane surface, as well as the entrapment of these compounds within the pores.

As previously mentioned, after each pressure cycle, a fresh membrane was employed, and subsequently, the membrane underwent cleaning using a 0.2 M NaOH solution in an effort to restore the initial PWF.

To examine membrane fouling, the permeate water flux (PWF) was measured at 20 bar after the cleaning step. This was done to compare the changes in permeability values. The calculation of flux recovery (FR) was then expressed as a percentage. **Table 6.1** presents the FR values obtained for both simple and nanocomposite NF membranes. The incorporation of nanoparticles into the membrane matrix significantly influenced the membrane's antifouling ability, as evidenced by the prominent impact of the fouling factor FR, which is considered the most crucial in this context. The FR for the bare PES membrane which was recorded at 74.3% was higher than the blended membranes (45.1% to39.2%) filled with 0.2 and 0.4 wt% ZnO-PANI nanoparticles. The decrease in flux recoveryis explained by the adsorptive effect of the used nanoparticles which produce a thin layer cake formed by the adsorption of phenolic compounds on the membrane surface. Therefore,membranes blended by high concentration of ZnO-PANI nanoparticles have exhibit enhanced capability to adsorb phenolic compounds molecules on their surface. The rise in FR observed in the membrane, when incorporating 0.6 wt% ZnO-PANI, could be explained by the agglomeration of nanoparticles at higher concentrations. This agglomeration may lead to a reduction in the effective surface area of the nanoparticles, subsequently resulting in a decrease in fouling occurrences.

Table 6.1: The flux recovery ratio of the membranes that were prepared.

Membrane Type	FR (%)
Bare PES	74.3
0.05wt% ZnO-PANI	65.3
0.1wt% ZnO-PANI	52.2
0.2wt% ZnO-PANI	45.1
0.4wt% ZnO-PANI	39.2
0.6wt% ZnO-PANI	42.2

In addition, the collected samples of cleaner permeate (0.2 M NaOH solution) from the cleaning step were subjected to analysis via HPLC to determine the membrane mostaffected by oleuropein deposition either within the membrane or in its pores. **Table 6.2** presents the obtained results. All cleaner samples showed evidence of oleuropein adsorption on their surfaces, as it was present in each of them. The 0.4 wt% ZnO-PANI membrane demonstrated the highest oleuropein adsorption, as anticipated due to its superior TPC and oleuropein rejection rates compared to other membranes, followed by membranes with 0.2, 0.1, 0.05, 0.6 wt% ZnO-PANI and, finally by bare PES membranes.

The level of oleuropein in the cleaner sample for each membrane appears to align with the findings presented in **section 6.5.4**.

Table 6.2: Oleuropein amount in membrane permeate after cleaning for each membrane.

Oleuropein (mg/g_{OLP})					
Bare PES	0.05wt% ZnO-PANI	0.1wt% ZnO-PANI	0.2wt% ZnO-PANI	0.4wt% ZnO-PANI	0.6wt% ZnO-PANI
1.1	1.5	1.9	2.0	2.3	2.1

6.6. Conclusions

The present study employed ZnO-PANI nanoparticles to fabricate PES nanocomposite membranes using the non-solvent induced phase inversion technique. The results of the filtration of the OLE led to the conclusion that permeate flux showed enhancement with higher ZnO-PANI content. Regarding the total phenolic compounds rejection, the highest rejection (97%) was offered by the membrane embedded with 0.4 wt% ZnO-PANI at 30 bar. In addition, in terms of oleuropein rejection, the 0.4 wt% ZnO-PANI membrane and the bare PES membrane exhibited the highest rejection (100%) at 30 bar, which is attributed to the high adsorptive effect of ZnO-PANI nanoparticles and membrane pore sizes, respectively. However, the fouling studies showed that the bare PES membrane had higher fouling resistance than the blended membranes. As a conclusion, membrane embedded with 0.2 wt% ZnO-PANI was selected as the best membrane compared to bare PES, which could offer the highest permeability of 7.18 Lm^{-2} h^{-1} bar with an oleuropein rejection of 95% from the OLE pre-treated by UF at 30 bar while lowering the fouling rate. Therefore, the results indicate the suitability of mixed matrix membranes with ZnO-PANI for the purification of oleuropein from natural OLE.

CHAPTER 7: Optimizing operating conditions for olive leaf valorization using activated carbon mixed matrix membrane

This Chapter is based on the publication:

7.1. Abstract

The processing of olive leaf extract (OLE) by membrane filtration frequently faces challenges in effectively separating total phenolic compounds (TPC) with a high permeate flux and minimal fouling, highlighting the need for advancements in membrane technology. In this study, the issue is addressed by preparing polysulfone/activated carbon nanoparticles (Psf/AC) mixed matrix membranes (MMM) using phase inversion technique. Impact of AC concentration on membrane structure and performance was investigated. Incorporation of AC in membrane matrix significantly enhanced membrane properties. Contact angle reduced from 66.7° (pristine Psf) to 48.2° for membrane containing 0.9% AC. Hydraulic permeability increased by 47.55% with 0.6% AC addition. The efficiency of prepared membranes in separating of total phenolic compounds (TPC) from olive leaf extract (OLE) was evaluated under various pressure. The membranes based on 0.3% AC demonstrated significantly improved performance, exhibiting a flux of 11.8 L m^{-2} h^{-1}, more than twice that of the pristine membranes (4.8 L m^{-2} h^{-1}), while also showing enhanced rejection of TPC. Furthermore, these membranes achieved over 97% water permeability recovery after OLE filtration and subsequent cleaning. Effect of pH, temperature, and pressure on the rejection of TPC was examined using 0.3% AC-based membranes based on a three- variable, three-level central composite design (CCD). It was found that extremely low pH (2.7) and temperature (25°C), along with a high pressure (30 bar) increased TPC rejection. This study developed AC-based NF membranes novel application in TPC separation from OLE, achieving 100% oleuropein (OLP) rejection under optimal conditions using 0.3% AC-based membranes.

Keywords: Activated carbon nanoparticles, Experimental design, Olive leaf extract, Phenolic compounds separation, Oleuropein, Mixed matrix membranes.

7.2 Graphical abstract
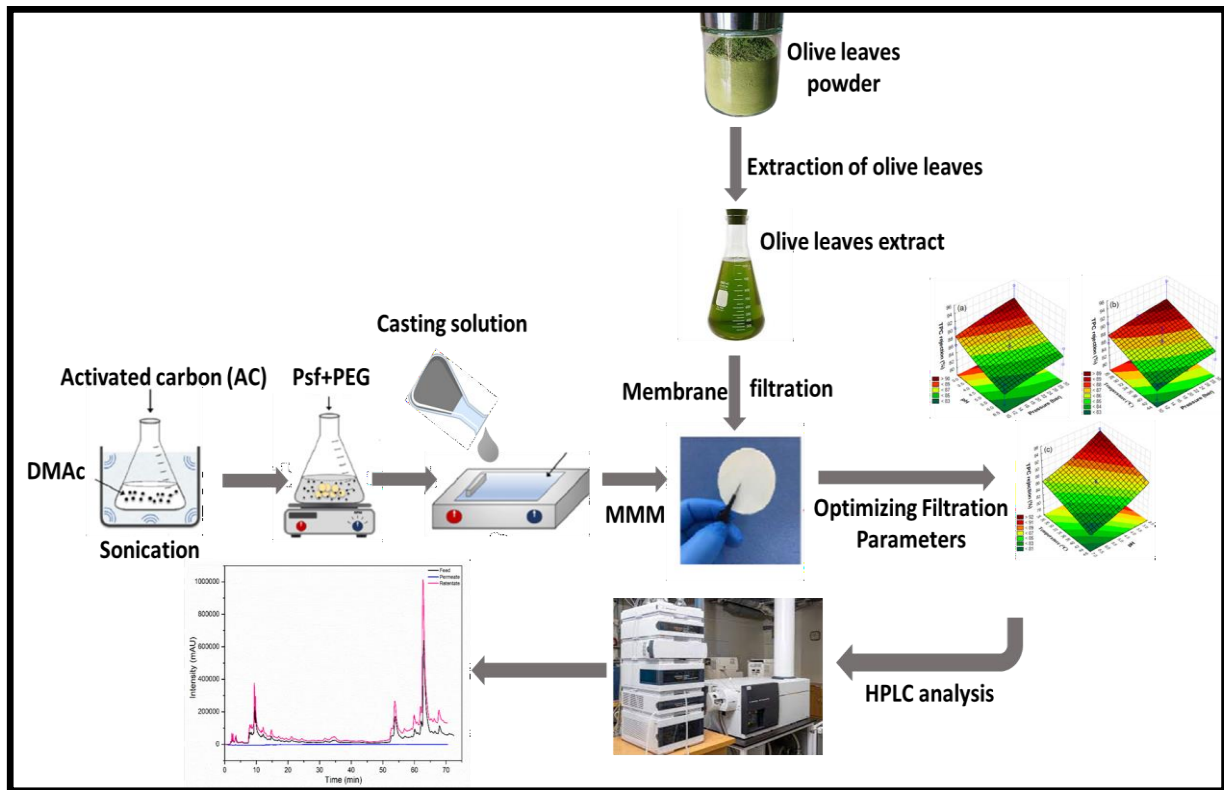
Figure 7.1: Graphical abstract.

7.3 Introduction

Over the last several years, the research focus was directed toward exploring the potential of agro-industrial residues as valuable resources for biorefineries, given their significance in both environmental impact and economic value. They present an appealing reservoir of various chemicals that can be transformed into products with significant added value (Gutierrez-Macias et al., 2017). Olive leaves represent one of these secondary outcomes, originating from both the cultivation of olive trees and the olive oil industry, which biorefineries could potentially utilize (Solarte-Toro et al., 2018). Only in Spain, the top global producer of olive oil (Lama-Muñoz et al., 2020), an annual production of over 300,000 tons of olive mill leaves is estimated, with Andalusia contributing the highest shareof production at 87.8% (Lama-Muñoz et al., 2020). This substantial quantity means a significant environmental issue, with solutions primarily revolving around their utilization

and dedication to the circular economy. One of the alternatives extensively explored by numerous researchers involves extracting bioactive compounds from olive leaves particularly polyphenols like oleuropein and other related compounds (Lama-Muñoz et al., 2019; Cruz et al., 2017).

In order to improve further the functional and nutritional characteristics of extracts, it is necessary to employ concentration techniques. This enhances the overall value of the end product (Erragued et al., 2022). Traditional approaches for concentrating extracts encompass adsorption technology, chromatography, coagulation, electrophoresis procedures and distillation, precipitation (Pereira et al., 2020). However, these techniques might result in elevated operational expenses, energy consumption and the use of high temperatures which can lead to the deterioration of thermosensitive compounds like phenolic species (Pereira et al., 2020).

Membrane technology has emerged as a promising substitute for concentrating delicate natural compounds, proving to be a viable alternative. When compared to traditional methods, membrane operations align seamlessly with the needs of the contemporary food industry. This operation guarantee the preservation of functional food properties, while also enhancing environmental friendliness, impressive efficiency, and minimal energy usage (Terki et al., 2018). This approach is based on the capacity to distinguish between various solute molecules. It selectively permits certain molecules to traverse either polymeric or semi-permeable membranes, while impeding others.

Regarding membrane separation techniques, the efficacy of separation process is affected by the materials constituting the membranes, thereby influencing the economic aspects of the operation (Sharma et al., 2023). For example, although membranes made from polymers offer efficient separation capabilities, they do exhibit certain drawbacks, such as instability when exposed to extreme temperatures and pH levels, limited selectivity for polyphenols, and the potential for polyphenol contamination by impurities of similar molecular weight (Manorma et al., 2021). Furthermore, a critical concern of utmost significance pertains to the substantial decline in permeate flux attributed to membrane fouling. This diminishment in flux emanates from the accumulation of contaminants and biomolecules onto the membrane's interface, or the obstruction of membrane pores. This

occurrence leads to a reduction in membrane lifetime, flux output, separation efficacy, and results in a noteworthy increase of trans-membrane pressure (TMP) alongside with operational costs (Zangeneh et al., 2019). Thus, membranes exhibiting excellent performance and effective fouling control are essential for the successful application of this technology in the pharmaceutical, cosmetic, and food sectors.

It is worth knowing that the hydrophilicity and microscopic structure of membranes are crucial factors in membrane separation processes. They hold the potential to diminish membrane fouling (Zinadini et al., 2017). In general, enhancing the hydrophilicity properties of the surface has been shown to effectively reduce fouling in nanofiltration membranes (Wang et al., 2018). To enhance the hydrophilicity and resistance to fouling in polymeric membranes, various approaches have been devised to address their constraints. These techniques include coating, blending with hydrophilic materials, grafting with hydrophilic monomers, surface modification, adding hydrophilic nanoparticles (Zinadini et al., 2017; Rahimi et al., 2015 ; Vatanpour et al., 2012 ; Hosseini et al., 2019). Among these various approaches, the introduction of nanoparticles as additives into the polymer membrane blend matrix (referred to as MMMs) gained significant attention. This growing interest is largely attributed to the potential to create customized membranes tailored for specific applications (Mukherjee et al., 2014).

The addition of nanoparticles within the membrane matrix has the capacity to improve the hydrophilicity, as well as the chemical, physical, and mechanical characteristics. Additionally, it can elevate porosity, improve solute rejection, increase water permeability, and augment the antifouling attributes of nanocomposite membranes based on polymers (Zangeneh et al., 2019; Vatanpour et al., 2012). Various types of nanomaterials have been experimented for this purpose in recent years. For example, Arsuaga et al., (2013) altered the PES membrane by introducing nanoparticles of TiO_2, Al_2O_3, and ZrO_2. As a result, they observed a consistently stable flux, along with improved resistance to fouling in the modified membrane. Safarpour et al., (2014) demonstrated that introduction of graphene $oxide/TiO_2$ nanoparticles into a PVDF nanofiltration membrane resulted in enhanced surface hydrophilicity and reduced surface roughness, and consequently enhanced water permeation and antifouling characteristics. Wang et al., (2015) have studied the impact of CNTs nanoparticles on both the performance and structure of PES membrane. They pointed

out that the incorporation of CNTs led to improvements in both water permeability and salt removal.

In this study, activated carbon nanoparticles were chosen to prepare mixed matrix membranes owing to their low cost and their effective ability to adsorb polyphenols (Montané et al., 2006). In fact, PES/AC nanofiltration membrane were prepared in previous study carried out by Manorma et al., (2023) to separate kraft lignin from black liquor. Jomekian et al., (2023) prepared PVA /AC mixed matrix membranes for CO_2/CH_4 separation. Furthermore, Hosseini et al., (2018) developed mixed matrix membranes PES/AC to remove sulfate and copper from water. However, there are no existing studies documented addressing separation of bioactive compounds (polyphenols) found in natural extracts using AC-based MMMs.

The novelty of this study lies in the use of activated carbon nanoparticles in mixed matrix membranes for separating polyphenols from olive leaf extract. To the best of our knowledge, this represents an innovative approach to separating bioactive compounds from natural extracts. This process yields a stream enriched with oleuropein, a compound with potential applications in both the cosmetic and pharmaceutical industries. The present study was, therefore, intended to investigate the preparation and utilization of AC-based NF membranes for recovering polyphenols from OLE (pre-filtered using UF). The effect of varying AC concentrations on the membranes morphology, porosity, hydrophilicity, separation performance and antifouling properties was carried out. Subsequently, the operational parameters were fine-tuned to optimize the performance of the best performant membrane. Effects of pH, temperature, and pressure, on the rejection of TPC were investigated through an optimization study using a central composite design (CCD). Finally, the filtration of OLE to concentrate oleuropein was carried out under optimized filtration conditions using the membrane, which was selected.

7.4 Materials and methods

7.4.1. Reagents and materials

Newly harvested olive leaves were acquired from the Chemlali cultivar growing in Sfax district (Tunisia). Collected leaves were subsequently dried for 24 h at 40°C in a

conventional oven and grounded in a laboratory mill. The dry ground material was kept in darkness at room temperature (RT) until needed. To prepare the olive leaf extract (OLE), distilled water (Direct-Pure Water System, Interlab, China) and ethanol (Fisher Chemical, 99.5%) were used. The study used activated carbon nanoparticles (AC) with a particle size of ≤100 nm as the inorganic filler additive, which were sourced from Sigma Aldrich. Polysulfone (PSf, Mw = 60,000 g/mol), supplied by Acros Organics, served as the foundational polymer for the study. N, N-Dimethyl acetamide (DMAc) and Polyethylene glycol (PEG, Mw = 1500 g/mol) procured from Merck and utilized as solvent and pore former, respectively. Phosphoric acid (85%) and acetronitrile (HPLC grade) were supplied by Fluka and Carlo Erba, respectively. Commercial standard of oleuropein was provided by Sigma-Aldrich.

7.4.2. Extract Preparation

Olive leaf extract was prepared as described below. The grounded olive leaves (1.2 g) were meticulously blended with 40 mL of 75% (v/v) ethanol-water solution in an erlenmeyer flask. The flask was positioned immediately in a thermostatic shaking water bath at 50°C and 120 rpm. After 90 min, the liquid extract was isolated from solids by vacuum pump using sintered glass at 0.45 μm. Afterwards, the mixture underwent centrifugation at 4000 rpm for about 15 min and the resulting supernatant was collected. This extract was then stored in a refrigerator for subsequent analyses.

7.4.3. Measurement of total phenolic compounds (TPC) in olive leaf extract

Total phenolic content (TPC) in various fractions of olive leaf extract was determined according the Folin–Ciocalteau method in our previous work (Erragued et al., 2022).Briefly, a 100 μL portion of extract solution was mixed with 100 μL of Folin-Ciocalteu reagent and left to incubate in the dark at 25°C. After 5 min, 300 μL of Na_2CO_3 solution (0.333 g/mL) was added to the mixture. Absorbance readings at 765 nm were taken using a SP-2000 UV spectrophotometer (Spectrum, Shanghai, China) after incubating for 30 min at 40°C. Calibration curve was generated by utilizing different concentrations of gallic acid

solutions within the range of (0.0005-0.02 g/mL). The findings were reported in milligrams of gallic acid equivalents (GAE) per gram of olive leaf powder (mg GAE/g OLP).

7.4.4. Determination of phenolic compounds by HPLC

The oleuropein in different fractions of olive leaf extract was identified and measured using the Waters separation model 2695 high-performance liquid chromatography (HPLC) system, following the method suggested by Mulinacci et al., (2001). Separation of oleuropein was carried out on a Brisa LC2 C18 column (250 × 4.6 mm id, 5 μm, Spain) andsubsequently analyzed using a Waters 2487 dual-absorbance detector.

The mobile phase consisted of a blend of two solutions: solution A, which contained water with a pH adjusted to 3.20 using phosphoric acid, and solution B, consisting of acetonitrile, flowing at a rate of 1 mL/min. The elution gradient was executed for a total period of 80 min according to the following schedule: 0-3 min, the solvent composition transitioned from 100% to 89% A, 3- 41 min, the composition changed from 89% to 87% A, 41-55 min, the composition shifted from 87% to 80% A, 55-70 min, the gradient moved from 80% to 75% A,70-71, a brief change from 75% to 100% and finally, an isocratic elution was maintained at 100% A for the last 9 min. The column temperature was held at aconstant 30°C, while the sampler temperature was maintained at 25°C. Prior to injection,the samples underwent filtration through a 0.1 μm microfilter with an injection volume of 10 μL. Chromatographic profiles were then recorded at both 215 and 280 nm. Oleuropein was detected by comparing its retention time with that of the standard solution, which was prepared using pure oleuropein in acetonitrile.

7.4.5. Preparation of AC-based NF membranes

The technique non-solvent induced phase separation (NIPS) was used for preparing the different flat sheet NF membranes. Casting solution was formulated following the detailed composition presented in **Table 7.1**. Psf was used as the base polymer, PEG as pore- forming agent, AC as the adsorbent or additive/organic filler and DMAc as a solvent. In brief, the required quantity of AC nanoparticles was introduced into DMAc, followed by 30min of sonication to enhance homogeneity in the solution. Then, the required amount of Psf

and PEG were slowly introduced into the mixture and stirred continuously overnight at ambient temperature. Resultant viscous solution underwent a 30min sonication to block the nanoparticles aggregation and left exposed to fresh air for 4 h at ambient temperature for air bubbles removal. Following that, the polymer solution was casted onto a new glass substrate using a film applicator, creating a membrane film with a thickness of 250 µm. Afterward, the glass substrate was submerged in a bath of distilled water (non-solvent) untilthe membrane film was separated from the glass substrate. After exchanging solvent and non-solvent and the formation of the membrane, the membranes were soaked in fresh distilled water for a duration of 24 h to thoroughly remove completely the residual solvents. At last, the membranes were air-dried for 24 h, placed between layers of filter paper at room temperature, and then stored in a dry location for future use.

Table 7.1: Formulation of casting solutions of the MMMs.

Number	Membrane	PSf (%)	PEG (%)	AC (%)	DMAc (%)
1	0 % AC	19	1	0	80.0
2	0.1 % AC	19	1	0.1	79.9
3	0.3 % AC	19	1	0.3	79.7
4	0.6 % AC	19	1	0.6	79.4
5	0.9 % AC	19	1	0.6	79.1

7.4.6. Characterization of NF membranes

The gravimetric method was employed to determine membrane water uptake and porosity, using Eq. (7.1) and Eq. (7.2), respectively. Initially, the samples of membrane were dipped in distilled water at room temperature for 24 h, then their surfaces were gently positioned between sheets of filter paper to remove any excess water, and their weights were promptly recorded. Afterwards, moist membranes were subjected to a 24 h drying period at 40°C until the constant weight was achieved. Following this, the membranes wererereweighed. To mitigate the experimental error, each membrane was subjected to the entire procedure three times.

$$Water\ upta(\%) = \frac{m_1 - m_2}{m_1} \times 100 \tag{7.1}$$

$$(\%) = \frac{\dfrac{m_1 - m_2}{\rho_w}}{V_m} \times 100 \tag{7.2}$$

where the weights of the wet and dry membrane are m_1 (g) and m_2 (g), respectively), while ρ_w (g cm^{-3}) and V_m (cm^3) denote the density of water at 20°C and the membrane volume, respectively. The volume of membranes was calculated using the value of known active area and the thickness of membrane, which was measured using a micrometer.

The membrane mean pore radius (r_m) was calculated using the Guerout-Elford-Ferry equation (Eq. (7.3)), which relied on the permeability and porosity data (Vatanpour et al., 2012).

$$r_m = \sqrt{\frac{(2.9 - 1.75\varepsilon)8\mu_w l L_P}{\varepsilon}} \tag{7.3}$$

where ε is the membrane porosity, μ_w is the water viscosity at RT (Pa.s), l is membrane thickness (m) and Lp is the membrane permeability (L m^{-2} h^{-1} bar^{-1}).

The hydrophilic properties of the surface of fabricated membrane was characterized through a standard technique known as water contact angle (WCA) measurement method. A goniometer instrument (Theta Flex, Biolin Scientific, Sweden) was utilized to gauge the static contact angle formed between the membrane's surface and water, using the sessile-drop method at 25°C. To get more accurate results, contact angle measurements were taken at five randomly chosen spots on each sample, and the average value was subsequently recorded.

To examine the cross-sectional and top surface morphology of the membranes, SEM analysis was applied using (Quantax 200 with XFlash 4010 detector, Bruker AXS machine). Preceding the SEM analysis, the samples of membrane were placed in liquid nitrogen for a duration of 5 min. Afterwards, the frozen membrane pieces were broken using tweezers, dried in air, and then sputtered with in a conductive layer. The SEM imageswere observed with the microscope set at 10 kV.

A MultiMode AFM microscope, outfitted with a NanoScope 3D controller from Veeco Instruments Inc. in New York, NY, USA, was employed to analyze the surface roughness and morphology of the fabricated membranes. A sufficient portion of the dried membranes,

measuring approximately 1 cm^2, was cut and securely affixed to a glass surface. To determine the roughness parameters, the NanoScope software was utilized within a scanning area of 10 μm × 10 μm. The surface roughness characteristics of membranes were described using average roughness (Ra) and root mean square (RMS) roughness parameters. The results shown represent the mean values obtained from a minimum of five separate measurements. All AFM tests were carried out under normal room temperature conditions.

7.4.7. Nanofiltration experiments

Experiments involving water and OLE were conducted utilizing a Sterlitech HP4750 stirred cell filtration system. This system, designed a dead-end configuration, is optimally suited for a membrane area of 14.6 cm² and can handle a maximum feed volume of 300 mL. The operating pressure was provided by a nitrogen gas cylinder connected to the top ofthe feed storage. To prevent concentration polarization on the membrane surface andregulate the filtration temperature, the cell was positioned on a hot plate that was fitted witha magnetic stirrer. Additionally, a thermostatic coil was wound around the cell to controlthe desired filtration temperature. The experiments were conducted in duplicates, and the mean results were presented.

This part of experiments was carried out to compare the filtration performance of the prepared membranes. The performance of the membranes was studied by evaluating their pure water flux and TPC rejection. The water filtration tests were done under 10-30 bar trans-membrane pressure (TMP) at 25°C. Filtration studies using OLE were conducted at different pressure values (10, 20 and 30 bar) at 25°C, constant feed pH of ~4.7 and fixed speed of 800 rpm.

Prior to the start of experiment, every membrane was soaked in distilled water for half an hour. Thereafter, the membrane was secured within the cell containing distilled water. Initially, each membrane was subjected to a pressure of 30 bar until the stable water flux was achieved. Following this, the pressure was reduced to the operational set up and collecting the permeate water was continued every 5 min up to 30 min.

The pure water flux (PWF), Jw, was estimated by the following equation:

$$J_w = \frac{V_w}{tA_m}$$
(7.4)

where J_w (L m^{-2} h^{-1}) represent the PWF, V_w (L) stands for the collected permeate volume, A_m (m^2) represents the membrane area, and t (h) indicates the sampling period.

The values of PWF that were acquired were graphed against the applied pressure, forming a linear curve. The slope of this curve was employed to calculate the water hydraulic permeability within the applied TMP range.

$$L_p = \frac{V_w}{tA_m \Delta P} = \frac{J_w}{\Delta P}$$
(7.5)

Lp, denoted in units of L m^{-2} h^{-1} bar^{-1}, represents hydraulic permeability, while ΔP, measured in bars, corresponds to the transmembrane pressure.

Following the experiments on water filtration, the membranes that were prepared were evaluated in relation to their permeate flow and their capability to remove TPC from OLE. It is important to remind that the feed (OLE) was the permeate from the UF process. As previously mentioned, in the OLE experiments, the TMP was changed after fixed time intervals and the filtration was performed continuously for 300 min. Permeate samples collected from these tests were analysed using a UV-Vis spectrometer to determine the concentrations of TPC. Subsequently, these values were utilized in Eq. (7.6) to calculate the retention values.

$$Rejection\ (\%) = (1 - \frac{C_p}{C_f}) \times 100$$
(7.6)

Cp represents the concentration of TPC in the permeate, while Cf represents the concentration of TPC in the feed solution.

The cleaning procedure involved a sequential approach, starting with rinsing using distilled water, and then proceeding to chemical cleaning using 0.1 M NaOH and 0.1 M HCl solutions at a temperature of 40°C. Subsequently, the membranes were cleaned by filtering distilled water at 20 bar until the pH of the feed reached a neutral level. Followingt the chemical cleaning, the permeate water flux (PWF) and hydraulic permeability were measured again at 20 bar. The permeability data obtained for the new membrane ($L_{p,i}$) and

the membrane after cleaning ($L_{p,f}$) were utilized to assess the antifouling properties of the prepared membranes. The antifouling ability was assessed by calculating the permeability recovery percentage, which was obtained as follows:

$$\text{Permeability Recovery (\%)} = \frac{L_{p,}}{L_{p,i}} \times 100 \tag{7.7}$$

$L_{p,i}$ (L m^{-2} h^{-1} bar^{-1}) represents the initial hydraulic permeability of the membrane, while $L_{p,f}$ (L m^{-2} h^{-1} bar^{-1}) represents the hydraulic permeability restored after OLE filtration and subsequent cleaning.

7.4.8. Experimental design

In this research, a three-variable-three-level central composite design (CCD) was employed to set up experiments aimed at determining the optimal filtration conditions for the removal of phenolic compounds. The independent variables were pH of feed solution, temperature and pressure, known to affect in the concentrated products in terms of polyphenols retention (Mello et al., 2013). The ideal operation setup (optimal variables) was determined based on one with the highest total phenolic compounds rejection value. The response variable for the experimental design was defined as the rejection of total phenolic compounds (Y).

Sixteen runs were carried out, with each experiment being duplicated. Every factor was coded at three levels, −1, 0, +1. The pH varied from 2.6 to 6.7, temperature ranged between 25 and 45°C and pressure between 10 and 30 (**Table 7.2**). In this situation, the values of every factor were chosen by considering both existing literature information and preliminary tests.

The obtained experimental data were fitted using a second-order polynomial equation, depicted in the following expression (Eq. (7.8)).

$$Y = \beta_0 + \sum_{i=1}^{n} \beta_i X_i + \sum_{i=1}^{n} \beta_{ii} X_{ii}^2 + \sum_{ij, i<j}^{n} \beta_{ij} \beta_i X_j \tag{7.8}$$

Y represents the dependent variable, β0 signifies the intercept, Xi or Xj represent the independent variables, while βi, βj, and βij denote the regression coefficients for the linear, quadratic, and interactive terms, respectively.

Table 7.2: The levels of independent factors in a central composite design.

Independent variables	Levels		
	-1	0	1
pH	2.7	4.7	6.7
Temperature (°C)	25	35	45
Pressure (bar)	10	20	30

7.4.9. Statistical Analysis

Every experiment was duplicated, and the outcomes were reported as means with their corresponding standard deviations. Central composite design was conducted and statistical analysis was performed with the assistance of JMP 16 Pro and STATISTICA 14.0 software. An analysis of variance (ANOVA) was conducted to assess the accuracy of the model that was fitted.

The quality of the fitted model was evaluated using the coefficient of determination (R^2), while the significance of the dependent variables was statistically analyzed by determining the F-value at a significance level of $p < 0.05$. From the obtained regression models, response surface design and corresponding contour plots were drawn to comprehend the correlations between the response and the various experimental factor levels.

7.5. Results and discussion

7.5.1. Characterization of membrane

7.5.1.1. Effect of AC nanoparticle content on membrane water uptake

The membrane water uptake is considered as a fundamental indicator for assessing hydrophilicity and the potential for swelling (Mobarakabad et al., 2015). **Figure 7.2** displays the impact of AC nanoparticles amount on the water uptake of different modified membranes. Based on the findings, when the amount of AC nanofillers content in the casting solution is raised from 0% to 0.6%, there is a corresponding rise in the membrane's water uptake from 72.2% to 78.1%. The reason for this could be attributed partially to the

hydrophilic moity nature of AC nanoparticles and partly to the augmentation in both the size and quantity of pores (Mobarakabad et al., 2015). The rise in AC content from 0.6% to 0.9% led to a reduction in the water uptake of the membranes. This phenomenon is linked to the filling of membrane pores by the employed nanoparticles, which can overcome their inherent hydrophilic nature (Hosseini et al., 2019), leading to lower porosity and smaller pore size, which restricts the water molecules accommodation (Bagheripour et al., 2016). The observed behavior aligns with findings documented in existing literature (Hosseini et al., 2019; Mobarakabad et al., 2015; Bagheripour et al., 2016).
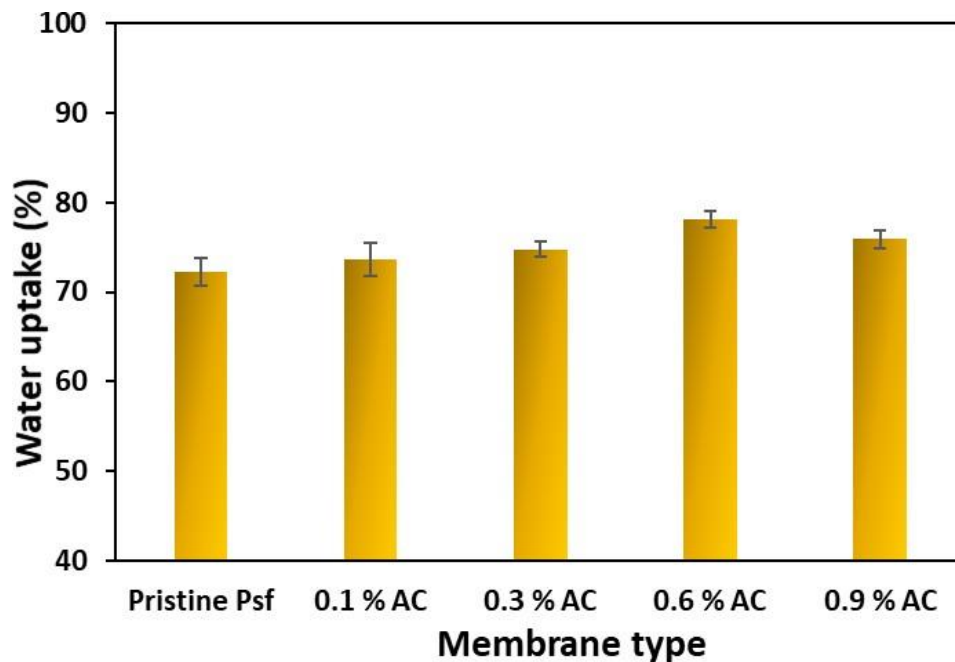
Figure 7.2: The impact of varying amount of AC nanoparticles on membrane water uptake.

7.5.1.2. Effect of AC nanoparticle content on membrane porosity and mean pore size

The results displayed in **Fig. 7.3** illustrates the porosity and pore size of the mixed matrix membranes prepared in this investigation. As depicted in this figure, the introduction of AC nanoparticles initially resulted in an improvement in the mean pore size and porosity up to 0.6% (Hosseini et al., 2019). However, with a further increase to 0.9% nanoparticle concentration, these values declined (Bagheripour et al., 2016). These phenomena align

with findings documented in previous studies (Wang et al., 2014; Bagheripour et al., 2016; Zinadini et al., 2014). The augmentation in membrane porosity and pore size can be linked to the ability of AC nanoparticles to enhance the exchange of solvent and non-solvent during the phase-inversion process. This could result to higher porosity on the membrane surface, enhancing water permeability (Zinadini et al., 2014). Furthermore, the potential interactions between nanoparticles and the polymer binder may result in decreased interactions between polymer-polymer chains, resulting in the formation of significantmicro-voids (Hosseini et al., 2019). The decrease in membrane porosity and pore size at higher nanoparticle ratios (0.9%) might be related to the increase in viscosity of the casting solution. This rise in viscosity, in turn, lowers the mass exchange rate (Hosseini et al., 2019). Likewise, Wang et al., (2018) demonstrated that as the additive content increased, there was a reduction in mean pore size and porosity of the modified membranes. They attributed this observation to the rise in viscosity as a probable explanation.
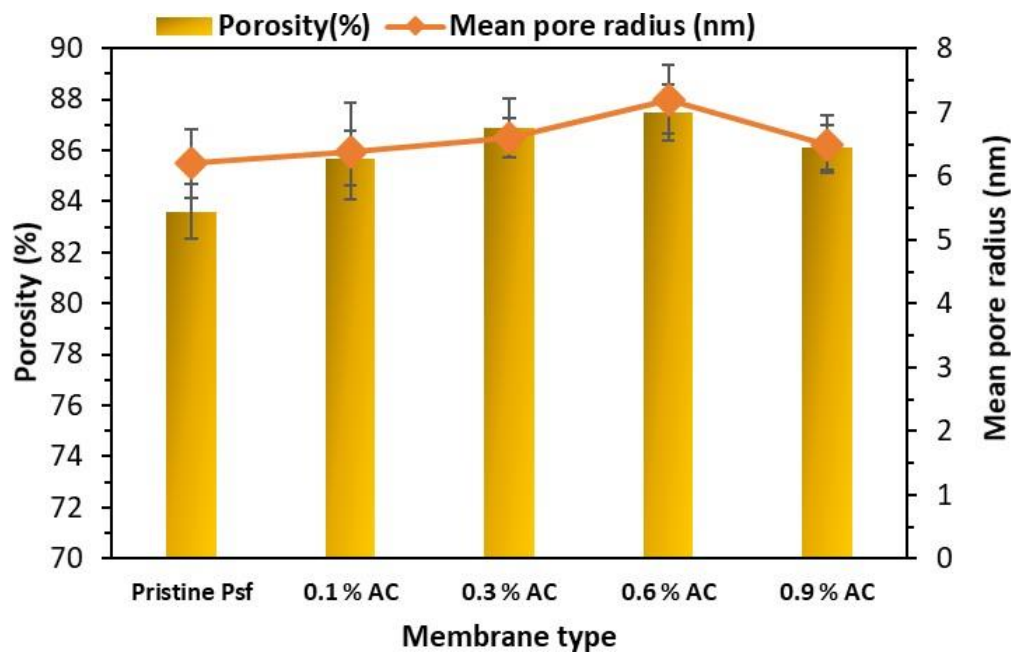
Figure 7.3: The impact of nanoparticles content (AC) on porosity and mean pore size.

7.5.1.3. Effect of AC nanoparticle content on contact angle

Membrane surface hydrophilicity is a crucial feature that significantly influences both permeability and ability to resist fouling. The hydrophilic nature of a membrane surface is

typically determined through the measurement of the contact angle formed by a water droplet on the membrane surface, as well as its water uptake capacity. It is worth knowing that a lower water contact angle indicates a more hydrophilic membrane (Zinadini et al., 2017; Hosseini et al., 2013).The contact angle values were shown in the **Fig. 7.4**. It is evident that adding of AC nanoparticles to the polymeric matrix significantly improved the hydrophilicity of the membrane. As depicted in **Fig.7.4**, an increase in the amount of nanoparticles within the mixed matrix membranes led to a reduction in the contact angle, decreasing from 66.7 (for the pristine Psf membrane) to 48.2 (for the Psf/AC MMMs with 0.9% AC). The decrease in the contact angle value might be explained by the phenomenon observed while preparing mixed matrix membranes during the phase inversion process. In this process, the AC present in the AC/Psf solution showed a spontaneous tendency to migrate towards the upper layer of the prepared membranes. This migration process leads to the decoration of AC nanoparticles on the top surface of the membrane, reducinginterfacial energy and an enhancement in the hydrophilicity of the membrane (Zangeneh et al., 2019; Zinadini et al., 2017; Wang et al., 2018; Vatanpour et al., 2011). The movementof AC to the surface of mixed membranes was clearly evident upon comparing the top and bottom surface images of the modified membranes (**Fig. 7.5)** (Vatanpour et al., 2011).
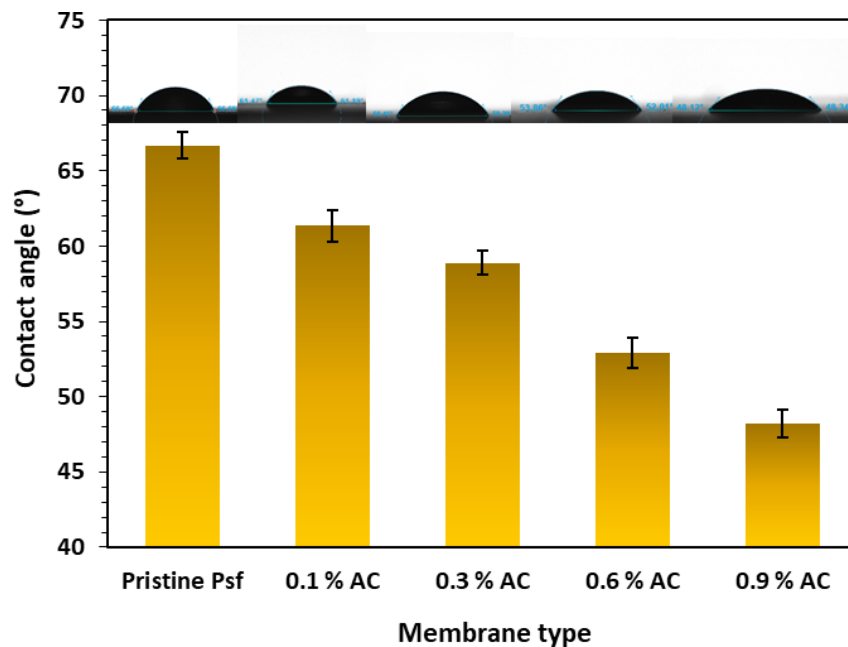
Figure 7.4: Contact angle measurement of prepared Psf membranes.
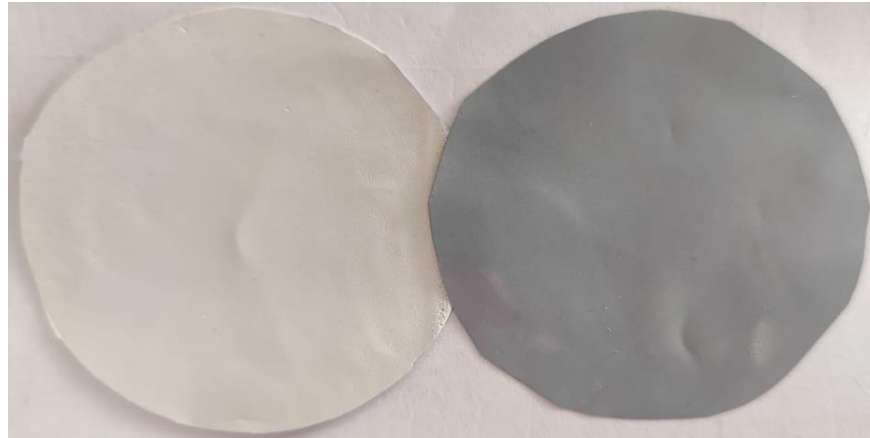
Figure 7.5: Digital images showing the top and bottom surfaces of AC/Psf membrane (0.9% AC).

7.5.1.4. Characterizing the morphology using SEM and AFM

To evaluate the influence of the incorporation of AC on polysulfone membrane structure, the cross-sectional views of the membranes prepared both with and without AC were examined using scanning electron microscopy (SEM). **Fig.7.6** shows cross-sectional images with two magnifications of membranes containing 0%, 0.1%, 0.3%, 0.6%, and 0.9% AC. Clearly, membranes prepared with varying loadings of AC exhibit a characteristic asymmetric structure consisting of a dense top layer (skin layer) and a porous lower sub-layer. This asymmetric structure designates the top dense layer as the active layer, serving as a selective barrier that facilitates the separation process, while the porous layer serves only as a mechanical support for the skin with negligible effects on separation. Among all the cross-sectional images, the pristine Psf membrane in **Fig.7.6 (a, a')** exhibits the smallestpore size in the top layer and a closed structure in the bottom layer. Through the introduction of nanoparticles into polymeric casting solution, significant alterations in membrane morphology were detected, affecting the kinetic and thermodynamic of the system (Hosseini et al., 2019; Nasrollahi et al., 2018). It could be observed from **Fig.7.6 (b,b') and (c, c')** that the incorporating of 0.1% and 0.3% AC into the polymer solution resulted in a significant change in morphology of both the skin layer and sub-layer. The porosity in the sub-layer increased, and the pores in the top layer became wider. Also, it's easy to observe that the volume of macro-voids in the sub-layer is open and larger

compared to the unfilled Psf. The appearance of the large macro-voids in downside layer made the sub-layer's sponge-like structure (**Fig.7.6b**) looks more obvious with more porosity and visibly bigger pore. As shown in **Fig. 7.6 (d, d')**, the addition of 0.6% AC intothe membrane casting solution resulted in a further increase in the quantity and volume of pores and macrovoids in the sub-layer. Additionally, there was a significant increase in the breadth of pores in the dense layer (See **Fig.7.6d'**). In addition, macro-pores are fully developed at the bottom result in a complete change in the sub layer, leading to theformation of a wide finger-like structure. The occurrence of this event can be related to the influence of phase inversion speed on the type of membrane structure, which arises fromthe interaction between the polymer film and non-solvent (water).Incorporating hydrophilicagents into the membrane matrix can significantly improve the speed of mass transfer between the solvent and non-solvent during phase inversion. Consequently, this results in the formation of more extensive pore channels within the sub-layer and a reduced thickness in the top layer (Hosseini et al., 2019; Bagheripour et al., 2016; Zinadini et al., 2014; Rahimpour et al., 2012). However, by further increase in AC until 0.9% **Fig.7.6 (e)**,macrovoid volume reduced. This is maybe due to the higher possibility of nanoparticles aggregating within the pore structure or on the membrane surface when the content is high. Additionally, it may be due to the rise in viscosity of the casting solution resulting from the addition of activated carbon (Sharma et al., 2013). In fact, increase of the viscosity typicallyprolongs the solvent and non-solvent exchange process resulting in suppression of macroporous structure in bottom layer leads to more closed structure (Zangeneh et al., 2019; Zinadini et al., 2017; Vatanpour et al., 2011). Similar behaviour is also observed for water uptake, porosity pore size and permeability results of prepared membranes (**Figs 7.2, 7.3 and 7.8**).
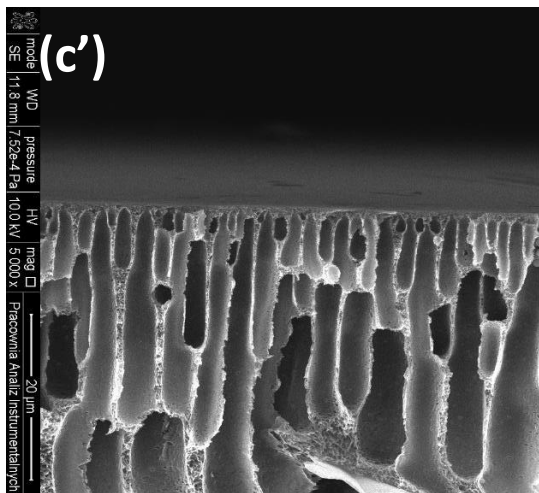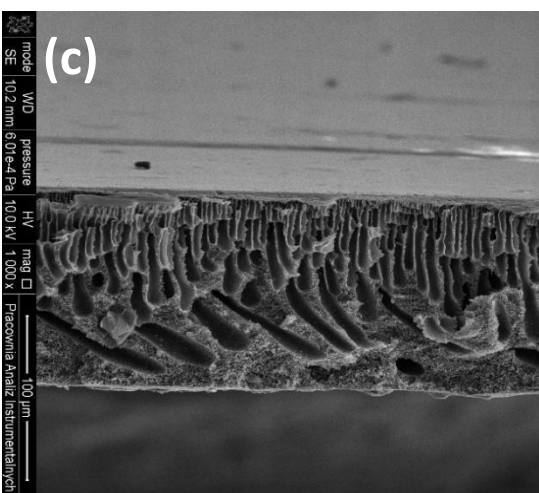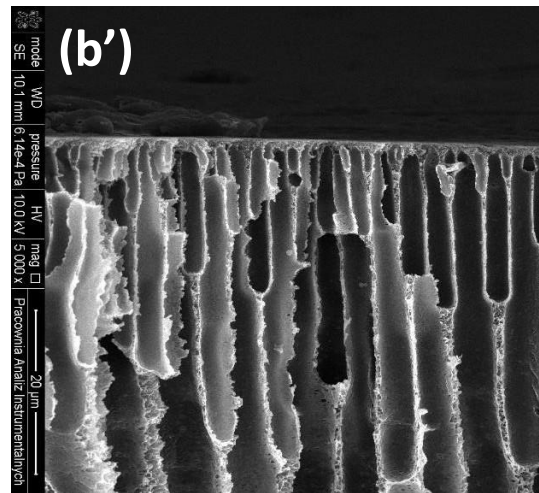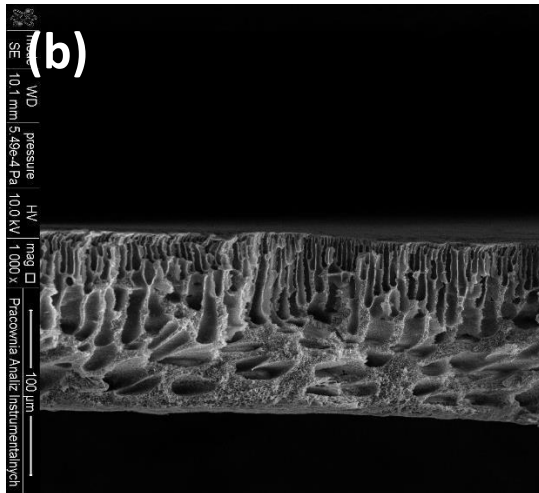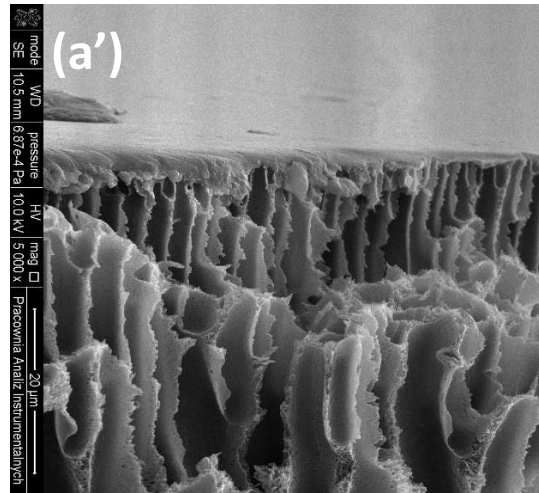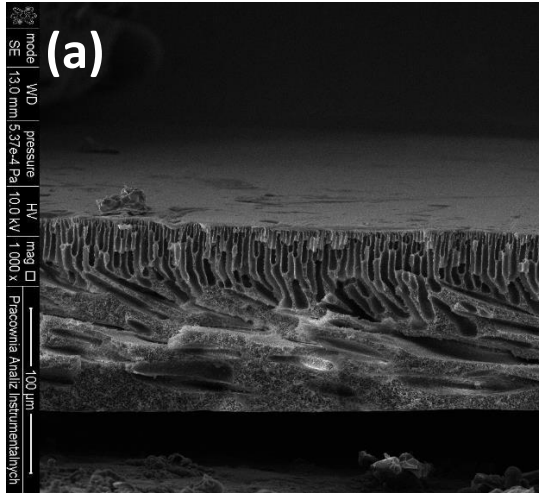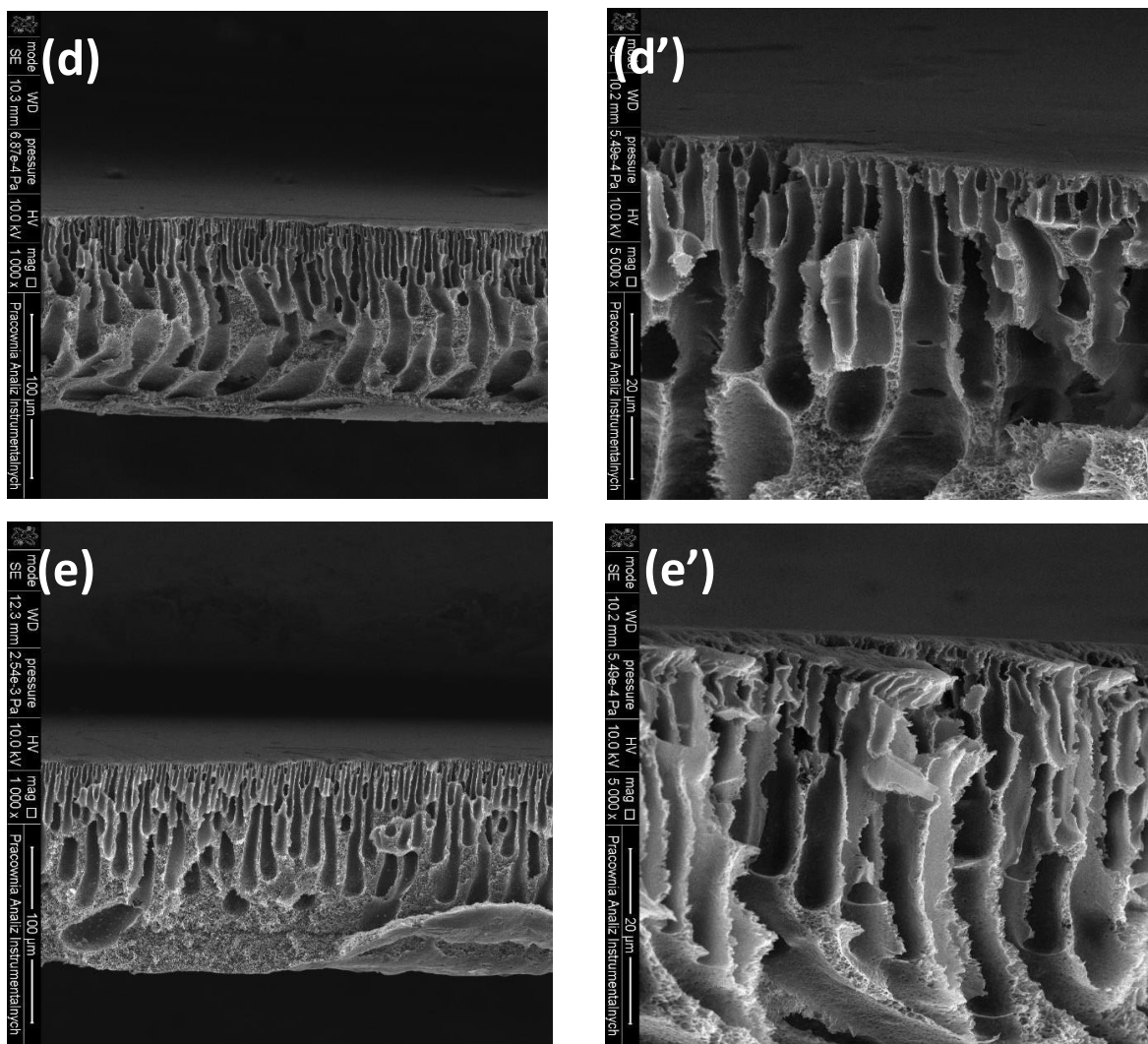
Figure 7.6: Images obtained through scanning SEM at a cross-sectional with two magnifications of various membranes filled with: 0% AC (a and a'), 0.1% AC (b and b'), 0.3% AC (c and c'), (d) 0.6% AC (d and d') and 0.9% AC (e and e').

Two and three-dimensional surface images, along with their measured roughness parameters generated by AFM technique, are presented in **Fig. 7.7** for both pristine membrane and those filled with AC. The average roughness (Ra) represents the average difference between surface peaks and valleys on a surface. A lower average roughness value indicates reduced variation between the peaks and troughs on a surface, resulting in a smoother surface. Root mean square (RMS) roughness, crucial for defining surface roughness; a higher value indicates high surface roughness. Based on the AFM analysis, it was observed that the incorporation of AC nanoparticles into the casting solution, at

loading ratios of 0.1% and 0.3%, led to an initial reduction in both average roughness and root mean square roughness. Therefore, these two membranes are smoother than that of the pristine Psf membrane. With a low nanoparticle content added to the membrane matrix, there are low interfacial interactions and an even regular distribution of the nanoparticles within the membrane. This results in a smoother membrane surface (Zangeneh et al., 2019; Vatanpour et al., 2012; Bagheripour et al., 2016). However, as seen in **Fig. 7.7**, the average roughness and root mean square of prepared mixed matrix membrane embedded with high nanoparticle content (0.6% and 0.9% AC) clearly increased, This observation can be attributed to an excessive dosage of activated carbon present on the surface of membrane, resulting in increased roughness (Zangeneh et al., 2019 ; Hosseini et al., 2019).

Ra(nm)=5.1
RMS(nm)=6.5

Ra(nm)=7.2
RMS(nm)=9.3

Ra(nm)=8.2
RMS(nm)=10.3
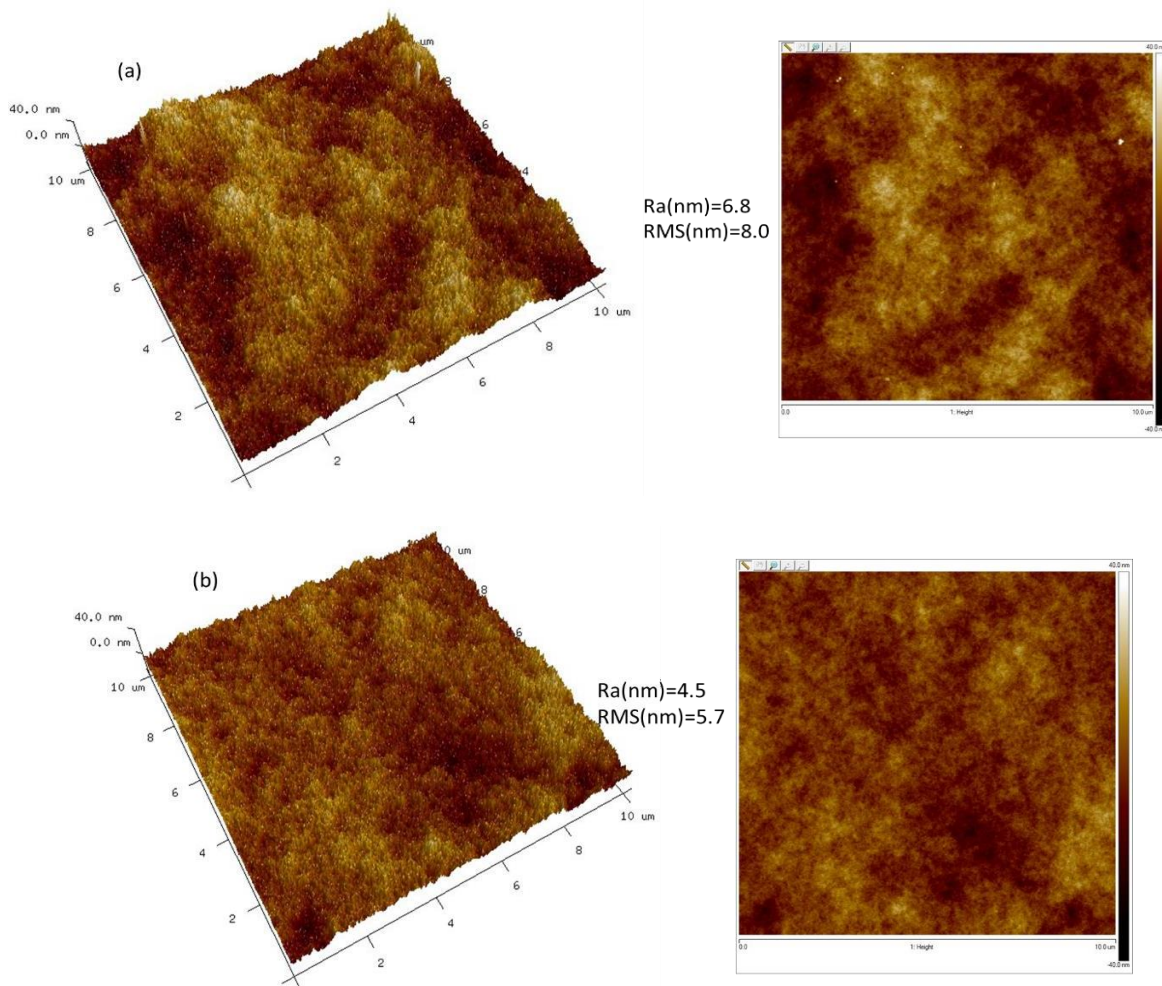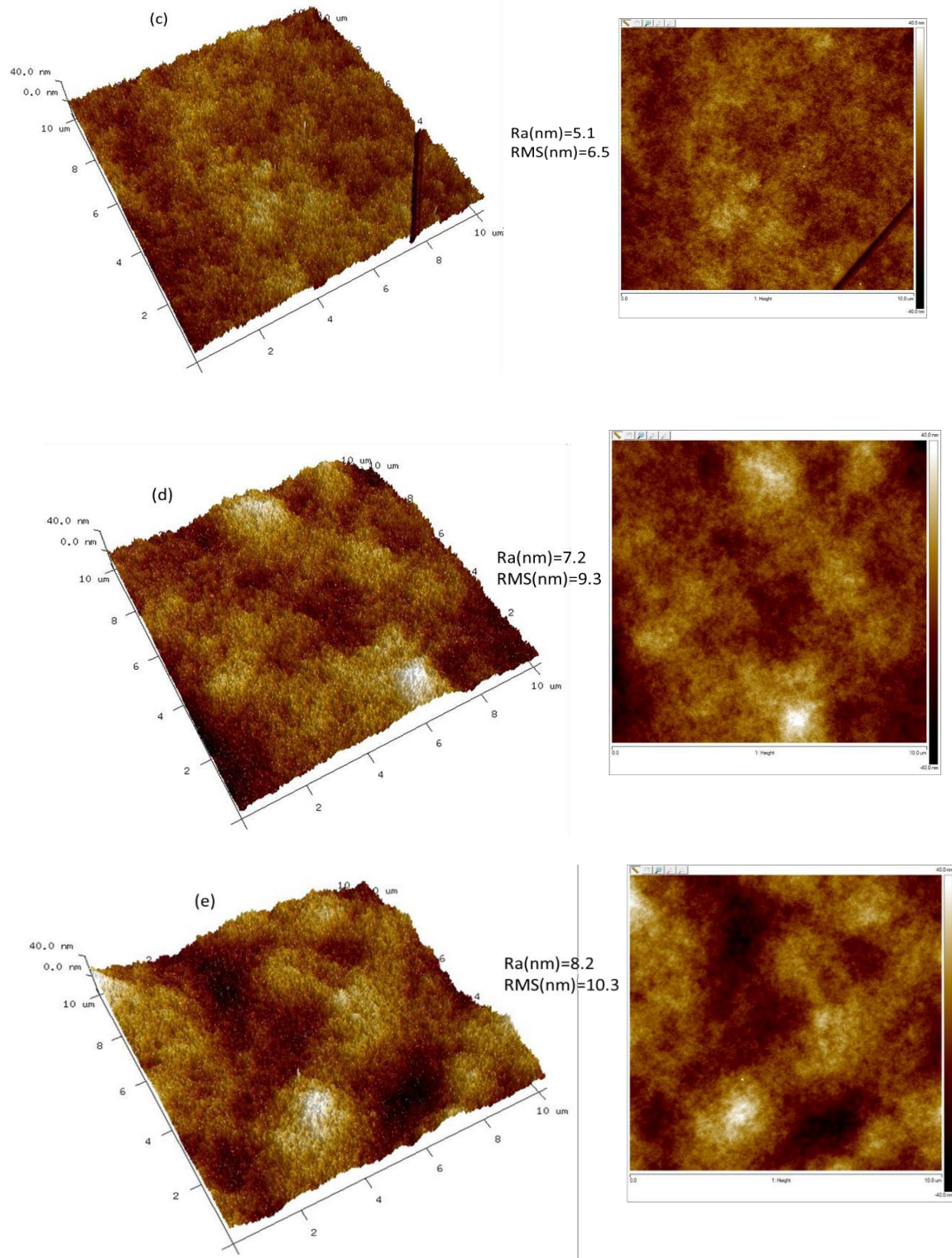
Figure 7.7: Two- and three-dimensional AFM micrographs of prepared membranes filled with 0% AC (a), 0.1% AC (b), 0.3%AC (c), 0.6% AC (d) and 0.9% AC (e) content.

7.5.1.5. Hydraulic permeability

An analysis of the filtration properties was conducted to explore the impact of nanoparticles content upon the filtration efficiency in the fabricated membranes. PWF and permeability of MMMs are presented in **Figs. 7.8 (a)** and **(b)**. Pure water fluxes of the modified membranes were determined at various TMP (from 5 to 25 bar) and presented in **Fig. 7.8 (a)**. The figure displays the mean of three measurements for the pure water flux, along with the corresponding standard deviation.

As it is obvious in **Fig. 7.8**, the PWF and permeability of all the modified membranes had a significant growth compared to unfilled Psf membrane. Furthermore, the prepared membranes exhibit an increase in pure water flux as the driving force increases, aligning with findings from other studies (Wang et al., 2015). The results indicated that the permeability increased initially and reached the highest rate when the amount of the AC was 0.6% (9.8 L m^{-2} h^{-1} bar^{-1}). This enhancement in water permeation can be attributed to two major parameters which are surface hydrophilicity and membrane structure (Wang et al., 2018; Bagheripour et al., 2016; Hosseini et al., 2013; Gholamzadeh et al., 2017). It is widely recognized that improving the hydrophilicity properties of membrane enhances the permeate flux. Generally, the hydrophilic nature of nanoparticles contributes to an increase in the membrane surface hydrophilicity. This enhancement leads to the improved water permeation by drawing water molecules into the membrane matrix and facilitating their movement across the membrane (Vatanpour et al., 2012; Xu et al., 2014). Moreover,membranes with a thinner skin layer, higher porosity, and larger pore size can enhance permeability by reducing the flow resistance of water. Consequently, this leads to an increase in the PWF of the prepared membranes.

Despite that the membrane hydrophilicity was enhanced with further increase of nanoparticles content (>0.6%) in polymer matrix, the permeability was diminished. This opposing behavior could be attributed to either a reduction in pore radius or the blockage of membrane pores caused by the accumulation of nanoparticles (Zangeneh et al., 2019; Zinadini et al., 2017). Moreover, when the AC concentration exceeds 0.6%, the highdensity of AC in the casting solution leads to an increase in the solution viscosity. Hence, this decreased porosity and narrowed pore size of the membrane led to a decrease in pure

water flux and subsequently the decrease of permeability (Zinadini et al., 2017; Vatanpour et al., 2011).This explanation is well matched with morphological results demonstrated in **Fig.7.3 and Fig.7.6** (SEM, porosity and mean pore size) and also with contact angle measurements in **Fig.7.4**. Zinadini et al., (2017) also observed a comparable behavior.
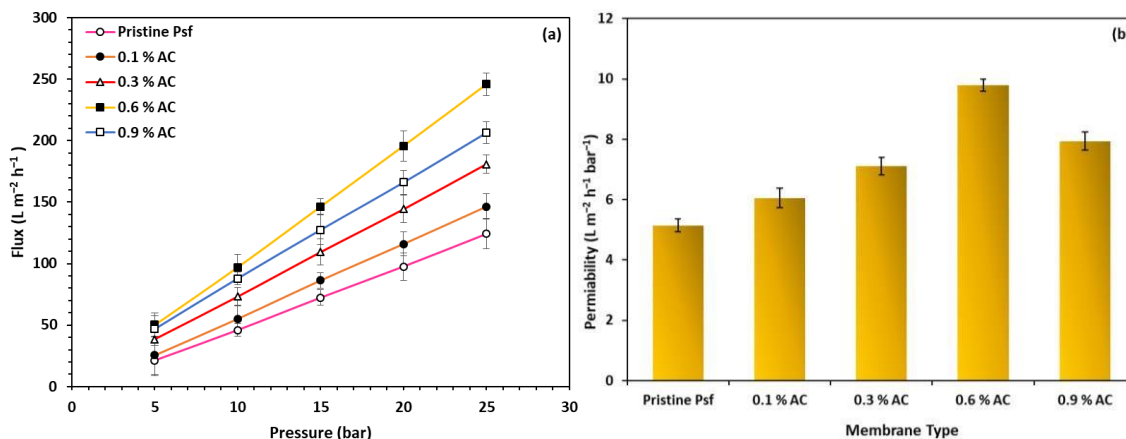
Figure 7.8: Variation of PWF versus TMP (a) and water permeability of NF membranes prepared with various content of AC nanoparticles (b).

7.5.2. Selection of membrane

7.5.2.1. Filtration experiments of OLE

The influence of content of activated carbon on the OLE filtration efficiency of the membranes was investigated at temperature of 25°C and within the TMP range of 10-30 bar. Filtration was carried out for a duration of 300 min at various pressures, and the resulting permeate was collected to analyze TPC rejection. **Figures 7.9 (a)** and **7.9 (b)** illustrate the changes in permeate flux and TPC rejection at different TMPs (10, 20, and 30 bar), respectively.
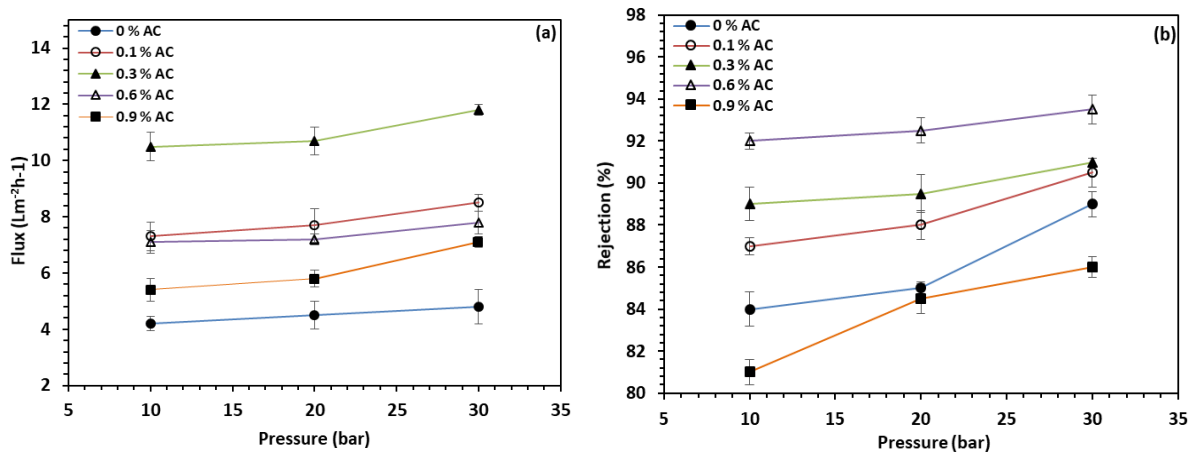
Figure 7.9: Variation in OLE permeate flux (a) and TPC rejection (b) with changing TMP for NF membranes fabricated with various content of AC nanoparticles.

When examining the impact of AC nanoparticles content on filtration, it becomes evident that AC-based membranes possess higher permeate flux than simple polymeric membrane. The membranes containing 0.3% AC demonstrated the highest observed permeate flux for OLE. This can be attributed to the enlargement of pore size and increase in porosity within the membranes. The larger pores and higher porosity provide a more efficient flow through the membrane, leading to higher permeate flux. However, a decrease in OLE permeate flux was noted when the concentration of AC in the casting solution was further increased to 0.6% and 0.9%. This reduction can be explained by the phenomenon ofagglomeration. At higher AC concentrations, nanoparticles tend to cluster together, formingaggregates that obstruct membrane pores. This obstruction surpasses the effect of membrane porosity and pore size in these specific membranes.

Furthermore, it's important to observe that the permeate flux exhibited a rise as the TMP increased, indicating that the permeate flux stayed below the maximum limit for all the membranes studied. Nevertheless, permeate flux of the basic polymeric membrane exhibited stabilization beyond 20 bar, indicating that it serves as the threshold TMP (flux) (Sharma et al., 2023; Luo et al., 2013). Nevertheless, in the case of AC-based membranes containing 0.1%, 0.3%, 0.6%, and 0.9% of nanoparticles, the permeate flux demonstrated a linear increase as the transmembrane pressure was raised. This suggests that these membranes exhibit enhanced stability at high (TMP) levels to achieve the maximum flux

owing to their smaller pore size and increased hydrophilicity of surface (see **Figs. 7.3** and **7.3**).

Moreover, the collected permeate samples at various pressures were subjected to analysis to determine the concentration of TPC, which was then used to assess the membrane properties. According to **Fig. 7.9 (b)**, the TPC rejection falls within the range of 81-93% for all the tested membranes. Despite that membranes containing 0.1%, 0.3%, and 0.6% AC nanoparticles possess larger pore sizes compared to the pristine Psf membrane, they demonstrated greater TPC rejection. The reason behind this can be attributed to the fact that the control of rejection by these membranes is attributed not just by their pore size but also by the interplay between the structural elements of the membrane (AC) and the solute molecules (polyphenols).

The TPC rejection increased as TMP increased within the 10–30 bar range. Permeate transport in a pressure-driven membrane system occurs either through convection or through diffusion. At elevated pressure, the significance of diffusion-based transport diminishes, with convection playing a predominant role. Consequently, the pressure gradient becomes closely linked to the flow of permeate. On the contrary, when operating under low pressure, permeate flow is primarily driven by diffusion transport. This situation leads to a decreased concentration gradient, causing permeate concentration to increase and rejection to decrease (Erragued et al., 2022; Manorma et al., 2022).

The observed decrease in rejection, which occurred with the use of a 0.9% AC-based membrane, could be linked to the significant aggregation of nanoparticles at a high content of AC in membrane matrix. As a result, the decrease in adsorptive active sites or active surface area led to a reduction in the adsorption of total phenolic compounds by nanoparticles.

7.5.2.2. Membrane fouling and cleaning

Membrane fouling, a significant challenge in membrane processes, comes with several disadvantages including reduced flux, higher operational and maintenance expenses, and membrane degradation. Furthermore, membrane filtration's performance is substantially influenced by the extent of membrane fouling (Zinadini et al., 2017; Hosseini et al., 2019).

Therefore, significant effort has been dedicated to enhancing and altering the antifouling performance of membranes.

In this study, an evaluation of the membranes' potential for reuse and their ability to resist fouling was conducted. This was achieved by subjecting the membranes to cleaning processes and then analyzing the extent of permeability recovery using distilled water. **Table 7.3** displays the outcomes of permeability recovery for the membranes that were prepared. As indicated in **Table 7.3**, the permeability of the examined membranes cannot be completely regained to their initial values following cleaning. This occurs due to the potent adsorption of polyphenols molecules onto the surface, making it difficult to remove them completely with simple cleaning. Comparing permeability recovery as a key indicator of membrane antifouling effectiveness indicated that the introduction of nanoparticles had a notable impact on reducing fouling. The permeability recovery for the pristine Psf (approximately 75%) was inferior to that of membranes produced by incorporating of AC (83.2% to 95.5%), confirming the enhanced antifouling capability of the membrane due to the presence of AC nanoparticles. Membrane containing 0.3% AC exhibited the highest permeability recovery at 95%. This could be attributed to a surface with higher hydrophilicity for the nanocomposite membranes (Zinadini et al., 2017; Hosseini et al., 2019). Membranes with increased surface hydrophilicity possess higher capacity to adsorb water molecules on their surface. This leads to the formation of a thin layer of water, improving their ability to reject foulants and contaminants. Therefore, this layer can serveas a barrier to prevent the deposition of phenolic molecules onto the surface of the membranes (Rahimi et al., 2015; Vatanpour et al., 2011; Wang et al., 2019). In addition, some decrease in the permeability recovery for the modified membranes at higher activated carbon concentration (0.6% and 0.9% AC) could be ascribed to the potential aggregation ofnanoparticles at elevated content ratios which decrease the effective surface area of nanoparticles. Hosseini et al., (2019) observed a comparable finding while employing a Fe_3O_4-polyvinylpyrrolidone nanoparticles-based mixed matrix membrane (MMMs) for BSA solution filtration, and Vatanpour et al., (2012) observed a similar phenomenon when utilizing TiO_2-coated multiwalled carbon nanotubes nanoparticles-based MMMs for whey filtration.

The aforementioned findings indicate that the membrane, which was fabricated with a 0.3% AC content, displayed the greatest flux and permeability. Furthermore, it showed TPC rejection levels within the acceptable range for NF membranes as anticipated. Consequently, this specific membrane was chosen for additional investigations into optimizing operational variables to improve its overall efficiency.

Table 7.3: Permeability recovery of different prepared membranes.

Membrane type	Pristine Psf	0.1% AC	0.3% AC	0.6% AC	0.9% AC
Permeability recovery (%)	75.6	92.5	95.04	86.31	83.21

7.5.3. Optimization of NF performance using CCD

Table 7.4 provides a comprehensive list of mixed matrix membranes from the literature, showcasing the integration of various nanoparticles (e.g., ZnO, CNT, and GO) into polymer matrices within the 0 to 3% wt range. Polyethersulfone and polysulfone were commonly used as base polymers, with PVP and PEG as pore formers. Results in **Table 7.4**reveal that nanoparticle incorporation significantly improves membrane morphology, enhancing porosity and reducing pore size and roughness. Regarding hydrophilicity, adding nanoparticles increases the water contact angle. Moreover, nanoparticle introduction improves the rejection of required solutes such as lignin, salt, and TPC and enhances membrane resistance to fouling.

Table 7.4: Comparison of various MMM properties and performance by using different kinds of nanoparticles fillers.

Base polymer	Pore former	Nanoparticles	Loading ratios (wt %)	Water uptake (%)	Porosity (%)	Pore size (nm)	Water contact angle ($\circ$)	Ra (nm)	RMS (nm)	PWF ($Lm^{-2}h^{-1}$) (Kg/m^2h)*	R (%)	FRR (%)	Ref
Psf	PVP	CNT	0, 0.1 and 0.5	73.20-79.10	74.40-79.70	2.82-8.26	57.6-70.8	5.01 -7.70	6.31-10.80	14.8-132.5	52-98 Lignin rejection (6-16 bar)	100	[11]
PES	PVP	L-Methionine (C,N,S triple doped)-TiO$_2$-ZnO	0, 0.1, 0.5 and 1	-	-	-	63.2-46.4	0.45-47.11	0.57-59.60	12.1-41.8* at 5 bar	91.99 Dye removal (at 5 bar)	52.4-88.9	[12]
PES	PVP	ZnO/MWCNTs	0, 0.1, 0.5 and 1	-	-	-	68.3-55.6	8.3-68.7	10.7-103.9	8.2-16.7* at 4 bar	91-99 Dye removal (4 bar, pH=6)	51.0-88.6	[13]
PES	PVP	SLS-CNT	0,0.5,1,1.5,2 and 2.5	-	65–74	37-59	79-57	7.0-10.4	9.4-14.3	150-590 at 1 bar	<95 BSA rejection at 1 bar	61.2-95.1	[14]
PES	PVP	NH$_2$-MWCNTs	0, 0.05, 0.1 and 1	-	78.4-89.3	-	63-52	-	-	78.55-106.75* at 2 bar	BSA rejection 25-52 at 2 bar	70-89.7	[15]
PES	PVP	TiO$_2$ coated MWCNTs	0, 0.1 and 1	-	70.1-78.1	2.15-2.52	66.1-61.5	7.9-13.9	9.5-18.0	3.71-5.66* at 5 bar	69.5-80.7 Na$_2$SO$_4$ rejection (at 5 bar)	53.1-83.0	[16]

Table 7.4: Comparison of various MMM properties and performance by using different kinds of nanoparticles fillers. (Continuation)

PES	PVP	Fe_3O_4-PVP	0, 0.05, 0.1, 0.5, 1 and 2	72.23-74.15	68.8-95.2	1.80-2.93	65.2-50.5	5.5-9.26	-	3.2-9.9 at 5 bar	77-90 Salt rejection (at 5 bar)	46.2-89.5	[17]
PES	PVP	GO nanoplate	0, 0.1, 0.5 and 1	-	73.2-83.1	3.2-4.5	65.2-53.2	8.0-20.4	10.0-28.1	8.2-20.4* at 4 bar	90-99 Dye removal (4 bar, pH=6)	35-90.5	[29]
PES	PVP	PAA-co-PMMA-g-ZnA	0, 0.05, 0.1, 0.5 and 1	-	64.8-79.9	-	65.38-48.33	-	-	10.2-35.6 at 5 bar	68.40-85.57 Salt rejection (at 5 bar)	-	[30]
PES	PVP	ZnO-PANI	0, 0.05, 0.1,0.2, 0.4 and 0.6	73.23-78.12	72.21-77.82	2.34-8.25	71.02-56.03	-	-	29.18-165.94 (at 20 bar)	83.3-92.1 TPC rejection (10- 30 bar)	47.1-74.3	[46]
PES	-	sulfated-TiO_2	0 and 2	33.8-68.9	75.3-80.2	11.6-16.6	67.9-52.9	-	-	57.6-106.3 at 1.4 bar	96.5- 99.0 BSA rejection at 1.4 bar	-	[47]
Psf	PEG	ZnO	0,0.2,0.5 and 1	76.40-78.17	66.80-90.66	21.13-36.38	65.7-59.9	17.53-22.36	21.84-27.74	525-975 at 4 bar	65–80 hemicellulose rejection (at 4 bar)	-	[48]
PES	PVP	boehmite	0, 0.5, 1, 2 and 3	-	65.6-68.1	2.36-2.81	66.3-40.4	4.2-14.5	5.2-18.1	3.90-4.14* at 5 bar	-	58.2-96.1	[49]
Psf	PEG	AC	0,0.1,0.3,0.6 and 0.9	72.2-78.1	83.6-87.5	6.3-7.2	66.6-48.2	4.6-8.2	5.7-10.3	46-87.9 at 10 bar	86-93.5 at 30 bar	75.6-95	Our work

7.5.3.1. Fitting the model

The study explored the efficiency of nanofiltration using a 0.3% AC-based membrane on the permeate derived from OLE processing via ultrafiltration using the CCD method. The 16 experimental designs and the response variable results (rejection of TPC) of eachrun based on the CCD are presented in **Table 7.5**.

Table 7.5: Experimental findings acquired from CCD for optimizing operational parameters with a 0.3% AC-based NF membrane.

			Independent variables		Response variable
Run	Level	pH	Temperature (°C)	Pressure (bar)	Rejection of TPC (%)
1	00+	4.7	35	30	88.54
2	000	4.7	35	20	86.75
3	000	4.7	35	20	86.80
4	--+	2.7	25	30	97.62
5	---	2.7	25	10	91.33
6	-+-	2.7	45	10	85.91
7	+++	6.7	45	30	82.75
8	++-	6.7	45	10	79.77
9	0+0	4.7	45	20	83.88
10	00-	4.7	35	10	85.21
11	-++	2.7	45	30	88.22
12	-00	2.7	35	20	89.71
13	+-+	6.7	25	30	87.87
14	+--	6.7	25	10	85.00
15	+00	6.7	35	20	83.33
16	0-0	4.7	25	20	89.52

The regression model that expresses the TPC rejection (%) as a function of the three experimental factors is presented in Equation (9). This equation aims to elucidate the correlation between the rejection of TPC from OLE and the various operational conditions, namely pH, temperature, and pressure.

$$Y = 86.564 - 3.407 \left(\frac{pH-4.7}{2}\right) - 3.081 \left(\frac{T-35}{10}\right) + 1.778 \left(\frac{P-20}{10}\right) - 0.343 \left(\frac{pH-4.7}{2}\right)\left(\frac{P-20}{10}\right) -$$

$$0.483 \left(\frac{T-35}{10}\right)\left(\frac{P-20}{10}\right) + 0.558 \left(\frac{pH-4.7}{2}\right)\left(\frac{T-35}{10}\right) + 0.061 \left(\frac{pH-4.7}{2}\right)^2 + 0.241 \left(\frac{T-35}{10}\right)^2 +$$

$$0.416 \left(\frac{P-20}{10}\right)^2 \tag{9}$$

The analysis of variance (ANOVA) holds significant importance as a widely employed statistical tool to validate the precision of models. In this study, an ANOVA was conducted specifically to ascertain the significance of the model. In **Table 7.6**, the ANOVA analysis results demonstrated a high level of significance ($p < 0.0001$) for the presented model. This was evident from the high F-test value and a small p-value, indicating strong statistical significance.

Table 7.6: ANOVA and estimated regression coefficients for the quadratic polynomial model.

Parameter	Estimated coefficient	Standard Error	Sum of Square	Degree of Freedom	F-value	P > F	Significance
Model	-	-	249.302	9	64.591	<0.0001	**
Intercept							
β_0	86.564	0.3100	-	-	-	-	
Linear							
pH	-3.407	0.2070	116.076	1	270.666	<0.0001	**
T	-3.081	0.2070	94.925	1	221.347	<0.0001	**
P	1.778	0.2070	31.612	1	73.714	0.0001	**
Interaction							
pH T	0.558	0.2315	2.497	1	5.823	0.0523	ns
pH P	-0.343	0.2315	0.945	1	2.204	0.1882	ns
T P	-0.483	0.2315	1.872	1	4.365	0.0817	ns
Quadratic							
pH^2	0.061	0.4033	0.009	1	0.022	0.8847	ns
T^2	0.241	0.4033	0.153	1	0.357	0.5719	ns
P^2	0.416	0.4033	0.456	1	1.064	0.3421	ns
Statistics							
R^2	0.9897	-	-	-	-	-	
$Radj^2$	0.9744	-	-	-	-	-	
RMSE	0.6549	-	-	-	-	-	
CV %	3.14	-	-	-	-	-	

pH: pH of feed; T: temperature ($\circ$C); P: pressure (bar). ** denotes statistical significance at a level of $p < 0.001$, whereas ns indicates no statistical significance.

The strong correlation between the experimental and predicted values is evident from the high linear regression coefficient ($R^2 = 0.989$), indicating that only 2% of the variations were unexplained by the model. An effective statistical model is characterized by the adjusted determination coefficient (R^2_{adj}) being close to R^2. In this case, both coefficients were almost identical, with R² being 0.989 and R²adj being 0.974, as shown in **Table 7.6**.

This close similarity suggests the robust correlation between the values obtained through experimentation and those predicted, as depicted in **Fig. 7.10a**.

Experimental and predicted values exhibit a high degree of similarity, as evidenced by a low coefficient of variation (CV = 3.14%) and a minimal root mean square error (RMSE = 0.6549).Consequently, the experimental values exhibit a high degree of precision and good accuracy (Fratoddi et al., 2018; Dairi et al., 2021). Hence, the suggested model provesto be suitable and has the potential to perform effectively in predicting the rejection of phenolic compounds using 0.3% AC-based membrane within the range of experimental variables.
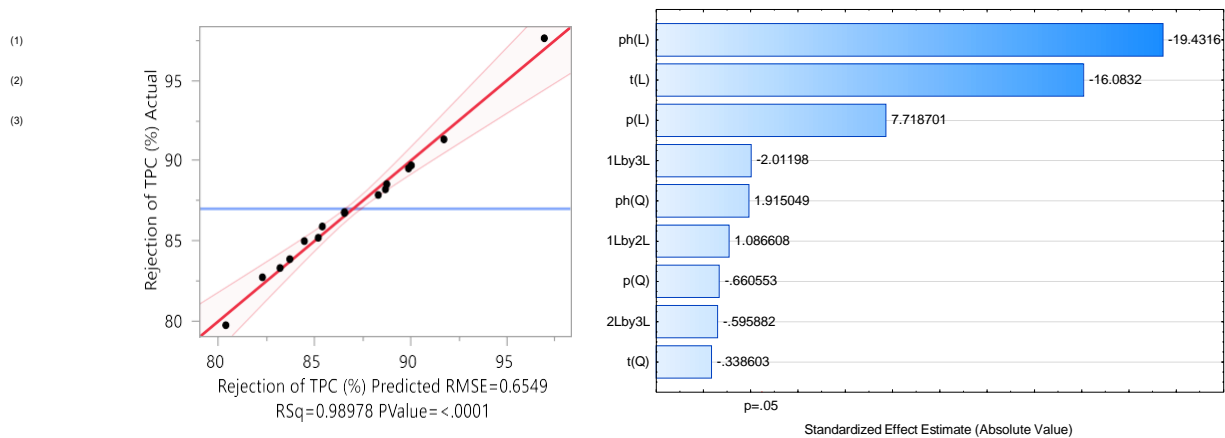
Figure 7.10: Experimental vs predicted value for TPC rejection (a) and Pareto chart presenting effects of the variables and their interactions on TPC rejection using membrane filled with 0.3 % AC (b).

The importance of each independent variable and their interactions in the process can be evaluated with a 95% confidence interval ($p \leq 0.05$) by examining the Pareto graph (**Fig. 7.10b**) of the dependent variable, which was generated using Statistica 14.0 software. According to the data presented in **Fig.7.10b**, it is evident that pressure drop, temperature, and pH significantly influence the rejection of TPC, while their mutual interaction does not exhibit significant effects. The pressure has a beneficial impact on the rejection of TPC, whereas the temperature and pH exert a negative impact. This outcome aligns with p-value and F-value provided in **table 7.6**. A reduced p-value and an increased F-value indicate the

significance of the analyzed variables in relation to the considered response (Dahmoune et al., 2014).

7.5.3.2. Response optimization of operating variables

To establish the most favorable conditions for maximizing TPC rejection in olive leaf extract and illustrate the influence of independent factors on this rejection, a desirability function was formulated. Additionally, response surfaces were constructed to graphically represent these effects. The optimal value for all the tested factors was determined using the Desirable Function (DF). Evaluating response desirability involved defining the DF foreach dependent variable by assigning predicted values on a scale ranging from 0.0 (indicating undesirability) to 1 (representing high desirability) (Khodadoust et al., 2018). **Figure 7.11** displays the graphs representing the desirability function for each factor.

Consequently, the anticipated ideal values for the independent variables turned out to be: pH at 2.7, temperature at 25°C, and pressure at 30.
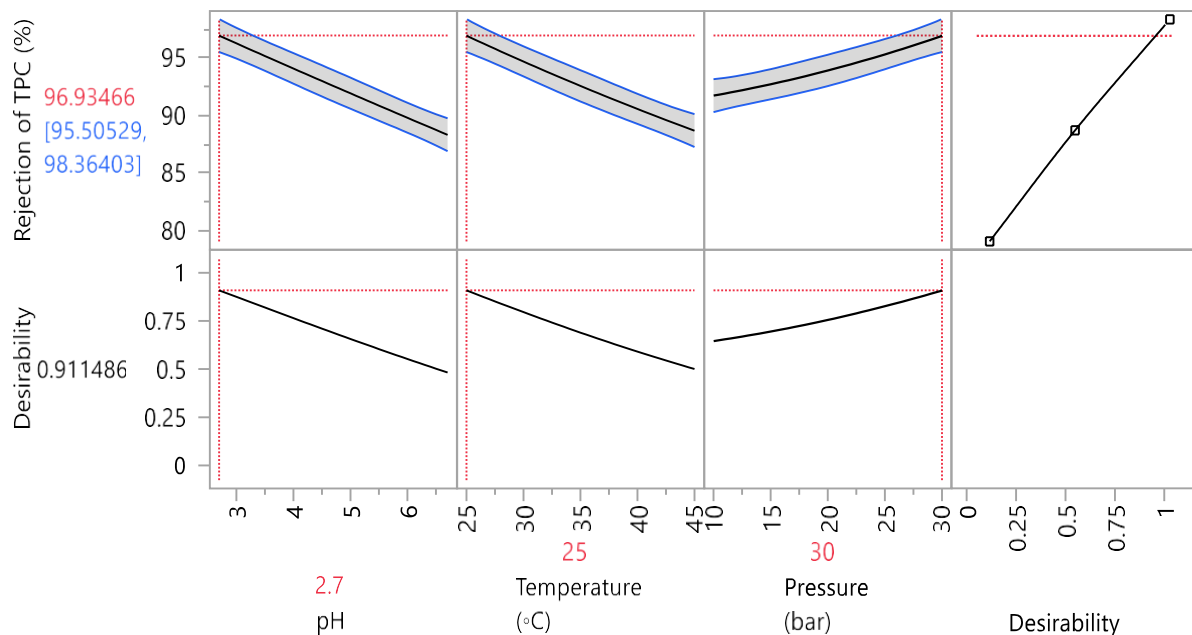
Figure 7.11: Desirability function for TPC rejection. The optimized values for every individual factor are indicated by the red lines

The three-dimensional graph presented in **Fig.7.12**, constructed using the mathematical equation outlined in Eq. (9), illustrates the impact of various combinations of independent

variables on TPC rejection. The polyphenols rejection response surface was graphed in relation to two operating variables, with the third variable held constant at a fixed value (level 0 as indicated in **Table 7.2**). It is feasible to observe the significant variation in the rejection of polyphenols when the operating conditions within the studied range are modified.

In particular, as depicted in **Fig. 7.12 (a)** and (**c**), the rise in TMP (within the 10-30 bar range) led to a higher rejection of phenolic compounds. This increase was attributed to the accumulation of particles or solutes on the membrane surface, creating a layer referred to as a "cake." This layer can act as an extra barrier, reducing the passage of substances through the membrane (Ruby-Figueroa et al., 2011). In addition, increasing TMP generally enhances rejection performance by forcing more solutes to be retained by the membrane. Giacobbo et al., (2017) and Cassano et al., (2018) were also demonstrated a linear correlation between TMP and phenolic compound removal in treating secondary racking wine lees and processing agro-food by-products, respectively. This phenomenon can be explained using the film layer theory, which suppose the creation of a narrow layer with a distinct thickness in the region next to the membrane's surface. In this area, the concentration gradually diminishes from the surface towards the bulk region. When the transmembrane pressure (TMP) is elevated, concentration polarization and fouling effects become more pronounced.   As a result, with higher TMP, an additional selective layer forms upon the surface of the membrane, resulting in an enhancement in the retention coefficient (Cassano et al., 2018).

By analyzing **Fig.7.12 (b)**, it becomes evident that the highest TPC removal values occurred at lower temperature. This can be linked to modification in the structure and morphology of the membrane. These findings align with the research conducted by Dang et al., (2014). They validated that raising the feed temperatures (from 20 to 40°C) results in a greater pore radius (0.39 to 0.44 nm) for the NF270 membrane. This occurrence occurs due to the active layer of the thin film composite membrane, made of polymer, expanding because of heat-induced thermal expansion. Consequently, the membrane's pore structure undergoes alterations as the temperature increases. Therefore, increasing the temperature ofthe feed had a negative impact on solute rejection. The behavior we observed is in accordance with findings outlined in previous research (Xie et al., 2013).

Besides to pore size and membrane structure, the filtration temperature can affect feed viscosity. It is worth mentioning that an increase in temperature of feed solution results an decrease in the viscosity (Cassano et al., 2018; Dang et al., 2014). Decreased viscosity can affect the ability of the membrane to effectively reject solutes. Viscosity may impact the solute's diffusion and transport through the membrane, which might impact the efficiency of the rejection. Regardless, when employing membrane processes for the recovery of phenolic compounds, it is essential to operate at the lowest possible temperature to preserve the bioactivity of the compounds (Cassano et al., 2018).
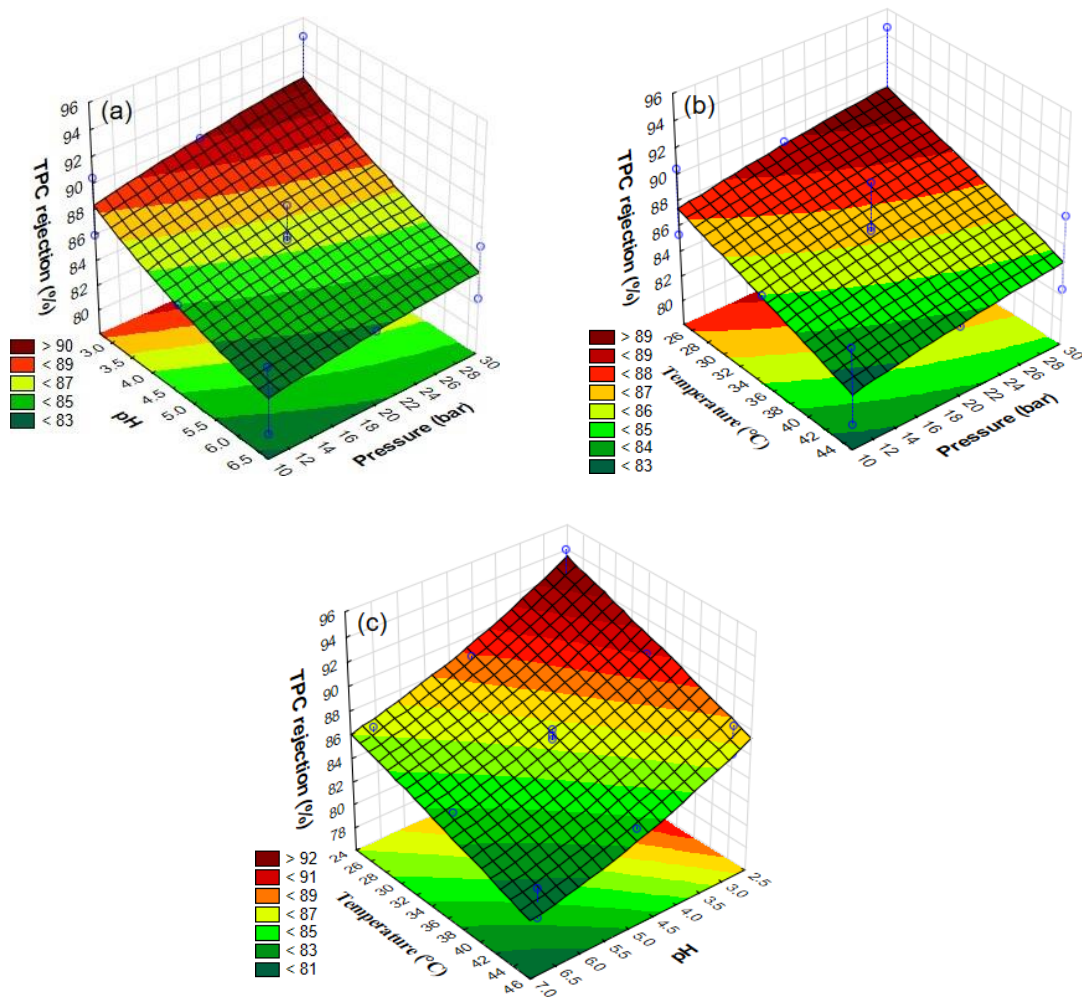
Figure 7.12: Response surface graphs for the effects of pressure and pH (a), temperature and pressure (b), and pH and temperature (c) on the rejection of TPC.

Figure 7.12(a) demonstrates that achieving a TPC removal rate exceeding 90% is possible at the lowest temperature and pH levels i, e., 25°C and 2.7, respectively. In processes like membrane filtration, the pH of the feed solution can have an impact on membrane performance and separation efficiency. The most crucial factor affecting TPC recovery is the pH of the feed stream. This factor regulates the charge of polyphenols molecules in the solution, influencing the interactions between the solute and the membrane and the hydrophilicity of membrane (De Almeida et al., 2018). Thus, analyzing the membrane's zeta potential reveals the impact of pH levels on it. The highest rejection coefficient was achieved at pH 2.7 when the membrane had a positive zeta potential and phenolic molecules remained undissociated (when the pH medium is lower than pKa), considering the standard pKa values for phenolic compounds are approximately 9.89 (Ahmadiaras et al., 2023). Consequently, the primary mechanism for rejection in these circumstances is size exclusion, which proves its superior efficiency in eliminating polyphenols (De Almeida et al., 2018).

As the pH increases to around 5 (while the membrane still maintains a positive zeta potential), there is a decrease in TPC Rejection. This phenomenon can be elucidated by the existence of two categories of phenolic compounds present in natural olive leaf extract. These categories comprise hydroxycinnamic acids, including ferulic acid, p-coumaric acid, chlorogenic acid, and caffeic acid, as well as hydroxybenzoic acids like gallic acid and vanillic acid. These compounds possess primary pKa because of their carboxylic group, usually around 4.5. Consequently, when the pH levels exceed 4.5, these phenolic compounds undergo deprotonation, causing them to carry a negative charge (Ferri et al., 2011). In such circumstances, the two aforementioned classes of phenolic compounds experience an electrostatic attraction that augments their passage, leading to reduced rejection coefficient and heightened permeate flux.

Once the pH level surpasses 5.5, the membrane acquires a negative charge in its zeta potential. Consequently, the membrane surface becomes more inclined towards hydrophilicity, resulting in an enhanced flow that facilitates greater permeation of neutral polyphenols molecules. On the other hand, phenolic compounds bearing a negative charge, especially phenolic acids, experience electrostatic repulsion from the membrane. Therefore,

the predominant phenolic compounds are likely to be in a non-deprotonated (neutral) state, as evidenced by the poorest rejection outcomes observed at pH levels exceeding 5.5. The noticed behavior is in accordance with results documented in existing literature (De Almeida et al., 2018). Moreover, under elevated pH conditions, the rise in permeate flux might be associated with pore expansion, which in turn leads to reduce in the rejection of phenolic compounds (De Almeida et al., 2018; Luo et al., 2013). Nevertheless, this effect isnot as noticeable in this study due to the use a low range of pH values in the experimental design.

7.5.4. Nanofiltration of OLE using optimal membrane under optimal conditions

Following the optimized parameters, OLE was systematically filtered through the best membrane (0.3% AC-based membrane) under following conditions: pH=2.7, T=25°C, TMP=30 bar. The oleuropein concentration in the initial feed, permeate, and retentate was analyzed using HPLC, and the findings are depicted in **Fig.7.13**.The chromatographicprofiles of the feed, permeate, and retentate are visually depicted in the same figure. The results illustrated in **Fig.7.13** highlight that the pre-ultrafiltration permeate, which constitutes the initial feed, showed that oleuropein was identified as the predominantpolyphenol, with a concentration of 41.98 mg/g OLP.A complete rejection (100%) of oleuropein (Mw = 540 g/mol) was achieved using 0.3% AC-based membrane. Comparable findings were recorded in the concentration of oleuropein from olive leaf aqueous extract through the integration of membrane operations (including microfiltration, ultrafiltration, and nanofiltration), as documented by Ibtihel et al., (2017). The achieved results can be ascribed to the strong adsorption of polyphenols onto the surfaces of activated carbon nanoparticles that have been incorporated into the membrane matrix. This explanation aligns with findings documented in existing literature regarding the high adsorption of polyphenols on AC nanoparticles (Benaddi et al., 2023; García-Pérez et al., 2019).

In this study, the main goal was to achieve the significant removal of polyphenols from olive leaf extract along with a high rate of flux. Based on the results, the optimal balance between the recovery of TPC and permeate flux was observed with 0.3% AC/Psf

membrane, attributed to the strong adsorption affinity of AC nanoparticles (indicated by the color of the retentate fraction in **Fig. 7.13**) and to hydrophilic properties of these nanoparticles, respectively.
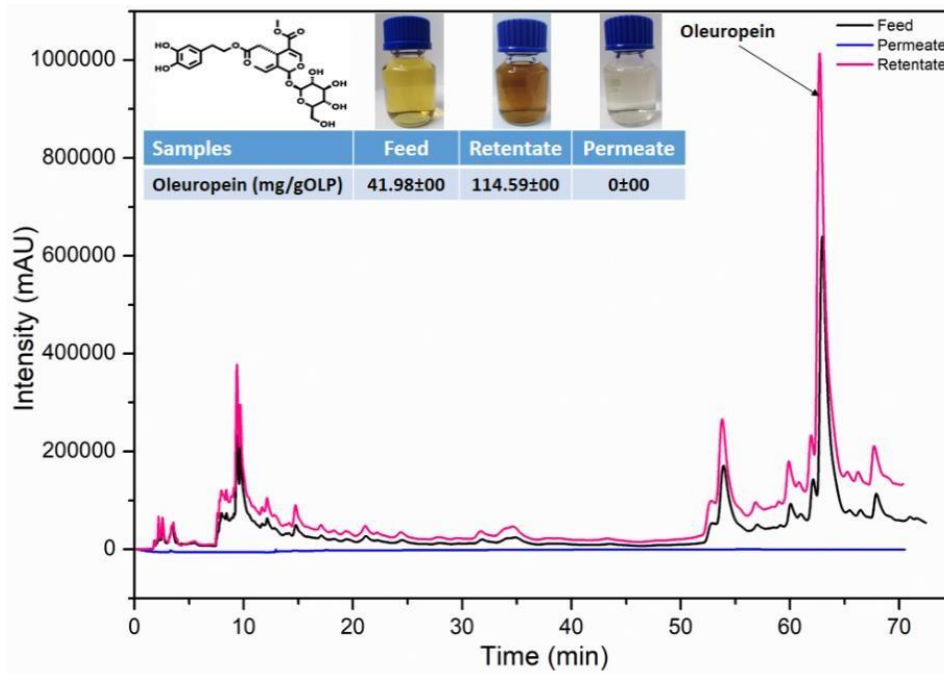
Figure 7.13: HPLC chromatographic profiles for phenolic compounds found in feed, permeate, and retentate.

7.6. Conclusions

The research explored the influence of AC nanoparticles content on the efficiency of Psf membranes during the TPC recovery from OLE. It also concentrated on enhancing operational parameters to improve filtration effectiveness. Incorporating of AC nanoparticles led to enhancements in all the favorable attributes of the membrane, includingporosity, pore size, surface hydrophilicity, permeability to water and OLE, as well as the resistance to fouling, when compared to pristine Psf membrane. The maximum hydrophilicity was noted at 0.9 % AC loading, reducing water contact angle by 18.4°. A significant improvement was found in water permeation, reaching to 9.8 L m^{-2} h^{-1} bar^{-1} (0.6 % AC content), as compared with the pristine one (5.14 L m^{-2} h^{-1} bar^{-1}). In the OLE filtration process, membranes fabricated using a 0.3% AC content demonstrated the

greatest permeability, achieving a flux rate of 11.8 ± 0.2 L m^{-2} h^{-1} under 30 bar pressure. These membranes also exhibited effective TPC rejection, ranging from 89% to 91% across pressures of 10 to 30 bar, and displayed an impressive flux recovery rate of 95% following membrane cleaning. In contrast, the pristine Psf membranes achieved a lower flux recovery rate of 75.6%. The investigation into enhancing operational factors was conducted employing membranes based on 0.3% AC, within the pH range of 2.7 to 6.7, temperatures between 25°C and 45°C, and pressures spanning from 10 to 30 bar. The outcomes of the experimental setup demonstrated substantial impacts of pH, temperature, and pressure on the rejection of TPC. The pressure showed a beneficial impact on the recovery of TPC, whereas the temperature and pH exerted an adverse influence. The desirability profiler was used to identify optimal pH, temperature, and pressure settings, resulting in maximum rejection of TPC. HPLC analysis of fractions produced by 0.3% AC-based membranes under the optimum conditions showed a complete rejection (100%) of oleuropein.

CHAPTER 8: General conclusions and future opportunities

8.1 Conclusions

In the studies carried out in the present work, phenolic compounds were effectively separated from olive leaf extract using a commercial polyethersulfone flat sheet nanofiltration membrane and mixed matrix membranes. However, the spotlight has been put on NF mixed matrix membranes modified with different nanoparticles, was an innovative approach for the separation of phenolic compounds from naturel extract. The work was accomplished by completing a various tasks and experiments, which allowed usto reach the following conclusions.

• Regarding the approach for integrating solvent extraction and membrane separation technique using a commercial polyethersulfone (PES) flat sheet nanofiltration (NF) membrane, In summary, this study optimized the extraction of phenolic compounds from olive leaves using ethanol: water (75:25%) and determined the optimal conditions (50°C, 30 mg/L, 90 min). The integration of solvent extraction and membrane filtration processes resulted in a purified fraction (NF retentate) rich in polyphenols, especially oleuropein, exhibiting high antioxidant activity. This approach shows promise for industrial applications in pharmacy and cosmetics.

• In the context of synthesizing ZnO-PANI nanoparticles for subsequent use in the preparation of mixed matrix membranes, these nanoparticles were successfully synthesized via a simple chemical oxidation polymerization process. SEM-EDX analysis confirmed their preparation. The experiments revealed that phenolic compound adsorption was more effective at high pH and at higher concentrations. Isotherm studies indicated that the Langmuir model best described the adsorption process, suggesting a monolayer adsorption mechanism. These results highlight the potential of ZnO-PANI nanoparticles for efficient phenolic compound removal from liquid effluents.

• In the study of preparing and applying NF mixed matrix membranes modified with ZnO-PANI nanoparticles, it was found that the addition of these nanoparticles improved the desirable membrane characteristics, such as hydraulic permeability, pore size, and surface hydrophilicity

• In addition, pertaining to NF mixed matrix membranes modified with ZnO-PANI, it was found that the incorporation of ZnO-PANI at a concentration of 0.2% (w/w) resulted in a balanced permeate flux and TPC rejection. These membranes offered higher permeate flux during the filtration of olive leaves extract, achieving an 87% TPC rejection and 95% rejection of OLE at 30 bar, however, they still suffer from low resistance to fouling compared to simple PES membrane.

• Furthermore, incorporating 0.4% (w/w) of ZnO-PANI resulted in the highest total phenolic compounds (TPC) rejection of 93-97% at pressures ranging from 10 to 30 bar,with complete oleuropein rejection reaching 100%.

• In a follow-up study, another type of NF mixed matrix membranes modified with activated carbon (AC) nanoparticles were prepared for TPC separation from OLE. It was found that the addition of these nanoparticles led to enhancements in all the favorable attributes of the membrane, including porosity, pore size, surface hydrophilicity,permeability to water and OLE, as well as the resistance to fouling, when compared to pristine Psf membrane.

• The membrane filled with 0.3% AC exhibited the highest permeate flux and effective total polyphenol compound (TPC) rejection, ranging from 89% to 91% across pressures of 10 to 30 bar, and displayed an impressive flux recovery rate of 95% following membrane cleaning. Using this membrane, the optimal operating conditions for pH, temperature, and pressure were found to be pH 2.7, 25°C, and 30 bar. HPLC analysis of fractions produced by 0.3% AC-based membranes showed a complete rejection (100%) of oleuropein.

Upon comparing these conclusions, it becomes easy to draw an overall conclusion about the tasks carried out in this thesis, which is that: The highest TPC rejection (92%- 93%) was found using ZnO-PANI-based membranes (0.4.wt %), followed by (93%-95%) and (92%-93%) for commercial polyethersulfone (PES) and AC-based membranes (0.6.wt %), respectively, at pressures ranging from 10 to 30 bar. In terms of OLE permeate flux, AC-based membranes, with the addition of AC at a concentration of 0.3% (w/w), outperform commercial polyethersulfone (PES) membranes and membranes filled withZnO-PANI nanoparticles, achieving a flux rate of 10.5-11.8 L/m²h at pressures ranging from 10 to 30 bar. In terms of oleuropein rejection, both the commercial polyethersulfone

(PES) and MMMs (with 0.4% ZnO-PANI and 0.3% AC) approaches provided complete rejection of oleuropein at 30 bar (100%).In terms of antifouling ability, the membrane filled with AC demonstrated higher antifouling ability compared to membranes filled with ZnO-PANI. Membranes containing 0.3% AC exhibited an impressive flux recovery rate of 95% after membrane cleaning.

8.2 Future work opportunities

A more comprehensive analysis of the studies in the thesis could help resolve certain issues. Based on the work described, potential future aspects for further research could include:

• Investigating the use of other types of nanoparticles for preparation of ultrafiltration and nanofiltration mixed matrix membranes, to observe if they can provide even better performance for natural extracts filtration in terms of flux, TPC rejection, and fouling resistance.

• Evaluating the impact of the size and shape of the nanoparticles on the performance of the modified membranes, to understand how these factors influence membrane characteristics and separation efficiency of phenolic compounds.

• Evaluating the performance of the modified membranes over longer periods of time, to assess their durability and potential for practical use in industrial processes.

• Exploring new approaches for cleaning and regenerating the used membranes, in order to extend their useful lifespan and reduce the cost of operation.

•Investigation of the influence of various membrane parameters, such as pore size, membrane thickness, surface charge, and morphology on the separation efficiency. Optimization studies have the potential to significantly enhance the selectivity and permeability of membranes.

• Exploration of different methods to modify the simple polymeric membrane and its surface properties to enhance its overall performance. By exploring innovative techniques for membrane modification, scientists and engineers can advance the field of membrane technology, leading to various applications in water treatment, healthcare, and beyond.

• Evaluating the potential for using the membrane filtration techniques to recover other valuable compounds from different natural extracts, which may have potential applications in a range of industries.

•Investigating the possibility of combining membrane filtration processes with other separation techniques to determine whether higher yields and purity of oleuropein can be obtained.

• Conduct studies to scale up the developed membrane separation processes from the laboratory scale to pilot or industrial scale. Investigate the economic feasibility, challenges, and cost-effectiveness of implementing these processes in large-scale applications.

• Development mathematical models and simulations to predict the behavior of polyphenol and oleuropein separation processes using membranes. Computational modeling can aid in optimizing process parameters and understanding the underlying mechanisms governing the separation processes.

• Exploration of the practical applications of polyphenol-enriched extracts in the food and pharmaceutical industries. Investigation of the potential health benefits, stability, and shelf life of separated polyphenols and oleuropein for various products and formulations.

• Studying the environmental impact of the developed membrane separation processes. Compare the environmental impact of membrane processes with conventional separation methods to assess their sustainability and eco-friendliness.

Bibliography

CHAPTER 1

Arkell A, Olsson J, Wallberg O (2014) Process performance in lignin separation from softwood black liquor by membrane filtration. Chemical Engineering Research and Design 92(9):1792-1800. DOI: 10.1016/j.cherd.2013.12.018.

Ayala-Zavala J.F, Vega-Vega V, Rosas-Domínguez C, Palafox-Carlos H, Villa- Rodriguez J.A, Wasim Siddiqui Md, Dávila-Aviña J.E, González-Aguilar G.A (2011)Agro-industrial potential of exotic fruit byproducts as a source of food additives. Food Research International 44(7):1866-1874. DOI: 10.1016/j.foodres.2011.02.021.

Bouaziz M, Fki I, Jemai H, Ayadi M, Sayadi S (2008) Effect of storage on refined and husk olive oils composition: Stabilization by addition of natural antioxidants from Chemlali olive leaves. Food Chemistry 108(1):253-262. DOI: 10.1016/j.foodchem.2007.10.074.

Briante R, Patumi M, Terenziani S, Bismuto E, Febbraio F, Nucci R (2002) Olea europaea L. Leaf Extract and Derivatives: Antioxidant Properties. J Agric Food Chem50(17):4934-4940.

Erbay Z, Icier F (2010) The Importance and Potential Uses of Olive Leaves. Food Reviews International 26(4):319-334. DOI: 10.1080/87559129.2010.496021.

Govaris A, Botsoglou E, Moulas A, Botsoglou N (2010) Effect of dietary olive leaves and rosemary on microbial growth and lipid oxidation of Turkey breast during refrigerated storage. South African Journal of Animal Science 40:145–155.

Herrero M, Temirzoda TN, Segura-Carretero A, Quirantes R, Plaza M, Ibañez E (2011) New possibilities for the valorization of olive oil by-products. Journal of Chromatography A 1218(42):7511-7520. DOI: 10.1016/j.chroma.2011.04.053.

Humpert D, Ebrahimi M, Czermak P (2016) Membrane Technology for the Recovery of Lignin: A Review. Membranes 6(3):42. DOI: 10.3390/membranes6030042.

International Olive Council (IOC) (2022) Trade standard applying to olive oils and olive pomace oils.

Kevlich N.S, Shofner M.L, Nair S (2017) Membranes for Kraft black liquor concentration and chemical recovery: Current progress, challenges, and opportunities. Separation Science and Technology 52(6):1070-1094. DOI: 10.1080/01496395.2017.1279180.

M.Z. Tsimidou, Papoti V.T (2010)Bioactive ingredients in olive leaves V.R. Preedy, R.R. Watson (Eds.), Olives and olive oil in health and disease prevention, Academic Press, San Diego pp. 349-356

.

Mello B.C.B.S, Petrus J.C.C, Hubinger M.D (2010) Concentration of flavonoids and phenolic compounds in aqueous and ethanolic propolis extracts through nanofiltration. Journal of Food Engineering 96(4):533-539. DOI: 10.1016/j.jfoodeng.2009.08.040.

Molina-Alcaide E, Yáñez-Ruiz D.R (2008) Potential use of olive by-products in ruminant feeding: A review. Animal Feed Science and Technology 147(1-3):247-264. DOI: 10.1016/j.anifeedsci.2007.09.021.

Mourtzinos I, Salta F, Yannakopoulou K, Chiou A, Karathanos V.T (2007) Encapsulation of Olive Leaf Extract in β-Cyclodextrin. J Agric Food Chem 55(20):8088-8094. DOI: 10.1021/jf0709698.

Obied H.K, Prenzler P.D, Omar S.H, et al. (2012) Pharmacology of Olive Biophenols. In: Advances in Molecular Toxicology. Vol 6. Elsevier: 195-242. DOI: 10.1016/B978-0-444-59389-4.00006-9

Peralbo-Molina Á, Luque de Castro M.D (2013) Potential of residues from the Mediterranean agriculture and agrifood industry. Trends in Food Science & Technology 32(1):16-24. DOI: 10.1016/j.tifs.2013.03.007.

Quirantes-Piné R, Lozano-Sánchez J, Herrero M, Ibáñez E, Segura-Carretero A,Fernández-Gutiérrez A (2012) HPLC–ESI–QTOF–MS as a Powerful Analytical Tool for Characterising Phenolic Compounds in Olive-leaf Extracts. Phytochemical Analysis 24(3):213-223. DOI: 10.1002/pca.2401.

Rahmanian N, Jafari S.M, Wani T.A (2015) Bioactive profile, dehydration, extraction and application of the bioactive components of olive leaves. Trends in Food Science & Technology 42(2):150-172. DOI: 10.1016/j.tifs.2014.12.009.

Romero-García J.M, Niño L, Martínez-Patiño C, Álvarez C, Castro E, Negro M.J (2014) Biorefinery based on olive biomass. State of the art and future trends. Bioresource Technology 159:421-432. DOI: 10.1016/j.biortech.2014.03.062.

Spinelli R, Picchi G (2010) Industrial harvesting of olive tree pruning residue for energy biomass. Bioresource Technology 101: 730–735.DOI: doi:10.1016/j.biortech.2009.08.039.

Wallberg O, Jönsson A.S. (2006) Separation of lignin in kraft cooking liquor from a continuous digester by ultrafiltration at temperatures above 100°C. Desalination 195(1-3):187-200. DOI: 10.1016/j.desal.2005.11.011.

Xie P jun, Huang L xin, Zhang C hong, You F, Zhang Y lei. (2015) Reduced pressure extraction of oleuropein from olive leaves (Olea europaea L.) with ultrasound assistance. Food and Bioproducts Processing 93:29-38. DOI: 10.1016/j.fbp.2013.10.004.

CHAPTER 2

Abaza L, Ben Youssef N, Manai H, Mahjoub Haddada F, Methenni K, Zarrouk M (2011) Chétoui olive leaf extracts: influence of the solvent type on phenolics and antioxidant activities. Grasas y Aceites 62(1):96-104. DOI: 10.3989/gya.044710.

Abaza L, Taamalli A, Nsir H, Zarrouk M (2015) Olive Tree (Olea europeae L.) Leaves: Importance and Advances in the Analysis of Phenolic Compounds. Antioxidants 4(4):682-698. DOI: 10.3390/antiox4040682.

Afaneh I, Yateem H, Al-rimawi F (2015) Effect of olive leaves drying on the content of oleuropein. American Journal of Analytical Chemistry 6: 246–252. DOI:10.4236/ajac.2015.63023.

Agalias A, Melliou E, Magiatis P, Mitaku S, Gikas E, Tsarbopoulos A (2005) Quantitation of Oleuropein and Related Metabolites in Decoctions of Olea europaea Leaves from Ten Greek Cultivated Varieties by HPLC with Diode Array Detection (HPLC-DAD). Journal of Liquid Chromatography & Related Technologies 28(10):1557-1571. DOI: 10.1081/JLC-200058355.

Agalias A, Melliou E, Magiatis P, Mitaku S, Gikas E, Tsarbopoulos A (2005) Quantitation of Oleuropein and Related Metabolites in Decoctions of Olea europaea Leaves from Ten Greek Cultivated Varieties by HPLC with Diode Array Detection (HPLC-DAD). Journal of Liquid Chromatography & Related Technologies 28(10):1557-1571. DOI: 10.1081/JLC-200058355.

Ahmad-Qasem M.H, Cánovas J, Barrajón-Catalán E, Carreres J.E, Micol V, García-Pérez J.V (2014) Influence of Olive Leaf Processing on the Bioaccessibility of Bioactive Polyphenols. J Agric Food Chem 62(26):6190-6198. DOI: 10.1021/jf501414h.

Ahmad-Qasem M.H, Cánovas J, Barrajón-Catalán E, Micol V, Cárcel J.A, García-Pérez J.V (2013) Kinetic and compositional study of phenolic extraction from olive leaves (var. Serrana) by using power ultrasound. Innovative Food Science & Emerging Technologies 17:120-129. DOI: 10.1016/j.ifset.2012.11.008.

Akhair S.M, Harun Z, Jamalludin M, Shuhor M, Kamarudin N, Yunos M, Ahmad A, Azhar M (2017) Polymer mixed matrix membrane with graphene oxide for humic acid performances. Chemical Engineering Transactions 56:697–702.

Alara O.R, Abdurahman N.H, Ukaegbu C.I (2021) Extraction of phenolic compounds: A review. Current Research in Food Science 4:200-214. DOI: 10.1016/j.crfs.2021.03.011.

Al-Rimawi F, Odeh I, Bisher A, Abbadi J, Qabbajeh M (2014) Effect of geographical region and harvesting date on antioxidant activity, phenolic and flavonoid content of olive leaves. Journal of Food Nutrition Research 2: 925–930. DOI: 10.12691/jfnr-2-12-11.

Altıok E, Bayçın D, Bayraktar O, Ülkü S (2008) Isolation of polyphenols from the extracts of olive leaves (Olea europaea L.) by adsorption on silk fibroin. Separation and Purification Technology 62 (2):342-348.DOI:10.1016/j.seppur.2008.01.022.

Altop A, Coskun I, Filik G, Kucukgul A , Bekiroglu Y.G, Çayan H, Gungor E, Sahin A, Erener G, Kırsehir Ahi Evran University; et al. (2018) Amino acid, mineral, condensed tannin, and other chemical contents of olive leaves (Olea europaea L.) processed via

solid-state fermentation using selected Aspergillus niger strains. Cien. Inv. Agr 45(2):220–230. DOI 10.7764/rcia.v45i3.1886.

Andreadou I, Iliodromitis E.K, Mikros E, Constantinou M, Agalias A, Magiatis P, Skaltsounis A.L, Kamber, E, Tsantili-Kakoulidou A, Kremastinos D.T (2006) The olive constituent oleuropein exhibits anti-ischemic, antioxidative, and hypolipidemic effects in anesthetized rabbits. J. Nutr. 136:2213–2219.

Andrikopoulos N.K, Antonopoulou S, Kaliora A.C (2002) Oleuropein Inhibits LDL Oxidation Induced by Cooking Oil Frying By-products and Platelet Aggregation Induced by Platelet-Activating Factor. LWT - Food Science and Technology 35(6):479- 484. DOI: 10.1006/fstl.2002.0893.

Ansari M, Kazemipour M, Fathi S (2011) Development of a simple green extraction procedure and HPLC method for determination of oleuropein in olive leaf extract applied to a multi-source comparative study. JICS 8(1):38-47. DOI: 10.1007/BF03246200.

Aouidi F, Dupuy N, Artaud J, et al. (2012) Rapid quantitative determination of oleuropein in olive leaves (Olea europaea) using mid-infrared spectroscopy combined with chemometric analyses. Industrial Crops and Products 37(1):292-297. DOI: 10.1016/j.indcrop.2011.12.024.

Baker RW, et al. (2004) Overview of membrane science and technology. Membrane technology and applications 3:1–14.

Balta S, Sotto A, Luis P, Benea L, Van der Bruggen B, Kim J (2012) A new outlook on membrane enhancement with nanoparticles: the alternative of zno. Journal of membrane science 389:155–161.

Benavente-García O, Castillo J, Lorente J, Ortuño A, Del Rio J.A (2000) Antioxidant activity of phenolics extracted from Olea europaea L. leaves. Food Chemistry 68(4):457-462. DOI: 10.1016/S0308-8146(99)00221-6.

Benavente-García O, Castillo J, Lorente J, Ortuño A, Del Rio J.A (2000) Antioxidant activity of phenolics extracted from Olea europaea L. leaves. Food Chemistry 68(4):457-462. DOI: 10.1016/S0308-8146(99)00221-6.

Bet-Moushoul E, Mansourpanah Y, Farhadi K, Tabatabaei M (2016) TiO2 nanocomposite based polymeric membranes: A review on performance improvement for various applications in chemical engineering processes. Chemical Engineering Journal 283:29–46. DOI: 10.1016/j. cej.2015.06.124.

Bilgin M, Şahin S (2013) Effects of geographical origin and extraction methods on total phenolic yield of olive tree (Olea europaea) leaves. Journal of the Taiwan Institute of Chemical Engineers 44(1):8-12. DOI: 10.1016/j.jtice.2012.08.008.

Botsoglou E, Govaris A, Fletouris D, Iliadis S (2013) Olive leaves (Olea europea L.) and α-tocopheryl acetate as feed antioxidants for improving the oxidative stability of α- linolenic acid-enriched eggs. Animal Physiology Nutrition 97(4):740-753. DOI:10.1111/j.1439-0396.2012.01316.

Bouallagui Z, Han J, Isoda H, Sayadi S (2011) Hydroxytyrosol rich extract from olive leaves modulates cell cycle progression in MCF-7 human breast cancer cells. Food and Chemical Toxicology 49(1):179-184. DOI: 10.1016/j.fct.2010.10.014.

Bouaziz M, Fki I, Jemai H, Ayadi M, Sayadi S (2008) Effect of storage on refined and husk olive oils composition: Stabilization by addition of natural antioxidants from Chemlali olive leaves. Food Chemistry 108(1):253-262. DOI: 10.1016/j.foodchem.2007.10.074.

Bouaziz M, Sayadi S (2005) Isolation and evaluation of antioxidants from leaves of a Tunisian cultivar olive tree. Euro J Lipid Sci & Tech 107(7-8):497-504. DOI: 10.1002/ejlt.200501166.

Boudhrioua N, Bahloul N, Ben Slimen I, Kechaou N (2009) Comparison on the total phenol contents and the color of fresh and infrared dried olive leaves. Industrial Crops and Products 29(2-3):412-419. DOI: 10.1016/j.indcrop.2008.08.001.

Brahmi F, Mechri B, Dhibi M, Hammami M (2013) Variations in phenolic compounds and antiradical scavenging activity of Olea europaea leaves and fruits extracts collected in

two different seasons. Industrial Crops and Products 49:256-264. DOI: 10.1016/j.indcrop.2013.04.042.

Brahmi F, Mechri B, Dhibi M, Hammami M (2014) Variation in antioxidant activity and phenolic content in different organs of two Tunisian cultivars of Olea europaea L. Acta Physiol Plant 36(1):169-178. DOI: 10.1007/s11738-013-1397-4.

Briante R, La Cara F, Febbraio F, Patumi M, Nucci R (2002a) Bioactive derivatives from oleuropein by a biotransformation on Olea europaea leaf extracts. Journal of Biotechnology 93(2):109-119. DOI: 10.1016/S0168-1656(01)00387-X

Briante R, Patumi M, Febbraio F, Nucci R (2004) Production of highly purified hydroxytyrosol from Olea europaea leaf extract biotransformed by hyperthermophilic β-glycosidase. Journal of Biotechnology 111(1):67-77. DOI: 10.1016/j.jbiotec.2004.03.011.

Briante R, Patumi M, Terenziani S, Bismuto E, Febbraio F, Nucci R (2002b) Olea europaea L. Leaf Extract and Derivatives: Antioxidant Properties. J Agric Food Chem 50(17):4934-4940. DOI: 10.1021/jf025540p.

Caballero B, Trugo L.C, Finglas P.M (2003) Encyclopedia of Food Sciences and Nutrition, 2nd ed.; Academic Press, Elsevier: Amsterdam, The Netherlands.

Capote F.P, Marinas A, Japo R (2008) Liquid chromatography/triple quadrupole tandem mass spectrometry with multiple reaction monitoring for optimal selection of transitions to evaluate nutraceuticals from olive-tree materials. Wiley InterScience 22:855–864. DOI: 10.1002/rcm.3423.

Chemat, Abert Vian, Ravi, et al. (2019) Review of Alternative Solvents for Green Extraction of Food and Natural Products: Panorama, Principles, Applications and Prospects. Molecules 24(16):3007. DOI: 10.3390/molecules24163007.

Chen Y, Zhang Y, Zhang H, Liu J, Song C (2013) Biofouling control of halloysite nanotubes decorated polyethersulfone ultrafiltration membrane modified with chitosan-

silver nanoparticles. Chemical Engineering Journal 228:12–20, DOI 10.1016/j.cej.2013.05.015.

Christophoridou S, Dais P (2009) Detection and quantification of phenolic compounds in olive oil by high resolution 1 H nuclear magnetic resonance spectroscopy. Analytica Chimica Acta 633(2)283–292. DOI:10.1016/j.aca.2008.11.048.

Contreras M.D.M, Lama-Muñoz A, Espínola F, Moya M, Romero I, Castro E (2020) Valorization of olive mill leaves through ultrasound-assisted extraction. Food Chemistry 314:126218. DOI: 10.1016/j.foodchem.2020.126218.

Coppa C, Gonçalves B, Lee S, et al. (2020) Extraction of oleuropein from olive leaves and applicability in foods. qas 12(4):50-62. DOI: 10.15586/qas.v12i4.779.

Dasgupta J, Chakraborty S, Sikder J, Kumar R, Pal D, Curcio S, Drioli E (2014) The effects of thermally stable titanium silicon oxide nanoparticles on structure and performance of cellulose acetate ultrafiltration membranes. Separation and Purification Technology 133:55–68, DOI 10.1016/j.seppur.2014.06.035.

De Leonardis A, Aretini A, Alfano G, Macciola V, Ranalli G (2008) Isolation of a hydroxytyrosol-rich extract from olive leaves (Olea Europaea L.) and evaluation of its antioxidant properties and bioactivity. Eur Food Res Technol 226(4):653-659. DOI: 10.1007/s00217-007-0574-3.

Diagne F, Malaisamy R, Boddie V, Holbrook RD, Eribo B, Jones KL (2012)Polyelectrolyte and silver nanoparticle modification of microfiltration membranes to mitigate organic and bacterial fouling. Environmental Science and Technology 46(7):4025–4033, DOI 10.1021/ es203945v.

El-Ghaffar M, Tieama HA (2017) A review of membranes classifications, configurations, surface modifications, characteristics and its applications in water purification. Chemical and Biomolecular Engineering 2(2):57–82.

Erbay Z, Icier F (2009) Optimization of hot air drying of olive leaves using response surface methodology. Journal of Food Engineering 91(4):533-541. DOI: 10.1016/j.jfoodeng.2008.10.004.

Esfahani MR, Aktij S.A, Dabaghian Z, Firouzjaei M.D, Rahimpour A, Eke J, Escobar I.C, Abolhassani M, Greenlee L.F, Esfahani A.R, Sadmani A, Koutahzadeh N (2019) Nanocomposite membranes for water separation and purification: Fabrication, modification, and applications. Separation and Purification Technology 213(September 2018):465–499, DOI: 10.1016/j. seppur.2018.12.050.

Fu S, Arráez-Roman D, Segura-Carretero A, et al. (2010) Qualitative screening of phenolic compounds in olive leaf extracts by hyphenated liquid chromatography and preliminary evaluation of cytotoxic activity against human breast cancer cells. Anal Bioanal Chem 397(2):643-654. DOI: 10.1007/s00216-010-3604-0.

García-Gómez A (2003) Composting of the solid fraction of olive mill wastewater with olive leaves: organic matter degradation and biological activity. Bioresource Technology 86(1):59-64. DOI: 10.1016/S0960-8524(02)00106-2.

Garcia-Ivars J, Alcaina-Miranda M.I, Iborra-Clar M.I, Mendoza-Roca J.A, Pastor-Alcañiz L (2014) Enhancement in hydrophilicity of different polymer phase-inversion ultrafiltration membranes by introducing PEG/Al2O3 nanoparticles. Separation and Purification Technology 128:45–57, DOI 10.1016/j.seppur.2014.03.012.

Garcia-Salas P, Morales-Soto A, Segura-Carretero A, Fernández-Gutiérrez A (2010) Phenolic-Compound-Extraction Systems for Fruit and Vegetable Samples. Molecules 15(12):8813-8826. DOI: 10.3390/molecules15128813.

Gilani AH, Khan A ullah (2010) Medicinal Value of Combination of Cholinergic and Calcium Antagonist Constituents in Olives. In: Olives and Olive Oil in Health and Disease Prevention. Elsevier: 835-843. DOI: 10.1016/B978-0-12-374420-3.00089-9.

Gohari B, Abu-Zahra N (2018) Polyethersulfone Membranes Prepared with 3-Aminopropyltriethoxysilane Modified Alumina Nanoparticles for Cu(II) Removal from Water. ACS Omega 3(8):10154–10162, DOI 10.1021/acsomega.8b01024.

Golemme G, Santaniello A (2019) Perfluoropolymer/Molecular Sieve Mixed-Matrix Membranes. Membranes 9(2):19, DOI 10.3390/membranes9020019.

Gómez-Caravaca A.M, Verardo V, Bendini A, Gallina-Toschi T (2014) From wastes to added value by-products: an overview on chemical composition and healthy properties of bioactive compounds of olive oil chain by-products. In A. De Leonardis (Ed.), Virgin olive oil (pp. 301–335). New York: Nova Publishers.

Goulas V, Papoti V.T, Exarchou V, Tsimidou M.Z, Gerothanassis I.P (2010) Contribution of Flavonoids to the Overall Radical Scavenging Activity of Olive (Olea europaea L.) Leaf Polar Extracts. J Agric Food Chem 58(6):3303-3308. DOI: 10.1021/jf903823x.

Goulas V, Papoti V.T, Exarchou V, Tsimidou M.Z, Gerothanassis I.P (2010) Contribution of Flavonoids to the Overall Radical Scavenging Activity of Olive (Olea europaea L.) Leaf Polar Extracts. J Agric Food Chem 58(6):3303-3308. DOI: 10.1021/jf903823x.

Guo J, Kim J (2017) Modifications of polyethersulfone membrane by doping sulfated-TiO2 nanoparticles for improving anti-fouling property in wastewater treatment. RSC Advances 7(54):33822–33828, DOI 10.1039/c7ra06406c.

Hamdi H.K, Castellon R (2005) Oleuropein, a non-toxic olive iridoid, is an anti-tumor agent and cytoskeleton disruptor. Biochemical and Biophysical Research Communications 334(3):769-778. DOI: 10.1016/j.bbrc.2005.06.161.

Harborne, J. B, Simmonds, N. W. (1964) Biochemistry of Phenolic Compounds, Academic Press, London, pp. 101.

Hassen I, Casabianca H, Hosni K (2015) Biological activities of the natural antioxidant oleuropein: Exceeding the expectation – A mini-review. Journal of Functional Foods 18:926-940. DOI: 10.1016/j.jff.2014.09.001.

Hayes JE, Allen P, Brunton N, O'Grady MN, Kerry JP (2011) Phenolic composition and in vitro antioxidant capacity of four commercial phytochemical products: Olive leaf extract (Olea europaea L.), lutein, sesamol and ellagic acid. Food Chemistry 126(3):948-955. DOI: 10.1016/j.foodchem.2010.11.092.

Heimler D, Pieroni A, Tattini M, Cimato A (1992) Determination of flavonoids, flavonoid glycosides and biflavonoids in Olea europaea L. Leaves. Chromatographia 33(7-8):369-373. DOI: 10.1007/BF02275920.

Herrero M, Temirzoda TN, Segura-Carretero A, Quirantes R, Plaza M, Ibañez E (2011) New possibilities for the valorization of olive oil by-products. Journal of Chromatography A 1218(42):7511-7520. DOI: 10.1016/j.chroma.2011.04.053.

Jamshidi Gohari R, Halakoo E, Lau W.J, Kassim M.A, Matsuura T, Ismail A.F (2014) Novel polyethersulfone (PES)/hydrous manganese dioxide (HMO) mixed matrix membranes with improved anti-fouling properties for oily wastewater treatment process. RSC Advances 4(34):17587–17596, DOI 10.1039/c4ra00032c.

Japón-Luján R, Luque De Castro M.D (2006) Superheated liquid extraction of oleuropein and related biophenols from olive leaves. Journal of Chromatography A 1136(2):185- 191. DOI: 10.1016/j.chroma.2006.09.081.

Japón-Luján R, Luque De Castro M.D (2008) Liquid–Liquid Extraction for the Enrichment of Edible Oils with Phenols from Olive Leaf Extracts. J Agric Food Chem 56(7):2505-2511. DOI: 10.1021/jf0728810.

Japón-Luján R, Luque-Rodríguez JM, Luque De Castro MD (2006a) Dynamic ultrasound-assisted extraction of oleuropein and related biophenols from olive leaves. Journal of Chromatography A 1108(1):76-82. DOI: 10.1016/j.chroma.2005.12.106.

Japón-Luján R, Ruiz-Jiménez J, Luque De Castro MD (2006b) Discrimination and Classification of Olive Tree Varieties and Cultivation Zones by Biophenol Contents. J Agric Food Chem 54(26):9706-9712. DOI: 10.1021/jf062546w.

Jemai H, Bouaziz M, Fki I, El Feki A, Sayadi S (2008) Hypolipidimic and antioxidant activities of oleuropein and its hydrolysis derivative-rich extracts from Chemlali olive leaves. Chemico-Biological Interactions 176(2-3):88-98. DOI: 10.1016/j.cbi.2008.08.014.

Jhaveri J.H, Murthy Z (2016) A comprehensive review on anti-fouling nanocomposite membranes for pressure driven membrane separation processes. Desalination 379:137–15.

Karioti A, Chatzopoulou A, Bilia AR, Liakopoulos G, Stavrianakou S, Skaltsa H (2006) Novel Secoiridoid Glucosides in Olea europaea Leaves Suffering from Boron

Deficiency. Bioscience, Biotechnology, and Biochemistry 70(8):1898-1903. DOI: 10.1271/bbb.60059.

Kashaninejad M, Sanz M.T, Blanco B, Beltrán S, Mehdi Niknam S (2020) Freeze dried extract from olive leaves: Valorisation, extraction kinetics and extract characterization. Food and Bioproducts Processing 124:196-207. DOI:10.1016/j.fbp.2020.08.015.

Kevlich N.S, Shofner M.L, Nair S (2017) Membranes for kraft black liquor concentration and chemical recovery: Current progress, challenges, and opportunities. Separation Science and Technology 52(6):1070–1094.

Kiritsakis K, Kontominas MG, Kontogiorgis C, Hadjipavlou-Litina D, Moustakas A, Kiritsakis A (2010) Composition and Antioxidant Activity of Olive Leaf Extracts from Greek Olive Cultivars. J Americ Oil Chem Soc 87(4):369-376. DOI: 10.1007/s11746-009-1517-x.

Kiritsakis K, Kontominas MG, Kontogiorgis C, Hadjipavlou-Litina D, Moustakas A, Kiritsakis A (2010) Composition and Antioxidant Activity of Olive Leaf Extracts from Greek Olive Cultivars. J Americ Oil Chem Soc 87(4):369-376. DOI: 10.1007/s11746-009-1517-x.

Kolah A.K, Lira C.T, Miller D.J (2013) Separation and Purification Technologies in Biorefineries. DOI 10.1002/9781118493441.

Krawczyk H (2013) Separation of Biomass Components by Membrane Filtration-Process Development for Hemicellulose Recovery. Lund University.

Laguerre M, López Giraldo LJ, Piombo G, et al. (2009) Characterization of Olive-Leaf Phenolics by ESI-MS and Evaluation of their Antioxidant Capacities by the CAT Assay. J Americ Oil Chem Soc 86(12):1215-1225. DOI: 10.1007/s11746-009-1452-x.

Lalas S, Athanasiadis V, Gortzi O, et al. (2011) Enrichment of table olives with polyphenols extracted from olive leaves. Food Chemistry 127(4):1521-1525. DOI: 10.1016/j.foodchem.2011.02.009.

Lalia B.S, Kochkodan V, Hashaikeh R, Hilal N (2013) A review on membrane fabrication: Structure, properties and performance relationship. Desalination 326:7.

Lama-Muñoz A, Contreras MDM, Espínola F, Moya M, Romero I, Castro E (2020) Content of phenolic compounds and mannitol in olive leaves extracts from six Spanish cultivars: Extraction with the Soxhlet method and pressurized liquids. Food Chemistry 320:126626. DOI: 10.1016/j.foodchem.2020.126626.

Lamuela-Raventós RM, Vallverdú-Queralt A, Jáuregui O, Martínez-Huélamo M, Quifer-Rada P (2014) Improved Characterization of Polyphenols Using Liquid Chromatography. In: Polyphenols in Plants. Elsevier: 261-292. DOI: 10.1016/B978-0- 12-397934-6.00014-0.

Le Floch F, Tena MT, Ríos A, Valcárcel M (1998) Supercritical fluid extraction of phenol compounds from olive leaves. Talanta 46(5):1123-1130. DOI: 10.1016/S0039-9140(97)00375-5.

Lee O-H, Lee B-Y, Lee J, et al. (2009) Assessment of phenolics-enriched extract and fractions of olive leaves and their antioxidant activities. Bioresource Technology 100(23):6107-6113. DOI: 10.1016/j.biortech.2009.06.059.

Leong S, Razmjou A, Wang K, Hapgood K, Zhang X, Wang H (2014) TiO2 based photocatalytic membranes: A review. Journal of Membrane Science 472:167–184.DOI: 10.1016/j. memsci.2014.08.016.

Lewis J, Al-sayaghi M.A, Buelke C, Alshami A (2021) Activated carbon in mixed-matrix membranes. Separation and Purification Reviews 50(1):1–31, DOI 10.1080/15422119.2019. 1609986.

Li H, Deng Y, Liu B, Ren Y, Liang J, Qian Y, Qiu X, Li C, Zheng D (2016a) Preparation of Nanocapsules via the Self-Assembly of Kraft Lignin: A Totally Green Process with Renewable Resources. ACS Sustainable Chemistry and Engineering 4(4):1946–1953, DOI 10.1021/acssuschemeng.5b01066.

Li H, Deng Y, Liu B, Ren Y, Liang J, Qian Y, Qiu X, Li C, Zheng D (2016b) Preparation of nanocapsules via the self-assembly of kraft lignin: A totally green process with renewable resources. ACS Sustainable Chemistry & Engineering 4(4):1946–1953.

Liakopoulos G, Karabourniotis G (2005) Boron deficiency and concentrations and composition of phenolic compounds in Olea europaea leaves: a combined growth chamber and field study. Tree Physiology 25(3):307-315. DOI: 10.1093/treephys/25.3.307.

Macheix J.-J, Fleuriet A, Sarni-Manchado P (2003). Composés phénoliques dans la plante - Structure, biosynthèse, répartition et rôles. Dans Les polyphénols en agroalimentaire; Sarni-Manchado P. et Cheynier V., Eds.; Lavoisier: Paris; pp 1-28.

Malik N.S.A, Bradford J.M (2006) Changes in oleuropein levels during differentiation and development of floral buds in 'Arbequina' olives. Scientia Horticulturae 110(3):274- 278. DOI: 10.1016/j.scienta.2006.07.016.

Malik N.S.A, Bradford J.M. (2006) Changes in oleuropein levels during differentiation and development of floral buds in 'arbequina' olives. Scientia Horticulturae 110(3) 274– 278. DOI:10.1016/j.scienta.2006.07.016.

Malik N.S.A, Bradford, J.M. (2008) Recovery and stability of oleuropein and other phenolic compounds during extraction and processing of olive (Olea europaea L.) leaves. Journal of Food, Agriculture and Environment 6(2):8–13.

Mannina L, Segre A.L (2010) Chapter 14 - NMR and Olive Oils: A Geographical Characterization V.R. Preedy, R.R. Watson (Eds.), Olives and Olive Oil in Health and Disease Prevention, Academic Press, San Diego (2010) pp. 117-124.

Martín García I, Yáñez Ruiz D, Moumen A, Molina Alcaide E (2006) Effect of polyethylene glycol, urea and sunflower meal on olive (Olea europaea var. europaea) leaf fermentation in continuous fermentors. Small Ruminant Research 61(1):53-61. DOI: 10.1016/j.smallrumres.2005.01.005.

Martin S, Andriantsitohaina R (2002) Mécanismes de la protection cardiaque et vasculaire des polyphénols au niveau de l'endothélium. Annales de Cardiologie et d'Angéiologie 51(6):304-315. DOI: 10.1016/S0003-3928(02)00138-5.

Meirinhos J, Silva BM, ValentÃo P, et al. (2005) Analysis and quantification of flavonoidic compounds from Portuguese olive (Olea Europaea L.) leaf cultivars. Natural Product Research 19(2):189-195. DOI: 10.1080/14786410410001704886.

Mert C, Barut E, Ipek A (2013) Quantitative seasonal changes in the leaf phenolic content related to the alternate-bearing patterns of olive (Olea europaea L. cv. Gemlik). Journal of Agricultural Science and Technology 15:995–1006.

Moghimifar V, Raisi A, Aroujalian A (2014) Surface modification of polyethersulfone ultrafiltration membranes by corona plasma-assisted coating TiO2 nanoparticles. Journal of Membrane Science 461:69–80, DOI 10.1016/j.memsci.2014.02.01.

Mohammad A.W, Teow Y, Ang W, Chung Y, Oatley-Radcliffe D, Hilal N (2015) Nanofiltration membranes review: Recent advances and future prospects. Desalination 356:226–254.

Mollahosseini A, Rahimpour A, Jahamshahi M, Peyravi M, Khavarpour M (2012) The effect of silver nanoparticle size on performance and antibacteriality of polysulfone ultrafiltration membrane. Desalination 306:41–50, DOI 10.1016/j.desal.2012.08.035.

Montenegro-Landívar MF, Tapia-Quirós P, Vecino X, et al. (2021) Polyphenols and their potential role to fight viral diseases: An overview. Science of The Total Environment 801:149719. DOI: 10.1016/j.scitotenv.2021.149719.

Mylonaki S, Kiassos E, Makris DP, Kefalas P (2008) Optimisation of the extraction of olive (Olea europaea) leaf phenolics using water/ethanol-based solvent systems and response surface methodology. Anal Bioanal Chem 392(5):977-985. DOI: 10.1007/s00216-008-2353-9.

Mylonaki S, Kiassos E, Makris DP, Kefalas P (2008) Optimisation of the extraction of olive (Olea europaea) leaf phenolics using water/ethanol-based solvent systems and response surface methodology. Anal Bioanal Chem 392(5):977-985. DOI: 10.1007/s00216-008-2353-9.

Omar SH (2010) Cardioprotective and neuroprotective roles of oleuropein in olive. Saudi Pharmaceutical Journal 18(3):111-121. DOI: 10.1016/j.jsps.2010.05.005.

Ortega-García F, Blanco S, Peinado MÁ, Peragón J (2009) Phenylalanine ammonia-lyase and phenolic compounds in leaves and fruits of Olea europaea L. cv. Picual during ripening. J Sci Food Agric 89(3):398-406. DOI: 10.1002/jsfa.3458.

Ortega-García F, Peragón J (2010) Phenol Metabolism in the Leaves of the Olive Tree (Olea europaea L.) cv. Picual, Verdial, Arbequina, and Frantoio during Ripening. J Agric Food Chem 58(23):12440-12448. DOI: 10.1021/jf102827m.

Othman N.H, Alias N.H, Fuzil N.S, Marpani F, Shahruddin M.Z, Chew C.M, David Ng K.M, Lau W.J, Ismail A.F (2021) A review on the use of membrane technology systems in developing countries. Membranes 12(1):30.

Paiva-Martins F, Correia R, Félix S, Ferreira P, Gordon MH (2007) Effects of Enrichment of Refined Olive Oil with Phenolic Compounds from Olive Leaves. J Agric Food Chem 55(10):4139-4143. DOI: 10.1021/jf063093y.

Paiva-Martins F, Pinto M (2008) Isolation and Characterization of a New Hydroxytyrosol Derivative from Olive (Olea europaea) Leaves. J Agric Food Chem 56(14):5582-5588. DOI: 10.1021/jf800698y.

Papoti VT, Tsimidou MZ (2009) Impact of Sampling Parameters on the Radical Scavenging Potential of Olive (Olea europaea L.) Leaves. J Agric Food Chem 57(9):3470-3477. DOI: 10.1021/jf900171d.

Pasković I, Lukić I, Žurga P, et al. (2020)Temporal variation of phenolic and mineral composition in olive leaves is cultivar dependent Plants 9 :1099. DOI: 10.3390/plants9091099.

Pendergast M.M, Hoek E.M (2011) A review of water treatment membrane nanotechnologies. Energy & Environmental Science 4(6):1946–1971.

Pereira A, Ferreira I, Marcelino F, et al. (2007) Phenolic Compounds and Antimicrobial Activity of Olive (Olea europaea L. Cv. Cobrançosa) Leaves. Molecules 12(5):1153-1162. DOI: 10.3390/12051153.

Pérez-Trujillo M, Gómez-Caravaca AM, Segura-Carretero A, Fernández-Gutiérrez A, Parella T (2010) Separation and Identification of Phenolic Compounds of Extra Virgin Olive Oil from Olea europaea L. by HPLC-DAD-SPE-NMR/MS. Identification of a New Diastereoisomer of the Aldehydic Form of Oleuropein Aglycone. J Agric Food Chem 58(16):9129-9136. DOI: 10.1021/jf101847e.

Polzonetti V, Egidi D, Vita A, Vincenzetti S, Natalini P. (2004) Involvement of oleuropein in (some) digestive metabolic pathways. Food Chemistry 88(1):11-15. DOI: 10.1016/j.foodchem.2004.01.029.

Qadir D, Mukhtar H, Keong LK (2017) Mixed Matrix Membranes for Water Purification Applications. Separation and Purification Reviews 46(1):62–80, DOI 10.1080/15422119.2016. 1196460.

Quirantes-Piné R, Lozano-Sánchez J, Herrero M, Ibáñez E, Segura-Carretero A, Fernández-Gutiérrez A. (2012) HPLC–ESI–QTOF–MS as a Powerful Analytical Tool for Characterising Phenolic Compounds in Olive-leaf Extracts. Phytochemical Analysis 24(3):213-223. DOI: 10.1002/pca.2401.

Quirantes-Piné R, Zurek G, Barrajón-Catalán E, et al. (2013) A metabolite-profiling approach to assess the uptake and metabolism of phenolic compounds from olive leaves in SKBR3 cells by HPLC–ESI-QTOF-MS. Journal of Pharmaceutical and Biomedical Analysis 72:121-126. DOI: 10.1016/j.jpba.2012.09.029.

Rahimpour A, Madaeni SS, Taheri AH, Mansourpanah Y (2008) Coupling TiO2 nanoparticles with UV irradiation for modification of polyethersulfone ultrafiltration membranes. Journal of Membrane Science 313(1-2):158–169, DOI 10.1016/j.memsci.2007.12.075

Rahmanian N, Jafari SM, Wani TA. (2015) Bioactive profile, dehydration, extraction and application of the bioactive components of olive leaves. Trends in Food Science & Technology 42(2):150-172. DOI: 10.1016/j.tifs.2014.12.009.

Ranalli A, Contento S, Lucera L, Di Febo M, Marchegiani D, Di Fonzo V. (2006) Factors Affecting the Contents of Iridoid Oleuropein in Olive Leaves (Olea europaea L.). J Agric Food Chem 54(2):434-440. DOI: 10.1021/jf051647b.

Rashidi NA, Yusup S (2017) A review on recent technological advancement in the activated carbon production from oil palm wastes. Chemical Engineering Journal 314:277– 290, DOI 10.1016/j.cej.2016.11.059.

Ray NB, Lam NT, Luc R, Bonvino NP, Karagiannis TC. (2015) Cellular and Molecular Effects of Bioactive Phenolic Compounds in Olives and Olive Oil. In: Olive and Olive Oil Bioactive Constituents. Elsevier: 53-91. DOI: 10.1016/B978-1-63067-041-2.50009-4.

Rezakazemi M, Dashti A, Riasat Harami H, Hajilari N, Inamuddin (2018) Fouling-resistant membranes for water reuse, vol 16. Springer International Publishing. DOI: 10.1007/s10311-018-0717-8.

Robards K, Prenzler PD, Tucker G, Swatsitang P, Glover W. (1999) Phenolic compounds and their role in oxidative processes in fruits. Food Chemistry 66(4):401-436. DOI: 10.1016/S0308-8146(99)00093-X.

Romero-García JM, Niño L, Martínez-Patiño C, Álvarez C, Castro E, Negro MJ. (2014) Biorefinery based on olive biomass. State of the art and future trends. Bioresource Technology 159:421-432. DOI: 10.1016/j.biortech.2014.03.062.

Romero-García JM, Niño L, Martínez-Patiño C, Álvarez C, Castro E, Negro MJ. (2014) Biorefinery based on olive biomass. State of the art and future trends. Bioresource Technology 159:421-432. DOI: 10.1016/j.biortech.2014.03.062.

Safarpour M, Vatanpour V, Khataee A (2016) Preparation and characterization of graphene oxide/TiO2 blended PES nanofiltration membrane with improved antifouling and separation performance. Desalination 393:65–78, DOI 10.1016/j.desal.2015.07.003.

Saitta M , Di Bella G , Turco V.L, La Torre G.L, Dugo G (2010) Low-level free phenols in Sicilian olive oils. In V.R. Preedy, & R.R. Watson (Eds.), Olives and olive oil in health and disease prevention (pp. 187–200). Elsevier Inc.DOI:10.1016/B978-0-12-374420-3.00021-8.

Santhosh R, Nath D, Sarkar P. (2021) Novel food packaging materials including plant- based byproducts: A review. Trends in Food Science & Technology 118:471-489. DOI: 10.1016/j.tifs.2021.10.013.

Savournin C, Baghdikian B, Elias R, Dargouth-Kesraoui F, Boukef K, Balansard G. (2001) Rapid High-Performance Liquid Chromatography Analysis for the Quantitative Determination of Oleuropein in Olea europaea Leaves. J Agric Food Chem 49(2):618-621. DOI: 10.1021/jf000596+.

Scognamiglio M, D'Abrosca B, Pacifico S, et al. (2012) Polyphenol characterization and antioxidant evaluation of Olea europaea varieties cultivated in Cilento National Park (Italy). Food Research International 46(1):294-303. DOI: 10.1016/j.foodres.2011.

Silva S, Gomes L, Leitao F, Coelho a. V , Boas L. V (2006) Phenolic compounds and antioxidant activity of Olea europaea L. fruits and leaves. Food Science and Technology International 12(5):385–396. DOI: 10.1177/1082013206070166.

Souilem S, Fki I, Kobayashi I, Khalid N, Neves M.A, Isoda H, Sayadi S, Nakajima M (2017)Emerging technologies for recovery of value-added components from oliveleaves and their applications in food/feed industries. Food bioprocess Technol 10:229- 248. DOI 10.1007/s11947-016-1834-7.

Taamalli A, Arráez-Román D, Barrajón-Catalán E, Ruiz-Torres V, Pérez-Sánchez A, Herrero M, Ibañez E, Micol V, Zarrouk M , Antonio Segura-Carretero A, Fernández-Gutiérrez A (2012a) Use of advanced techniques for the extraction of phenolic compounds from Tunisian olive leaves: phenolic composition and cytotoxicity against human breast cancer cells. Food and Chemical Toxicology 50(6):1817–1825.DOI:10.1016/j.fct.2012.02.090.

Taamalli A, Arráez-Román D, Ibañez E, Zarrouk M, Segura-Carretero A, Fernández-Gutiérrez A (2012b) Optimization of Microwave-Assisted Extraction for the Characterization of Olive Leaf Phenolic Compounds by Using HPLC-ESI-TOF-MS/IT-MS². J Agric Food Chem 60(3):791-798. DOI: 10.1021/jf204233u.

Taamalli A, Gómez-Caravaca AM, Zarrouk M, Segura-Carretero A, Fernández-Gutiérrez A (2010) Determination of apolar and minor polar compounds and other chemical parameters for the discrimination of six different varieties of Tunisian extra-virgin olive oil cultivated in their traditional growing area. Eur Food Res Technol 231(6):965-975. DOI: 10.1007/s00217-010-1350-3.

Talhaoui N, Gómez-Caravaca AM, León L, De La Rosa R, Segura-Carretero A, Fernández-Gutiérrez A (2014) Determination of phenolic compounds of 'Sikitita' olive leaves by HPLC-DAD-TOF-MS. Comparison with its parents 'Arbequina' and 'Picual' olive leaves. LWT - Food Science and Technology 58(1):28-34. DOI: 10.1016/j.lwt.2014.03.014.

Talhaoui N, Gómez-Caravaca AM, Roldán C, et al. (2015b) Chemometric Analysis for the Evaluation of Phenolic Patterns in Olive Leaves from Six Cultivars at Different Growth Stages. J Agric Food Chem 63(6):1722-1729. DOI: 10.1021/jf5058205.

Talhaoui N, Taamalli A, Gómez-Caravaca AM, Fernández-Gutiérrez A, Segura-Carretero A (2015a) Phenolic compounds in olive leaves: Analytical determination, biotic and abiotic influence, and health benefits. Food Research International 77:92-108. DOI: 10.1016/j.foodres.2015.09.011.

Tayoub G, Sulaiman H, Hassan A.H, Alorfi M (2012) Determination of oleuropein in leaves and fruits of some Syrian olive varieties. International Journal of Medicinal and Aromatic Plants 2: 428–433.

Tijink M, Kooman J, Wester M, Sun J, Saiful S, Joles J, Borneman Z, Wessling M, Stamatialis D (2014) Mixed Matrix Membranes: A New Asset for Blood Purification Therapies. Blood Purification 37(1):1–3, DOI 10.1159/000356226.

Van der Bruggen B, Vandecasteele C, Van Gestel T, Doyen W, Leysen R (2003) A review of pressure-driven membrane processes in wastewater treatment and drinking water production. Environmental progress 22(1):46–56.

Vidal-Casanella O, Núñez O, Granados M, Saurina J, Sentellas S. (2021) Analytical Methods for Exploring Nutraceuticals Based on Phenolic Acids and Polyphenols. Applied Sciences 11(18):8276. DOI: 10.3390/app11188276.

Visioli F, Bellosta S, Galli C (1998) Oleuropein, the bitter principle of olives, enhances nitric oxide production by mouse macrophages. Life Sci 62:541–546.

Vuolo MM, Lima VS, Maróstica Junior MR. (2019) Phenolic Compounds. In: Bioactive Compounds. Elsevier: 33-50. DOI: 10.1016/B978-0-12-814774-0.00002-5.

Warsinger D.M, Chakraborty S, Tow E.W, Plumlee M.H, Bellona C, Loutatidou S, Karimi L, Mikelonis A.M, Achilli A, Ghassemi A, et al. (2018) A review of polymeric membranes and processes for potable water reuse. Progress in polymer science 81:209–237.

Yahfoufi N, Alsadi N, Jambi M, Matar C. (2018) The Immunomodulatory and Anti-Inflammatory Role of Polyphenols. Nutrients 10(11):1618. DOI: 10.3390/nu10111618.

Yang D, Li J, Jiang Z, Lu L, Chen X (2009) Chitosan/TiO2 nanocomposite pervaporation membranes for ethanol dehydration. Chemical Engineering Science 64(13):3130–3137, DOI 10.1016/j.ces.2009.03.042.

Ye J, Wijesundera C, Shi M (2014) Effects of agronomic and oil processing conditions on natural antioxidative phenolics in olive (Olea europaea L.). Austin Journal of Nutrition and Food Sciences 2:1–8.

Yu H, Zhang X, Zhang Y, Liu J, Zhang H (2013) Development of a hydrophilic PES ultrafiltration membrane containing SiO2@N-Halamine nanoparticles with bothorganic antifouling and antibacterial properties. Desalination 326:69–76, DOI 10.1016/j.desal.2013.07.018.

Zhang Y, Cai P, Cheng G, Zhang Y. (2022) A Brief Review of Phenolic Compounds Identified from Plants: Their Extraction, Analysis, and Biological Activity. Natural Product Communications 17(1):1934578X2110697. DOI: 10.1177/1934578X211069721.

Zhang Y.J, Gan R.Y, Li S, Zhou Y, Li A.N, Xu D.P, Bin Li H, Kitts D.D (2015)Antioxidant phytochemicals for the prevention and treatment of chronic diseases,Molecules 20: 21138e21156. DOI: 10.3390/ molecules201219753.

Zhao W, Huang J, Fang B, Nie S, Yi N, Su B, Li H, Zhao C (2011) Modification of polyethersulfone membrane by blending semi-interpenetrating network polymeric nanoparticles. Journal of Membrane Science 369(1-2):258–266.

Zhu Y, Yu X, Zhang T, Hua W, Wang X (2019) Nanofibrous composite hemodiafiltration membrane: A facile approach towards tuning the barrier layer for enhanced performance. Applied Surface Science 465(September 2018):950–963, DOI 10.1016/j.apsusc.2018.09.201.

Zinadini S, Zinatizadeh A.A, Rahimi M, Vatanpour V, Zangeneh H (2014) Preparation of a novel antifouling mixed matrix PES membrane by embedding graphene oxide nanoplates. Journal of Membrane Science 453:292–301, DOI 10.1016/j.memsci.2013.10.070.

Zipori I, Erel R, Yermiyahu U, Ben-Gal A, Dag A. (2020) Sustainable Management of Olive Orchard Nutrition.

CHAPTER 3

Ben Salah M, Abdelmelek H, Abderraba M 2012 Study of phenolic composition and biological activities assessment of olive leaves from different varieties grown in Tunisia. Med. Chem 2:107–111.DOI:10.4172/2161-0444.1000124.

Bilgin M, Şahin S 2013 Effects of geographical origin and extraction methods on total phenolic yield of olive tree (Olea europaea) leaves. J. Taiwan Inst. Chem. Eng. 44:8–12.DOI:10.1016/j.jtice.2012.08.008.

Di Donna L, Mazzotti F, Naccarato A, Salerno R, Tagarelli A, Taverna D 2010 Secondary metabolites of Olea europaea leaves as markers for the discrimination of cultivars and cultivation zones by multivariate analysis. Food Chem. 121:492–496. DOI: 10.3390/agronomy12092007.

El NS, Karakaya S 2009 Olive tree (Olea europaea) leaves: potential beneficial effects on human health. Nutr Rev 67(11):632–8. DOI: 10.1111/j.1753-4887.2009.00248.x.

Fabbri A, Galaverna G, Ganino T 2008 Polyphenol composition of olive leaves with regard to cultivar, time of collection and shoot type. Acta Hortic 791:459–464. DOI:10.17660/ActaHortic.2008.791.69

Felhi S, Hajlaoui H, Ncir M, Bakari S, Ktari N, Saoudi M, Gharsallah N, Kadri A 2016 Nutritional, phytochemical and antioxidant evaluation and FT-IR analysis of freeze dried extracts of Ecballium elaterium fruit juice from three localities. Food Sci. Tech. 36:646–655.DOI:10.1590/1678-457X.12916.

Japón-Luján R, Ruiz-Jiménez J, Luque De Castro MD 2006 Discrimination and classification of olive tree varieties and cultivation zones by biophenol contents. J Agric Food Chem 54(26):9706–12.DOI: 10.1021/jf062546w.

Kallithraka S, Mohdaly AAA, Makris DP, Kefalas P 2004 Determination of major anthocyanin pigments in Hellenic native grape varieties (Vitis vinifera sp.). J. Food Compos. Anal 18:375–386. DOI:10.1016/j.jfca.2004.02.010.

Lorini A, Aranha BC, da Antunes BF, Otero DM, Jacques AC, Zambiazi RC 2021Metabolic Profile of Olive Leaves of Different Cultivars and Collection Times. Food Chem 345:128758. DOI:10.1016/j.foodchem.2020.128758.

Markakis E.A, Tjamos S.E, Antoniou P.P, Roussos P.A, Paplomatas E.J, Tjamos E.C 2010 Phenolic responses of resistant and susceptible olive cultivars induced by defoliating and non defoliatingVerticilliumdahliaepathotypes. Am. Phytopathol. Soc. 94:1156 1162. DOI: 10.1094/PDIS-94-9-1156.

Mohamed M.B, Guasmi F, Ali S.B, Radhouani F, Faghim J, Triki T, Kammoun N.C, Baffi C, Lucini L, Benincasa C 2018 The LC-MS/MS characterization of phenolic compounds in leaves allows classifying olive cultivars grown in SouthTunisia. Biochem. Syst. Ecol 78:84–90. DOI:10.1016/j.bse.2018.04.005.

Papoti VT, Tsimidou MZ (2009) Impact of sampling parameters on the radical scavenging potential of olive (Olea europaea L.) leaves. J Agric Food Chem 57 (9):3470–7.DOI: 10.1021/jf900171d.

Petridis A, Therios I, Samouris G 2012 Genotypic variation of total phenol and oleuropein concentration and antioxidant activity of 11 Greek olive cultivars (Olea europaea L.). Hortscience 47 (3):339–342.DOI:10.21273/HORTSCI.47.3.339.

Quirantes-Piné R, Lozano-Sánchez J, Herrero M, Ibáñez E, Segura-Carretero A, Fernández-Gutiérrez A 2012 HPLC–ESI–QTOF–MS as a powerful analytical tool for characterising phenolic compounds in olive-leaf extracts. Phytochem. Anal. 24 (3):213–223. DOI: 10.1002/pca.2401

Szydłowska-Czerniak A, Łaszewska A 2015 Effect of refining process on antioxidant capacity, total phenolics and prooxidants contents in rapeseed oils, LWT - Food Sci Technol 64:853–859. DOI:10.1016/j.lwt.2015.06.069.

Talhaoui N, Gómez-Caravaca A.M, Roldán C, León L, De la Rosa R, Fernández-Gutiérrez A, Segura-Carretero A 2015 Chemometric analysis for the evaluation of phenolic patterns in olive leaves from six cultivars at different growth stages. J. Agric. Food Chem. 63:1722–1729.DOI: 10.1021/jf5058205.

Veličković DT, Milenović DM, Ristic′ MS, Veljkovic′ VB 2008 Ultrasonic extraction of waste solid residues from the Salvia sp. essential oil hydrodistillation. Biochem Eng J 42(1)97–104. DOI:10.1016/j.bej.2008.06.003.

Vinha AF, Ferreres F, Silva BM, Valentão P, Gonc¸alves A, Pereira JA, Oliveira MB, Seabra RM, Andrade PB 2005 Phenolic profiles of Portuguese olive fruits (Oleaeuropaea L.): influences of cultivar and geographical origin. Food Chem 89(4):561–8.DOI:10.1016/j.foodchem.2004.03.012.

Zakraoui M, Hannachi H, Pasković I,Vidović N ,Pasković MP,Palčić I,Major N,Ban SG, Hamrouni L 2023 Effect of Geographical Location on the Phenolic and Mineral Composition of Chetoui Olive Leaves. Foods 12:2565. DOI: 10.3390/foods12132565.

CHAPTER 4

Ahmad-Qasem M.H, Canovas J, Barrajon-Catalan E, Micol V, Carcel J.A, Garcia-Perez J.V (2013) Kinetic and compositional study of phenolic extraction from olive leaves (var. Serrana) by using power ultrasound. Innovative Food Science & Emerging Technologies 17:120–129. DOI: 10.1016/j.ifset.2012.11.008.

Al-Azzawie H.F, Alhamdani M.S (2006) Hypoglycemic and antioxidant effect of oleuropein in alloxan-diabetic rabbits. Life Sciences 78(12):1371–1377.

Alonso-Riano P, Sanz Diez M.T, Blanco B, Beltran S, Trigueros E, Benito-Roman O (2020) Water ultrasound-assisted extraction of polyphenol compounds from brewer's spent grain: Kinetic study, extract characterization, and concentration. Antioxidants 9:265. DOI: 10.3390/antiox9030265.

Altiok E, Bayçin D, Bayraktar O, Ülkü S (2008) Isolation of polyphenols from the extracts of olive leaves (Olea europaea L.) by adsorption on silk fibroin. Separation and Purification Technology 62(2):342–348. DOI: 10.1016/j.seppur.2008.01.022.

Alu'datt M.H, Alli I, Ereifej K, Alhamad M.N, Alsaad A, Rababeh T (2011) Optimization and characterisation of various extraction conditions of phenolic compounds and antioxidant activity in olive seeds. Natural Product Research 25(9):876–889.

Arend G.D, Adorno WT, Rezzadori K, Di Luccio M, Chaves V.C, Reginatto F.H, Petrus J.C.C (2017) Concentration of phenolic compounds from strawberry (Fragaria X ananassa Duch) juice by nanofiltration membrane. Journal of Food Engineering 201:36–41. DOI: 10.1016/j.jfoodeng.2017.01.014.

Arslan D, Schreiner M (2012) Chemical characteristics and antioxidant activity of olive oils from Turkish varieties grown in Hatay province. Scientia Horticulturae 144:141–152. DOI: 10.1016/j.scienta.2012.07.006.

Avram A.M, Morin P, Brownmiller C, Howard L.R, Sengupta A, Wickramasinghe R (2017) Concentrations of polyphenols from blueberry pomace extract using nanofiltration. Food and Bioproducts Processing 106:91–101. DOI: 10.1016/j.fbp.2017.07.006.

Babbar N, Oberoi H.S, Uppal D.S, Patil R.T (2011) Total phenolic content and antioxidant capacity of extracts obtained from six important fruit residues. Food Research International 44(2):391–396. DOI: 10.1016/j.foodres.2010.10.001.

Bashi D.S, Mortazavi S.A, Rezaei K, Rajaei A, Karimkhani M.M (2012) Optimization of ultrasound-assisted extraction of phenolic compounds from yarrow (Achillea beibrestinii) by response surface methodology. Food Science and Biotechnology 21(4):1005–1011. DOI: 10.1007/s10068-012-0131-0.

Bellona C, Drewes J.E, Xu P, Amy G (2004) Factors affecting the rejection of organic solutes during NF/RO treatment – a literature review. Water Research 38(12):2795– 2809. DOI: 10.1016/j.watres.2004.03.034.

Ben Othman N, Roblain D, Thonart P, Hamdi M (2008) Tunisian table olive phenolic compounds and their antioxidant capacity. Journal of Food Science 73:235–240. DOI: 10.1111/j.1750-3841.2008.00711.x.

Benedetti S, Prudêncio E.S, Nunes G.L, Guizoni K, Fogaça L.A, Petrus J.C.C.C (2015) Antioxidant properties of tofu whey concentrate by freeze concentration and nanofiltration processes. Journal of Food Engineering 160:49–55. DOI: 10.1016/j.jfoodeng.2015.03.021.

Bouallagui Z, Han J, Isoda H, Sayadi S (2011) Hydroxytyrosol rich extract from olive leaves modulates cell cycle progression in MCF-7 human breast cancer cells. Food and Chemical Toxicology 49:179–184.

Bouaziz M, Sayadi S (2005) Isolation and evaluation of antioxidants from leaves of a Tunisian cultivar olive tree. European Journal of Lipid Science and Technology 107:497–504. DOI: 10.1002/ejlt.200501166.

Bras T, Guerreiro O, Duarte M.F, Neves L.A (2015) Impact of extraction parameters and concentration by nanofiltration on the recovery of phenolic compounds from Cynara cardunculus var. altilis: Assessment of antioxidant activity. Industrial Crops and Products 67:137–142. DOI: 10.1016/j.indcrop.2015.01.005.

Carbone K, Amoriello T, Iadecola R (2020) Exploitation of kiwi juice pomace for the recovery of natural antioxidants through microwave-assisted extraction. Agriculture 10:435. DOI 10.3390/agriculture10100435.

Cassano A, Cabri W, Mombelli G, Peterlongo F, Giorno L (2016) Recovery of bioactive compounds from artichoke brines by nanofiltration. Food and Bioproducts Processing 98:257–265.

Cassano A, Conidi C, Giorno L, Drioli E (2013) Fractionation of olive mill wastewaters by membrane separation techniques. Journal of Hazardous Materials 248–249:185–193. DOI: 10.1016/j.jhazmat.2013.01.006.

Cifá D, Skrt M, Pittia P, Mattia C.D, Ulrih N.P (2018) Enhanced yield of oleuropein from olive leaves using ultrasound-assisted extraction. Food Science & Nutrition 6:1128– 1137. DOI: 10.1002/fsn3.654.

Cokgezme O.F, Icier F (2022) Frequency and wave type effects on extractability of oleuropein from olive leaves by moderate electric field assisted extraction. Innovative Food Science & Emerging Technologies 77:102985. DOI: 10.1016/j.ifset.2022.102985.

Conidi C, Cassano A (2015) Recovery of phenolic compounds from bergamot juice by nanofiltration membranes. Desalination and Water Treatment 56(14):3510–3518. DOI: 10.1080/19443994.2014.968219.

Conidi C, Cassano A, Caiazzo F, Drioli E (2017) Separation and purification of phenolic compounds from pomegranate juice by ultrafiltration and nanofiltration membranes. Journal of Food Engineering 195:1–13. DOI: 10.1016/j.jfoodeng.2016.09.017.

Conidi C, Cassano A, Drioli E (2012) Recovery of phenolic compounds from orange press liquor by nanofiltration. Food and Bioproducts Processing 90(4):867–874. DOI: 10.1016/j.fbp.2012.07.0050.

Conidi C, Fuca L, Drioli E, Cassano A (2019) A membrane-based process for the recovery of glycyrrhizin and phenolic compounds from licorice wastewaters. Molecules 24(12):2279. DOI: 10.3390/molecules24122279.

Costa A.S, Alves R.C, Vinha A.F, Barreira S.V, Nunes M.A, Cunha L.M, Oliveira M (2014) Optimization of antioxidants extraction from coffee silverskin a roasting by- product, having in view a sustainable process. Industrial Crops and Products 53:350– 357. DOI: 10.1016/j.indcrop.2014.01.006.

Da Rosa G.S, Martiny T.R, Dotto G.L, Vanga S.K, Parrine D, Gariepy Y, Lefsrud M, Raghavan V (2021) Eco-friendly extraction for the recovery of bioactive compounds from Brazilian olive leaves. Sustainable Materials and Technologies 28:e00276. DOI: 10.1016/j.susmat.2021.e00276.

Da Rosa G.S, Vanga S.K, Gariepy Y, Raghavan V (2019) Comparison of microwave, ultrasonic and conventional techniques for extraction of bioactive compounds from olive leaves (Olea europaea L.). Innovative Food Science & Emerging Technologies 58:102234.

Dahmoune F, Nayak B, Moussi K, Remini H, Madani K (2015) Optimization of microwave-assisted extraction of polyphenols from Myrtus communis L. leaves. Food Chemistry 166:585–595. DOI: 10.1016/j.foodchem.2014.06.066.

Dahmoune F, Spigno G, Moussi K, Remini H, Cherbal A, Madani K (2014) Pistacia lentiscus leaves as a source of phenolic compounds: microwave-assisted extractionoptimized and compared with ultrasound-assisted and conventional solvent extraction. Industrial Crops and Products 61:31–40. DOI: 10.1016/j.indcrop.2014.06.035.

Dairi S, Dahmoune F, Belbahi A, Remini H, Kadri N, Aoun O, Bouaoudia N, Madani K, Madani K (2021) Optimization of microwave extraction method of phenolic compounds from red onion using response surface methodology and inhibition of lipoprotein low-density oxidation. Journal of Applied Research on Medicinal and Aromatic Plants 22:100301.

Dammak I, Neves M.A, Nabetani H, Isoda H, Sayadi S, Nakajima M (2015) Transport properties of oleuropein through nanofiltration membranes. Food and Bioproducts Processing 94:342–353.

De Santana Magalhães F, De Souza Martins M, Sa V.L, Cardoso M, Hespanhol Miranda Reis (2019) Recovery of phenolic compounds from pequi (Caryocar brasiliense Camb.)

fruit extract by membrane filtrations: comparison of direct and sequential processes. Journal of Food Engineering 257:26–33. DOI: 10.1016/j.jfoodeng.2019.03.025.

Dekanski D, Ristic S, Radonjic N, Petronijevic N, Dekanski A, Mitrovic D (2011) Olive leaf extract modulates cold restraint stress-induced oxidative changes in rat liver. Journalof the Serbian Chemical Society 76(9):1207–1218.

Del Contreras M, Lama-Munoz A, Espínola F, Moya I, Romero I, Castro E (2020) Valorization of olive mill leaves through ultrasound-assisted extraction. Food Chemistry.

Difonzo G, Russo A, Trani A, Paradiso VM, Ranieri M, Pasqualone A, Summo C, Tamma G, Silletti R, Caponio F (2017) Green extracts from Coratina olive cultivar leaves: Antioxidant characterization and biological activity. Journal of Functional Foods 31:63–70. DOI: 10.1016/j.jff.2017.01.039.

Fratoddi I, Rapa M, Testa G, Venditti I, Scaramuzzo F.A, Vinci G (2018) Response surface methodology for the optimization of phenolic compounds extraction from extra virgin olive oil with functionalized gold nanoparticles. Microchemical Journal 138:430–437. DOI: 10.1016/j.microc.2018.01.043.

Goulas V, Papoti V.T, Exarchou V, Tsimidou M.Z, Gerothanassis I.P (2010) Contribution of flavonoids to the overall radical scavenging activity of olive (Olea europaea L.) leaf polar extracts. Journal of Agricultural and Food Chemistry 58(6):3303–3308. DOI: 10.1021/jf903823x.

Japon-Luján R, Luque de Castro M.D (2006) Superheated liquid extraction of oleuropein and related biophenols from olive leaves. Journal of Chromatography A 1136(2):185– 191.

Jaski J.M, Barao C.E, Liao L.M, da Silva Pinto V, Zanoelo E.F, Cardozo-Filho L (2019) β-Cyclodextrin complexation of extracts of olive leaves obtained by pressurized liquid extraction. Industrial Crops and Products 129:662–672. DOI: 10.1016/j.indcrop.2018.12.045.

Jemai H, El Feki A, Sayadi S (2009) Antidiabetic and antioxidant effects of hydroxytyrosol and oleuropein from olive leaves in alloxan-diabetic rats. Journal of Agricultural and Food Chemistry 57(19):8798–8804.

Kashaninejad M, Sanz MT, Blanco B, Beltrán S, Niknam SM (2020) Freeze dried extract from olive leaves: Valorisation, extraction kinetics and extract characterization. Food and Bioproducts Processing 124:196–207.

Khemakhem I, Dridi Gargouri O, Dhouib A, Ali Ayadi M, Bouaziz M (2017) Oleuropein rich extract from olive leaves by combining microfiltration, ultrafiltration and nanofiltration. Separation and Purification Technology 172:310–317. DOI: 10.1016/j.seppur.2016.08.003.

Khodadoust S, Nasiriani T, Zeraatpisheh F (2018) Preparation of a magnetic molecularly imprinted polymer for the selective adsorption of chlordiazepoxide and its determination by central composite design optimized HPLC. New Journal of Chemistry 42:14444–14452. DOI: 10.1039/c8nj02643b.

Kiai H, García-Payo M.C, Hafidi A, Khayet M (2014) Application of membrane distillation technology in the treatment of table olive wastewaters for phenolic compounds concentration and high quality water production. Chemical Engineering and Processing 86:153–161. DOI: 10.1016/j.cep.2014.09.007.

Kiritsakis K, Kontominas MG, Kontogiorgis C, Hadjipavlou-Litina D, Moustakas A, Kiritsakis A (2010) Composition and antioxidant activity of olive leaf extracts from Greek olive cultivars. Journal of the American Oil Chemists' Society 87(4):369–376. DOI: 10.1007/s11746-009-1517-x.

Lafka T.I, Lazou A.E, Sinanoglou V.J, Lazos E.S (2013) Phenolic extracts from wild olive leaves and their potential as edible oils antioxidants. Foods 2:18–31. DOI: 10.3390/foods2010018.

Lama-Munoz A, Contreras M.M, Espínola F, Moya M, de Torres A, Romero I, Castro E (2019a) Extraction of oleuropein and luteolin-7-O-glucoside from olive leaves: Optimization of technique and operating conditions. Food Chemistry 293:161–168. DOI: 10.1016/j.foodchem.2019.04.075.

Lama-Munoz A, Contreras M.M, Espínola F, Moya M, Romero I, Castro E (2020) Content of phenolic compounds and mannitol in olive leaves extracts from six Spanish cultivars: extraction with the Soxhlet method and pressurized liquids. Food Chemistry 320:126626. DOI: 10.1016/j.foodchem.2020.126626.

Lama-Munoz A, Contreras M.M, Espínola F, Moya M, Romero I, Castro E (2019b) Optimization of oleuropein and luteolin-7-o-glucoside extraction from olive leaves by ultrasound-assisted technology. Energies 12:2486. DOI: 10.3390/en12132486.

Lee O-H, Lee B-Y (2010) Antioxidant and antimicrobial activities of individual and combined phenolics in Olea europaea leaf extract. Bioresource Technology 101:3751–3754314:126218. DOI: 10.1016/j.biortech.2009.12.052.

Liu Y, Wei S, Liao M (2013) Optimization of ultrasonic extraction of phenolic compounds from Euryale ferox seed shells using response surface methodology. Industrial Crops and Products 49:837–843. DOI: 10.1016/j.indcrop.2013.07.023.

Ma S-C, He Z-D, Deng X-L, But P-H, Ooi V-C, Xu H-X, Lee S-S, Lee S-F (2001) In Vitro Evaluation of Secoiridoid Glucosides from the Fruits of Ligustrum lucidum as Antiviral Agents. Chemical and Pharmaceutical Bulletin 49(11):1471–1473.

Manorma, Ferreira I, Alves P, Gil M.H, Gando-Ferreira L.M (2021) Lignin separation from black liquor by mixed matrix polysulfone nanofiltration membrane filled withmultiwalled carbon nanotubes. Separation and Purification Technology 260:118231. DOI: 10.1016/j.seppur.2020.118231.

Martín-García B, Pimentel-Moral S, Gomez-Caravaca A.M, Arraez-Román D, Segura-Carretero A (2020) A Box-Behnken design for optimal green extraction of compounds from olive leaves that potentially activate the AMPK pathway. Applied Sciences 10:462. DOI: 10.3390/app10134620.

Martín-García B, Pimentel-Moral S, Gomez-Caravaca A.M, Arráez-Román D, Segura-Carretero A (2020) Box-Behnken experimental design for a green extraction method of phenolic compounds from olive leaves. Industrial Crops and Products 154:112741. DOI: 10.1016/j.indcrop.2020.112741.

Mello B.C, Petrus J.C.C, Hubinger M.D (2010) Concentration of flavonoids and phenolic compounds in aqueous and ethanolic propolis extracts through nanofiltration. Journal of Food Engineering 96:533–539. DOI: 10.1016/j.jfoodeng.2009.08.040.

Mulinacci N, Romani A, Galardi C, Pinelelli P, Giaccherini C, Vincieri FF (2001) Polyphenolic content in olive oil waste waters and related olive samples. Agricultural and Food Chemistry 49:3509–3514. DOI: 10.1021/jf000972q.

Murakami N.N, Amboni R.D.M.C, Prudˆencio E.S, Amante E.R, De Moraes Zanotta L, Maraschin M, Petrus J.C.C, Teofilo R.F (2011) Concentration of phenolic compounds in aqueous mate (Ilex paraguariensis A, St. Hil) extract through nanofiltration. LWT - Food Science and Technology 44:2211–2216.

Naleini N, Rahimi M, Heydari R (2015) Oleuropein extraction using microfluidic system. Chemical Engineering and Processing: Process Intensification 92:1–6. DOI: 10.1016/j.cep.2015.03.023.

Orak H.H, Karama M, Amarowicz R, Orak A, Penkacik K (2019) Genotype-related differences in the phenolic compound profile and antioxidant activity of extracts from olive (Olea europaea L.) Leaves. Molecules 24(6):1130. DOI: 10.3390/molecules24061130.

Park J, Min J.S, Chae U, Lee J.Y, Song K.S, Lee H.S, Lee H.J, Lee S.R, Lee D.S (2017) Anti-inflammatory effect of oleuropein on microglia through regulation of Drp1-dependent mitochondrial fission. Journal of Neuroimmunology 306:46–52. DOI: 10.1016/j.jneuroim.2017.02.019.

Pereira D.T.V, Marson G.V, Barbero G.F, Tarone A.G, Cazarin C.B.B, Hubinger M.D, Martínez J (2020) Concentration of bioactive compounds from grape marc using pressurized liquid extraction followed by integrated membrane processes. Separation and Purification Technology 250:117206. DOI: 10.1016/j.seppur.2020.117206.

Putnik P, Barba F.J, Spanič V, Zorić Z, Dragović-Uzelac V, Bursać Kovačević D (2017) Green extraction approach for the recovery of polyphenols from Croatian olive leaves (Olea europea). Food and Bioproducts Processing 106:19-28. DOI: 10.1016/j.fbp.2017.08.004.

Şahin S, Şamli R (2013) Optimization of olive leaf extract obtained by ultrasound-assisted extraction with response surface methodology. Ultrasonics Sonochemistry 20:595–602. DOI: 10.1016/j.ultsonch.2012.07.029.

Sherif I.O, Al-Gayyar M.M (2018) Oleuropein potentiates anti-tumor activity of cisplatin against HepG2 through affecting proNGF/NGF balance. Life Sciences 198:87–93. DOI: 10.1016/j.lfs.2018.02.027.

Socaci S.A, Farcas A.C, Diaconeasa Z.M, Vodnar D.C, Rusu B, Tofana M (2018) Influence of the extraction solvent on phenolic content, antioxidant, antimicrobial and antimutagenic activities of brewers' spent grain. Journal of Cereal Science 80:180–187. DOI: 10.1016/j.jcs.2018.03.006.

Stamatopoulos K, Katsoyannos E, Chatzilazarou A, Konteles S.J (2012) Improvement of oleuropein extractability by optimizing steam blanching process as pre-treatment of olive leaf extraction via response surface methodology. Food Chemistry 133:344–351. DOI: 10.1016/j.foodchem.2012.01.038.

Susalit E, Agus N, Effendi I, Tjandrawinata R.R, Nofiarny D, Perrinjaquet-Moccetti T, Verbruggen M (2011) Olive (Olea europaea) leaf extract effective in patients with stage-1 hypertension: Comparison with Captopril. Phytomedicine 18:251–258.

Szydłowska-Czerniak A, Bartkowlak-Broda I, Karlovic I, Karlovits G, Zlyk E.S (2011) Antioxidant capacity, total phenolics, glucosinolates and colour parameters of rapeseed cultivars. Food Chemistry 127:556–563. DOI: 10.1016/j.foodchem.2011.01.040.

Szydłowska-Czerniak A, Łaszewska A (2015) Effect of refining process on antioxidant capacity, total phenolics and prooxidants contents in rapeseed oils. LWT - Food Science and Technology 64:853–859. DOI: 10.1016/j.lwt.2015.06.069.

Szydłowska-Czerniak A, Tułodzieckaa A, Szłyk E (2012) A silver nanoparticle-based method for determination of antioxidant capacity of rapeseed and its products. Analyst 137:3750–3759. DOI: 10.1039/c2an35326a.

Talhaoui N, Gomez-Caravaca A.M, Leon L, De la Rosa R, Segura-Carretero A, Fernandez-Gutierrez A (2014) Determination of phenolic compounds of 'Sikitita' olive leaves by

HPLC-DAD-TOF-MS. Comparison with its parents 'Arbequina' and 'Picual' olive leaves. LWT - Food Science and Technology 58:28–34. DOI: 10.1016/j.lwt.2014.03.014.

Vural N, Cavuldak O.A, Akay M.A (2021) D-Optimal design and multi-objective optimization for green extraction conditions developed with ultrasonic probe for oleuropein. Journal of Applied Research on Medicinal and Aromatic Plants 20:100279. DOI: 10.1016/j.jarmap.2020.100279.

Yateem H, Afaneh I, Al-Rimawi F (2014) Optimum conditions for oleuropein extraction from olive leaves. International Journal of Applied Science and Technology 4:153–157.

Yingngam B, Monschein M, Brantner A (2014) Ultrasound-assisted extraction of phenolic compounds from Cratoxylum formosum ssp. formosum leaves using central composite design and evaluation of its protective ability against H2O2-induced cell death. Asian Pacific Journal of Tropical Medicine 7(Supplement 1):S497–S505. DOI: 10.1016/S1995-7645(14)60281-9.

Yu L, Haley S, Perret J, Harris M, Wilson J, Qian M (2002) Free radical scavenging properties of wheat extracts. Journal of Agricultural and Food Chemistry 50(6):1619–1624. DOI: 10.1021/jf010964p.

Yuan J-J, Tu J-L, Qin F G.F, Xu Y-J, Li B (2018) Phenolic composition of oleuropein extract after enzymatic process by HPLC-MS and their antioxidant and antibacterial activities. Journal of Food Biochemistry 42(3). DOI: 10.1111/jfbc.12517.

CHAPTER 5

Achak M, Hafidi A, Mandi L, Ouazzani N (2014) Removal of phenolic compounds from olive mill wastewater by adsorption onto wheat bran. Desalination and Water Treatment 52:2875-2885. DOI: 10.1080/19443994.2013.819166.

Adhoum N, Monser L (2004) Decolourization and removal of phenolic compounds from olive mill wastewater by electrocoagulation. Chemical Engineering and Processing: Process Intensification 43:1281-1287. DOI: 10.1016/j.cep.2003.12.001.

Aghili F, Ghoreyshi A.A, Rahimpour A, Rahimnejad M (2017) Coating of mixed-matrix membranes with powdered activated carbon for fouling control and treatment of dairy effluent. Process Safety and Environmental Protection 107:528-539. DOI: 10.1016/j.psep.2017.03.013.

Ahmadiaras A, Mehrdadi N (2023) Extracting minerals from desalination brine using innovative capacitive photo electrocatalytic desalination cells (cPEDC). Chemical Science, Chemical Engineering and Engineering Education 7:100356. DOI: 10.1016/j.cscee.2023.100356.

Almanassra I.W, Jaber L, Backer S.N, Chatla A, Kochkodan V, Al-Ansari T, Shanableh A, Atieh M.A (2023) Oxidized carbide-derived carbon as a novel filler for improved antifouling characteristics and permeate flux of hybrid polyethersulfone ultrafiltration membranes. Chemosphere 313:137425. DOI: 10.1016/j.chemosphere.2022.137425.

Alves K.G.B, Felix J.F, De Melo E.F, Dos Santos C.G, Andrade C.A.S, De Melo C.P (2012) Characterization of ZnO/polyaniline nanocomposites prepared using surfactant solutions as polymerization media. Journal of Applied Polymer Science 125: E141- E147. DOI: 10.1002/app.35502.

Ansari S, Moghadassi R, Hosseini M (2015) Fabrication of novel poly (phenylene ether ether sulfone) based nanocomposite membrane modified by Fe_2NiO_4 nanoparticles and ethanol as organic modifier. Desalination 357:189-196. DOI: 10.1016/j.desal.2014.11.022.

Bagheripour E, Moghadassi A.R, Hosseini S.M (2016) Synthesis of PANI-co-MWCNT composite nanoparticles for enhancing the performance of PES-based nanofiltration membrane. Korean Journal of Chemical Engineering 33:1462-1471. DOI: 10.1007/s11814-015-0257-x.

Baruah P, Mahanta D (2016) Adsorption and reduction of Cr (VI) from aqueous medium using polyaniline emeraldine salt: a combined approach. Bulletin of Materials Science 39:875-882. DOI: 10.1007/s12034-016-1204-0.

Belabed C, Tab A, Belhamdi B, Boudiaf S, Bellal B, Benrekaa N, Trari M (2021) Optical and dielectric properties of polyaniline-ZnO nanoparticles for enhancing the

photodegradation of organic pollutants. Optik 248:168066. DOI: 10.1016/j.ijleo.2021.168066.

Bubela H, Konovalova V, Kujawa J, Kolesnyk I, Burban A, Kujawski W (2023) Enhancement of transport parameters and antifouling properties of PVDF membranes modified with Fe3O4 nanoparticles in proteins fractionation. Separation and Purification Technology 124573. DOI: 10.1016/j.seppur.2023.124573.

Buran T.J, Sandhu A.K, Zheng L, Rock C.R, Yang W.W, Gu L (2014) Adsorption/desorption characteristics and separation of anthocyanins and polyphenols from blueberries using macroporous adsorbent resins. Journal of Food Engineering 128:167-173. DOI: 10.1016/j.jfoodeng.2013.12.029.

Buthiyappan A, Gopalan J, Abdul Raman A.A (2019) Synthesis of iron oxides impregnated green adsorbent from sugarcane bagasse: characterization and evaluation of adsorption efficiency. Journal of Environmental Management 249:109323. DOI: 10.1016/j.jenvman.2019.109323.

Daraei P, Madaeni S.S, Ghaemi N, Salehi E, Khadivi M.A, Moradian R, Astinchap B (2012) Development of a novel polyethersulfone nanocomposite membrane using PANI/Fe3O4 nanoparticles for enhanced Cu(II) removal from water. Journal of Membrane Science 415-416:250-259. DOI: 10.1016/j.memsci.2012.05.007.

De Peres M.L, De Avila Delucis R, Amico S.C, Gatto D.A (2019) Zinc oxide nanoparticles from microwave-assisted solvothermal process: Photocatalytic performance and use for wood protection against xylophagous fungus. Nanomaterials and Nanotechnology 9:1-8. DOI: 10.1177/1847980419876201.

Dhole S.G, Adake S.A, Prajapati T.A, Helambe S.N (2018) Effect of ZnO filler on structural and optical properties of polyaniline-ZnO nanocomposites. Procedia Manufacturing 20:27-134. DOI: 10.1016/j.promfg.2018.02.018.

El-Abbassi A, Khayet M, Hafidi A (2011) Micellar enhanced ultrafiltration process for the treatment of olive mill wastewater. Water Research 45:4522-4530. DOI: 10.1016/j.watres.2011.05.044.

Erragued R, Braga MEM, Bouaziz M, Gando-Ferreira LM (2022) Integration of solvent extraction and membrane processes for the production of an oleuropein extract from olive leaves. Separation and Purification Technology 299:121751. DOI: 10.1016/j.seppur.2022.121751.

Fezzani B, Ben Cheikh R (2010) Two-phase anaerobic co-digestion of olive mill wastes in semi-continuous digesters at mesophilic temperature. Bioresource Technology 101:1628-1634. DOI: 10.1016/j.biortech.2009.09.067.

Galván D'Alessandro L, Vauchel P, Przybylski R, Chataigné G, Nikov I, Dimitrov K (2013) Integrated process extraction–adsorption for selective recovery of antioxidant phenolics from Aronia melanocarpa berries. Separation and Purification Technology 120:92-101. DOI: 10.1016/j.seppur.2013.09.027.

Ghaemi N, Madaeni S.S, Daraei P, Rajabi H, Shojaeimehr T, Rahimpour F, Shirvani B (2015) PES mixed matrix nanofiltration membrane embedded with polymer wrapped MWCNT: fabrication and performance optimization in dye removal by RSM. Journal of Hazardous Materials 298:111-121. DOI: 10.1016/j.jhazmat.2015.05.018.

Goswami B, Mahanta D (2019) Removal of phenolic compounds using polyaniline-coated nickel oxide nanoparticles: Equilibrium, kinetics, and thermodynamic studies. Colloids and Surfaces A: Physicochemical and Engineering Aspects 582:123843. DOI: 10.1016/j.colsurfa.2019.123843.

Gu W, Zhang H, Chen C, Zhang J (2022) Design of ZnO/PANI composites and the mechanism of enhanced humidity sensing properties. Current Applied Physics 34:112-121. DOI: 10.1016/j.cap.2021.11.013.

Guo J, Kim J (2017) Enhancement of polyethersulfone membrane's anti-fouling property in wastewater treatment through sulfated TiO2 nanoparticle doping. RSC Advances 7:33822. DOI: 10.1039/C7RA06406C.

Hashim H, Wan Ahmad W.Y, Zubairi S.I, Maskat M.Y (2018) Effect of pH on adsorption of organic acids and phenolic compounds by amberlite IRA 67 resin. Jurnal Teknologi 81:69-81. DOI: 10.11113/jt.v81.12606.

Hosseini S.M, Afshari M, Fazlali A.R, Farahani S.K, Bandehali S, Van der Bruggen B, Bagheripour E (2019) Fabrication of antifouling mixed matrix nanofiltration membrane decorated with (Fe3O4-polyvinylpyrrolidone) composite nanoparticles. Chemical Engineering Research and Design 147:390-398. DOI: 10.1016/j.cherd.2019.05.025.

Hosseini S.M, Amini S.H, Khodabakhshi A.R, Bagheripour E, Van der Bruggen B (2018) Activated carbon nanoparticles entrapped mixed matrix polyethersulfone based nanofiltration membrane for sulfate and copper removal from water. Journal of Taiwan Institute of Chemical Engineers 82:169-178. DOI: 10.1016/j.jtice.2017.11.017.

Hosseini S.M, Bagheripour E, Hamidi A.R, Moghadassi A.R, Madaeni S.S (2016) Fabrication of PES-based nanofiltration membrane modified with composite PAA-co-PMMA-g-ZnA nanoparticles. Journal of the Iranian Chemical Society 13:1749-1758. DOI: 10.1007/s13738-016-0892-0.

Hosseini S.M, Bagheripour E, Hamidi A.R, Moghadassi A.R, Madaeni S.S (2016) Fabrication of PES-based nanofiltration membrane modified with composite PAA-co-PMMA-g-ZnA nanoparticles. Journal of the Iranian Chemical Society 13:1749-1758. DOI: 10.1007/s13738-016-0892-0.

Majumdar S, Nath J, Mahanta D (2018) Efficient removal of phenolic compounds from aqueous medium using surface-modified polypyrrole. Journal of EnvironmentalChemical Engineering 6:2588. DOI: 10.1016/j.jece.2018.04.002.

Manorma, Ferreira I, Alves P, Gil M.H, Gando-Ferreira L.M (2021) Lignin separation from black liquor by mixed matrix polysulfone nanofiltration membrane filled withmultiwalled carbon nanotubes. Separation and Purification Technology 260:118231. DOI: 10.1016/j.seppur.2020.118231.

Maruthi N, Faisal M, Raghavendra N, Prasanna B.P, Manohara S.R, Revanasiddappa M (2021) Tunable electrical properties of anticorrosive polyaniline-coated copper oxide (PANI/CuO) nanocomposites for broadband electromagnetic interference shielding. Colloids and Surfaces A: Physicochemical and Engineering Aspects 621:126611. DOI: 10.1016/j.colsurfa.2021.126611.

Mobarakabad P, Moghadassi A.R, Hosseini S.M (2015) Fabrication and characterization of poly (phenylene ether-ether sulfone) based nanofiltration membranes modified by titanium dioxide nanoparticles for water desalination. Desalination 365:227-233. DOI: 10.1016/j.desal.2015.03.002.

Mostafaei A, Zolriasatein A (2012) Synthesis and characterization of conductingpolyaniline nanocomposites containing ZnO nanorods. Progress in Natural Science: Materials International 22:273-280. DOI: 10.1016/j.pnsc.2012.07.002.

Mukherjee R, De S (2016) Development of a novel carbon-nanoparticle polysulfone hollow fiber mixed matrix ultrafiltration membrane for adsorptive removal of benzene, phenol, and toluene from aqueous solution. Separation and Purification Technology 157:229- 240. DOI: 10.1016/j.seppur.2015.11.015.

Nasrollahi N, Aber S, Vatanpour V, Mahmoodi NM (2018) Influence of amine-functionalized CuO and ZnO nanoparticles on the morphology and permeation properties of polyethersulfone ultrafiltration nanocomposite membranes. Composites Part B: Engineering 154:388-409. DOI: 10.1016/j.compositesb.2018.09.027.

Rahimi Z, Zinatizadeh A.A.L, Zinadini S (2015) Preparation of highly antibiofoulingamino-functionalized MWCNTs/PES nanocomposite ultrafiltration membrane for membrane bioreactor applications. Journal of Industrial and Engineering Chemistry 29:366-374. DOI: 10.1016/j.jiec.2015.04.017.

Rahimpour A, Jahanshahi M, Khalili S, Mollahosseini A, Zirepour A, Rajaeian B (2012) Enhancement of surface properties and performance of polyethersulfone (PES)membrane using novel functionalized carbon nanotubes. Desalination 286:99-107. DOI: 10.1016/j.desal.2011.10.039.

Ruby-Figueroa R, Cassano A, Drioli E (2012) Ultrafiltration of orange press liquor: Optimization of operating conditions for the recovery of antioxidant compounds by response surface methodology. Separation and Purification Technology 98:255-261.DOI: 10.1016/j.seppur.2012.07.022.

Salem A.N.M, Ahmed M.A, El-Shahat M.F (2016) Selective adsorption of amaranth dye on Fe3O4/MgO nanoparticles. Journal of Molecular Liquids 219:780-788. DOI: 10.1016/j.molliq.2016.03.084.

Sharma M, Alves P, Gil M.H, Gando-Ferreira L.M (2022) Fractionation of black liquor using ZnO nanoparticles/PES ultrafiltration membranes: Effect of operating variables. Journal of Cleaner Production 345:131183. DOI: 10.1016/j.jclepro.2022.131183.

Shen J, Ruan H, Wu L, Gao C (2011) Development and characterization of a PES-SiO$_2$ organic-inorganic composite ultrafiltration membrane for raw water pretreatment. Chemical Engineering Journal 168:1272-1278. DOI: 10.1016/j.cej.2011.02.039.

Sohail A, Sarfraz M, Nawaz S, Tahir Z (2023) Enhancing carbon capture efficiency of zeolite-embedded polyether sulfone mixed-matrix membranes via annealing process. Journal of Cleaner Production 399:136617. DOI: 10.1016/j.jclepro.2023.136617.

Stasinakis A.S, Elia I, Petalas A.V, Halvadakis C.P (2008) Removal of total phenols from olive-mill wastewater using an agricultural by-product, olive pomace. Journal of Hazardous Materials 160:408-413. DOI: 10.1016/j.jhazmat.2008.03.012.

Szydlowska-Czerniak A, Tulodziecka A, Szlyk E (2012) A silver nanoparticle-based method for the determination of antioxidant capacity in rapeseed and its products. Analyst 137:3750-3759. DOI: 10.1039/C2AN35326A.

Thomas D, Thomas A, Tom A.E, Sadasivuni K.K, Ponnamma D, Goutham S, Cabibihan J.J, Venkateswara Rao K (2017) Highly selective gas sensors from photo-activated ZnO/PANI thin films synthesized by mSILAR. Synthetic Metals 232:123-130. DOI: 10.1016/j.synthmet.2017.08.006.

Tri N.L.M, Thang P.Q, VanTan L, Huong T, Kim J, Viet N.M, Phuong N.M, Al Tahtamouni T.M (2020) Removal of phenolic compounds from wastewaters by using synthesized Fe-nano zeolite. Journal of Water Process Engineering 33:101070. DOI: 10.1016/j.jwpe.2019.101070.

Tseng H.H, Zhuang G.L, Su Y.C (2012) The effect of blending ratio on the compatibility, morphology, thermal behavior and pure water permeation of asymmetric CAP/PVDF membranes. Desalination 284:269-278. DOI: 10.1016/j.desal.2011.09.011.

Vatanpour V, Madaeni S.S, Khataee A.R, Salehi E, Zinadini S, Monfared H.A (2012) Influence of different sizes and types of TiO2 nanoparticles embedded in mixed matrix PES nanocomposite membranes on antifouling and performance properties. Desalination 292:19-29. DOI: 10.1016/j.desal.2012.02.006.

Vatanpour V, Madaeni S.S, Moradian R, Zinadini S, Astinchap B (2012) Preparation and characterization of an innovative antibiofouling nanofiltration polyethersulfone membrane incorporating TiO2-coated multiwalled carbon nanotubes. Separation and Purification Technology 90:69-82. DOI: 10.1016/j.seppur.2012.02.014.

Vatanpour V, Madaeni SS, Moradian R, Zinadini S, Astinchap B (2011) Fabrication and characterization of a new anti-fouling nanofiltration membrane composed of oxidized multiwalled carbon nanotube/polyethersulfone nanocomposite. Journal of Membrane Science 375:284-294. DOI: 10.1016/j.memsci.2011.03.055.

Wang L, Song X, Wang T, Wang S, Wang Z, Gao C (2015) Fabrication and characterization of polyethersulfone/carbon nanotubes (PES/CNTs) based mixed matrix membranes (MMMs) for nanofiltration application. Applied Surface Science 330:118- 125. DOI: 10.1016/j.apsusc.2014.12.183.

Wang W, Zhu L, Shan B, Xie C, Liu C, Cui F, Li G (2018) Development and characterization of SLS-CNT/PES ultrafiltration membrane with anti-fouling and antibacterial features. Journal of Membrane Science 548:459-469. DOI: 10.1016/j.memsci.2017.11.046.

Wang X, Feng M, Liu Y, Deng HN, Lu J (2019) Preparation of polyethersulfone membranes blended with graphene oxide using electric field-assisted phase inversion forenhanced separation and anti-fouling performance. Journal of Membrane Science 577:41-50. DOI: 10.1016/j.memsci.2019.01.055.

Xia S, Yao L, Zhao Y, Li N, Zheng Y (2015) Preparation of graphene oxide modified polyamide thin film composite membranes with improved hydrophilicity for natural

organic matter removal. Chemical Engineering Journal 280:720-727. DOI: 10.1016/j.cej.2015.06.063.

Xu Z, Zhang J, Shan M, Li Y, Li B, Niu J, Zhou B, Qian X (2014) Organosilane-functionalized graphene oxide for enhanced antifouling and mechanical properties of polyvinylidene fluoride ultrafiltration membranes. Journal of Membrane Science 458:1-13. DOI: 10.1016/j.memsci.2014.01.050.

Zaini M.S.M, Arshad M, Syed-Hassan S.S.A (2022) Adsorption isotherm and kinetic study of methane on palm kernel shell-derived activated carbon. Journal of Bioresource and Bioproducts 8:66-77. DOI: 10.1016/j.jobab.2022.11.002.

Zam W, Bashour G, Abdelwahed W, Khayata W (2012) Effective extraction of polyphenols and proanthocyanidins from Pomegranate's peel. International Journal of Pharmacy and Pharmaceutical Sciences 4:675-682.

Zangeneh H, Zinatizadeh A, Zinadini S, Feyzi M, Bahnemann D (2019) Preparation of ultrafine L-Methionine (C, N, S triple doped)-TiO2-ZnO nanoparticles and their application in fouling alleviation in PES nanocomposite membrane. Composites Part B: Engineering 176:107158. DOI: 10.1016/j.compositesb.2019.107158.

Zangeneh H, Zinatizadeh A.A, Feyzi M, Zinadini S, Bahnemann D.W (2019) Preparation of ultrafine L-Methionine (C,N,S triple doped)-TiO2-ZnO nanoparticles for fouling alleviation in PES nanocomposite membrane. Composites Part B: Engineering 176:107158. DOI: 10.1016/j.compositesb.2019.107158.

Zhou Q, Yuan Y, Wu Y, Liu Y (2017) Sensitive determination of typical phenols in environmental water samples using magnetic solid-phase extraction with polyaniline@SiO$_2$@Fe as adsorbents followed by HPLC. Journal of Separation Science 40:4032-4040. DOI: 10.1002/jssc.201700644.

Zinadini S, Rostami S, Vatanpour V, Jalilian E (2017) Development of a photocatalytic ZnO/MWCNTs nanocomposite for antibiofouling polyethersulfone mixed matrix nanofiltration membrane. Journal of Membrane Science 529:133-141. DOI: 10.1016/j.memsci.2017.01.047.

Zinadini S, Zinatizadeh A.A, Rahimi M, Vatanpour V, Zangeneh H (2014) Preparation of a novel antifouling mixed matrix PES membrane by embedding graphene oxide nanoplates. Journal of Membrane Science 453:292-301. DOI: 10.1016/j.memsci.2013.10.070.

CHAPTER 6

Bagheripour E, Moghadassi A, Hosseini S.M (2016) Preparation of mixed matrix PES- based nanofiltration membrane filled with PANI-co-MWCNT composite nanoparticles. Korean Journal of Chemical Engineering 33:1462-1471. DOI: 10.1007/s11814-015-0257-x.

Beek W.J, Wienk M.M, Janssen R.A (2004) Efficient hybrid solar cells from zinc oxide nanoparticles and a conjugated polymer. Advanced Materials 16:1009-1013. DOI: 10.1002/adma.200306659.

Bunani S, Yörükoğlu E, Sert G, Yüksel Ü, Yüksel M, Kabay N (2013) Application of nanofiltration for reuse of municipal wastewater and quality analysis of product water. Desalination 315:33-36. DOI: 10.1016/j.desal.2012.11.015.

Cassano A, Cabri W, Mombelli G, Peterlongo F, Giorno L (2016) Recovery of bioactive compounds from artichoke brines by nanofiltration. Food and Bioproducts Processing 98:257-265. DOI: 10.1016/j.fbp.2016.02.004.

Cifá D, Skrt M, Pittia P, Di Mattia C, Poklar Ulrih N (2018) Enhanced yield of oleuropein from olive leaves using ultrasound-assisted extraction. Food Science & Nutrition 6:1128-1137. DOI: 10.1002/fsn3.654.

Conidi C, Cassano A, Drioli E (2012) Recovery of phenolic compounds from orange press liquor by nanofiltration. Food Bioprod Process 90:867–874. DOI: 10.1016/j.fbp.2012.07.005.

Contreras .del M.M, Lama-Muñoz A, Espínola F, Moya M, Romero I, Castro E (2020) Valorization of olive mill leaves through ultrasound-assisted extraction. FoodChemistry 314:126218. DOI: 10.1016/j.foodchem.2020.126218.

Cruz R.M.S, Brito R, Smirniotis P, Nikolaidou Z, Vieira M.C (2017) Extraction of bioactive compounds from olive leaves using emerging technologies. In: Ingredients Extraction by Physicochemical Methods in Food, Elsevier Ed., Amsterdam, pp. 441- 461. DOI: 10.1016/B978-0-12-811521-3.00011-9.

Daraei P, Madaeni S.S, Ghaemi N, Salehi E, Khadivi M.A, Moradian R, Astinchap B (2012) Novel polyethersulfone nanocomposite membrane prepared by PANI/Fe3O4 nanoparticles with enhanced performance for Cu (II) removal from water. Journal of Membrane Science 415–416:250-259. DOI: 10.1016/j.memsci.2012.05.007.

Diawara C.K, Diop S.N, Diallo M.A, Farcy M, Deratani A (2011) Performance of Nanofiltration (NF) and Low Pressure Reverse Osmosis (LPRO) Membranes in the Removal of Fluorine and Salinity from Brackish Drinking Water. Journal of Water Resource and Protection 3:912-917. DOI: 10.4236/jwarp.2011.312101.

Erragued R, Braga M.E.M, Bouaziz M, Gando-Ferreira L.M (2022) Integration of solvent extraction and membrane processes to produce an oleuropein extract from olive leaves. Separation and Purification Technology 299:121751. DOI: 10.1016/j.seppur.2022.121751.

Günes S, Neugebauer H, Sariciftci N.S (2007) Conjugated polymer-based organic solar cells. Chemical Reviews 107:1324-1338. DOI: 10.1021/cr050149z.

Guo J, Kim J (2017) Modifications of polyethersulfone membrane by doping sulfated-TiO2 nanoparticles for improving anti-fouling property in wastewater treatment. RSC Advances 7:33822. DOI: 10.1039/C7RA06406C.

Hosseini S.M, Amini S.H, Khodabakhshi A.R, Bagheripour E, Van der Bruggen B (2017) Activated carbon nanoparticles entrapped mixed matrix polyethersulfone based nanofiltration membrane for sulfate and copper removal from water. Journal of the Taiwan Institute of Chemical Engineers 000:1-10. DOI: 10.1016/j.jtice.2017.11.017.

Hosseini S.M, Bagheripour E, Hamidi A.R, Moghadassi A.R, Madaeni S.S (2016) Fabrication of PES based nanofiltration membrane modified by composite PAA co PMMA g ZnA nanoparticles. Journal of the Iranian Chemical Society 13:1749-1758. DOI: 10.1007/s13738-016-0892-0.

Huang J, Xia C, Cao L, Zeng X (2008) Facile microwave hydrothermal synthesis of zinc oxide one-dimensional nanostructure with three-dimensional morphology. Materials Science and Engineering B: Solid-State Materials for Advanced Technology 150:187–193. DOI: 10.1016/j.mseb.2008.05.014.

Irakli M, Chatzopoulou P, Ekateriniadou L (2018) Optimization of ultrasound-assisted extraction of phenolic compounds: Oleuropein, phenolic acids, phenolic alcohols and flavonoids from olive leaves and evaluation of its antioxidant activities. Industrial Crops and Products 124:382-388. DOI: 10.1016/j.indcrop.2018.07.070.

Kashaninejad M, Sanz M, Blanco B, Beltrán S, Niknam S (2020) Freeze dried extract from olive leaves: valorization, extraction kinetics and extract characterization. Food and Bioproducts Processing 124:196-207. DOI: 10.1016/j.fbp.2020.08.015.

Khan A.A, Khalid M (2010) Synthesis of nano-sized ZnO and polyaniline-zinc oxide composite: characterization, stability in terms of DC electrical conductivity retention and application in ammonia vapor detection. Journal of Applied Polymer Science 117:1601–1607. DOI: 10.1002/app.32037.

Khemakhem I, Gargouri O.D, Dhouib A, Ayadi M.A, Bouaziz M (2017) Oleuropein rich extract from olive leaves by combining microfiltration, ultrafiltration and nanofiltration. Separation and Purification Technology 172:310-317. DOI: 10.1016/j.seppur.2016.08.003.

Lama-Muñoz A, Contreras del M.M, Espínola F, Moya M, Romero I, Castro E (2019) Optimization of oleuropein and luteolin-7-o-glucoside extraction from olive leaves by ultrasound-assisted technology. Energies 12:2486. DOI: 10.3390/en12132486.

Manorma, Ferreira I, Alves P, Gil M.H, Gando-Ferreira L.M (2021) Lignin separation from black liquor by mixed matrix polysulfone nanofiltration membrane filled with multiwalled carbon nanotubes. Separation and Purification Technology 260:118231. DOI: 10.1016/j.seppur.2020.118231.

Markhali F.S, Teixeira J.A, Rocha .CM.R (2020) Olive tree leaves - A source of valuable active compounds. Processes 8:1177. DOI: 10.3390/pr8091177.

Mudimu O.A, Peters M, Brauner F, Braun G (2012) Overview of membrane processes for the recovery of polyphenols from olive mill wastewater. American Journal of Environmental Sciences 8(3):195-201. DOI: 10.3844/ajessp.2012.195.201.

Mulinacci N, Romani A, Galardi C, Pinelelli P, Giaccherini C, Vincieri F.F (2001) Polyphenolic content in olive oil waste waters and related olive samples. Journal of Agricultural and Food Chemistry 49:3509-3514. DOI: 10.1021/jf000972q.

Nasrollahi N, Aber S, Vatanpour V, Mahmoodi N.M (2018) The effect of amine functionalization of CuO and ZnO nanoparticles used as additives on the morphology and the permeation properties of polyethersulfone ultrafiltration nanocomposite membranes. Composites Part B: Engineering 154:388-409. DOI: 10.1016/j.compositesb.2018.09.027.

Pereira D.T.V, Marson G.V, Barbero G.F, Tarone A.G, Cazarin C.B.B, Hubinger M.D, Martínez J (2020) Concentration of bioactive compounds from grape marc using pressurized liquid extraction followed by integrated membrane processes. Separation and Purification Technology 250:117206. DOI: 10.1016/j.seppur.2020.117206.

Rahimi Z, Zinatizadeh A.A.L, Zinadini S (2015) Preparation of high antibiofouling amino functionalized MWCNTs/PES nanocomposite ultrafiltration membrane for application in membrane bioreactor. Journal of Industrial and Engineering Chemistry 29:366-374. DOI: 10.1016/j.jiec.2015.04.017.

Rahimpour A, Jahanshahi M, Khalili S, Mollahosseini A, Zirepour A, Rajaeian B (2012) Novel functionalized carbon nanotubes for improving the surface properties and performance of polyethersulfone (PES) membrane. Desalination 286:99-107. DOI: 10.1016/j.desal.2011.10.039.

Schaep J, Vandecasteele C, Peeters B, Luyten J, Dotremont C, Roels D (1999) Characteristics and retention properties of a mesoporous γ-Al2O3 membrane for nanofiltration. Journal of Membrane Science 163:229-237. DOI: 10.1016/S0376- 7388(99)00163-5.

Sharma M, Alves P, Gil M.H, Gando-Ferreira L.M (2022) Fractionation of black liquor using ZnO nanoparticles/PES ultrafiltration membranes: Effect of operating variables. Journal of Cleaner Production 345:131183. DOI: 10.1016/j.jclepro.2022.131183.

Todisco S, Tallarico P, Gupta B.B (2002) Mass transfer and polyphenols retention in the clarification of black tea with ceramic membranes. Innovative Food Science and Emerging Technologies 3:255-262. DOI: 10.1016/S1466-8564(02)00046-2.

Tundis R, Loizzo M.R, Bonesi M, Sicari V, Ursino C, Manfredi I, Conidi C, Figoli A, Cassano A (2018) Concentration of Bioactive Compounds from Elderberry (Sambucus nigra L.) Juice by Nanofiltration. Membranes Plant Foods Hum Nutr. 73(4):336-343. DOI: 10.1007/s11130-018-0686-x.

Van Gestel T, Vandecasteele C, Buekenhoudt A, Dotremont C, Luyten J, Leysen R, Van der Bruggen B, Maes G (2002) Salt retention in nanofiltration with multilayer ceramic TiO2 membranes. Journal of Membrane Science 209:379-389. DOI: 10.1016/S0376-7388(02)00311-3.

Vatanpour V, Madaeni S.S, Moradian R, Zinadini S, Astinchap B (2012) Novel antibiofouling nanofiltration polyethersulfone membrane fabricated from embedding TiO2 coated multiwalled carbon nanotubes. Separation and Purification Technology 90:69-82. DOI: 10.1016/j.seppur.2012.02.014.

Wang L, Song X, Wang T, Wang S, Wang Z, Gao C (2015) Fabrication and characterization of polyethersulfone/carbon nanotubes (PES/CNTs) based mixed matrix membranes (MMMs) for nanofiltration application. Applied Surface Science 330:118-125. DOI: 10.1016/j.apsusc.2014.12.183.

Xu F, Lu Y, Yan X, Liu Y (2009) Synthesis and photoluminescence of assembly- Controlled ZnO architectures by Aqueous Chemical growth. The Journal of Physical Chemistry C 113:1052–1059. DOI: 10.1021/jp808456r.

Yateem H, Afaneh I, Al-Rimawi F (2014) Optimum conditions for Oleuropein extraction from olive leaves. International Journal of Applied Science and Technology 4:153-157.

Yousefi R, Sheini F.J, Muhamad M.R (2010) Characterization and field emission properties of ZnMgO nanowires fabricated by thermal evaporation process. Solid State Sciences 12:1088-1093. DOI: 10.1016/j.solidstatesciences.2010.04.019.

Zinadini S, Rostami S, Vatanpour V, Jaliliana E (2017) Preparation of antibiofouling polyethersulfone mixed matrix NF membrane using photocatalytic activity of ZnO/MWCNTs nanocomposite. Journal of Membrane Science 529:133-141. DOI: 10.1016/j.memsci.2017.01.047.

Zinadini S, Zinatizadeh A.A, Rahimi M, Vatanpour V, Zangeneh H (2014) Preparation of a novel antifouling mixed matrix PES membrane by embedding graphene oxide nanoplates. Journal of Membrane Science 453:292-301. DOI: 10.1016/j.memsci.2013.10.070.

<u>CHAPTER 7</u>

Ahmadiaras A, Mehrdadi N (2023) Extracting minerals from desalination brine using innovative capacitive photo electrocatalytic desalination cells (cPEDC). CSCEE 7:100356. DOI: 10.1016/j.cscee.2023.100356.

Arsuaga J.M, Sotto A, del Rosario G, Martínez A, Molina S, Teli S.B, de Abajo J (2013) Influence of the type, size, and distribution of metal oxide particles on the properties of nanocomposite ultrafiltration membranes. J Membr Sci 428:131–141. DOI: 10.1016/j.memsci.2012.11.008.

Bagheripour E, Moghadassi A, Hosseini S.M (2016) Preparation of Mixed Matrix PES-Based Nanofiltration Membrane Filled with PANI-Co-MWCNT Composite Nanoparticles. Korean J Chem Eng 33:1462-1471. DOI: 10.1007/s11814-015-0257-x.

Benaddi R, Osmane A, Zidan K, El Harfi K, Ouazzani N (2023) A Review on Processes for Olive Mill Waste Water Treatment. EEET 7:196-207. DOI: 10.12912/27197050/169876.

Cassano A, Conidi C, Ruby-Figueroa R, Castro-Muñoz R (2018) Nanofiltration and tight ultrafiltration membranes for the recovery of polyphenols from agro-food by-products. Int J Mol Sci 19:351. DOI: 10.3390/ijms19020351.

Cruz R.M.S, Brito R, Smirniotis P, Nikolaidou Z, Vieira M.C (2017) Extraction of bioactive compounds from olive leaves using emerging technologies. In: Ingredients Extraction by Physicochemical Methods in Food, Elsevier Ed., pp. 441-461. DOI: 10.1016/B978-0-12-811521-3.00011-9.

Dahmoune F, Spigno G, Moussi K, Remini H, Cherbal A, Madani K (2014) Pistacia lentiscus leaves as a source of phenolic compounds: Microwave-assisted extraction optimized and compared with ultrasound-assisted and conventional solvent extraction. Ind Crop Prod 61:31–40. DOI: 10.1016/j.indcrop.2014.06.035.

Dairi S, Dahmoune F, Belbahi A, Remini H, Kadri N, Aoun O, Bouaoudia N, Madani K (2021) Optimization of microwave extraction method of phenolic compounds from red onion using response surface methodology and inhibition of lipoprotein low-density oxidation. J Appl Res Med Aromat Plants 22:100301. DOI: 10.1016/j.jarmap.2021.100301.

Dang H.Q, Price W.E, Nghiem L.D (2014) The effects of feed solution temperature on pore size and trace organic contaminant rejection by the nanofiltration membrane NF270. Sep Purif Technol 125:43–51. DOI: 10.1016/j.seppur.2013.12.043.

De Almeida M.S, Martins R.C, Quinta-Ferreira R.M, Gando-Ferreira L.M (2018) Optimization of operating conditions for the valorization of olive mill wastewater using membrane processes. Environ Sci Pollut Res 25:21968–21981. DOI: 10.1007/s11356-018-2323-5.

Erragued R, Braga M.E.M, Bouaziz M, Gando-Ferreira L.M (2022) Integration of solvent extraction and membrane processes to produce an oleuropein extract from olive leaves. Sep Purif Technol 299:121751. DOI: 10.1016/j.seppur.2022.121751.

Ferri F, Bertina L, Scoma A, Marchetti L, Fava F (2011) Recovery of low molecular weight phenols through solid-phase extraction. Chem Eng J 166:994–1001. DOI: 10.1016/j.cej.2010.11.090.

Fratoddi I, Rapa M, Testa G, Venditti I, Scaramuzzo F.A, Vinci G (2018) Response surface methodology for the optimization of phenolic compounds extraction from extra virgin

olive oil with functionalized gold nanoparticles. Microchem J 138:430–437. DOI: 10.1016/j.microc.2018.01.043.

García-Pérez P, Losada-barreiro S, Gallego P.P, Bravo-díaz C (2019) Adsorption of gallic acid, propyl gallate and polyphenols from Bryophyllum extracts on activated carbon. Nat Sci Reports 9:1-9. DOI: 10.1038/s41598-019-51322-6.

Gholamzadeh N, Peyravi M, Jahanshahi M, Hoseinpour H, Rad A.S (2017) Developing PES membrane by modified Co3O4–OA nanoparticles for direct contact membrane distillation process. Asia-Pacific J Chem Eng 12:582–594. DOI: 10.1002/apj.2100.

Giacobbo A, Bernardes A.M, de Pinho M.N (2017) Sequential pressure-driven membrane operations to recover and fractionate polyphenols and polysaccharides from second racking wine lees. Sep Purif Technol 173:49–54. DOI: 10.1016/j.seppur.2016.09.007.

Gutierrez-Macias P, De Jesus M.L.H, Barragan-Huerta B.E (2017) The production of biomaterials from agro-industrial waste. Fresenius Environ Bull 26:4128-4152. DOI: 10.1007/s00253-017-8583-y.

Hosseini S, Afshari M, Fazlali A, Farahani S.K, Bandehali S, Van der Bruggen B, Bagheripour E (2019) Mixed matrix PES-based nanofiltration membrane decorated by (Fe3O4-polyvinylpyrrolidone) composite nanoparticles with intensified antifouling and separation characteristics. Chem Eng Res Des 147:390–398. DOI: 10.1016/j.cherd.2019.05.025.

Hosseini S, Bagheripour E, Hamidi A, Moghadassi A, Madaeni S (2013) Fabrication of PES-based nanofiltration membrane modified by composite PAA-co-PMMA-g-ZnA nanoparticles. J Iran Chem Soc 13:1749-1758. DOI: 10.1007/s13738-016-0892-0.

Hosseini S.M, Amini S.H, Khodabakhshi A.R, Bagheripour E, Van der Bruggen B (2018) Activated carbon nanoparticles entrapped mixed matrix polyethersulfone based nanofiltration membrane for sulfate and copper removal from water. J Taiwan Inst Chem Eng 82:169–178. DOI: 10.1016/j.jtice.2017.11.017.

Jomekian A, Bazooyar B, Mansoori S.A.A (2023) The experimental, technical, and economical evaluations of green fabricated activated carbon/PVA mixed matrix

membrane for enhanced CO2/CH4 separation. J Membr Sci Res 9:563685. DOI: 10.22079/JMSR.2023.563685.1571.

Khemakhem I, Dridi Gargouri O, Dhouib A, Ali Ayadi M, Bouaziz M (2017) Oleuropein rich extract from olive leaves by combining microfiltration, ultrafiltration and nanofiltration. Sep Purif Technol 172:310–317. DOI: 10.1016/j.seppur.2016.08.003.

Khodadoust S, Nasiriani T, Zeraatpisheh F (2018) Preparation of a magnetic molecularly imprinted polymer for the selective adsorption of chlordiazepoxide and its determination by central composite design optimized HPLC. New J Chem 42:14444– 14452. DOI: 10.1039/c8nj02643b.

Lama-Muñoz A, Contreras M.M, Espínola F, Moya M, de Torres A, Romero I, Castro E (2019) Extraction of oleuropein and luteolin-7-O-glucoside from olive leaves: Optimization of technique and operating conditions. Food Chem 293:161–168. DOI: 10.1016/j.foodchem.2019.04.075.

Lama-Muñoz A, Contreras M.M, Espínola F, Moya M, Romero I, Castro E (2020) Characterization of the lignocellulosic and sugars composition of different olive leaves cultivars. Food Chem 329:127153. DOI: 10.1016/j.foodchem.2020.127153.

Luo J, Wan Y (2013) Effects of pH and salt on nanofiltration—A critical review. J Membr Sci 438:18–28. DOI: 10.1016/j.memsci.2013.03.029.

Luo J, Zhu Z, Ding L, Bals O, Wan Y, Jaffrin M.Y, Vorobiev E (2013) Flux behavior in clarification of chicory juice by high-shear membrane filtration: Evidence for threshold flux. J Membr Sci 435:120–129. DOI: 10.1016/j.memsci.2013.01.057.

Manorma, Ferreira I, Alves P, Gil M.H, Gando-Ferreira L.M (2021) Lignin separation from black liquor by mixed matrix polysulfone nanofiltration membrane filled with multiwalled carbon nanotubes. Sep Pur Technol 260:118231–118232. DOI: 10.1016/j.seppur.2020.118231.

Mello B.C.B.S, Petrus J.C.C, Hubinger M.D (2013) Nanofiltration of aqueous propolis extracts and the effects of temperature, pressure and pH in the concentrated product. Stud Chem Process Technol 4:55-65.

Mobarakabad P, Moghadassi A.R, Hosseini S.M (2015) Fabrication and characterization of poly(phenylene ether-ether sulfone) based nanofiltration membranes modified by titanium dioxide nanoparticles for water desalination. Desalination 365:227-233. DOI: 10.1016/j.desal.2015.03.002.

Montané D, Nabarlatz D, Martorell A, Torné-Fernández V, Fierro V (2006) Removal of Lignin and Associated Impurities from Xylo-oligosaccharides by Activated Carbon Adsorption. Ind Eng Chem Res 45:2294–2302. DOI: 10.1021/ie051051d.

Mukherjee R, De S (2014) Adsorptive removal of phenolic compounds using cellulose acetate phthalate-alumina nanoparticle mixed matrix membrane. J Hazard Mater 265:8–19. DOI: 10.1016/j.jhazmat.2013.11.012.

Mulinacci N, Romani A, Galardi C, Pinelelli P, Giaccherini C, Vincieri F.F (2001) Polyphenolic content in olive oil waste waters and related olive samples. J Agric Food Chem 49:3509–3514. DOI: 10.1021/jf000972q.

Nasrollahi N, Aber S, Vatanpour V, Mahmoodi N.M (2018) The effect of amine functionalization of CuO and ZnO nanoparticles used as additives on the morphology and the permeation properties of polyethersulfone ultrafiltration nanocomposite membranes. Compos Part B Eng 154:388–409. DOI: 10.1016/j.compositesb.2018.09.027.

Nasrollahi N, Aber S, Vatanpour V, Mahmoodi N.M (2018) The effect of amine functionalization of CuO and ZnO nanoparticles used as additives on the morphology and the permeation properties of polyethersulfone ultrafiltration nanocomposite membranes. Compos Part B Eng 154:388–409. DOI: 10.1016/j.compositesb.2018.09.027.

Pereira D.T.V, Marson G.V, Barbero G.F, Tarone A.G, Cazarin C.B.B, Hubinger M.D, Martínez J (2020) Concentration of bioactive compounds from grape marc using pressurized liquid extraction followed by integrated membrane processes. Sep Purif Technol 250:117206. DOI: 10.1016/j.seppur.2020.117206.

Rahimi Z, Zinatizadeh A.A.L, Zinadini S (2015) Preparation of high antibiofouling amino functionalized MWCNTs/PES nanocomposite ultrafiltration membrane for application in membrane bioreactor. J Ind Eng Chem 29:366–374. DOI: 10.1016/j.jiec.2015.04.01.

Rahimpour A, Jahanshahi M, Khalili S, Mollahosseini A, Zirepour A, Rajaeian B (2012) Novel functionalized carbon nanotubes for improving the surface properties and performance of polyethersulfone (PES) membrane. Desalination 286:99–107. DOI: 10.1016/j.desal.2011.10.039.

Rahimpour A, Jahanshahi M, Khalili S, Mollahosseini A, Zirepour A, Rajaeian B (2012) Novel functionalized carbon nanotubes for improving the surface properties and performance of polyethersulfone (PES) membrane. Desalination 286:99–107. DOI: 10.1016/j.desal.2011.10.039.

Ruby-Figueroa R.A, Cassano A, Drioli E (2011) Ultrafiltration of orange press liquor: Optimization of operating conditions for the recovery of antioxidant compounds by response surface methodology. Sep Purif Technol 80:1-10. DOI: 10.1016/j.seppur.2011.03.030.

Safarpour M, Khataee A, Vatanpour V (2014) Preparation of a novel PVDF ultrafiltration membrane modified with reduced graphene oxide/TiO2 nanocomposite with enhanced hydrophilicity and antifouling properties. Ind Eng Chem Res 53:13370–13382. DOI: 10.1021/ie502407g.

Sharma M, Alves P, Gando-Ferreira L.M (2023) Effect of Activated Carbon Nanoparticles on the Performance of PES Nanofiltration Membranes to Separate Kraft Lignin from Black Liquor. J Water Process Eng 52:103487. DOI: 10.1016/j.jwpe.2023.103487.

Solarte-Toro J.C, Romero-García J.M, López-Linares J.C, Ramos E.R, Castro E, Alzate C.A.C (2018) Simulation Approach Through the Biorefinery Concept of the Antioxidants, Lignin and Ethanol Production using Olive Leaves as Raw Material. Chem Eng Trans 70:925–930. DOI: 10.3303/CET1870155.

Terki L, Kujawski W, Kujawa J, Kurzawa M, Filipiak-Szok A, Chrzanowska E, Khaled S, Madani K (2018) Implementation of osmotic membrane distillation with various hydrophobic porous membranes for concentration of sugars solutions and preservation

of the quality of cactus pear juice. J Food Eng 230:28–38. DOI: 10.1016/j.jfoodeng.2018.02.023.

Vatanpour V, Madaeni S.S, Moradian R, Zinadini S, Astinchap B (2012) Novel antibifouling nanofiltration polyethersulfone membrane fabricated from embedding TiO2 coated multiwalled carbon nanotubes. Sep Purif Technol 90:69–82. DOI: 10.1016/j.seppur.2012.02.014.

Vatanpour V, Madaeni S.S, Moradian R, Zinadini S, Astinchap B (2011) Fabrication and characterization of novel antifouling nanofiltration membrane prepared from oxidized multiwalled carbon nanotube/polyethersulfone nanocomposite. J Membr Sci 375:284–294. DOI: 10.1016/j.memsci.2011.03.055.

Wang L, Song X, Wang T, Wang S, Wang Z, Gao C (2015) Fabrication and characterization of polyethersulfone/carbon nanotubes (PES/CNTs) based mixed matrix membranes (MMMs) for nanofiltration application. Appl Surf Sci 330:118–125. DOI: 10.1016/j.apsusc.2014.12.183.

Wang W, Zhu L, Shan B, Xie C, Liu C, Cui F, Li G (2018) Preparation and characterization of SLS-CNT/PES ultrafiltration membrane with antifouling and antibacterial properties. J Membr Sci 548:459–469. DOI:10.1016/j.memsci.2017.11.046.

Wang X, Feng M, Liu Y, Deng H, Lu J (2019) Fabrication of graphene oxide blended polyethersulfone membranes via phase inversion assisted by electric field for improved separation and antifouling performance. J Membr Sci 577:41–50. DOI: 10.1016/j.memsci.2019.01.055.

Xie M, Price W.E, Nghiem L.D, Elimelech M (2013) Effects of feed and draw solution temperature and transmembrane temperature difference on the rejection of trace organic contaminants by forward osmosis. J Membr Sci 438:57–64. DOI: 10.1016/j.memsci.2013.03.031.

Xu Z, Zhang J, Shan M, Li Y, Li B, Niu J, Zhou B, Qian X (2014) Organosilane-functionalized graphene oxide for enhanced antifouling and mechanical properties of

polyvinylidene fluoride ultrafiltration membranes. J Membr Sci 458:1–13. DOI: 10.1016/j.memsci.2014.01.050.

Zangeneh H, Zinatizadeh A.A, Zinadini S, Feyzi M, Bahnemann D.W (2019) Preparation ultrafine L-Methionine (C, N, S triple doped)-TiO_2-ZnO nanoparticles and their photocatalytic performance for fouling alleviation in PES nanocomposite membrane. Compos Part B Eng 176:107158. DOI: 10.1016/j.compositesb.2019.107158.

Zinadini S, Rostami S, Vatanpour V, Jalilian E (2017) Preparation of antibiofouling polyethersulfone mixed matrix NF membrane using photocatalytic activity of ZnO/MWCNTs nanocomposite. J Membr Sci 529:133–141. DOI: 10.1016/j.memsci.2017.01.047.

Zinadini S, Zinatizadeh A.A, Rahimi M, Vatanpour V, Zangeneh H (2014) Preparation of a novel antifouling mixed matrix PES membrane by embedding graphene oxide nanoplates. J Membr Sci 453:292-301. DOI: 10.1016/j.memsci.2013.10.070.